

Alma Mater Studiorum – Università di Bologna

DOTTORATO DI RICERCA IN
COGNITIVE NEUROSCIENCE

Ciclo XXX

Settore Concorsuale di afferenza: 11/E1
Settore Scientifico disciplinare: M-PSI/02

**TMS highlights the functional relevance and malleability of cortico-cortical
connections to motion and action perception**

Presentata da: Emilio Chiappini

Coordinatore Dottorato

Prof.ssa Monica Rubini

Relatore

Prof. Alessio Avenanti

Esame finale anno 2018

TABLE OF CONTENTS

| | |
|--|-----|
| ABSTRACT | 5 |
| GENERAL INTRODUCTION | 6 |
| I. Perception of visual motion..... | 6 |
| II. Perception of actions..... | 7 |
| III. Feedforward and feedback architecture..... | 12 |
| IV. Neural Plasticity..... | 13 |
| V. Contribution of cortical connectivity to action perception..... | 15 |
| CHAPTER I | |
| Enhancing goal-directed action performance following TMS manipulation of associative plasticity in ventral premotor-motor pathway..... | 17 |
| CHAPTER II | |
| Empowering re-entrant projections from V5 to V1 boosts sensitivity to motion..... | 39 |
| CHAPTER III | |
| Strengthening functionally specific neural pathways with TMS..... | 55 |
| CHAPTER IV | |
| Grounding motor resonance in the PMv-M1 connectivity..... | 72 |
| CHAPTER V | |
| Strengthening PMv-STs feedback projections enhances action prediction accuracy..... | 90 |
| GENERAL DISCUSSION | 107 |

APPENDIX A

Long-latency modulation of motor cortex excitability by ipsilateral posterior inferior frontal gyrus and pre-supplementary motor area.....114

APPENDIX B

Long-latency interhemispheric interactions between motor-related areas and the primary motor cortex: a dual site TMS study.....132

REFERENCES..... 154

ABSTRACT

In a social environment the human brain evolves systems to make sense of others' actions and behaviours, allowing the development of social interactions and reactions. Influential theories supported by growing evidence, posit that the understanding of others' actions is realised through the activation of one's motor system that internally simulates the motor kinematics of the ongoing observed action, and predicts its sensorial outcome. This process engages an action observation network (AON) that encompasses temporal-occipital visual and parietal-frontal motor regions. The flowing visual information is coupled with motor representations through recursive bidirectional fronto-temporal interactions that are modelled by sensorimotor experience allegedly via Hebbian plastic mechanisms. However, to date there is no direct evidence on the role that connectivity plays in carrying crucial information for the AON functioning. Recent studies demonstrated the efficacy of a transcranial magnetic stimulation (TMS) protocol, named cortico-cortical paired associative stimulation (ccPAS), able to induce transient Hebbian-like plastic potentiation in motor neural circuits. For a mechanistic understanding of the relevance of the AON connections for simulative processes and action prediction, we used ccPAS with the aim of empowering the synaptic efficacy, and thus the connectivity, between the nodes of the system to evaluate the impact on behaviour and on neurophysiological responses. Yet, ccPAS is a tool of novel conception, therefore, we firstly demonstrated its impact on motor behaviour revealing that a ccPAS to empower the premotor-motor circuit (particularly relevant also for AON simulative processes) improved dexterity and revealed the circuit's functional malleability (Study I). On low-level visual perception, ccPAS, boosting the re-entrant connectivity of visual cortices (source of AON inputs) revealed changes in motion perception and in specific features of it (Studies II-III). We then demonstrated that premotor-motor circuit conveys crucial information for the motor simulation of observed movements (Study IV), and finally, that empowering feedback connectivity in the AON enhances action prediction accuracy (Study V). We therefore provided evidence on the functional relevance of AON connectivity that supports theoretical models, and we developed an innovative tool able to promote AON functionality by inducing plastic changes in its connections.

INTRODUCTION

I. Perception of visual motion

The human being highly relies on the sense of vision to represent the surrounding reality, and the detection of motion is a key element of the visual processing, essential for example to react to nearing threats or to detect gestures during courtship behaviour. Visual motion is the change of elements' position over time, with respect to one's frame of reference and it is computed by visual regions that compares over time information from the retinal photoreceptors array (Borst, 2014). The majority of retinal inputs reach the striate visual area (V1) via the lateral geniculate nucleus (Kennedy and Bullier, 1985) and then are further processed through several stages in higher order extrastriate areas for perceptual interpretation (Lamme et al., 1998). Although a strict functional specificity is still disputed (Binkofski and Buxbaum, 2013; Gilaie-Dotan, 2016), classical theoretical accounts (Mishkin and Ungerleider, 1982; Goodale and Milner, 1992) identify in the "where" (or "how") stream a fast dorsal pathway for the visual coding of stimuli position on a moment-to-moment basis and thus critical for motion perception, in opposition to a "what" slower ventral pathway involving areas for the analysis of an object's qualities, colour and form. The motion pathway consists of neural detectors represented by several visual areas that hierarchically process the image displacement over time in increasing complexity, from low-level neurons of V1 with small receptive fields and selective for directions in the preferred orientation (see Giese and Poggio, 2003). Higher level neurons located in MT/V5+ and MST regions are responsive to whole pattern motion regardless of the individual constituents (Rust et al., 2006), selective for speed, tuned for direction, and relatively insensitive to form or colour (Rodman and Albright, 1989; Gross, 1991). The extrastriate MT/V5+ area is acknowledged as a specialised one dedicated to the perception of moving stimuli (Zeki et al., 1991). Indeed it is crucial for perceiving structure from motion, and its disruption impairs visual motion perception (Zihl et al., 1983; Beckers and Hömberg, 1992). Despite learning models based on neurophysiological mechanisms of hierarchical feedforward connectivity may explain various experimental results (Giese and Poggio, 2003), the study of the anatomical connections (carried out especially in non-human primates; see Orban et al., 2004)

indicates a more complex hierarchy (Lamme et al., 1998). Visual areas are often reciprocally interconnected with higher and lower cortices, as compellingly demonstrated in monkeys, consistently MT/V5+ has bidirectional connections with lower areas such as V1, V2, V3, V4, but also with later temporal and parietal regions such as MST, FST, VIP (Maunsell and Van Essen, 1983a). The architecture of re-entrant connections is believed to be the neural scaffold to top-down influences in a variety of visual elaborations including visual motion processing (Hochstein and Ahissar, 2002; Giese and Poggio, 2003; Bastos et al., 2015).

MT/V5+ also projects to multifarious brain regions either cortical (visual, temporal, parietal, frontal areas) or subcortical (e.g. thalamus, pons; see Vaina et al., 2001; Gilaie-Dotan, 2016). Among these cortical projections, the posterior part of the superior temporal sulcus (STS) represents a noteworthy area, being able to integrate visual information about form and motion, received from the ventral and the dorsal visual stream respectively (Felleman and Vanessen, 1991; Giese and Poggio, 2003; Puce and Perrett, 2003). Several studies showed the central role acted by this area in perceiving biological motion (Vaina et al., 2001; Giese and Poggio, 2003; Puce and Perrett, 2003) being endowed with neurons sensitive to hand-object interactions, specifically tuned to the shape of the hand executing the action. Furthermore its dense anatomical connectivity with the frontal and parietal regions of the motor system (Puce and Perrett, 2003) puts STS in a convenient anatomical and functional position to link perception to action.

II. Perception of actions

It has been shown that our brain is endowed with structures specific for processing visual motion and biological motion, that are fundamental for primary activities since birth, but more recently in the human history, we took advantage of living together with other conspecifics and organise our lives in families, communities and societies. It is straightforward to think that our brain developed structures and specific functions for social behaviours. Nowadays, the normal man of whatsoever social extraction or culture, lives in a social world and is endowed with brain structures that consent for example, to

speak, to empathise, and in general to understand the inner life of others, with increasing efficacy at increasing “similarity”. In everyday life we have to face other people that interact with us moving, and we always try to figure out what these actions mean, as soon as possible, to readily prepare an appropriate response. It is the case, for example, that meeting someone else smiling and extending the hand will prompt you to extend your hand as well and shake her hand. Conversely, the hand extension of someone with a threatening expression will engage your sympathetic system and ready fight or flight responses. In competitive sports, such as football, a defender should quickly predict the outcome of the striker actions to anticipate her moves, and the former must keep in consideration that the latter will try to mask her intentions, allegedly using feints.

In these kind of situations, and more in general, when one observes someone else moving, neuroimaging studies showed the compelling engagement of a widespread neural system called action observation network (AON) in the onlooker (Grafton et al., 1996; Nishitani and Hari, 2000; Buccino et al., 2001; Gazzola and Keysers, 2009; Van Overwalle and Baetens, 2009; Caspers et al., 2010). The AON includes three core areas: the biological motion area STS (often the middle temporal gyrus (MTG) in humans), the anterior sector of the inferior parietal lobule (IPL) and the posterior aspect of the inferior frontal gyrus (IFG) that encompasses the ventral part of the premotor cortex (PMv). Visual input access to the AON from the STS that is endowed with multimodal cells activated by motion that parse motion into sequential discrete units, reducing it to changes in spatial location over time (Barracough et al., 2005; Redcay, 2008). IPL is an area that bridges perception and action, it is dedicated to online control of hand-object interactions and involved in the representation of actions at a goal level (Hamilton and Grafton, 2006; Tunik et al., 2007). PMv stores the representations of motor acts in a rough somatotopic organisation (Buccino et al., 2001) and ultimately transforms the visual information into motor representation (Rizzolatti and Craighero, 2004).

The processing of other actions actually gathers a larger network of areas that constitute the extended AON and involves the primary motor cortex (M1), the dorsal premotor cortex (PMd), the supplementary

motor cortex (SMA) and the extrastriate visual area of motion (V5) (Nishitani and Hari, 2000; Caspers et al., 2010; Mukamel et al., 2010; Fig.1.1). It is assumed that the engagement of this system enables the onlooker to recognise the goal of behaviours by matching the observed action with its own motor repertoire and the most common purposes associated with it (Van Overwalle and Baetens, 2009). This leads to understand the observed action and to infer the underlying intentions (Cattaneo and Rizzolatti, 2009).

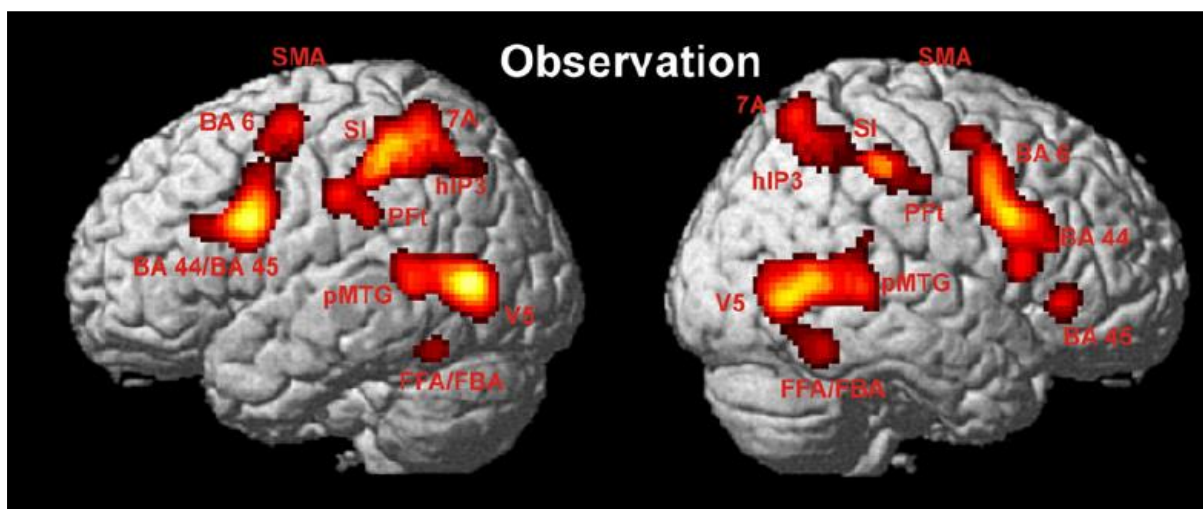


Fig.1.1 Significant meta-analysis results for action observation. From Caspers et al. 2010.

Action understanding, direct matching hypothesis

The parietal and frontal areas of the AON strongly overlap with regions involved in movement execution (Grèzes and Decety, 2001; Gazzola and Keysers, 2009). Motor areas are activated somatotopically by action observation (Buccino et al., 2001) and transcranial magnetic stimulation (TMS) of the primary motor cortex (M1) shows muscular specific facilitations that are congruent with the movement observed and its kinematic (Fadiga et al., 1995; Strafella and Paus, 2000; Gangitano et al., 2001) prompted by PMv engagement (Avenanti et al., 2007; Koch et al., 2010; Catmur et al., 2011). These findings, together with the discovery in the homologue areas of the macaque cortex of mirror neurons (di Pellegrino et al., 1992; Gallese et al., 1996), i.e. bimodal neuronal cells active both during action execution and observation, brought to the development of embodied theories for action understanding

(Grafton, 2009). In this framework, the observation of someone else's movement automatically induces a subliminal activation of the motor representation corresponding to that generated during the execution of the same movement, the effects of which are well known by the individual. Such resonating mechanisms have been indicated as responsible to transform visual information into knowledge of the observed movement and the neuronal substrate of such processes has been identified in the mirror neurons (Rizzolatti et al., 2001; Rizzolatti and Craighero, 2004), for this reason, the AON is often referred to as the mirror neurons system. In this model, the information carried by visual signals, flowing through the forward connections $STS \rightarrow IPL \rightarrow PMv$, is transformed from low-level kinematic representations to high-level representations of intentions (Nishitani and Hari, 2000, 2002; Keysers and Perrett, 2004; Kilner et al., 2007a; Van Overwalle and Baetens, 2009; Fig.1.2).

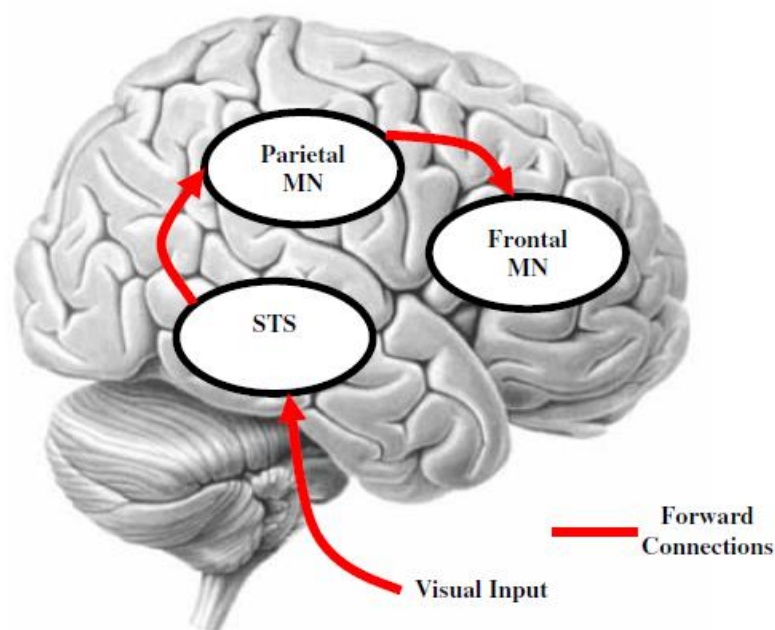


Fig.1.2 Schematic representation of areas and connections of the forward recognition model as conceptualised in the direct matching hypothesis. From Kilner et al. 2007b.

Predictive coding, Bayesian perspective

A recent theory of action perception challenges the view of the AON as a mere feedforward model for the passive recognition of action. Kilner and co-workers (2007a) suggest an active role of the system in inferring the intentions using a predictive coding approach based on hierarchical Bayesian inference of

different descriptive levels of action: muscle activity, kinematics, goals and intentions (Hamilton and Grafton, 2007). Here, action understanding is the comprehension of the intentions and the goals of an observed movement from the available visual representation of the kinematic level (Kilner et al., 2007b). Contextual information and short and long-term experience elicits a multi-level cascade of neural representations, where higher level predictions influence processing at lower levels (Friston, 2010; Kilner, 2011). In this view, the AON act as a Bayesian device that empirically infers the most likely cause of an action by minimising the prediction error through recurrent reciprocal interactions among every level of actions that are represented in hierarchically organised cortical areas. The prediction error is the mismatch between the neural representation at each step and the predictions generated by the lower, or feeding back from, higher cognitive level.

This processing is granted by the dynamicity of a system having feedforward and feedback connections that allows the functional communication between the nodes of the network. The feedforward STS→IPL→PMv connectivity recognise the cause of an action activating the best suiting motor representations given the visual input and so allows the backward PMv→IPL→STS generative stream to provide a sensory prediction underlying an expectation of the goal (Fig.1.3). Importantly, the prediction can be adjusted through the feedforward flow if a mismatch between the incoming perceptual inputs and the prediction itself is detected by the feedback flow. The prediction is therefore a hypothesis that is tested by constantly matching the top-down prediction with incoming bottom-up sensorial inputs.

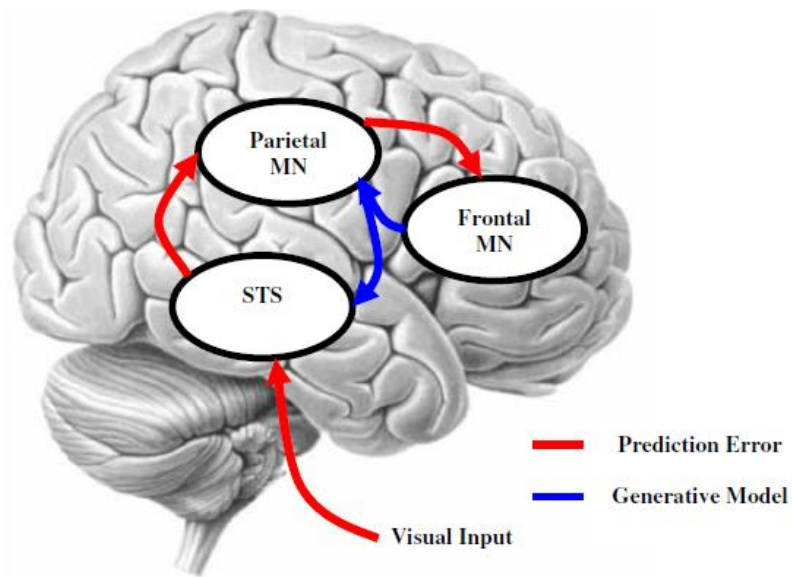


Fig.1.3 Schematic representation of areas and connections of the predictive coding model. From Kilner et al. 2007b.

III. Feedforward and feedback architecture

The study of the neural networks highlighted the interactions among the hubs of the network itself and thus of their anatomical and functional connectivity. It is not uncommon to observe in the central nervous system, complex systems having fine-tuned neural interactions resulting in an efficient functional operativity (Avenanti et al., 2012b; Plow et al., 2014; Fiori et al., 2017) prompted by the reciprocal exchange of information between homologue regions or hierarchically/functionally distinct areas. The concept of recurrent interactions is appropriate for characterising both the visual system for motion perception and the AON.

The feedforward architecture of the visual system allows sensory input to be swiftly represented from low levels in early cortices to higher levels in later cortices following a bottom-up processing (Felleman and Vanessen, 1991; Lamme et al., 1998). At the same time, it has been widely shown how visual perception is constantly modulated through influences exerted by high order cortices on the encoding of early ones in a top-down fashion (Hochstein and Ahissar, 2002; Gilbert and Li, 2013; Wyatte et al., 2014) through re-entrant projections (Lamme and Roelfsema, 2000; Bastos et al., 2015). For example visual recurrent processing allow the attentional grouping of object's features (Desimone and Duncan,

1995) and provide access of stimuli encoded in MT/V5 to consciousness (Pascual-Leone and Walsh, 2001; Silvanto et al., 2005a).

Similarly, the predictive coding account of action observation, puts much emphasis on the recursive connections between the areas of the AON that underpin forward and inverse models for action perception, making of the STS-PMv loop, the dynamic system performing predictive coding (Keysers and Gazzola, 2014). Scholars proposed that inverse models use forward visual-to-motor connections to convert the visual information in a predicted motor plan, while the forward (generative) models involve backward motor-to-visual connections to generate the sensory outcome expected as triggered by the representation of the observed action (Miall, 2003; Wolpert et al., 2003; Kilner et al., 2007a, 2007b; see Fig.1.3). In support, evidence of dominant fronto-temporal connectivity has been found when individuals observe predictable actions (Kokal and Keysers, 2010; Schippers and Keysers, 2011). These findings suggest a prominent role of the feedback pathways in inhibiting incoming redundant input from lower-level hierarchical cortical representations as far as the prediction is correct. Otherwise, a prediction error is generated and conveyed through forward projections to frontal regions for revising the prediction (Kilner, 2011).

Therefore, inter-cortical loops represent a functioning scheme that belongs to the general architecture of the nervous system and assists perceptual systems to sense unisensorial stimuli (e.g. visual motion) but also more complex multimodal stimuli (e.g. actions). However, these connectivity models for perception and understanding of the observed action are mainly based on theoretical assumptions and indirect observation. For a mechanistic comprehension of the role of the connectivity it is needed to directly manipulate the information flow from one node of the network to another; that is, investigate the functional response to an exogenous change of the feedforward or feedback flow of information.

IV. Neural Plasticity

Neural plasticity defines the essential ability of the human brain to modify the functioning of specific neural circuitries in response of environmental demands, leading to perceptual, emotional, cognitive

and behavioural changes. Continuous use-dependent plasticity mechanisms drive structural modifications or modulation of molecular activity and determine short- or long-term changes in the morphological or functional connectivity between cells or neural networks (Xerri, 2012). Repetitive activation of neuronal circuits can induce long-term changes in subsequent responses generated by synapses, such plasticity of synaptic connections is regarded as a cellular basis for adaptive functions during developmental age as well as adulthood, having a major impact on the organisation of cortical representations responsible for learning, perception and motor control (Hebb, 1949; Bliss and Collingridge, 1993; Kalia, 2008; Xerri, 2012). Motion and action perception systems are not exempt from plastic neural reorganisation during developmental age (Bedny et al., 2010; Keysers and Gazzola, 2014; Agyei et al., 2016), and across humans or primates lifespan as consequence of training and exposition (Calvo-Merino et al., 2005; Catmur et al., 2007, 2011; Aglioti et al., 2008; Cross et al., 2009; Beste et al., 2011; Chen et al., 2015) or brain lesions (Avenanti et al., 2013a; Sokolov et al., 2014; Dettmers et al., 2015; Burnat et al., 2017).

The efficiency of neuronal signal transmission can be enhanced if the activity of the presynaptic cell persistently assists the firing of the postsynaptic cell (Markram et al., 1997; Bi and Poo, 2001; Jackson et al., 2006). This type of plasticity postulated by Hebb (Hebb, 1949) is referred to as spike-timing dependent plasticity (STDP), since it hinges on strict temporal constraints that define whether long-term potentiation (LTP) will arise or not. In synapses that show STDP phenomena, long-term depression (LTD) can be triggered by reversed stimulation order (i.e. post-pre), leading to dampened postsynaptic response (Bi and Poo, 2001; Caporale and Dan, 2008; Keysers and Gazzola, 2014).

Recently, plasticity with STDP properties has been induced by pairing cortical stimulation of two physiologically interconnected human motor-related regions using dual-coil transcranial magnetic stimulation (TMS; Rizzo et al., 2009; Buch et al., 2011; Veniero et al., 2013; Johnen et al., 2015). Notably, this cortico-cortical paired associative stimulation (ccPAS) has been shown to strengthen connectivity between the stimulated regions and improve motor performance.

V. Contribution of cortical connectivity to movement and action perception

The research exposed here aims at modulating the connectivity between the nodes of the motion and action perception systems, by taking advantage of the ccPAS tool, in order to understand the role of the connectivity between them. The underlying hypothesis is that if a connection subserves a function, then the manipulation of the information flow of such connection will impact on the expression of the function. This hypothesis was tested on the theoretical models of the feedforward and feedback functional architecture involved in the elaboration of low level visual stimuli and in the representation of complex visual stimuli that requires visuo-motor processing, specifically observed actions (see Fig.I.4).

In chapter I, it is illustrated how the efficacy of ccPAS in inducing appreciable behavioural changes was demonstrated. Thus far, ccPAS behavioural impact was controversial (Rizzo et al., 2009; Chao et al., 2015) or non-controlled (Koganemaru et al., 2009). The PMv-M1 circuit is known for being involved in the execution of goal-directed actions (Davare, 2006) and for its involvement on M1 activity modulation during action observation (Avenanti et al., 2007; Koch et al., 2010; Catmur et al., 2011). Neurophysiological (Buch et al., 2011) and functional connectivity (Johnen et al., 2015) evidence on the impact of ccPAS have been adequately demonstrated, therefore, the PMv-M1 connectivity represented the ideal testbed circuit for verifying the behavioural effects of ccPAS.

In the experiments presented in chapter II, ccPAS was administrated for the first time over non-motor-related areas, to test its efficacy on the visual system. The aim was to provide behavioural evidence that fostering the re-entrant information from V5 to V1 drove to behavioural performance improvement on a visual motion task. On the grounds of the results obtained, the V5-V1 feedback circuit was further investigated with the aim of suggesting the existence of specific visual motion pathways carrying functionally direction-specific re-entrant information. A novel ccPAS protocol, able to differentiate its neural targets on a functional basis, was thereby developed, the study is reported in chapter III.

Successful experiments demonstrating motor and visual low-level behavioural improvements following connectivity boosting through ccPAS in the premotor-motor and in the motion visual systems paved the way for exploring the relevance of feedforward and feedback connectivity in the AON, encoding complex and hybrid visuo-motor stimuli such as observed actions. In keeping, experiments in chapter IV further explored the PMv-M1 connectivity, here in relation to the observed actions to demonstrate ccPAS efficacy in action perception modulation. Specifically, we addressed the question of whether boosting the information flowing from the core region of the AON, PMv, to the connected M1, caused the enhancement of the motor resonance phenomenon, as neurophysiological index of AON engagement during action observation (Fadiga et al., 1995, 2005).

Once proved with neurophysiological evidence the possibility of action perception modulation, in chapter V experiments, visuo-to-motor feedback connectivity of the AON was manipulated to assess on a behavioural level, its role in the prediction of others' actions.

In compliance with STDP rules, the success of the ccPAS protocol critically hinges on the selection of timing between the two pulses. In Appendix A and B are reported neurophysiological dual-coil TMS studies that focus on the timing of interactions between motor-related areas and M1. Interactions revealed in these studies at long-latency timings, thus far scarcely explored, may underpin intercortical functions and fine-tuning mechanisms that can be altered via ccPAS.

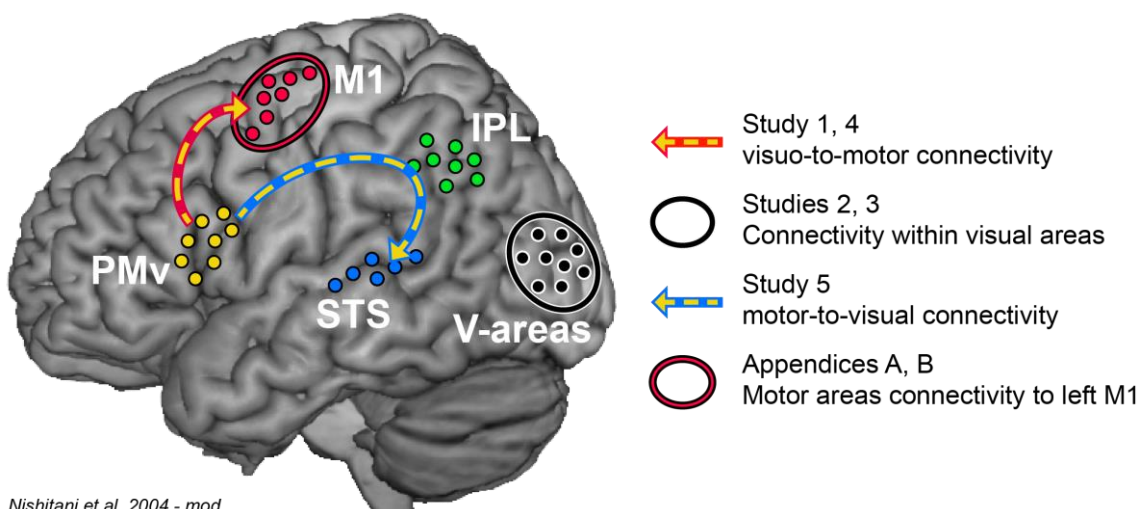


Fig.I.4 Schematic representation of areas and connectivity tested in the studies reported in the present thesis.

CHAPTER I

Enhancing goal-directed action performance following TMS manipulation of associative plasticity in ventral premotor-motor pathway

1.1 Introduction

Goal-directed actions such as grasping, manipulating and moving objects are the result of complex interactions within dorsal occipito-parieto-frontal streams involved in sensorimotor transformations (Jeannerod et al., 1995; Castiello, 2005; Grol et al., 2007; Cavina-Pratesi et al., 2010; Davare et al., 2011). At least part of this process is thought to occur in a serial, hierarchical fashion: monkey studies have suggested that, within a dorsolateral stream, the ventral premotor cortex (PMv) transforms visual information about object properties (e.g., their shape, size, etc.) into appropriate motor commands; these commands are conveyed to the primary motor cortex (M1), allowing fine control of individual finger movements (Muir and Lemon, 1983; Murata et al., 1997; Fagg and Arbib, 1998; Fogassi et al., 2001; Lang and Schieber, 2004; Raos et al., 2006). Although alternative/parallel pathways also exist (e.g., Dum and Strick, 1991; He et al., 1995), these monkey studies point to a pivotal role of the PMv-to-M1 hierarchy in performing skilled, visually guided object-oriented manual actions such as grasping observed objects (Prabhu et al., 2009; Rizzolatti et al., 2014).

Neuroimaging and transcranial magnetic stimulation (TMS) studies suggest that the human brain is endowed with neural systems for goal-directed actions analogous to those of monkeys (Castiello, 2005; Kroliczak et al., 2007; Tunik et al., 2007; Davare et al., 2008, 2009, 2010). These studies have shown that visually guided goal-directed actions are at least partly underpinned by neural interactions within the dorsolateral stream (Davare et al., 2010, 2011; see Vesia et al., 2017). For example, Grol and colleagues reported increased connectivity between occipito-parieto-frontal nodes of the dorsolateral stream (i.e., V3A, AIP and PMv) during precision grasping (Grol et al., 2007). In addition, Davare and colleagues have shown that, during grasp preparation, short-latency PMv-to-M1 connections are

facilitated in a muscle-specific manner (i.e., grasp-related facilitation is specific to those circuits controlling the muscles involved in the upcoming grasp; see Davare et al., 2008, 2009, 2010). These studies converge with monkey findings and support the notion of a human PMv-to-M1 hierarchy in fine motor control of goal-directed actions.

A variety of experiences ranging from learning new motor skills to experiencing a stroke in motor areas have been associated with neuroplastic changes in premotor and motor areas and the connection between them (Nelles et al., 2001; Sun et al., 2007; Albert et al., 2009; Taubert et al., 2011; Wiestler and Diedrichsen, 2013; Horn et al., 2016). For example, training in a fine motor task involving grasping and moving pegs and marbles strengthened functional connectivity between PMv and primary sensorimotor representations of the hand (Hamzei et al., 2012). Increased functional connectivity between PMv and sensorimotor cortex was also found following training in a precision drawing task (Philip and Frey, 2016). Moreover, performing skilful hand actions after extensive training was associated with increased premotor-motor connectivity (Dayan and Cohen, 2011). However, these previous studies used a correlational approach that does not address the critical question of whether direct strengthening of premotor-motor connectivity (e.g., via exogenous brain manipulation) would cause an enhancement in hand motor functions. Answering this outstanding question is the goal of the present study.

Recent advances in TMS allow us to directly address this question through a new protocol called cortico-cortical paired associative stimulation (ccPAS Koganemaru et al., 2009; Rizzo et al., 2009, 2011; Arai et al., 2011; Buch et al., 2011; Lu et al., 2012; Veniero et al., 2013; Koch et al., 2013; Johnen et al., 2015; Casula et al., 2016; Romei et al., 2016a). This protocol involves repeated paired stimulation of two interconnected brain areas with the aim of inducing spike-timing-dependent plasticity (STDP), a form of synaptic plasticity meeting the Hebbian principle that synapses are potentiated if the presynaptic neuron fires repeatedly before the postsynaptic neuron (Jackson et al., 2006; Caporale and Dan, 2008; Markram et al., 2011). In the ccPAS protocol, pre- and post-synaptic coupling is achieved by repeatedly

administering pairs of TMS pulses. In each pair, a first pulse over a target area is followed by a second pulse over an interconnected target area with an inter-stimulus interval (ISI) consistent with the activation of short-latency connections between the two areas. In a recent study, Buch and colleagues (2011) administered a ccPAS protocol by delivering the first pulse in each pair over PMv and the second over M1 using an ISI of 8 ms, i.e., the critical ISI at which the PMv exerts a short-latency physiological effect on the excitability of the ipsilateral M1 (see dual-site TMS studies of Davare et al., 2008, 2009, 2010). It was shown that this repeated stimulation of the PMv-to-M1 pathway enhanced the physiological effect of PMv conditioning over M1 excitability, and that the time-course of the long-term potentiation (LTP)-like effect resembled that of STDP effects observed in animal studies (Buch et al., 2011). In a further study, the PMv-to-M1 ccPAS protocol was found to increase the functional connectivity of the stimulated pathway, as measured by functional magnetic resonance imaging (fMRI). Increased connectivity was anatomically specific and did not occur in non-stimulated parallel motor pathways (Johnen et al., 2015).

These physiological studies provided direct evidence that ccPAS can transiently strengthen PMv-to-M1 connections by increasing synaptic efficiency in a hierarchical motor pathway involved in visually guided object grasping and manipulation. However, these studies did not answer the critical question of whether exogenous enhancement of PMv-to-M1 synaptic efficiency also causes an improvement in performing goal-directed actions.

In the present study, we sought to investigate the malleability and behavioural relevance of PMv-to-M1 connectivity by combining a ccPAS PMv-to-M1 protocol with two behavioural tasks. Based on the notion that the PMv-to-M1 hierarchy is involved in the control of goal-directed actions, we hypothesised that administering a ccPAS protocol aimed at enhancing PMv-to-M1 connectivity would improve performance on the Nine-Hole Peg Test (9-HPT; (Mathiowetz et al., 1985; Oxford Grice et al., 2003), a well-established manual dexterity task tapping into the ability to grasp and manipulate small

objects – i.e., goal-directed actions underpinned by the recruitment of PMv and M1 (Binkofski et al., 1999; Ehrsson et al., 2000; Kuhtz-Buschbeck et al., 2001; Davare, 2006; Horn et al., 2016).

We hypothesised this behavioural enhancement would be specific. No improvement was expected following a M1-to-PMv ccPAS protocol –controlling for the directionality of the stimulated pathway– or a sham ccPAS protocol –controlling for nonspecific effects of TMS. Additionally, we expected no ccPAS-induced changes in performance on a visual choice reaction time (cRT) task. Although both 9-HPT and cRT are visuomotor tasks, the latter does not tap into the ability to efficiently shape the hand to manipulate objects, and it was thus expected to be less sensitive to manipulation of PMv-M1 connectivity.

1.2 Methods

Participants

Fifty-four healthy participants (16 males, mean age 23.1 ± 3.3 years) took part in the study. All were right handed, based on the Edinburgh Handedness Inventory (Oldfield, 1971), had normal or corrected-to-normal vision and were naïve to the purpose of the experiment. All participants gave written informed consent prior to the study, and were screened to avoid adverse reactions to TMS (Rossi et al., 2009; Rossini et al., 2015). The experimental procedures were in accordance with the 1964 Declaration of Helsinki and approved by the local ethics Committee. None of the participants reported adverse reactions or discomfort related to TMS.

General experimental design and procedures

To test the malleability and functional relevance of PMv-M1 connections, we administered ccPAS over the left PMv and the left M1, to repeatedly activate the neural pathways between them (Buch et al., 2011; Johnen et al., 2015). The participants were randomly assigned to 1 of 3 groups, accordingly to the administered ccPAS protocol (see Table 1.1 and Fig. 1.1). In the experimental group ($\text{Exp}_{\text{PMv} \rightarrow \text{M1}}$; $N = 18$), we administered a PMv-to-M1 ccPAS protocol. In the active control group ($\text{Ctrl}_{\text{M1} \rightarrow \text{PMv}}$; $N = 18$) we

administered a M1-to-PMv ccPAS protocol, whereas in the sham control group (Ctrl_{sham}, N = 18) we administered a sham PMv-to-M1 ccPAS protocol. We used a double-blind procedure, as both the participants and the experimenter assessing behavioural performance were blind to participants' allocation.

| | Exp_{PMv→M1} (N=18) | Ctrl_{sham} (N=18) | Ctrl_{M1→PMv} (N=18) | Statistical comparison |
|--|--|---|---|--|
| Age (years) | 22.9 ± 2.6 | 24.1 ± 4.3 | 22.7 ± 2.9 | $F_{2,51} = .94, p = .40;$ $\eta_p^2 = .04; BF_{01} = 3.5$ |
| Gender (F/M) | 13 F / 5 M | 12 F / 6 M | 13 F / 5 M | $\chi^2 = .18, p = 1;$ $\phi = .06; BF_{01} = 5.0$ |
| PMv pulse intensity (% of monophasic M.O.S.) | 37.9% ± 7.3 ^(a) | 38.8% ± 6.0 ^(a) | 36.8% ± 5.8 ^(a) | $F_{2,51} = 0.47, p = .63;$ $\eta_p^2 = .02; BF_{01} = 4.9$ |
| M1 pulse intensity (% of biphasic M.O.S.) | 68.8% ± 11.6 ^(b) | not assessed ^(c) | 68.6% ± 9.5 ^(b) | $F_{1,34} < .01, p = .96;$ $\eta_p^2 < .01; BF_{01} = 3.1$ |
| 9-HPT performance at baseline (s) | 20.8 ± 2.1 | 20.6 ± 1.8 | 21.2 ± 1.5 | $F_{2,51} = .47, p = .63;$ $\eta_p^2 = .02; BF_{01} = 4.9$ |
| cRT performance at baseline (ms) | 397 ± 29 | 421 ± 59 | 425 ± 43 | $F_{2,51} = 1.97, p = .15;$ $\eta_p^2 = .07; BF_{01} = 1.7$ |
| cRT performance at baseline (%Corr) | 96 % ± 3 | 95 % ± 5 | 96 % ± 4 | $F_{2,51} = .83, p = .44;$ $\eta_p^2 = .03; BF_{01} = 4.5$ |

Table1.1 Demographic characteristics, TMS parameters (as the maximum output stimulator; M.O.S.) and performance at Baseline across the three groups (expressed as Mean ± S.D.). A series of null hypothesis-testing analyses (one-way ANOVAs and χ^2) and their Bayesian implementations showed no differences between groups. **Notes:** ^(a) TMS intensity corresponding to 90% of the rMT as assessed with the coil of the monophasic stimulator over M1. ^(b) TMS intensity required to elicit a MEP of ~1-mV amplitude as assessed with the coil of the biphasic stimulator over M1; ^(c) In the sham group the biphasic stimulator was set at an intensity of 65% in all participants.

Participants performed two behavioural visuomotor tasks (i.e., 9-HPT and cRT). After they were familiarised with the tasks for about 10 min (training), their performance was recorded in four experimental sessions (Fig.1.1). Two sessions were recorded before the ccPAS (constituting the

“Baseline” and “Pre” sessions) and two sessions were recorded after the ccPAS (“Post-0” and “Post-30”). Each session lasted ~5 minutes, during which the two tasks were administered in a counterbalanced order across participants. Behavioural performance was followed by ~25 minutes of rest (i.e., sessions were separated by 30 minutes each). TMS parameters and coil positions (see *ccPAS protocol* and *neuronavigation* paragraphs below) were identified in the rest periods before and after the Baseline session. Fifteen minutes after the beginning of the Pre session, the ccPAS protocol was administered for 15 minutes and performance was recorded immediately (Post-0) and 30 minutes (Post-30) after the end of the stimulation. Participants were invited to remain sit throughout the duration of the experiment and keep their hands completely relaxed in the rest periods. The experiment lasted approximately 2.5 hours.

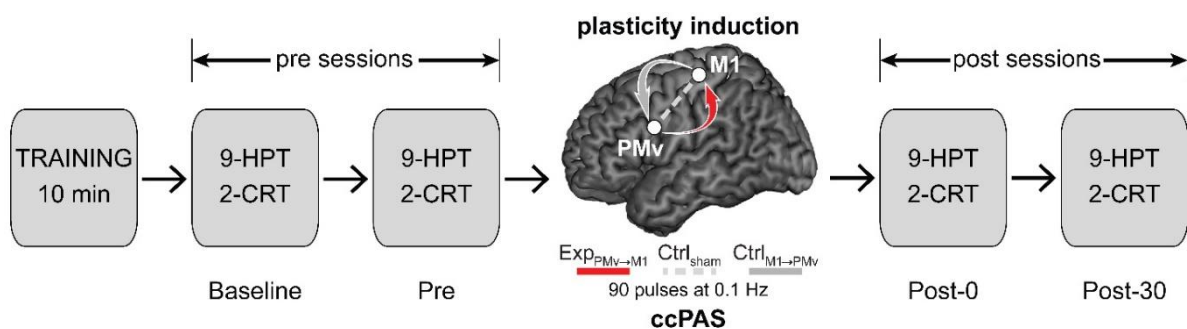


Fig.1.1 Schematic representation of the experimental procedure.

ccPAS protocol

The ccPAS pulses were administered by means of two 50-mm figure-of-eight branding coils. These small focal coils are designed with the handle pointing perpendicular to the plane of the wings and could be positioned nearby without interference from the handles. One coil was placed over the left PMv and connected to a Magstim 200 monophasic stimulator; the other coil was placed over the left M1 and connected to a Magstim Rapid2 biphasic stimulator (The Magstim Company, Carmarthenshire, Wales, UK). Ninety pairs of TMS pulses were delivered continuously at a rate of 0.1 Hz for 15 min (Rizzo et al., 2009, 2011; Buch et al., 2011; Johnen et al., 2015; Romei et al., 2016a). In each pair, PMv and M1 were

stimulated with an ISI of 8 ms (Buch et al., 2011; Johnen et al., 2015) to activate short-latency connections between the two regions (e.g. Davare et al., 2009).

The $\text{Exp}_{\text{PMv} \rightarrow \text{M1}}$ group received PMv-to-M1 ccPAS with the PMv pulse always administered before the M1 pulse. The $\text{Ctrl}_{\text{M1} \rightarrow \text{PMv}}$ group received the pulses in the reverse order, i.e., with the M1 pulse prior to the PMv pulse, to control for the direction of stimulation. The $\text{Ctrl}_{\text{sham}}$ group received PMv-to-M1 ccPAS, but the coils were held perpendicularly to the scalp so that no current was induced in the brain. The pulses were triggered remotely using MATLAB (MathWorks, Natick, USA) to control both stimulators.

Coil positions for targeting the PMv were determined based on a neuronavigation system (see next paragraph), whereas M1 was localised functionally as the optimal scalp position for inducing motor-evoked potentials (MEPs) of maximal amplitude in the right first dorsal interosseous (FDI; Rossini et al., 2015). During active ccPAS (i.e., in the $\text{Exp}_{\text{PMv} \rightarrow \text{M1}}$ and $\text{Ctrl}_{\text{M1} \rightarrow \text{PMv}}$ groups), coils were oriented to induce current flows consistent with previous dual-site TMS and ccPAS studies targeting PMv and M1 (e.g., Davare et al., 2008; Bäumer et al., 2009; Buch et al., 2010; see Fig.1.2, panel A and B). The left PMv was targeted using the monophasic stimulator and the coil was placed tangentially to the scalp, inducing a posterior-to-anterior and lateral-to-medial current flow. The left M1 was targeted using the biphasic stimulator with the coil placed tangentially to the scalp and oriented at a $\sim 45^\circ$ angle to the midline. In this way, the second and most effective component of the biphasic waveform induced a current flowing in an anterior direction, optimal for M1 stimulation (e.g. Kammer et al., 2001; Di Lazzaro et al., 2004). Table 1.1 reports the intensity of PMv and M1 stimulations across the three groups. TMS intensities were set based on MEPs induced by single pulse TMS over the left M1. MEPs were recorded from the right FDI by means of surface Ag/AgCl electrodes placed in a belly-tendon montage, with the ground electrode placed on the right wrist. EMG signals were acquired by means of a Biopac MP-35 (Biopac, USA) electromyograph, band-pass filtered (30-500 Hz) and digitised at a sampling rate of 5 kHz. The intensity of PMv stimulation was individually adjusted to 90% of each participant's resting motor threshold (rMT), which was assessed by placing the coil of the monophasic stimulator tangentially to

the scalp over the left M1, at a $\sim 45^\circ$ angle to the midline, inducing a posterior-anterior current direction (Kammer et al., 2001; Di Lazzaro et al., 2004). The rMT was defined as the minimum stimulator output intensity that induced a MEP with $> 50 \mu\text{V}$ amplitude in 5 out of 10 consecutive trials (Rossini et al., 2015). Although previous ccPAS studies focusing on PMv-to-M1 interactions have used higher intensities for targeting PMv (i.e., 110% of rMT; Buch et al., 2011; Johnen et al., 2015), subthreshold stimulation minimises potential discomfort associated with inferior frontal sites. Importantly, the effectiveness of subthreshold conditioning has been demonstrated in other ccPAS studies (e.g. Koch et al., 2013; Veniero et al., 2013) and finds specific support from dual-coil TMS studies testing early PMv-to-M1 interactions (e.g. Davare et al., 2008, 2009, 2010; Bäumer et al., 2009; Cattaneo and Barchiesi, 2011). To minimise discomfort and surprise, before starting the administration of the active ccPAS protocols, we made participants experience active stimulation of PMv, using 3-4 pulses of increasing intensity. All participants reported to tolerate well the stimulation. In the active ccPAS groups ($\text{Exp}_{\text{PMv} \rightarrow \text{M1}}$ and $\text{Ctrl}_{\text{M1} \rightarrow \text{PMv}}$), the intensity of M1 stimulation was adjusted to elicit MEPs of about 1 mV in amplitude following a single TMS pulse over the left M1 (Buch et al., 2011; Johnen et al., 2015). In the $\text{Ctrl}_{\text{sham}}$ group, M1 stimulation was set at 65% of maximal stimulator output in all participants. No between-group differences were found in the intensities of PMv and M1 stimulation (Table 1.1).

During the ccPAS protocol, participants remained relaxed with the eyes open and EMG activity was constantly monitored from the right FDI to ensure that full muscle relaxation was maintained during the protocol.

Neuronavigation

The coil positions to target the left PMv and left M1 were identified using established methods. As reported above, the hand representation in the left M1 was identified functionally based on MEPs from the FDI muscle. The left PMv was identified on each participant's scalp using the SofTactic Navigator System (Electro Medical System, Bologna, IT) as in previous studies (Avenanti et al., 2013a; Tidoni et al., 2013; Paracampo et al., 2016). Skull landmarks (nasion,inion and 2 preauricular points) and ~ 80 points

providing a uniform representation of the scalp were digitised by means of a Polaris Vicra digitiser (Northern Digital Inc., Ontario, CAN). An individual estimated magnetic resonance image (MRI) was obtained for each subject through a 3D warping procedure fitting a high-resolution MRI template to the participant's scalp model and craniometric points. This procedure has been proven to ensure a global localisation accuracy of roughly 5 mm (Carducci and Brusco, 2012). To target the left PMv, the coil was placed over a scalp region overlying the Talairach coordinates: $x = -54$, $y = 10$, $z = 24$, corresponding to the mean coordinates of a ventral frontal site (at the border between the anterior sector of the PMv and the posterior sector of the inferior frontal gyrus) whose conditioning was found to affect planning, execution and perception of hand actions (Davare, 2006). These coordinates are consistent with those used in previous ccPAS (Buch et al., 2011; Johnen et al., 2015) and dual-site TMS studies targeting PMv-to-M1 connections (Davare et al., 2008, 2009, 2010, Fiori et al., 2016, 2017).

The Talairach coordinates corresponding to the projections of the left PMv and left M1 scalp sites onto the brain surface were automatically estimated by the SofTaxis Navigator from the MRI-constructed stereotaxic template, and resulted in the following Talairach coordinates (mean \pm S.D.) across the three experiments: left PMv: $x = -54 \pm 1$, $y = 10 \pm 1$, $z = 24 \pm 1$; left M1: $x = -35 \pm 4$, $y = -19 \pm 6$, $z = 60 \pm 3$. These coordinates are consistent with regions defined as human PMv and M1, respectively (Mayka et al., 2006). A series of ANOVAs ensured that PMv and M1 coordinates were comparable across the three groups (all $F < 1.96$, all $p > .15$). Fig.1.2, panels C-E, shows individual targeted sites converted in MNI space for illustrative purpose.

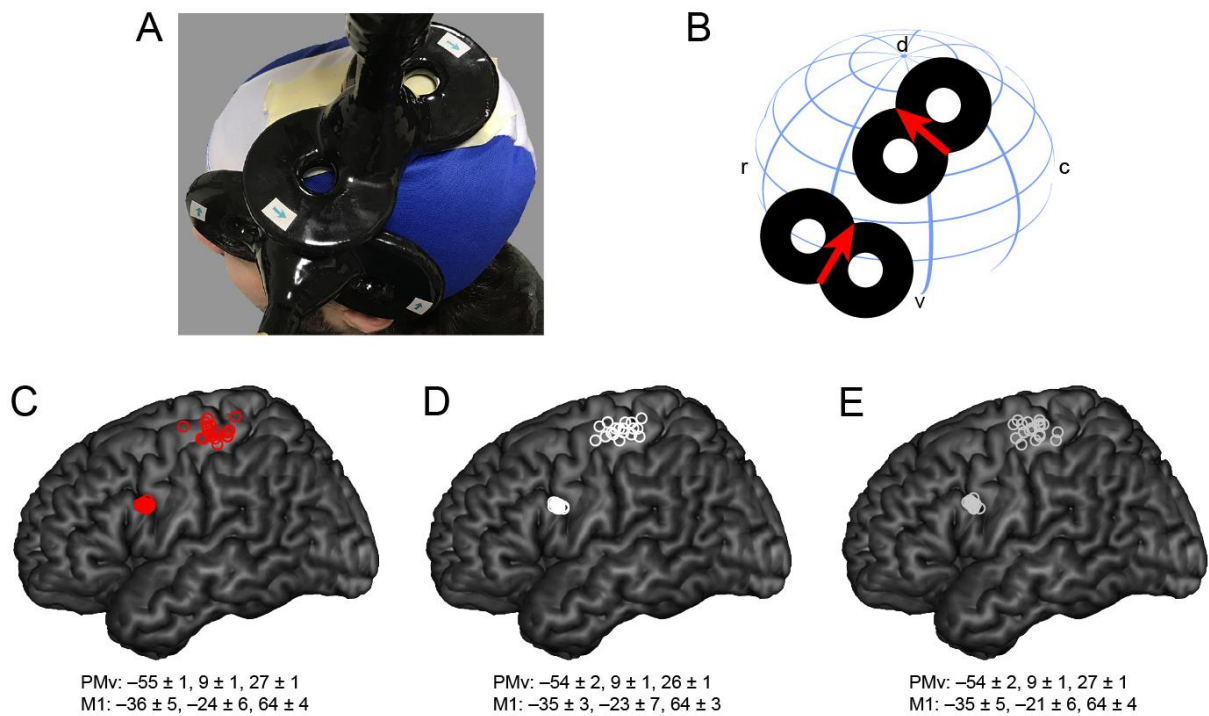


Fig.1.2 Targeted sites and coils placement. (A) Coils' positions and orientation during ccPAS on a representative participant and (B) corresponding schematic representation of induced currents. For M1 stimulation the arrow indicates the direction of the most effective phase of the biphasic pulse (see Methods). (C-E) Individual subjects targeted sites reconstructed on a standard template using MRICron software (MRICron/NPM/dcm2nii) after conversion to MNI space and corresponding mean \pm S.D. coordinates. (C) $Exp_{PMV \rightarrow M1}$, (D) $Ctrl_{sham}$ and (E) $Ctrl_{M1 \rightarrow PMV}$ group.

Visuomotor tasks

The 9-HPT is a widely-used test to assess fine hand dexterity. It requires participants to finely shape their hand in order to grasp and manipulate small objects (Mathiowetz et al., 1985; Oxford Grice et al., 2003), an ability tapping into the activation of the dorsolateral stream (Grol et al., 2007; Davare et al., 2010; Hamzei et al., 2012; Philip and Frey, 2016). Performance on the 9-HPT was found to be sensitive to exogenous non-invasive manipulations of the motor system (Koch et al. 2008; Avenanti et al. 2012; Di Lazzaro et al. 2013) and correlate with the recruitment of sensorimotor areas including PMv and M1 (Hamzei et al., 2012). The 9-HPT apparatus (Fig.1.3, panel A) consisted of a plastic board with 9 small holes organised in a 3 x 3 matrix. The distance between holes was 3.2 cm, and pegs were placed in a tray of 8.5 x 10.4 x 2.3 cm fixed adjacent to the board. Upon receiving the start command, participants picked up the nine small pegs one by one with their right hand, put all of them into the nine holes and

then removed them one by one, returning them to the box. Participants were required to execute the task as quickly as possible. The time taken to complete the task was recorded from the starting movement to the drop of the last peg into the tray by an experimenter blind to the ccPAS condition. In each session (Baseline, Pre, Post-0, Post-30), participants performed 5 repetitions of the task.

The cRT was used as a control task to assess visuomotor reaction times (Fig.1.3, panel B). We used a 2-choice version of the cRT to assess simple visuomotor mapping based on learned visuomotor associations. Although the cRT is sensitive to non-invasive brain stimulation of the motor system (Kobayashi et al., 2004; Mansur et al., 2005), this task does not involve dexterous hand shaping and object manipulation – as required by the 9-HPT– and relies less on the PMv-M1 circuit. Participants were instructed to respond by releasing the key pressed by the index or middle finger of the right hand according to the number '1' or '2' displayed on a monitor placed ~80 cm in front of them. Participants were instructed to perform the task as quickly and accurately as possible. The probability of appearance of each number was set to 50%. Each task consisted of 40 trials. The mean reaction times (RTs) and the accuracy (%Corr) of responses were collected.

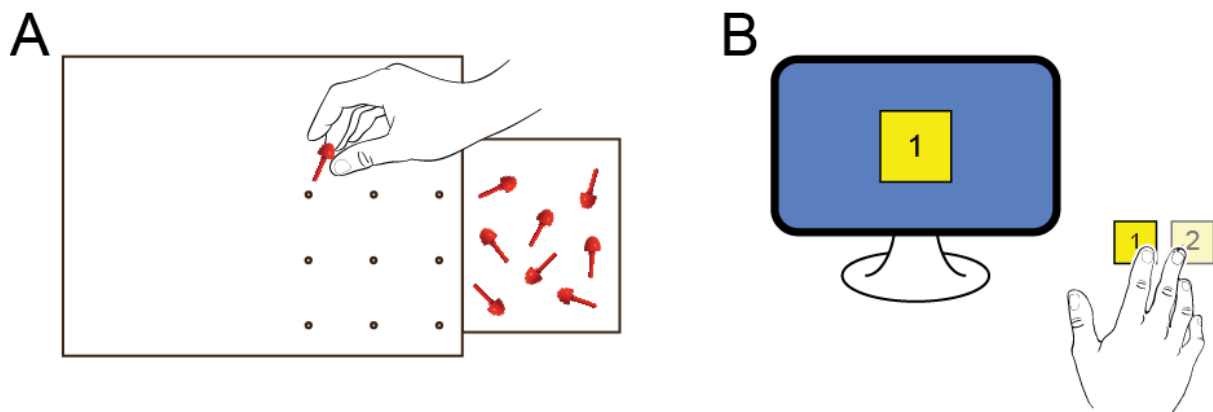


Fig.1.3 Schematic representation of the A) 9-HPT and B) cRT tasks.

Data analysis

Demographic data (age and gender) and scores on the Edinburgh Handedness Inventory were analysed between the three groups by means of one-way ANOVAs or Fisher exact tests. For the 9-HPT task, the

mean execution time across the 5 repetitions was computed for each session, and data were entered into a two-way mixed factor ANOVA with ccPAS ($\text{Exp}_{\text{PMV} \rightarrow \text{M1}}$, $\text{Ctrl}_{\text{M1} \rightarrow \text{PMV}}$, $\text{Ctrl}_{\text{sham}}$) as a between-subjects factor and Session (Baseline, Pre, Post-0, Post-30) as a within-subjects factor. For the cRT task, we computed the mean reaction times (RTs) and accuracy (%Corr) from each session. RTs associated with incorrect response or deviating more than 3 standard deviations from the mean RT in each task were excluded from analyses (< 5% of trials, comparably distributed across groups and sessions). RTs and %Corr were analysed through a ccPAS x Session ANOVA. The Greenhouse-Geisser correction was applied when appropriate. Post-hoc analyses were performed using the Newman-Keuls test to correct for multiple comparisons. Partial η^2 (η_p^2) was computed as a measure of effect size for significant main effects and interactions, whereas repeated measures Cohen's *d* indices were computed for significant post-hoc comparisons. By convention, η_p^2 effect sizes of ~ 0.01 , ~ 0.06 , and ~ 0.14 are considered small, medium, and large, respectively; Cohen's *d* effect sizes of ~ 0.2 , ~ 0.5 , and ~ 0.8 are considered small, medium, and large, respectively (Cohen, 1992).

All the ANOVAs were conducted using STATISTICA v12 and/or SPSS v23 with the significance level set at 0.05. These null hypothesis-testing analyses were complemented by their Bayesian implementations using JASP v 0.8.4 (JASP team 2017). With Bayesian hypothesis testing, we could directly evaluate the relative strength of evidence for the null and alternative hypotheses, providing quantification of the degree to which the data support either hypothesis (Dienes, 2011; Wagenmakers et al., 2017). We used default priors in JASP (*r* scale fixed effects = 0.5; *r* scale random effects = 1). Following the current standards, we report subscripts on Bayes Factors to refer to the models compared. Accordingly, the Bayes Factor for the alternative relative to the null hypothesis is denoted BF_{10} , while the Bayes Factor for the null relative to the alternative hypothesis is denoted BF_{01} .

1.3 Results

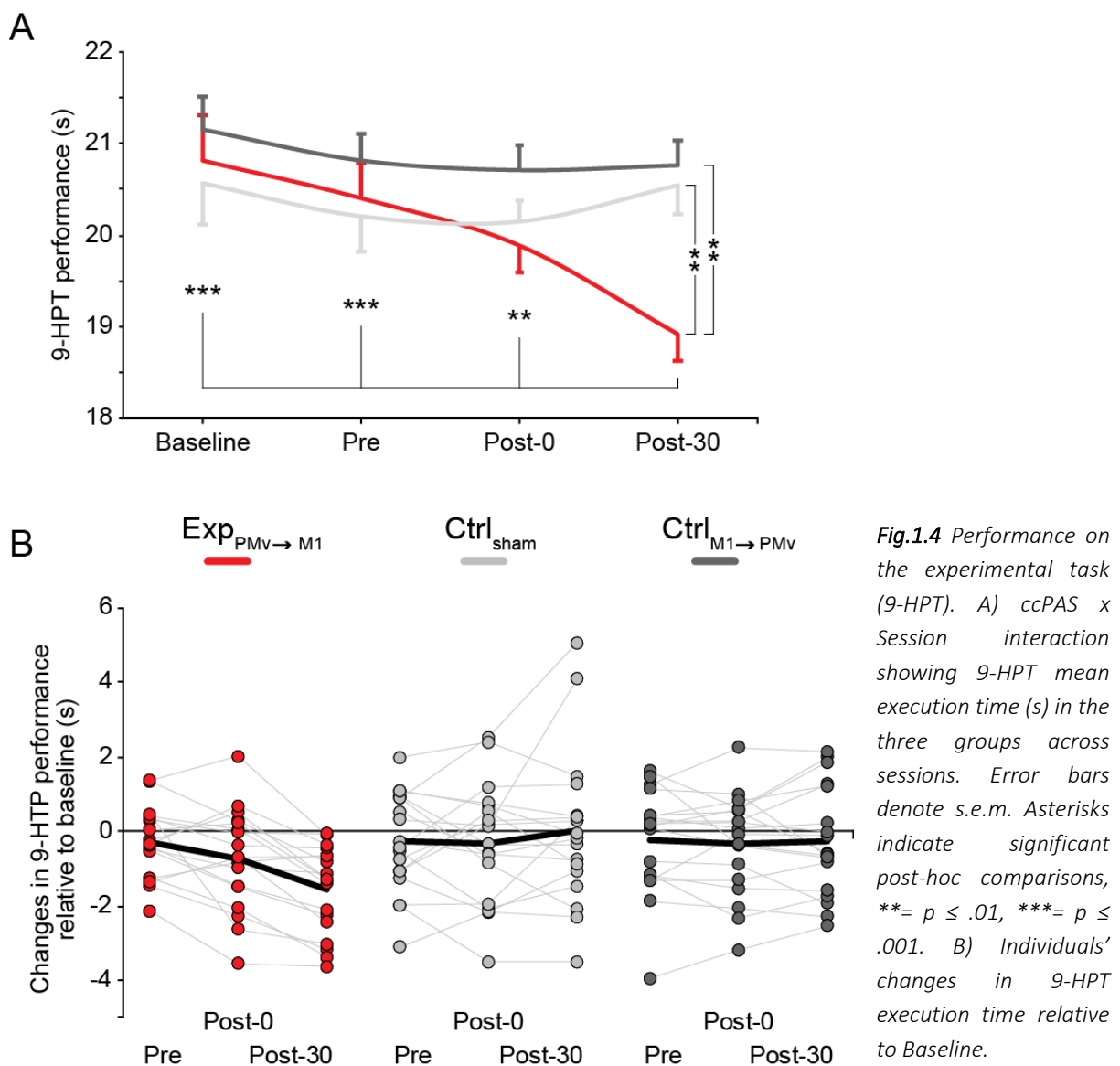
All participants tolerated the ccPAS protocol well and no adverse effects were noted or reported.

Preliminary comparisons

Table 1.1 shows that participants in the three ccPAS groups did not differ in age or gender. Moreover, they showed comparable 9-HPT and cRT performance at Baseline and similar left M1 excitability.

Experimental task (9-HPT)

The ccPAS x Session ANOVA conducted on the mean execution time showed no main effect of ccPAS ($F_{2,51} = 2.80$, $p = .07$; $\eta_p^2 = .10$), but a main effect of Session ($F_{2,3,117.6} = 5.12$, $p = .005$; $\eta_p^2 = .09$) that was qualified by a ccPAS x Session interaction ($F_{4,6,117.6} = 3.31$, $p = .009$; $\eta_p^2 = .11$), indicating that changes in 9-HPT performance over time depended on the ccPAS protocol being administered (Fig. 1.4).



Post-hoc analysis of the ccPAS interaction showed the following. The $\text{Exp}_{\text{PMV} \rightarrow \text{M1}}$ group showed a reduction in the mean time necessary to complete the 9-HPT after ccPAS (Fig.1.4). In this group, execution time in the Baseline (mean \pm S.D.: 20.8 s \pm 2.1) and Pre (20.4 s \pm 1.6) sessions were comparable ($p = .86$). At Post-0 (19.9 s \pm 1.2), execution time appeared lower than at Baseline and Pre, although the relevant post-hoc comparisons were not significant (all $p \geq .19$; trends for reductions were detected with uncorrected planned comparisons: Post-0 vs. Baseline: $p = .02$, *Cohen's d* = .59; Post-0 vs. Pre: $p = .06$, *Cohen's d* = .45). Importantly, at Post-30 (18.9 s \pm 1.3), mean execution time appeared strongly reduced relative to Baseline, Pre and Post-0 (all $p \leq .007$, all *Cohen's d* ≥ 1.14).

No consistent changes in mean execution time were found in the $\text{Ctrl}_{\text{M1} \rightarrow \text{PMV}}$ (all $p \geq .35$) or the $\text{Ctrl}_{\text{sham}}$ groups (all $p \geq .60$) across time points; moreover, no differences were found between these two groups across time points (all $p \geq .83$).

The $\text{Exp}_{\text{PMV} \rightarrow \text{M1}}$ group showed comparable performance to the $\text{Ctrl}_{\text{M1} \rightarrow \text{PMV}}$ and $\text{Ctrl}_{\text{sham}}$ groups in Baseline and Pre sessions (all $p \geq .86$). At Post-0, the execution time of the $\text{Exp}_{\text{PMV} \rightarrow \text{M1}}$ group (19.9 s \pm 1.3) started to appear shorter than the execution times of the $\text{Ctrl}_{\text{M1} \rightarrow \text{PMV}}$ (20.1 s \pm 0.9) and the $\text{Ctrl}_{\text{sham}}$ groups (20.7 s \pm 1.2), although the relevant post-hoc comparisons were not significant (all $p \geq 0.59$; uncorrected planned comparisons detected a difference relative to the $\text{Ctrl}_{\text{M1} \rightarrow \text{PMV}}$ group, $p = .03$, *Cohen's d* = .70). In contrast, at Post-30, the execution time of the $\text{Exp}_{\text{PMV} \rightarrow \text{M1}}$ group (18.9 s \pm 1.3) was significantly reduced relative to the $\text{Ctrl}_{\text{M1} \rightarrow \text{PMV}}$ (20.6 s \pm 1.2; $p = .005$; *Cohen's d* = 1.53) and the $\text{Ctrl}_{\text{sham}}$ groups (20.5 \pm 1.3 s; $p = .009$; *Cohen's d* = 1.27).

These findings were further corroborated by a Bayesian ANOVA with factors ccPAS and Session. The models including the main effect of Session ($\text{BF}_{10} = 7.4$) and both main effects ($\text{BF}_{10} = 8.1$) showed positive evidence favouring the alternative hypothesis, but the model that outperformed the null model the most was the model which also included the interaction ($\text{BF}_{10} = 75.2$). Data were ~ 8.8 times more likely under that model than under a null model including the main effects, thus providing positive

evidence indicating that 9-HTP performance changed over time depending on the type of the ccPAS protocol. Additionally, a series of Bayesian one-way ANOVAs with the factor Session provided very strong evidence supporting the alternative hypothesis for the $\text{Exp}_{\text{PMV} \rightarrow \text{M1}}$ group data ($\text{BF}_{10} = 7.6 \cdot 10^4$), whereas they provided positive evidence supporting the null hypothesis of no change across sessions in the $\text{Ctrl}_{\text{M1} \rightarrow \text{PMV}}$ ($\text{BF}_{01} = 6.2$) and the $\text{Ctrl}_{\text{sham}}$ ($\text{BF}_{01} = 7.5$) groups

Fig.1.4, panel B, shows the distribution of individual changes in 9-HPT performance (relative to Baseline). In the $\text{Exp}_{\text{PMV} \rightarrow \text{M1}}$ group, the effect of ccPAS was variable at Post-0 with 13 participants showing a reduction and 5 showing an increase in 9-HPT execution time (range -4.2 to +2.3 s). At Post-30, all participants showed a reduction in 9-HPT execution time, although, also the magnitude of the reduction was still variable across participants, ranging from -130 ms to -4.3 s (corresponding to reductions of ~1% to ~17% relative to Baseline performance). The other two groups showed a more distributed performance centred at zero and no net change at the group level.

Control task (cRT)

The ccPAS x Session ANOVA conducted on the mean RTs showed no main effect of ccPAS ($F_{2,48} = 1.82$, $p = .17$), but a main effect of Session ($F_{2,6,132,3} = 15.66$, $p < .001$; $\eta_p^2 = .23$), showing that participants, regardless of the group to which they belonged (i.e., also in the $\text{Ctrl}_{\text{sham}}$ group), became faster as task repetitions increased (Fig.1.5). Post-hoc analysis of the main effect of Session indicates that cRTs were comparable at Post-0 and Post-30 (398 ± 35 ms vs. 392 ± 30 ms; $p = .08$); however, cRTs in these sessions were lower than at Pre (405 ± 39 ms; $p \leq .03$) and cRTs in the Pre, Post-0 and Post-30 sessions were lower than at Baseline (414 ± 46 ms; $p \leq .01$). No significant ccPAS x Session interaction was revealed ($F_{5,2,132,3} = .71$, $p = .62$), suggesting similar trends across groups (Table1.2).

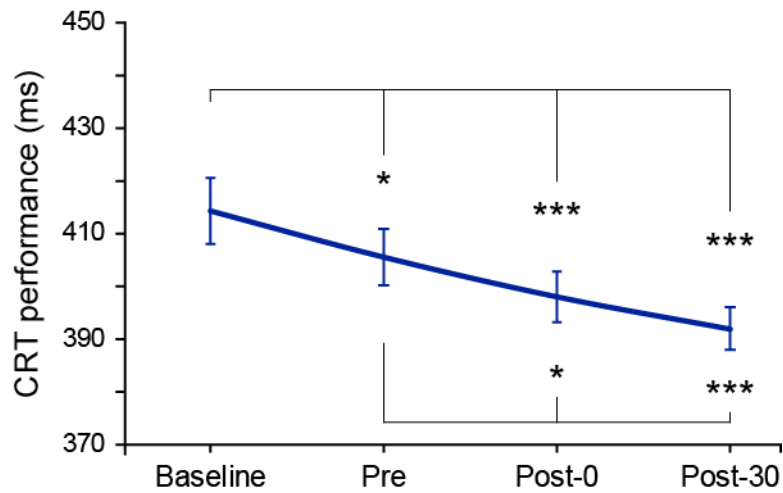


Fig.1.5 Performance on the control task (cRT). Main effect of Session. Error bars denote s.e.m. Asterisks indicate significant post-hoc comparisons (* = $p < .05$, *** = $p < .001$).

| | Baseline | Pre | Post-0 | Post-30 | |
|-------------------------|----------|----------|----------|----------|---------------------|
| Exp _{PMv} →M1 | 397 ± 29 | 393 ± 28 | 388 ± 25 | 382 ± 24 | RTs (ms) |
| Ctrl _{M1} →PMv | 425 ± 43 | 416 ± 40 | 402 ± 35 | 401 ± 28 | |
| Ctrl _{sham} | 421 ± 59 | 407 ± 46 | 402 ± 43 | 393 ± 36 | |
| Exp _{PMv} →M1 | 96 ± 3 | 96 ± 4 | 96 ± 3 | 96 ± 5 | Accuracy (%Corr) |
| Ctrl _{M1} →PMv | 96 ± 4 | 97 ± 4 | 96 ± 3 | 96 ± 3 | |
| Ctrl _{sham} | 95 ± 3 | 97 ± 4 | 95 ± 3 | 95 ± 3 | |

Table1.2 Performance on the control task. Mean cRTs ± S.D. (ms) and accuracy (% correct responses) ± S.D. in the three groups across sessions.

These findings were further corroborated by a ccPAS x Session Bayesian ANOVA. The analysis showed very strong evidence supporting all the alternative models (all $BF_{10} > 10^5$) – with the exception of the model including the main effect of ccPAS, which weak evidence in favour of the null hypothesis ($BF_{01} = 1.3$). The model that outperformed the null model the most was the model including the main effect of Session ($BF_{10} > 2.3 \times 10^6$) which was ~20 times more likely than the model with the interaction. Thus, the reduction of RTs over sessions likely reflected an effect of practice as data provided evidence against an influence of ccPAS.

The ccPAS x Session ANOVA conducted on accuracy data (%Corr; Table1.2) showed no main effects or interaction (all $F < 1.45$, all $p \geq .23$) and Bayes ANOVA showed positive evidence supporting the null hypothesis of no change in cRTs accuracy (all alternative models with $BF_{01} \geq 4.2$).

1.4 Discussion

Seminal studies in animals have provided in vitro and in vivo evidence that repetitive paired stimulation of interconnected neurons, evoking sequential pre- and postsynaptic activity in such neurons, can induce STDP and elicit a transient (Hebbian) enhancement of the synaptic efficacy of those connections (Hebb, 1949; Markram et al., 1997, 2011; Antonov et al., 2003; Jackson et al., 2006; Caporale and Dan, 2008). Previous TMS studies in humans have shown that similar STDP-like synaptic strengthening can be induced in the motor system between two interconnected motor areas through ccPAS administered at an optimal ISI (Koganemaru et al., 2009; Rizzo et al., 2009, 2011; Arai et al., 2011; Buch et al., 2011; Lu et al., 2012b; Veniero et al., 2013; Chao et al., 2015; Johnen et al., 2015). These studies showed that the ISI at which one targeted region (e.g., a premotor area) exerts a physiological effect on an anatomically connected second region (i.e., the M1) is also the ISI at which ccPAS can induce Hebbian-like cortico-cortical connection changes (e.g., ~8 ms for premotor-motor circuits; Davare et al., 2008; Buch et al., 2010, 2011). In particular, it has been demonstrated that the repeated pairing of PMv and M1 stimulation (i.e., PMv-to-M1 ccPAS) with an ISI of 8 ms, induces a transient enhancement of the effect of PMv stimulation on M1 excitability, thus providing direct evidence of increased PMv-to-M1 effective connectivity (Buch et al., 2011; Johnen et al., 2015).

Yet, these studies did not answer the critical question of whether PMv-to-M1 ccPAS is functionally relevant to behaviour. To address this outstanding question, we combined a ccPAS protocol with a visuomotor task tapping into PMv-M1 interactions (i.e., the 9-HPT) and a control visuomotor task (i.e., the cRT). Based on prior neuroimaging studies suggesting that improved motor performance following training is associated with increased premotor-motor connectivity (Hamzei et al., 2012; Philip and Frey, 2016) and with evidence showing a hierarchy in PMv-M1 interactions underpinning skilful goal-oriented

actions (Muir and Lemon, 1983; Murata et al., 1997; Fagg and Arbib, 1998; Fogassi et al., 2001; Lang and Schieber, 2004; Raos et al., 2006; Rizzolatti et al., 2014), here, we sought to examine whether exogenous manipulation of PMv-M1 connectivity through ccPAS can affect performance on the 9-HPT. Our study provides the first evidence that PMv-to-M1 ccPAS meeting the physiological constraint of PMv-to-M1 short-latency connectivity (i.e., an 8-ms ISI) improves performance on the 9-HPT. Such a task requires dexterous control of grasping and manipulation of small objects (Mathiowetz et al., 1985; Oxford Grice et al., 2003), and PMv-to-M1 interactions are thought to underpin this type of fine motor control (Grol et al., 2007; Davare et al., 2010). Critically, improvement on the 9-HPT was selectively found in the $\text{Exp}_{\text{PMv} \rightarrow \text{M1}}$ group that underwent a ccPAS protocol aimed at boosting synaptic efficiency in PMv-to-M1 connections. No similar changes in 9-HPT performance were detected when reversing the order of the repeated PMv-M1 stimulation (i.e. in the $\text{Ctrl}_{\text{M1} \rightarrow \text{PMv}}$ group that underwent active M1-to-PMv ccPAS) or when administering repeated PMv-to-M1 sham stimulation (in the $\text{Ctrl}_{\text{sham}}$ group), thus ruling out that mere repeated stimulation of PMv and M1, task practice or other nonspecific effects could explain the selective increase in 9-HPT performance. These findings indicate that hierarchical connections between frontal nodes of the network underlying motor control of object grasping and manipulation (Davare et al., 2008, 2009, 2010) are functionally malleable and sensitive to ccPAS.

Behavioural enhancement in the 9-HPT was weak and non-significant at Post-0 and increased at Post-30, i.e., 30 minutes after the end of the PMv-to-M1 ccPAS. This building up of the plastic effect within the first minutes after the end of the stimulation is consistent with the time course of Hebbian plasticity (Bi and Poo, 2001; Caporale and Dan, 2008) and, more generally, with LTP-like effects induced in the human motor cortex (Stefan et al., 2000; Huang et al., 2005; Ziemann et al., 2008). Notably, we found similar time course of behavioural gain in a previous study in which we administered ccPAS over extrastriate motion areas (V5) and primary visual cortex (V1; Romei et al., 2016a). In that study, we found that ccPAS aimed at increasing V5-to-V1 (re-entrant) connectivity improved perceptual visual sensitivity at 30 min, whereas nonsignificant effects were observed immediately after ccPAS (Romei et

al., 2016a). Based on physiological evidence (Buch et al., 2011), we would expect that behavioural improvements could be detected at even later time points – before returning toward baseline levels – although future studies are needed to directly test this prediction.

A growing literature shows that the effect of brain stimulation is highly variable across individuals (Ridding and Ziemann, 2010; Jones et al., 2016; Palmer et al., 2016; Valchev et al., 2016, 2017; Avenanti et al., 2017; Paracampo et al., 2018). Our data show that the behavioural effects of PMv-to-M1 ccPAS are highly variable at Post-0 and become more consistent at Post-30, with all 18 participants in the Exp_{PMv→M1} group showing a reduction in 9-HTP execution time. However, the magnitude of the effect was also variable at Post-30, ranging from a gain of ~1% to ~18% of baseline performance. Understanding the physiological and neural bases of this variability is an important avenue for research, and future ccPAS studies combining behavioural and neurophysiological, neuroimaging and/or genetic assessments (Cheeran et al., 2008, 2009; Ridding and Ziemann, 2010; Groppa et al., 2012; List et al., 2013) could play a role in delineating factors contributing to inter-individual variability.

Our study expands previous evidence by showing that plastic changes induced by ccPAS are functionally specific. Indeed, PMv-to-M1 ccPAS, but not the two control ccPAS protocols, improved motor functions tapping on PMv-to-M1 connectivity (i.e., 9-HTP performance), but no similarly selective effects were detected in the control visuomotor cRT task. In that task, we observed a linear increase in performance over time in all groups, irrespective of the ccPAS manipulation they underwent. Improvements were also detected in the Pre session relative to Baseline, clearly indicating a practice effect due to task repetition. Critically, these improvements were similar across the three groups – i.e., they were also found in the Ctrl_{sham} group – suggesting they were not due to active ccPAS but merely reflected a practice effect. While these data indicate functional specificity, future ccPAS studies might further assess specificity using experimental and control tasks with comparable learning rates over time.

Our study adds to previous physiological studies by showing that ccPAS over motor regions can improve motor performance. Our findings converge with two previous studies that suggested similar

behavioural effects following ccPAS over bilateral M1 (Koganemaru et al., 2009; Rizzo et al., 2009). These studies showed directional- and time-specific effects of ccPAS at a physiological level: for example, Koganemaru and colleagues administered right-to-left M1 ccPAS at an optimal ISI and induced physiological changes in left M1; no similar changes were observed following ccPAS protocols with suboptimal ISIs or when reversing the order of the ccPAS pulses (i.e., after left-to-right M1). Interestingly, in a separate behavioural experiment, better right-hand motor performance was observed after right-to-left M1 ccPAS, pointing to a behavioural counterpart of the physiological plastic changes. However, no control ccPAS protocol (e.g., sham or left-to-right) was used to examine behavioural effects of ccPAS and, thus, it remained unclear whether changes in motor performance in that experiment were specifically due to Hebbian changes or to nonspecific effects (see Rizzo et al., 2009). Our study expands these previous findings by showing that ccPAS over motor regions can induce directionally specific effects not only at a physiological level, but also at a behavioural level. Because we observed improved 9-HPT performance following PMv-to-M1 ccPAS ($Exp_{PMv \rightarrow M1}$ group), but not following M1-to-PMv ($Ctrl_{M1 \rightarrow PMv}$) or sham ccPAS ($Ctrl_{sham}$), our study allows us to rule out the possibility that changes in 9-HPT performance were merely due to repeated stimulation of PMv and M1, to practice effects or to other nonspecific effects. However, it is worth noting that a limitation of our study is that we do not have an electrophysiological evidence to support our finding. Future studies should assess behavioural and electrophysiological output resulting from ccPAS administration. Rather, building on previous ccPAS evidence suggestive of STDP in PMv-to-M1 connections (Buch et al., 2011; Johnen et al., 2015), our study allows us to conclude that ccPAS aimed at enhancing the synaptic efficacy of PMv-to-M1 connections has a clear and specific impact on behaviour.

We focused on a motor task tapping into the ability to grasp and manipulate objects – i.e, goal-directed actions underpinned by the recruitment of PMv and M1 (Binkofski et al., 1999; Ehrsson et al., 2000; Kuhtz-Buschbeck et al., 2001; Davare, 2006; Horn et al., 2016). Yet, because PMv-to-M1 connections are modulated during object-oriented grasping (e.g. Davare et al., 2008), but also during response inhibition or action reprogramming (e.g., Buch et al., 2010; Neubert et al., 2010; Picazio et al., 2014;

Bestmann and Duque, 2016), future studies might systematically evaluate the impact of PMv-to-M1 ccPAS on different domains of motor control.

We did not assess the impact of ccPAS at a neural level and this represents a limitation of our study. The effects of brain stimulation are known to spread along interconnected brain areas (Siebner et al., 2009a, 2009b; Dayan et al., 2013a; Bortoletto et al., 2015b; Valchev et al., 2015). Although the behavioural effects of our PMv-to-M1 ccPAS protocol were directionally specific, it is likely that they were not limited to the PMv-to-M1 hierarchical connections and may have extended to other components of the dorsolateral stream (e.g. as in Johnen et al., 2015) and/or nearby ventral and dorsal fronto-parietal areas involved in attention and higher-levels aspects of motor control (Vossel et al., 2014; Borra et al., 2017; Gerbella et al., 2017; Ptak et al., 2017). Understanding how different components of these networks reconfigure following PMv-to-M1 ccPAS is an important avenue for future work.

In conclusion, our study demonstrates that ccPAS aimed at strengthening the synaptic efficacy of PMv-to-M1 connections selectively enhances motor functions tapping into PMv-M1 networks. Plastic enhancement critically depended on the repeated pairing of pre-and post-synaptic nodes of the PMv-to-M1 pathway – meeting the physiological constraint of the premotor-motor hierarchy – and showed a time course consistent with Hebbian-like effects. Our findings provide the first causal evidence that PMv-to-M1 connections are behaviourally malleable and sensitive to exogenous manipulations of cortico-cortical connectivity.

Our study provides proof-of-principle evidence that ccPAS can be used to improve motor functions in healthy humans. These findings have important theoretical and methodological implications, as they suggest that ccPAS might be a useful tool for targeting specific cortico-cortical pathways and they demonstrate a causal effect of directional connectivity on behaviour (Romei et al., 2016a, 2016b). Moreover, these findings add to the growing literature showing the potential utility of non-invasive brain stimulation for improving cortical functions in humans (Fregni et al., 2005; Vallar and Bolognini,

2011; Krause and Cohen Kadosh, 2014; Romei et al., 2016a; Avenanti et al., 2017). By showing that increasing the synaptic efficacy of cortico-cortical pathways can lead to behavioural gains, our study suggests potential applications to neuroenhancement (e.g., in healthy people who need to improve their skills for professional reasons, like elite athletes or soldiers) and clinical uses (e.g., in conditions where recovery of a function depends on establishing new activity patterns across cortico-cortical pathways, or re-establishing old ones). In particular, our findings may have implications for designing novel therapeutic strategies based on associative brain stimulation of cortico-cortical pathways for the recovery of abilities that have been lost due to brain injury or neurodegenerative disease. Therefore, future studies should carefully assess the clinical and applied potentialities of ccPAS.

CHAPTER II

Empowering re-entrant projections from V5 to V1 boosts sensitivity to motion¹

2.1 Introduction

Repetitive paired stimulation, evoking sequential pre- and post- synaptic activity in interconnected neurons, induces Hebbian associative plasticity, prompting those synaptic connections to transiently strengthen (Hebb, 1949; Markram et al., 1997; Jackson et al., 2006; Caporale and Dan, 2008). Seminal research in animals have also provided in vitro and in vivo evidence of Hebbian plasticity in the visual system (Zhang et al., 1998; Caporale and Dan, 2008; Frégnac et al., 2010). Previous transcranial magnetic stimulation (TMS) studies have shown that similar synaptic strengthening can be induced in the human motor system over two interconnected motor areas through a novel cortico-cortical paired associative stimulation protocol (ccPAS), administered at an optimal timing (Koganemaru et al., 2009; Rizzo et al., 2009; Arai et al., 2011; Buch et al., 2011; Koch et al., 2013; Veniero et al., 2013; Johnen et al., 2015). These studies have shown that the timing (expressed as the inter-stimulus interval; ISI) at which one targeted region (e.g., the premotor cortex) exerts a physiological effect on an anatomically connected second region (i.e., the motor cortex) is also the ISI at which ccPAS can induce Hebbian-like cortico-cortical connection changes (e.g., 6–8 ms for premotor-motor circuits; compare Arai et al., 2011; Buch et al., 2011 with Buch et al., 2010; Arai et al., 2012). The specific ISI used is therefore critical to create sequential pre- and post-synaptic activity in the targeted pathway and this is essential for the occurrence of spike timing-dependent plasticity (STDP; Markram et al., 1997; Jackson et al., 2006; Caporale and Dan, 2008), a form of synaptic plasticity that meets the Hebbian principle and predicting that synapses are potentiated if the pre-synaptic neuron fires repeatedly before the post-synaptic neuron (Hebb, 1949; Caporale and Dan, 2008). ccPAS studies have supported the notion of STDP by showing a causal and directional change of influence of the first over the second targeted region (Buch

¹ Published paper: Romei V, Chiappini E, Hibbard PB, Avenanti A (2016a) Empowering Reentrant Projections from V5 to V1 Boosts Sensitivity to Motion. *Curr Biol* 26:2155–2160

et al., 2011; Johnen et al., 2015). However, little is known about the impact on behaviour of such an experimental increase in synaptic efficiency, and no study to date has tested ccPAS protocols over the visual system.

Our study goes beyond previous evidence by providing the first demonstration that directly fostering Hebbian plasticity in a cortical visual circuit has an impact on behaviour. We demonstrated for the first time that ccPAS over two interconnected visual regions with an ISI consistent with evoking pre- and post-synaptic activity necessary for STDP (Pascual-Leone and Walsh, 2001; Silvanto et al., 2005a, 2005b; Koivisto et al., 2010; Silvanto, 2015) affects visual perception.

Animal studies have shown that suppression of MT/V5 in the visual system weakens V1 responses to moving bar stimuli, in particular when stimuli have low salience (Hupé et al., 1998), which suggests a top-down amplification mechanism in the processing of visual motion. This mechanism is also thought to promote visual awareness of motion (Lamme et al., 1998; Dehaene et al., 2006; Lamme, 2006), and TMS studies in humans have provided causal evidence of the role of MT/V5-V1 backward connectivity on motion visual awareness as probed by TMS-induced visual phosphenes (Silvanto et al., 2005a, 2005b). However, evidence indicates that backward connectivity is important also for efficient processing of actual moving stimuli (Silvanto et al., 2005b; Koivisto et al., 2010; Silvanto, 2015; Vetter et al., 2015), even when motion stimuli are not consciously perceived (Koivisto et al., 2010). This suggests that the top-down gain control function of backward connections (Hupé et al., 1998; Silvanto, 2015) is not limited to subserving awareness (Pascual-Leone and Walsh, 2001; Silvanto et al., 2005a) and reflects a general principle of visual cortical information processing (Gilbert and Li, 2013; Wyatte et al., 2014; Silvanto, 2015).

We showed that stimulation aimed at increasing synaptic efficacy in back projections from MT/V5 to V1 transiently boosted visual motion sensitivity. Such perceptual enhancement was evident for at least 60 min, and its time course resembled that of Hebbian-like physiological effects observed in animal studies as well as in studies using ccPAS over the human motor system (Markram et al., 1997; Jackson

et al., 2006; Caporale and Dan, 2008; Koganemaru et al., 2009; Rizzo et al., 2009; Arai et al., 2011; Buch et al., 2011; Koch et al., 2013; Veniero et al., 2013; Johnen et al., 2015).

2.2 Methods

Participants

Thirty-two healthy volunteers (11 male, 21 female; mean age \pm SD: 22.31 \pm 4.22 years) were recruited for the study. They were right-handed by self-report and naive as to the purpose of the study. All participants gave written informed consent before taking part in the study, which had been approved by the University of Essex Research Ethics Committee.

General design

Participants were randomly assigned to four different groups according to the cortico-cortical Paired Associative Stimulation (ccPAS) protocol they would undergo. To test the effect of ccPAS on motion perception, participants performed a motion coherence discrimination task (see Stimuli and task). After having familiarized themselves with the task and achieving a stable performance on it in a training session, participants performed their baseline session (BSL) before undergoing their assigned ccPAS protocol. Participants performed the task again, immediately (T0), 30 (T30), 60 (T60) and 90 (T90) minutes after the ccPAS (See Fig.2.1, panel A).

Stimuli and task

Stimuli were generated and presented using MATLAB (MathWorks, Natick, USA) and the Psychophysics Toolbox extensions (Brainard, 1997; Pelli, 1997; Kleiner et al., 2007). They were presented on an 18-inch CRT monitor (ViewSonic G90fB, ViewSonic Corporation, Walnut, CA) with a resolution of 1280 x 1024 pixels and a refresh rate of 85 Hz. A chin rest was used to keep the viewing distance at 57 cm. Every stimulus consisted of 400 white dots (6 pixels each) moving within a square region subtending 12.8 x 12.8 degrees of visual angle, which could be on the left or on the right side of a white fixation cross (20 x 20 pixels) located in the centre of the screen on a grey background. The inner border of the

square region was 2.2° to the side of the fixation spot. Half of the trials were randomly presented in the left and half in the right visual hemifield (see Fig.2.1, panel B).

In each trial, dots moved with a different level of motion coherence (0, 4, 8, 12, 16, 20, 25, 35, 50 or 80%) leftward or rightward. Motion coherence was expressed as the percentage of dots that were moving in the signal direction. For example, in the 0% coherence trials all the dots moved randomly, in the 80% coherence trials, 320 dots (80%) moved coherently towards leftwards or rightwards, while the remaining 80 dots (20%) were each given a randomly selected direction of motion (see Fig.2.1, panel C). Each dot moved at a speed of $4.5^\circ/\text{sec}$.

The task was a two-alternative forced choice. After each trial participants were asked to make unspeeded responses by pressing the left arrow or the right arrow key to indicate the perceived global direction of motion. Each trial began with a fixation cross appearing in the middle of the screen for 500 ms, followed by the stimulus, the duration of which was 400 ms (see Fig.2.1, panel B). A task block consisted of 160 trials: 4 trials x 2 directions (left/right-ward coherent direction of motion) x 2 hemifields (left/right hemifield presentation) x 10 coherence levels. Each session consisted of 4 blocks, for a total of 640 trials and it lasted approximately 13 minutes.

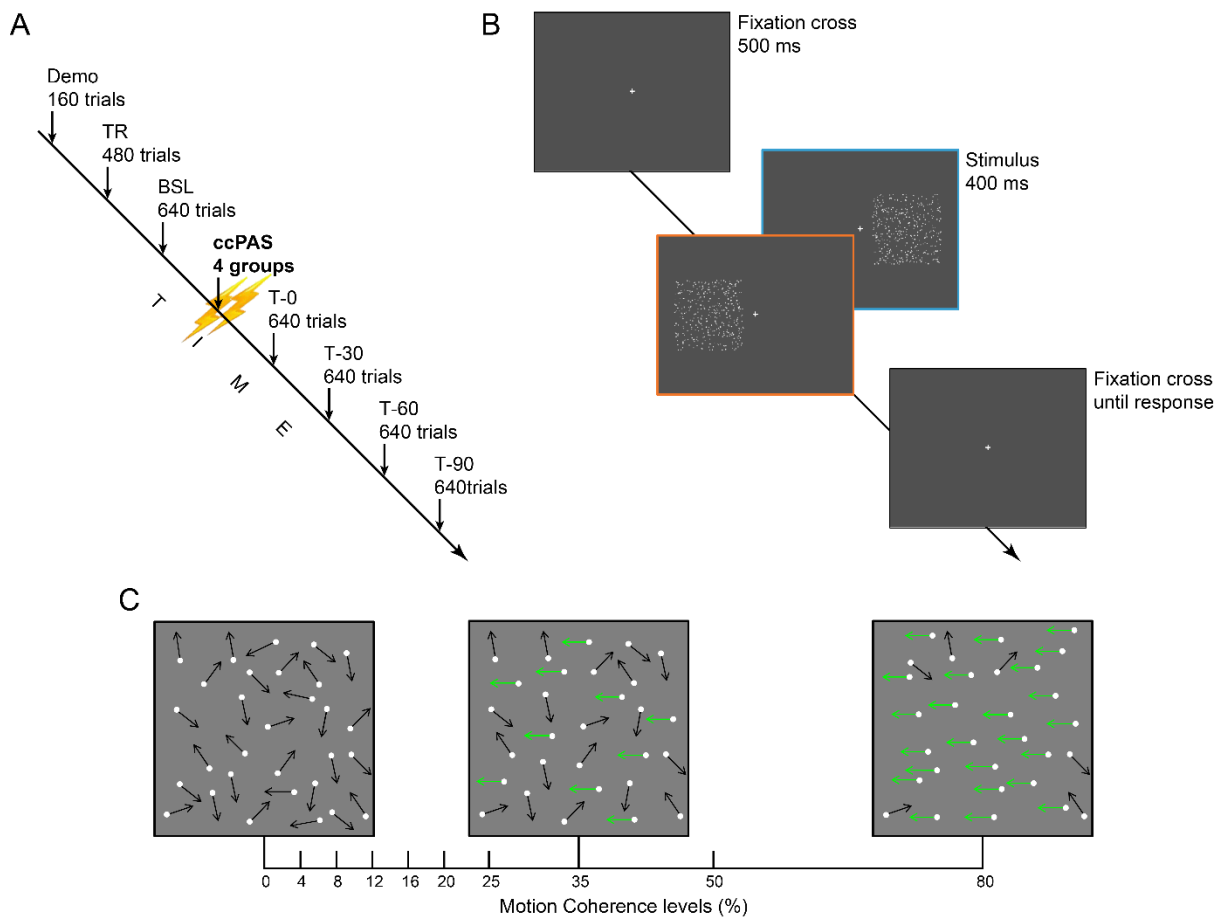


Fig.2.1 Experimental Design and Procedures. A) Timeline of the experiment, composed by a demo block (Demo) to familiarize the participant with the basic mechanisms of the task, a training session (TR) of three blocks to reach a stable performance level before the actual experiment, a baseline session (BSL), the ccPAS phase for plasticity induction, and task again, immediately (T0), 30 (T30), 60 (T60), and 90 (T90) minutes following the end of ccPAS protocol administration. One session consisted of four blocks of 160 trials each. B) Task sequence consisted of a white central fixation cross (500 ms) followed by a motion coherence stimulus (400 ms) that could appear either on the left or on the right side of the cross (a single frame of the motion coherence stimulus used in the study is depicted), and fixation cross until response (left or right arrow to indicate the leftward or rightward coherent motion perception, respectively). Motion coherence varied across trials. C) Schematic representation of the stimuli used to test the coherence threshold. 400 moving dots, a proportion of which moves in a coherent direction (except for 0% motion coherence condition), while the remainder move in random directions. Coherence of the motion ranged from 0% to 80%, distributed in ten levels (represented on the line below). Left panel represents a schematic trial with 0% coherence as all the dots are moving randomly. Central panel represents a trial with 35% coherence in the leftward direction. Right panel represents a trial with 80% coherence in the leftward direction. The arrows illustrate the motion direction of each dot. Green arrows represent the directions of signal dots; black arrows represent the directions of noise dots.

ccPAS protocol

ccPAS was delivered by means of a Magstim BiStim2 machine (Magstim Company, UK) via two 50 mm figure-of-eight coils. 90 pairs of stimuli were continuously delivered at a rate of 0.1 Hz for ~15 min (Rizzo

et al., 2009; Buch et al., 2011; Veniero et al., 2013), each pair of stimuli consisted of two monophasic transcranial magnetic pulses. The pulses were triggered remotely using a computer that controlled both stimulators. Left MT/V5 and central V1 were stimulated using established procedures (Beckers and Hömberg, 1992; Hotson et al., 1994; Walsh et al., 1998; Pascual-Leone and Walsh, 2001; Silvanto et al., 2005a; Laycock et al., 2007; Koivisto et al., 2010). To target left MT/V5, the coil was centred 3 cm dorsal and 5 cm lateral to the inion, corresponding to the average functionally localized scalp position where perception of moving phosphenes and disruption of motion perception can be elicited by TMS. The coil was held tangentially to the scalp with the handle pointing upwards and laterally at 45° angle to the sagittal plane. To target V1, the coil was centred 2 cm dorsal to the inion, corresponding to the scalp position where phosphenes in the centre of the visual field are typically elicited. From this position it is expected that V1 of both hemispheres is recruited during stimulation. The handle was held tangentially to the scalp and pointed downwards at an angle of 120° clockwise. For both areas intensity of TMS was set at 70% of the maximum stimulator output.

The ccPAS protocol was manipulated in four different groups of participants:

1. Experimental group (Exp_{V5-V1}). The first pulse was given to MT/V5 followed by another pulse, delivered to V1 with an ISI of 20 ms. This ISI was selected in accordance with the average timing of MT/V5-V1 interactions reported by Pascual-Leone & Walsh (2001) and Silvanto and colleagues (2005a) and corresponds to the optimal timing at which MT/V5 exerts a physiological effect on V1. Thus, this ISI was critical to repeatedly activate presynaptic and postsynaptic neurons in re-entrant MT/V5-V1 connections in a way that is consistent with STDP mechanisms, i.e. a form of synaptic plasticity meeting the Hebbian principle and predicting that synapses are potentiated if the presynaptic neuron fires repeatedly before the postsynaptic neuron (Markram et al., 1997; Jackson et al., 2006). Thus, ccPAS in the Exp_{V5-V1} group was aimed at strengthening re-entrant connections from MT/V5 to V1.

2. Control group 1 (Ctrl_{V1-V5}, control for direction). In this control group we switched the direction of the associative pulses: the first pulse was given to V1 and the second pulse to MT/V5 at the same ISI as the experimental condition (20 ms). The Ctrl_{V1-V5} group controlled for direction dependent effects, i.e. we verify that any effect as found in the Exp_{V5-V1} group is the result of enforced feedback connections (MT/V5 to V1) and should not be found when feedforward connections (V1 to MT/V5) are instead stimulated.
3. Control group 2 (Ctrl_{0ms}, control for timing). In this group both pulses were delivered simultaneously (ISI = 0 ms). According to the Hebbian principle (Markram et al., 1997; Jackson et al., 2006; Caporale and Dan, 2008; Koganemaru et al., 2009), a synapse will increase its efficiency if it persistently takes part in firing the postsynaptic target neuron. However, if two neurons fire at the same time, then one cannot have caused, or taken part in causing the other to fire. Thus, although neural interactions may occur during simultaneous TMS pairing (Prabhu et al., 2009), no net STDP is expected. This ccPAS condition therefore controlled for timing dependent effects, i.e. we verify that any effect as found in the Exp_{V5-V1} group is timing dependent and not provoked merely by a consistent stimulation pairing of the targeted areas.
4. Control group 3 (Ctrl_{sham}, control for unspecific effects): stimulation in this group was identical to that of the Exp_{V5-V1} group except for the fact that the TMS coils were tilted at 90 degrees so that no TMS pulses were effectively applied throughout the ccPAS session.

Data analysis

For each experimental condition and time, we determined the motion sensitivity threshold value on the data of the motion coherence discrimination task. By presenting several different levels of coherent motion, we could observe a sigmoid distribution of correctly perceived coherent motion as a function of the degree of coherence. We fitted the data with the logistic function:

$$y = \frac{a}{1 + e^{-\frac{x-b}{c}}}$$

and defined the motion sensitivity threshold as the coherence level at which the direction was correctly perceived 75% of the times. We used motion sensitivity threshold as our dependent variable to assess the impact of ccPAS in the 4 groups.

To assess the effect of ccPAS on motion sensitivity threshold we performed a 5 x 2 x 4 overall mixed ANOVA with STIMULATION (Exp_{V5-V1}, Ctrl_{V1-V5}, Ctrl_{0ms}, Ctrl_{sham}) as a between subject factor, and HEMIFIELD (LEFT, RIGHT) and TIME (BSL, T0, T30, T60, T90) as within subject factors. In order to readily compare performance across the 4 groups (Exp_{V5-V1}, Ctrl_{V1-V5}, Ctrl_{0ms}, Ctrl_{sham}) as a function of time (T0, T30, T60 and T90), variations in motion sensitivity threshold were baseline corrected such that the values obtained in the performance at each time after the stimulation were subtracted from the value obtained in the performance at baseline. In this way, any negative value reflects enhancement in performance, while positive values reflect reduction in performance, compared to baseline values. To validate our comparison approach, we evaluated whether baseline differed across groups. A mixed ANOVA with STIMULATION (Exp_{V5-V1}, Ctrl_{V1-V5}, Ctrl_{0ms}, Ctrl_{sham}) as a between subject factor and HEMIFIELD (LEFT, RIGHT) as within subject factor did not reveal any significant difference among the baselines of the 4 groups ($F_{3,28}=1.05$, $p=0.39$). T-tests (one-tailed, as directionality of the effects was predictable based on our theoretical assumptions) were Bonferroni corrected for multiple comparisons as a function of TIME (4 comparisons) and STIMULATION (3 comparisons).

2.3 Results

A 5 x 2 x 4 mixed-factors ANOVA showed a main effect of time ($F_{4,112} = 2.51$, $p = 0.046$), suggesting that motion sensitivity threshold changed as a function of testing time. Crucially, there was an interaction between time and experimental manipulation ($F_{12,112} = 2.51$, $p = 0.006$), suggesting that any modification of motion sensitivity threshold depended on the specific ccPAS condition. No other main effects or interactions were significant (all $p > 0.1$; see Supplemental analyses on HEMIFIELD non-significant effects). As clearly reported in figure 2.2, only the experimental group (Exp_{V5-V1}) showed motion sensitivity enhancements, as evidenced by significant threshold shifts toward lower levels of

motion coherence between 30 and 60 min following the ccPAS phase, before returning toward baseline values (see also Fig.2.3). Bonferroni-corrected t tests indicate that participants assigned to Exp_{V5-V1} are more sensitive to visual motion (lower motion sensitivity threshold) at T30 ($p = 0.003$) and T60 ($p = 0.048$) relative to baseline. Moreover, Bonferroni-corrected t tests comparing Exp_{V5-V1} versus all the other groups confirmed the greater sensitivity of the Exp_{V5-V1} group at T30 (Exp_{V5-V1} versus Ctrl_{V1-V5}: $p = 0.008$; Exp_{V5-V1} versus Ctrl_{0ms}: $p = 0.034$; Exp_{V5-V1} versus Ctrl_{sham}: $p = 0.003$) and T60 (Exp_{V5-V1} versus Ctrl_{V1-V5}: $p = 0.006$; Exp_{V5-V1} versus Ctrl_{0ms}: $p = 0.046$; Exp_{V5-V1} versus Ctrl_{sham}: $p = 0.025$). Perceptual enhancement in the Exp_{V5-V1} group was similar across hemifields as suggested by the non-significance of the triple interaction (see also Fig.2.4).

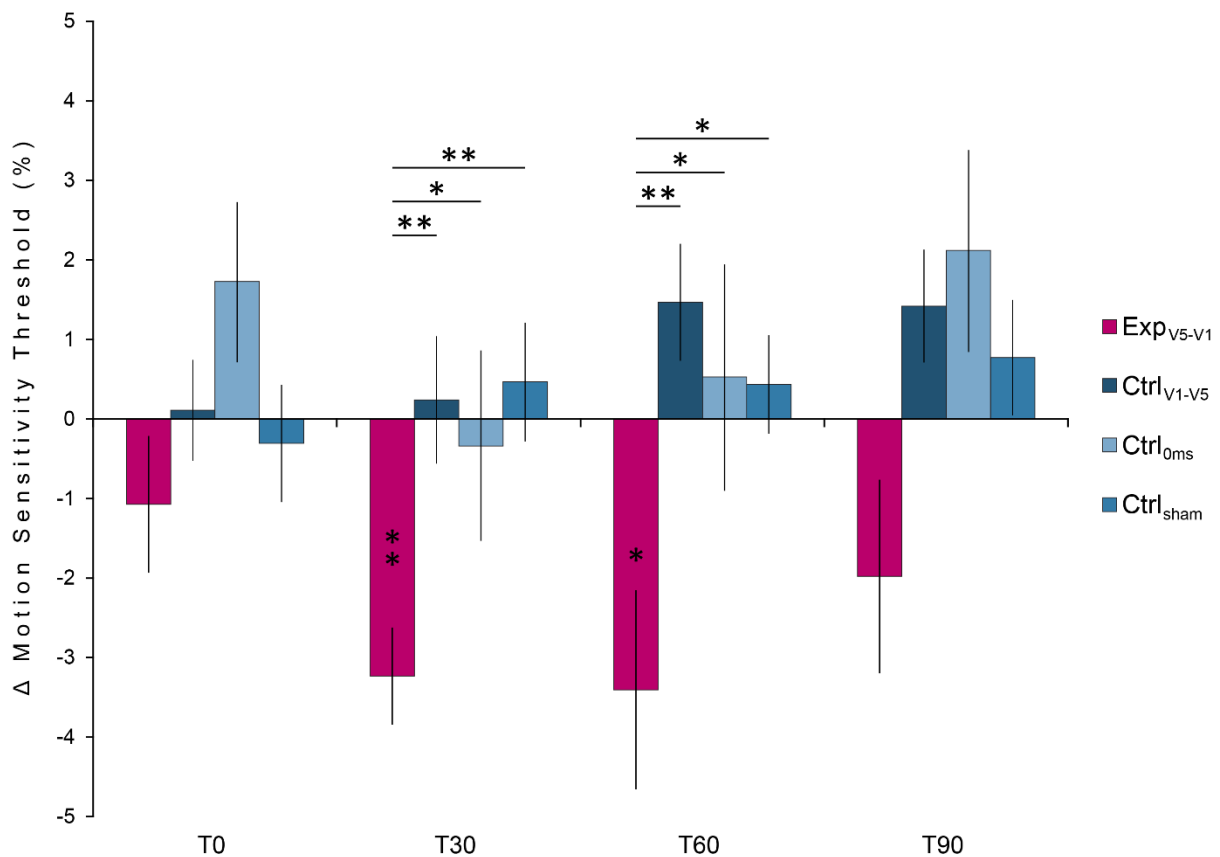


Fig.2.2 Changes in visual motion sensitivity induced by ccPAS. Only participants assigned to the experimental group (Exp_{V5-V1}; ccPAS: direction MT/V5-V1, ISI 20 ms) showed a reduction of motion sensitivity threshold (baseline corrected) at 30 and 60 min after ccPAS, indicating enhanced visual motion sensitivity. Participants in control group 1 (Ctrl_{V1-V5}; ccPAS: direction V1-to-MT/V5, ISI 20 ms), control group 2 (Ctrl_{0ms}; ccPAS: simultaneous MT/V5-V1 stimulation, ISI 0 ms), and control group 3 (Ctrl_{sham}; MT/V5-to-V1 sham stimulation, ISI 20 ms) showed no significant changes in motion sensitivity threshold over time. Error bars denote ± 1 SEM. Asterisks indicate significant differences ($*p < 0.05$, $**p < 0.01$).

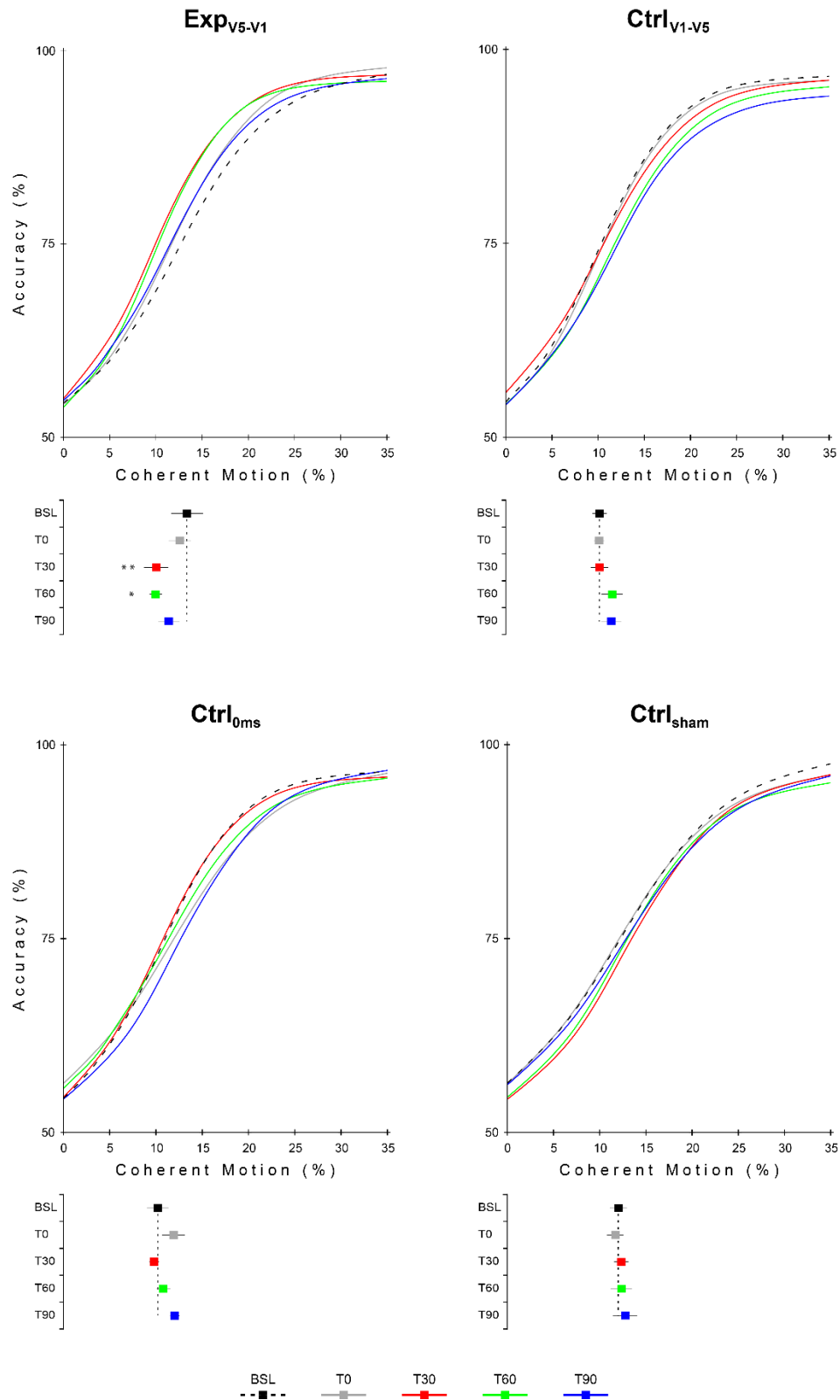


Fig.2.3 Curve Fitting and Groups' Performance Sigmoid curve fits (top panels) and participants' average performance (bottom panels) are plotted for each group as a function of time before and after the ccPAS protocol has been applied. Below each graph, the averaged motion sensitivity threshold (and s.e.) across participants, in each of the four groups, are plotted for each session. Only in the EXP_{V5-V1} group is there a significant TMS-induced decrease in the motion sensitivity threshold, at T30 and T60 relative to BSL, as indicated by the asterisks (* $p < 0.05$, ** $p < 0.01$). This reduction shows an enhancement in sensitivity to the global motion task.

None of the control groups showed a similar increase in performance after ccPAS (Ctrl_{V1-V5}: all $p > 0.19$; Ctrl_{0ms}: all $p > 0.12$; Ctrl_{sham}: $p > 0.53$), suggesting that perceptual boosting was specifically determined by the ccPAS manipulation when stimulation directionality (from MT/V5 to V1) and timing (20 ms) met the physiological constraints of re-entrant connectivity (Pascual-Leone and Walsh, 2001; Silvanto et al., 2005a). This pattern of results was substantially replicated when using non-parametric tests (see Supplemental analyses).

2.4 Discussion

Our findings provide causal evidence that short-term synaptic strengthening of re-entrant MT/V5-V1 connections can enhance motion perception. This supports the view that re-entrant connectivity from higher-order to early visual areas subserves integrative visual functions (Lamme et al., 1998; Pascual-Leone and Walsh, 2001; Silvanto et al., 2005a, 2005b; Koivisto et al., 2010; Gilbert and Li, 2013; Wyatte et al., 2014; Silvanto, 2015; Vetter et al., 2015). Remarkably, our study is the first to directly show that synchronous stimulation of MT/V5 and V1 aimed at strengthening backward connections improves the perceptual processing of coherent motion. Notably, we specifically tested for a novel account of the functionality of re-entrant projections, namely the plasticity of the MT/V5-V1 circuit, by manipulating its pre- and post-synaptic nodes according to the Hebbian rule as implemented through this novel ccPAS protocol. The most immediate consequence of this novel intervention approach is that participants in the experimental group (Exp_{V5-V1}) experienced an enhanced perception of motion coherence. In contrast, none of the participants in the control groups (including Ctrl_{V1-V5} controlling for directionality of the stimulation) improved their perception at any testing time following the TMS application, when compared to their pre-TMS BSL measure.

One may wonder why no change in performance was detected following ccPAS in the Ctrl_{V1-V5} group. In principle, reversing the order of the stimulation (i.e., first TMS pulse over V1, second over MT/V5) would strengthen feedforward rather than backward connectivity in the network. Our findings suggest that

backward more than feedforward connections are amenable to plastic boosting of visual perception, which is in keeping with their top-down modulatory role (Hupé et al., 1998; Lamme et al., 1998; Pascual-Leone and Walsh, 2001; Silvanto et al., 2005a, 2005b; Koivisto et al., 2010; Gilbert and Li, 2013; Wyatte et al., 2014; Silvanto, 2015; Vetter et al., 2015). However, it should be noted that the ISI of the ccPAS was selected based on the timing of causal interactions that MT/V5 exerts over V1 (Pascual-Leone and Walsh, 2001; Silvanto et al., 2005a), and, thus, other ISIs may be effective for modulating perceptual function via changes in feedforward connectivity. Visual tasks strongly relying on bottom-up processes may be particularly sensitive to manipulations of feedforward connectivity (Girelli and Luck, 1997).

It might be worth noting that during Exp_{V5-V1} ccPAS, the stimulation of MT/V5 may induce not only orthodromic activation of backward MT/V5-to-V1 connections, but also antidromic activation of feedforward V1-to-MT/V5 connections. Thus, one may consider the possibility that during Exp_{V5-V1} ccPAS, stimulation of V1 could reactivate the same feedforward connections, and this repeated pairing may also contribute to the observed plastic effect. Indeed, studies have shown that repeated TMS pairing over the same region can induce STDP (Thickbroom et al., 2006). However, such induction is selective for very short ISIs (~1.5 ms; Kidgell et al., 2016), making it unlikely that it played a major role in the plastic effects we detected. While our study supports the hypothesis of Hebbian strengthening of MT/V5-V1 backward connections, future studies are needed to elucidate the possible contribution of additional mechanisms underlying ccPAS aftereffects.

In sum, our study suggests that ccPAS can enhance visual perception of motion in participants where the MT/V5-V1 circuit is critically manipulated by repeatedly pairing pre- and post-synaptic nodes in the direction and timing that are optimal for strengthening these re-entrant connections. This provides a novel mechanistic insight into the circuit and computational basis of visual perception by providing causal evidence of its malleability and demonstrating that this strictly depends on the timing and directionality of the repeated ccPAS manipulation.

This new demonstration of the malleability of the network governing visual processing paves the ground for future exploration of brain mechanisms responsible for integrative visual functions. While our offline ccPAS procedure addressed the basic features of associative plasticity in the cortical network for motion perception, future investigations might use a state-dependent approach (Silvanto and Muggleton, 2008a; Silvanto et al., 2008; Jacquet and Avenanti, 2015) and pair ccPAS with specific motion directions in order to boost direction-specific perceptual tuning. Our study may also have implications for understanding more general mechanisms of perceptual learning (Levi et al., 2014) and fine-tuning interventional approaches aimed at enhancing perception, for example by combining training and neuromodulation strategies. However, physiological evidence indicates that ccPAS aimed at strengthening a given pathway may also induce weakening of non-stimulated pathways (Johnen et al., 2015). Thus, future studies are needed to understand the impact of such neural changes on behaviour, as, in principle, the ccPAS protocol may be useful but also detrimental depending on the stimulated pathway and the task at hand.

We have probed the effects of associative plasticity on the motion perception re-entrant network. There has been no attempt in the previous literature to explore this aspect of motion perception. Currently, it is not obvious whether and how our ability to make sense of motion signals depends on the capacity of the circuit to adapt to the environment. Here, we specifically shed light on the mechanisms by which re-entrant connections become functionally adaptive. This has important implications for the way we perceive, conceptualize, interpret, and learn motion patterns, from simple to more complex spatio-temporal structures. Our study may have implications for the recovery of abilities that have been lost as a result of disorders such as stroke, as it suggests possible therapeutic interventions aimed at enhancing motion perception, and sensory processing in general.

In summary, we have enhanced motion coherence perception for an extended period through the application of the ccPAS protocol. This enhancement was critically dependent on mimicking the temporal features of Hebbian plasticity, by exactly pairing the nodes of the network subserving motion

perception in the right direction and at the right time. The effects we observed are the result of a plastic modification of the circuit and not a mere interference with the circuit. As such, they provide novel mechanistic insights into the way the circuit functions. These findings have implications for theoretical models of visual perception as well as for the rehabilitation of visual deficits through non-invasive brain stimulation. Moreover, this novel protocol provides a novel perspective on current models of perceptual learning and its potential underlying neurophysiology.

2.5 Supplemental analyses

Similar changes in motion sensitivity threshold were found in the two hemifields. This is not surprising because our ccPAS protocol included stimulation of lateralized left MT/V5 but central V1. Indeed a TMS coil positioned 2 cm above theinion is likely to stimulate V1 over both hemispheres. It should also be noted that neurons in MT/V5 (and in neighbouring motion-sensitive areas like the medial superior temporal area) possess large receptive fields covering the contralateral visual field and spreading up to 10 degrees across the ipsilateral visual field (Gattass and Gross, 1981; Raiguel et al., 1997; Kolster et al., 2010). Therefore, it is likely that our ccPAS protocol may have recruited a bilateral cortical network with aftereffects spread across both hemifields. To test for any possible hemifield specific effect we presented lateralized rather than central motion stimuli (see also Fig.2.1). We did not observe any significant difference in performance as a function of hemifield (no main effect of Hemifield, nor interaction with this condition in the experimental as well as in the control groups; all $p > 0.1$). Rather, the ExpV5-V1 group showed a similarly enhanced performance in global motion perception for both left (LHF) and right (RHF) visual hemifields, with only a slight trend by visual inspection for a better performance over the right hemifield. The idea that ExpV5-V1 ccPAS may have activated a bilateral MT/V5-V1 pathway is well in keeping with the known transmission time of the circuit. Indeed, it is likely that during ccPAS activation of left MT/V5 spreads interhemispherically through the homologue right MT/V5 and reaches the right V1 within a fast transmission time (as early as 4 ms for interhemispheric transfer (Marzi, 2010; Nowicka and Tacikowski, 2011) and as early as 5-10 ms for MT/V5-V1 (Pascual-

Leone and Walsh, 2001; Silvanto et al., 2005a)). This is coherent with the possibility of inducing associative plasticity between right MT/V5 and V1 (that was centrally stimulated by the second TMS pulse in the ExpV5-V1 ccPAS protocol). Additionally, instead of the interhemispheric spreading of stimulation during ccPAS induction, spreading of excitation during the expression phase of plasticity could have occurred between the two hemispheres.

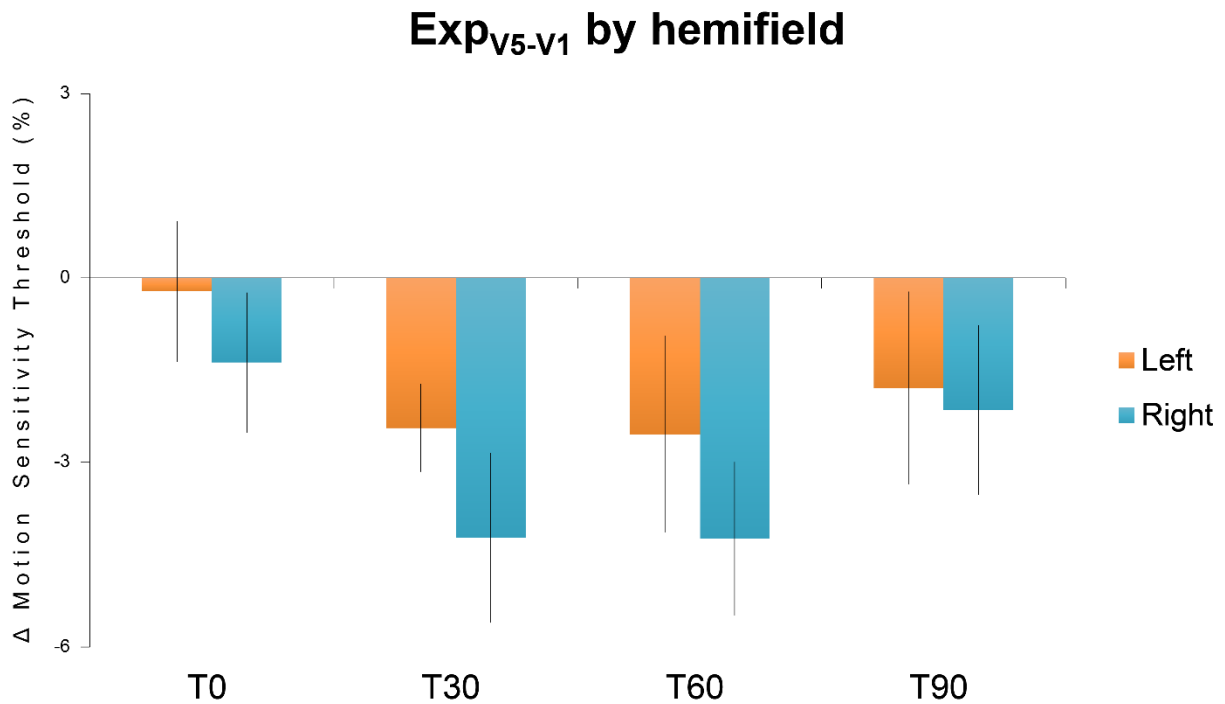


Fig.2.4 ccPAS-induced changes in visual motion sensitivity for stimuli occurring in the left and right hemifields of the ExpV5-V1 group. Error bars denote ± 1 s.e.m.

In the main parametric analyses we found that the Exp_{V5-V1} group was the only to show the expected decrease in motion sensitivity threshold at T30 and T60. The statistical results reported in the main ANOVA were also substantially replicated using other fittings, i.e., Hill equation:

$$y = \frac{x^a}{x^a + b^a}$$

Although motion sensitivity threshold was normally distributed, we additionally performed Bonferroni-corrected non-parametric analyses in view of the relatively low sample size. These analyses substantially replicated the effects detected with parametric analyses as reported in the following.

When comparing post-ccPAS performance relative to baseline values, we found that only the Exp_{V5-V1} group showed a significant change over time (Friedman ANOVA: $\chi^2(4) = 19.5$, $p = 0.003$), with significant lower motion sensitivity threshold detected at T30 and T60 (Wilcoxon tests: all $p < 0.023$), but not at T0 or T90 (all $p > 0.25$). No change over time was found in the other groups (all Friedman ANOVAs with $p > 0.11$). Baseline-corrected motion sensitivity threshold values in the 4 groups differed at T30 and T60 (Kruskal-Wallis ANOVA: all $\chi^2(3) > 11.51$, all $p < 0.023$) but not at T0 or T90 (all Kruskal-Wallis ANOVAs with $p > 0.24$). In particular, these threshold values were lower for the Exp_{V5-V1} group relative to the Ctrl_{V1-V5} (Mann-Whitney Test: all $p < 0.0035$) and Ctrl_{sham} (all $p < 0.0095$) at both time points. Moreover, relative to the Ctrl_{oms} group, the Exp_{V5-V1} group presented significantly lower threshold values at T30 ($p = 0.018$) and marginally significantly lower values at T60 ($p = 0.069$).

CHAPTER III

Strengthening functionally specific neural pathways with TMS

3.1 Introduction

An important use of transcranial magnetic stimulation (TMS) in humans is the induction of neural plasticity (see Thickbroom, 2007; Dayan et al., 2013). Such plastic changes, for which various paradigms have been developed, can be used to target cortical areas (Pascual-Leone et al., 1998; Nitsche et al., 2003; Huang et al., 2005) or, in the case of the cortico-cortical paired associative stimulation (ccPAS; Buch et al., 2011; Veniero et al., 2013; Johnen et al., 2015; Romei et al., 2016), pathways linking two cortical regions. However, an important limitation of these paradigms is the approximation of spatial specificity (see Kammer, 1999; Walsh and Rushworth, 1999) as well as the lack of functional specificity (Silvanto et al., 2007; Silvanto and Muggleton, 2008b); these paradigms are non-specific with regards to the functional type of neurons they target within the stimulated area. It has been proposed however, that a way to overcome these limitations is to rely on specific interaction between TMS intervention and state of the brain at the time of stimulation. Such state-dependent TMS approach allows targeting of functionally specific neuronal representations (Silvanto and Muggleton, 2008b) and enhances TMS specificity. Furthermore, online TMS studies revealed the crucial effect that TMS can induce depending on the intensity of the stimulation applied to the relevant cortical area (Abrahamyan et al., 2011; Schwarzkopf et al., 2011). Specifically, low-intensity TMS can generate stochastic resonant mechanisms that facilitate the perception of a stimulus by adding low-levels of neural noise that fosters the encoding of those neurons activated by the stimulus itself. On the other hand, high TMS intensities may be detrimental for perception provoking generalised noise.

In principle, state-dependent TMS at individually-definite intensities should allow tailored interventions promoting plastic changes in functionally specific neuronal representations and pathways. Therefore, the purpose of the present study is to provide proof-of-principle empirical support that enhanced TMS specificity can be achieved. Specifically, we reasoned that by pairing a recently developed paradigm

aiming at plastic modulation of functional connectivity, namely ccPAS (see Chapter II; i.e. Romei et al., 2016a) with concurrent time-locked pre- and post-synaptic tuning of interconnected neurons encoding a specific feature, we can test the selective plastic modulation of those neurons encoding the specific feature only. For this purpose we built up on our previous work (Chapter II; i.e. Romei et al., 2016a) by targeting the neural pathway carrying crucial visual motion information, namely the MT/V5-V1 re-entrant projections (Pascual-Leone and Walsh, 2001; Silvanto et al., 2005a).

Cells in MT/V5 are essential to perceive visual motion and the presence in this area of distinct populations of neurons selectively sensitive to different direction of motion has been compellingly evidenced in monkeys and strongly suggested in humans (Maunsell and Newsome, 1987; Zeki, 2004; Bartels et al., 2008; Cattaneo and Silvanto, 2008). Studies on monkeys (Lamme et al., 2000) and humans (Pascual-Leone and Walsh, 2001; Silvanto et al., 2005a) suggest that the re-entrant connectivity between MT/V5 and V1 plays a key role for moving visual stimuli to reach consciousness, conveying encoded information of motion to V1, the activity of which gates visual motion awareness. Furthermore, the MT/V5-V1 pathway has been shown to be susceptible of plastic modifications exogenously induced via ccPAS and measurable as behavioural changes (Romei et al., 2016a). These characteristics make the MT/V5-V1 circuit an ideal candidate to test whether priming a specific stimulus feature (e.g. a particular motion direction) can induce a state-dependent plastic modulation selectively encoding the primed feature whose characteristic would comply with the Hebbian principles of associative plasticity.

3.2 Methods

Phosphenes perception screening & induction

Phosphenes perception was tested on 37 right-handed subjects with no counterindications to TMS as assessed by a screening questionnaire approved by the University of Essex Research Ethics Committee in compliance with the guidelines for non-invasive magnetic brain stimulation for research application (Rossini et al., 2015). Phosphene perception thresholds from the V1 and the left MT/V5 were assessed

using a 50 mm figure-of-eight coil, connected to a mono-phasic Magstim BiStim² stimulator (Magstim Co., Whitland). To target V1 the coil was centered 2 cm dorsal to theinion, holding the handle tangential to the scalp and pointing downwards at an angle of $\sim 120^\circ$ clockwise. This location is expected to activate V1 bilaterally. To target left MT/V5 the coil was centered 3 cm dorsal and 5 cm lateral (left) to theinion, holding the handle tangential to the scalp and pointing upwards and laterally at an angle of $\sim 45^\circ$ to the sagittal plane (see also Fig.3.1, panel A). These positions are consistent with those of our previous study (Romei et al., 2016a) and also correspond to the average V1 and MT/V5 stimulation sites functionally assessed in previous studies (Silvanto et al., 2005a; Silvanto and Muggleton, 2008a). Single TMS pulses were repeatedly applied with increasing intensity, starting from 30% of the maximum stimulator output (MOS), until participants reliably perceived phosphenes; intensity was then adjusted to evoke phosphenes in 3 out of 6 consecutive pulses. Self-reported phosphenes for both V1 and MT/V5 had to fulfil the following criteria: phosphenes should be perceived with both eyes open and shut; no phosphene should be perceived during in sham stimulation; only for V1, coarse retinotopical perception should be observed, depending on the site of stimulation (i.e. phosphene on the left visual field if right hemisphere was stimulated and vice versa). Only 16 subjects (43% of the sample tested) fulfil the criteria and were therefore eligible for the experiment.

Sample

16 healthy volunteers (11 female; mean \pm s.d. age 25.3 ± 7.7 years) were recruited for the study. They were right-handed according to the Edinburgh handedness inventory (Oldfield, 1971). All of them perceived phosphenes evoked by V1 and MT/V5 TMS. They reported no neurological history and all of them gave written informed consent before taking part to the experimental procedures, which had been approved by the University of Essex Research Ethics Committee.

Task

A motion direction discrimination task was used to determine the global motion perception threshold in every participant at different timepoints. The task was very similar to the one used in a previous

experiment of our group (Romei et al., 2016a). It was created and displayed using MATLAB (version 2015a, The MathWorks Inc., Natick, MA) and the Psychophysics Toolbox 3 extensions (Brainard, 1997; Pelli, 1997; Kleiner et al., 2007) and presented on an 18-inch CRT monitor (ViewSonic G90fB, ViewSonic Corp., Walnut, CA) with a resolution of 1280 x 1024 pixels and a refresh rate of 85 Hz. Participant's viewing distance was kept at 57 cm using a chin rest. A stimulus consisted of 400 white (RGB: [255 255 255]) dots (6 pixels each) moving within an imaginary squared region subtending 12 x 12 degrees of visual angle, the centre of which was 8° to the right of a white central fixation cross (20 x 20 pixels) on a grey (RGB [80 80 80]) background (see Fig.3.1, panel B).

In each trial, dots could move coherently either leftward or rightward with 10 different percentages of motion coherence (0, 2, 4, 6, 9, 12, 16, 20, 35, 80). Motion coherence value indicates the percentage of dots that move in the signal direction. For example, in trials with 0% of coherence, each of the 400 dots moved with a randomly selected direction motion (0% of signal, 100% of noise); in trials with 80% of coherence, 320 dots moved coherently towards either left or right (80% of signal), while each of the remaining 80 dots moved in randomly determined directions (20% of noise). Dots moved at a speed of 4.5°/s.

The task was a two-alternative forced choice task. Participants were instructed to always keep the gaze on the fixation cross that was constantly present at the centre of the screen. Each trial began with the fixation cross for 500 ms, then the moving stimulus appeared on its right side for 400 ms. Once the stimulus ended, only the fixation cross persisted and participants had to make an unspeeded response by pressing the left or the right arrow key to indicate which was the perceived global coherent direction of the motion (Fig.3.1, panel B). One task block consisted of 600 trials having 30 repetitions for each of the 10 coherence percentages in 2 possible (right/leftward) directions (30 x 10 x 2; Fig.3.1, panel A). A block lasted approximately 13 minutes.

ccPAS phase

ccPAS was administered through two 50 mm figure-of-eight coil, connected to a mono-phasic dual pulse Magstim stimulator (Magstim Co., Whitland), consisting of a BiStim² and a 200² module. Coils positioning and orientation were consistent with those adopted for the assessment of phosphenes thresholds (see *Phosphenes induction* section). ccPAS protocol combined TMS pulse pairs with a motion stimulus having 100% of coherent motion towards a specific direction (either left or right). Specifically, the E-Prime software (Psychology Software Tools, Pittsburgh, PA) controlled the onset of the motion stimulus and TMS pulses that were delivered at a specific stimulus onset asynchrony (SOA; see below). Throughout this phase, participants were asked to maintain the head still on the chinrest, to keep their gaze on the fixation cross and to simply watch the stimuli appearing on the screen passively, since no response was required. Stimuli were identical to those presented in the motion direction discrimination task, except for the coherence of the motion that was always at 100% i.e. all the dots where coherently moving in the same direction. Each participant underwent 3 sessions of stimulation differing for ccPAS configuration in different days, while the direction of movement was consistent throughout the session and across the sessions, randomly determined and counterbalanced (8 participants were presented with 100% leftward motion, 8 with 100% rightward motion). Along with the motion stimulus presentation, the first TMS pulse of the ccPAS was delivered with a SOA of 150 ms, whereas the second pulse occurred 20 ms after the first (interstimulus interval; ISI). There were 90 motion stimuli paired with TMS (double) pulses administered at a rate of 0.1 Hz. These parameters were selected for the following reasons:

- i. SOA of 150 ms seems consistent with the peak of temporal activation course of V1 and MT/V5 in response to a motion stimulus in which MT/V5 feeds back the processed information to V1 (Prieto et al., 2007);
- ii. ISI of 20 ms corresponds to the timing at which MT/V5 exerts a physiological effect on V1 (Pascual-Leone and Walsh, 2001; Silvanto et al., 2005a), thus represents a critical timing to

- optimally activate the pre- and post-synaptic neuronal populations of MT/V5-V1 connection (Romei et al., 2016a), and comply with the spike timing-dependent plasticity (STDP) principles (Bi and Poo, 2001; Caporale and Dan, 2008; Keyzers and Gazzola, 2014);
- iii. 90 is a standard amount of (double) pulses delivered for ccPAS protocol intended to repeatedly activate the cortico-cortical connection and foster the establishment of STDP-like phenomena (Rizzo et al., 2009; Romei et al., 2016a);
 - iv. Stimulation rate of 0.1 Hz (intertrial interval: 10 s) assures no temporal summation effects of TMS pulses per se (Stefan et al., 2000).

The ccPAS condition varied depending on the session, the order of which was counterbalanced between subjects. ISI and TMS intensity were manipulated across the ccPAS sessions.

ISI: STDP phenomena of long-term potentiation (LTP) revealed in cells (Bi and Poo, 2001; Caporale and Dan, 2008; Keyzers and Gazzola, 2014) and mimicked by ccPAS protocols (Koch et al., 2013; Johnen et al., 2015) depend on the exact timing of the connection, since the pre-synaptic node needs to causally assist the activation of the post-synaptic node to establish associative plasticity. We therefore expected that the ISI of 20 ms was optimal to induce LTP-like phenomena whilst ISI of -20 ms (determining a stimulation of opposite direction) was not (Pascual-Leone and Walsh, 2001; Silvanto et al., 2005a; Romei et al., 2016a).

Intensity: Research showed that depending on TMS intensity, stochastic resonance can be induced with online TMS (Abrahamyan et al., 2011; Schwarzkopf et al., 2011). In keeping, low-intensities TMS (80% of phosphene threshold) can induce low-levels of noise that may foster the encoding of motion signals in MT/V5, thus having a specific effect on those neurons activated by the motion stimulus. On the contrary, high-intensities TMS (at 100% of phosphene threshold) are supposed to induce a generalised noise and thus no facilitations for stimulus encoding.

Based on these considerations, we expect to have one experimental ccPAS session that in consistency with STDP rules and stochastic resonance mechanisms optimally targets the MT/V5-V1 pathway for the direction of motion congruent with the motion stimulus observed during ccPAS protocol.

Experimental session (eV5-V1_80): the first pulse was delivered over MT/V5, the second over V1 at the intensity of 80 and 100% of the phosphene threshold, respectively. This ccPAS condition was expected to potentiate the MT/V5-V1 re-entrant connectivity specifically for the congruent direction of the motion. The subthreshold intensity at which MT/V5 was stimulated, was intended to facilitate pathways conveying information about the displayed motion direction, while no effect was expected on non-congruent ones, having a higher threshold and being inhibited by the congruent stimuli. Hence, we expected this ccPAS condition to be optimal to enhance the connectivity between the presynaptic node (MT/V5), and the postsynaptic node (V1) selectively for the neurons coding for the primed direction of motion.

Control session for intensity (cV5-V1_100): identical to the eV5-V1_80 session except for the intensity applied to MT/V5 stimulation that was at 100% of the phosphene threshold. This stimulation was expected to have no effects on motion perception.

Control session for directionality (cV1-V5_80): identical to the eV5-V1_80 session except for the order of stimulation, i.e. V1 pulse was delivered prior to MT/V5 pulse. This stimulation was expected to have no effects on motion perception.

Procedure

The experiment was a within subject design carried out in 3 sessions, separated by at least 1 day (average: 7.9 days). Each session was defined by the specific ccPAS condition whose order was randomly determined and counterbalanced across participants. In all the sessions, prior the beginning of the experiment, phosphene threshold was assessed for both V1 and MT/V5 areas (see *phosphenes induction* section).

Participant's sensitivity to global motion (in both the congruent and incongruent direction relative to the priming stimulus presented during ccPAS) was tested before (PRE) and 30 minutes after the end of (POST) the ccPAS phase. This timing (POST) was selected based on previous evidence suggesting a maximum effect after 30 minutes following ccPAS protocol (Romei et al., 2016a). In addition, a training block of 200 trials was performed in order to achieve a stable performance before the PRE, and, only in the first session a familiarisation block of 400 trials of the task was executed at the very beginning of the experiment (Fig.3.1, panel A).

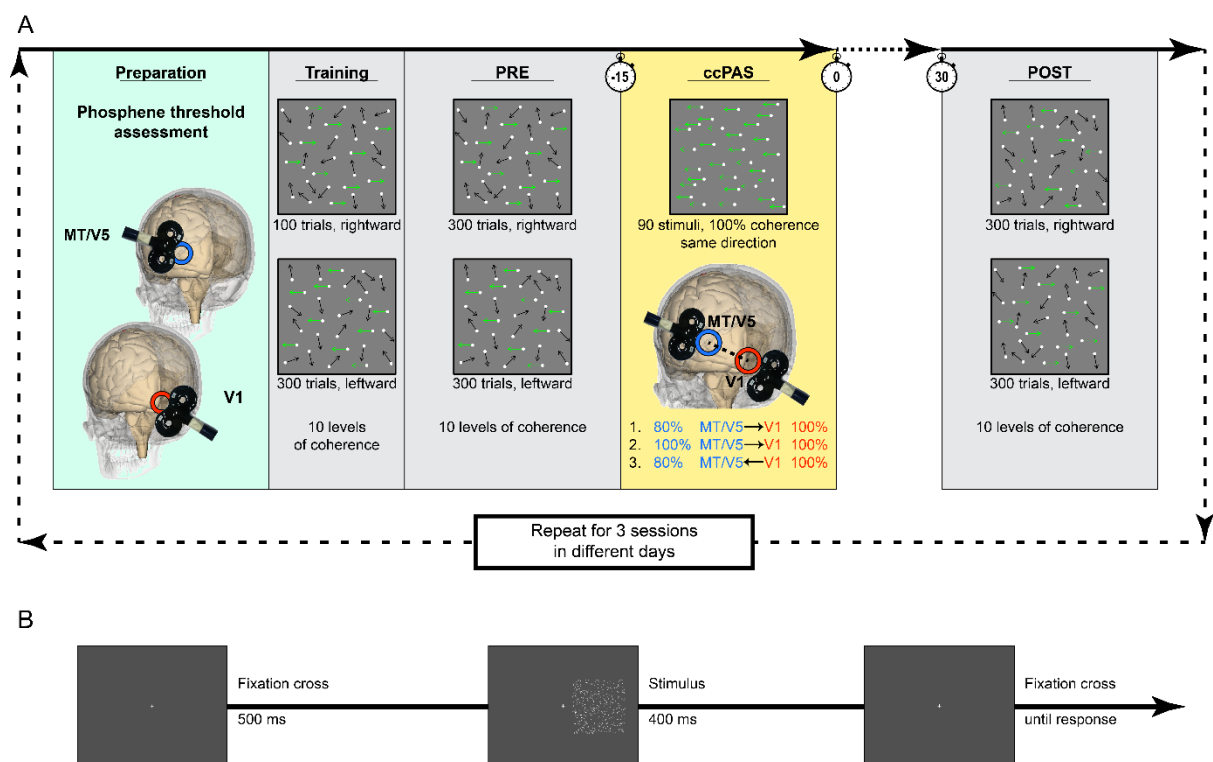


Fig.3.1 (A) Timeline of experiment. At the beginning of each session the phosphene threshold was assessed for both MT/V5 and V1. Training consisted of a single block (200 trials) of the global motion discrimination task, while PRE (before ccPAS) and POST (30 min after ccPAS) consisted of 3 blocks (600 trials) each. Motion coherence varied across trials in 10 levels (0-80%), here are depicted schematic trials, arrows illustrate the motion direction of each dot; green arrows represent the directions of signal dots (35%), black arrows represent the directions of noise dots (65%). ccPAS protocol could be delivered in 3 configurations differing for directionality and intensity. It consisted of 90 pairs of pulses over MT/V5 and V1, administered at a rate of 0.1 Hz, time locked to the motion stimulus with 100% of coherence moving in the same direction (either leftward or rightward, balanced across participants). The whole procedure was repeated for 3 sessions separated by at least 24h, and differing for the ccPAS configuration applied. (B) Task sequence consisted of a white central fixation cross (500 ms) followed by a motion coherence stimulus (400 ms) that appeared on the right side of the cross (a single frame of the motion coherence stimulus used in the study is depicted), and fixation cross until response (left or right arrow to indicate the leftward or rightward coherent motion perception, respectively). Motion coherence varied across trials.

Data handling

Data collected through the task were plotted on a cartesian plane with the X axis representing the motion coherence and the Y axis the percentage of accuracy. As expected from our previous study (Romei et al., 2016a), data distribution described a psychophysics curve having a sigmoidal shape roughly ranging between 50 (at 0% of motion coherence; guessing threshold) and 100% (at 80% of motion coherence) of accuracy. Therefore, data well fitted a nonlinear function modelled on the logistic curve:

$$y = \frac{a}{1 + e^{-\frac{x-b}{c}}}$$

where a assumes the value of the upper horizontal asymptote; b represents the value of the point of critical change in the function behaviour at half the way between the lower and the upper asymptotes, named the inflexion point of the curve; c defines the slope.

For each participant, the value of the inflexion points for each block and each motion direction (congruent or non-congruent to that presented in the ccPAS phase) was calculated using MATLAB (version 2016b, the MathWorks, Natick, MA), applying the Levenberg-Marquardt algorithm. This value represents the motion sensitivity threshold, intended as the percentage of coherent motion that mathematically describes the change in the global motion perception.

A factorial ANOVA with Stimulation (eV5-V1_80, cV5-V1_100, cV1-V5_80), Direction (Congruent, non-Congruent) and Time (PRE, POST) on the raw values of the motion sensitivity threshold was performed. Post-hoc T-tests with Bonferroni corrections were performed on relevant comparisons. To compare the modulatory effect of the ccPAS independently of the PRE values, we calculated a modulation index by subtracting the motion sensitivity values of POST to those of PRE (POST-PRE). Negative values reflect less percentage of coherent global motion necessary to change the perception, thus a performance enhancement, while positive values index a performance decay. Based on previous findings (Romei et al., 2016a) and on our a priori theoretical assumptions, one-tailed T-tests (with Bonferroni correction

for multiple comparisons) were performed on the modulation index (i) to compare the effect of the experimental ccPAS configuration (eV5-V1_80) on congruent and non-congruent direction of motion, and (ii) to compare the effect of the experimental ccPAS configuration (eV5-V1_80) with the effects of the control ccPAS configurations (cV5-V1_100 and cV1-V5_80) on the perception of the motion direction congruent to that observed during the ccPAS protocol. The Statistica software (version 12, StatSoft Inc., Tulsa, OK) was used to compute the analyses.

3.3 Results

Phosphenes thresholds

In line with previous studies (Silvanto et al., 2005a) the average phosphene threshold was lower for V1 than MT/V5 (MOS mean \pm s.d.) $58 \pm 8\%$ and $62 \pm 9\%$ respectively, as shown by a paired 2-tailed t test ($t_{15} = -4.48$, $p < 0.001$).

Threshold values did not significantly fluctuate across the sessions either for V1 [(session: MOS mean) session1: 59%, session2: 57%, session3: 58%; one-way ANOVA $p=0.63$] or MT/V5 [(session: MOS mean) session1: 62%, session2: 61%, session3: 62%; one-way ANOVA $p=0.65$].

Behavioural results

The repeated measures ANOVA with the factors Session (3), Direction (2) and Time (2) conducted on the inflection points of the logistic curves fitted on data of the task performance revealed a significant three-way interaction ($F_{2,30} = 3.86$, $p = 0.032$) and no other main effects or interactions (all p s > 0.14). Motion sensitivity threshold differences within the same factor Direction before ccPAS (at Time PRE) were tested with post-hoc comparisons; analyses revealed no differences (Congruent: all p s > 0.08 ; non-Congruent: all p s > 1), indicating comparable performance in the different sessions before TMS intervention. With the same post-hoc analysis motion sensitivity threshold differences within the factor Stimulation and Direction were tested, results showed that no comparisons between PRE and POST were significant (all p s = 1) except for the congruent direction in the eV5-V1_80 experimental Session

[PRE vs. POST (mean \pm s.e.); 11.14% \pm 1.51% vs. 7.72% \pm 1.78%, $p = 0.017$], proving an enhancement of motion sensitivity threshold occurring only for moving stimuli whose direction was congruent with the primed direction presented during the ccPAS protocol (Fig.3.2).

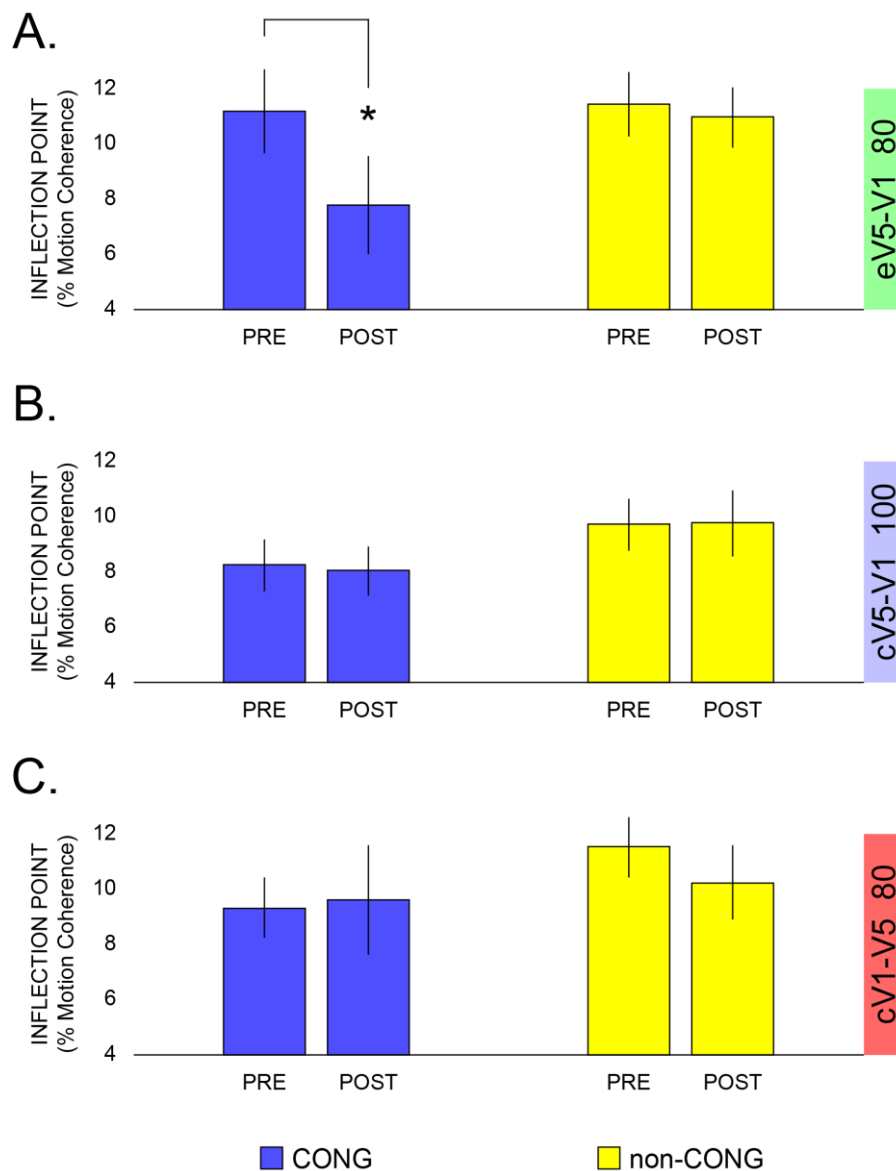


Fig.3.2 Results of three-way interaction ANOVA on visual motion sensitivity threshold defined by the inflection point of the psychophysics curve. Post-hoc analyses comparing motion sensitivity threshold before (PRE) and 30 min after (POST) ccPAS within the Direction and Session of ccPAS. Asterisk indicate the significant improvement of perception following the experimental (eV5-V1_80) ccPAS session for stimuli moving in the congruent direction (A). No difference between PRE and POST of the same direction resulted significant either for cV5-V1_100 (B) or cV1-V5_80 (C) configuration. Error bars denote s.e.m..

Modulation indices

To verify the functional specificity of motion sensitivity improvements, the modulatory effect of the experimental eV5-V1_80 ccPAS on the congruent and non-congruent direction of motion was analysed, revealing that ccPAS enhanced sensitivity for congruent moving stimuli relative to the non-congruent moving stimuli direction [Congruent vs. non-Congruent (mean \pm s.e.); $-3.42\% \pm 1.29\%$ vs. $-0.46\% \pm 0.95\%$, $p = 0.035$] (Fig.3.3, panel A).

To test the efficacy of the experimental ccPAS in changing functionally specific motion sensitivity, the modulatory effect of experimental ccPAS session (eV5-V1_80) was directly compared against both the control ccPAS sessions (cV5-V1_100 and cV1-V5_80). Specifically, when comparing the impact of ccPAS sessions on the congruent primed motion direction, a significant enhancement in motion sensitivity was observed for the experimental vs. the control ccPAS sessions [eV5-V1_80 vs. cV5-V1_100 (mean \pm s.e.); $-3.42\% \pm 1.29\%$ vs. $-0.19\% \pm 0.7\%$, $p = 0.018$ and eV5-V1_80 vs. cV1-V5_80 (mean \pm s.e.); $-3.42\% \pm 1.29\%$ vs. $0.3\% \pm 1.39\%$, $p = 0.019$] (Fig.3.3, panel B).

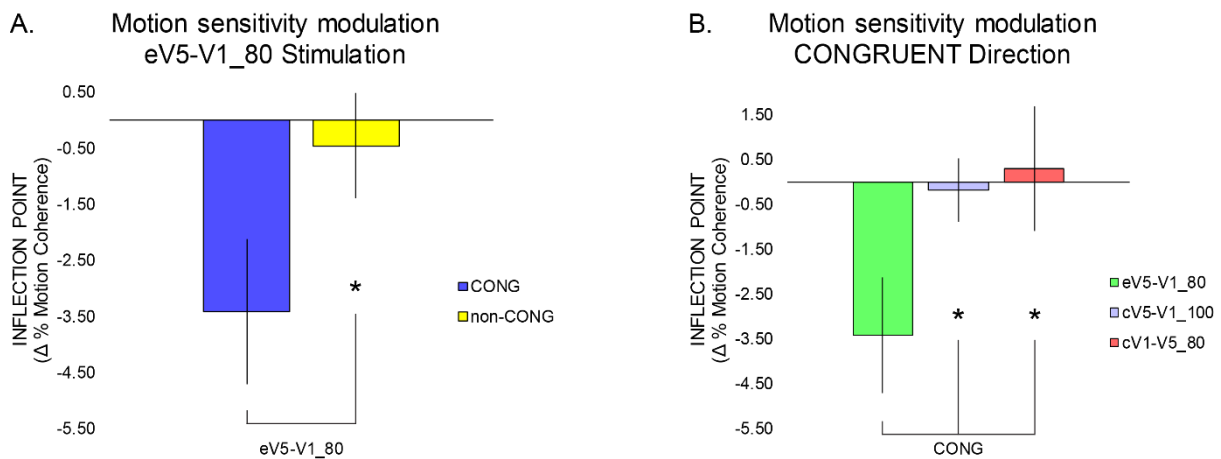


Fig.3.3 (A) experimental ccPAS: change in motion sensitivity for congruent vs. non-congruent motion direction stimuli. (B) change in sensitivity for congruent motion direction stimuli across experimental and control ccPAS sessions. Asterisks indicate Bonferroni corrected significant comparisons; error bars denote s.e.m..

3.4 Discussion

In the present study, the neural pathway between MT/V5 and V1 was repeatedly activated by means of dual-coil TMS, applying the ccPAS protocol. This stimulation has been shown to empower the targeted pathways leading to long-lasting behavioural improvements in motion perception (Romei et al., 2016a). Importantly, the presentation of a stimulus involving a pattern of dots coherently moving in a specific direction (either left or rightward) was paired with the ccPAS stimulation in order to modulate the activation of MT/V5 neurons that encode the direction of moving stimuli just before the subthreshold TMS pulse was delivered over this area. According to the state-dependency properties of TMS (Silvanto and Muggleton, 2008b; Silvanto et al., 2008), subthreshold MT/V5 stimulation during the vision of the moving stimulus should selectively interact with those neurons that are activated by the direction of the stimulus. Furthermore, mechanisms of stochastic resonance triggered by online TMS have been shown to facilitate the encoding of moving stimuli only when TMS was applied over the relevant site at low-intensities (Abrahamyan et al., 2011; Schwarzkopf et al., 2011). Therefore, we hypothesised that ccPAS specifically boosted the MT/V5-V1 pathway encoding for motion perception in the direction of motion congruent to that paired during ccPAS protocol, leading to functional specific perceptual improvements.

To test for the impact of ccPAS protocol on motion sensitivity, participants performed a motion discrimination task before and 30 minutes after the ccPAS protocol. Specifically, we looked for changes in sensitivity threshold for the motion stimuli whose direction could be either congruent or non-congruent (opposite) to the motion direction of those stimuli paired with the ccPAS session. Our key result was the increased sensitivity threshold for the motion stimulus direction congruent with that viewed during the application of ccPAS. No effect was found for the motion direction opposite (i.e. non-congruent) to that. This pattern of result is likely to reflect a summation between the impact of TMS and the visual presentation of motion during the ccPAS protocol.

We also included two conditions in which TMS was applied first over MT/V5 and then over V1. TMS was applied either below phosphene threshold (experimental configuration) or at its 100% (control configuration for intensity). A third condition controlled for the directionality of the stimulation where V1 stimulation preceded MT/V5 stimulation. Effects were specific for the ccPAS targeting re-entrant projections rather than feedforward connections (for MT/V5-to-V1 stimulation), and selectively for the subthreshold stimulation intensity of MT/V5.

In this study we have manipulated and empirically tested 3 key elements: cortical connectivity, plasticity and state-dependency.

Connectivity: MT/V5-V1 connectivity functionally links the motion visual area and the primary visual areas in a reversed hierarchical fashion (Lamme and Roelfsema, 2000). The importance of the re-entrant information to early visual cortices has been demonstrated to be essential for a conscious visual representation of the stimuli moving in the environment (Lamme et al., 2000; Pascual-Leone and Walsh, 2001; Silvanto et al., 2005a). The recurrent crosstalk of these areas is supported by the study of Prieto and colleagues (2007) that using magnetoencephalography (MEG) showed two peaks of activation for both MT/V5 and V1, following the presentation of a moving stimulus. Crucially, correlational analyses on timings and amplitude of the peaks strongly suggested a strict interaction between these structures that activate repeatedly through forward and feedback connections contributing to the visual motion analysis. The motion stimulus used in that experiment involved a random dot kinematogram with 100% of coherence, conceptually similar to our visual stimulus used during ccPAS. In keeping, we decided to deliver the first TMS pulse following by 150 ms the presentation of our motion stimulus, that is the timing corresponding to the mean maximum peak latency of the first MT/V5 MEG component (M1-MT/V5) reported by Prieto and collaborators (2007), the amplitude of which positively correlates with the M2-V1, the following component recorded in V1. The M2-V1 component peaks approximately 24 ms after M1-MT/V5, a latency that is consistent with the conduction time observed by paired-pulse TMS paradigms of the MT/V5-V1 feedback connectivity (Pascual-Leone and Walsh, 2001; Silvanto et al.,

2005a). Accordingly to these studies and to our previous study (Romei et al., 2016a), the second TMS pulse was delivered 20 ms after the first.

Plasticity: The ccPAS paradigm is a unique tool able to induce plastic changes in the interaction between two distant cortical sites at synaptic level. It is believed to mimic on a larger scale the long-term potentiation (LTP) mechanisms of associative synaptic plasticity intensively studied in cellular preparations (Bliss and Lømo, 1973; Zhang et al., 1998; Caporale and Dan, 2008), derived from the Hebbian principles of synaptic plasticity (Hebb, 1949) and considered at the base of learning, memory and behavioural changes. Neurophysiological evidence in the motor-related areas showed that ccPAS, by repeatedly and persistently activating a specific cortico-cortical connection at rest, alters the connectivity between the stimulated sites in an LTP-like manner (Koganemaru et al., 2009; Buch et al., 2011; Veniero et al., 2013; Johnen et al., 2015), impacting on motor behaviour (Koganemaru et al., 2009; Fiori et al., 2018). Similar synaptic potentiation is supposed to account for long-term behavioural perceptual changes observed after ccPAS administration at rest over the MT/V5-V1 backward connections (Romei et al., 2016a). In the mentioned experiment, a peak of motion perception sensitivity was reported 30 minutes after the stimulation (hinting the selection of timing for the post-ccPAS measurement in the present experiment), however, this performance enhancement was non-specific for the motion direction, on the contrary, it was generalised to both left and rightward motion sensitivity. We believe that such a crucial difference hinges on both the intensity of TMS delivered for ccPAS, and the state of neuronal pools implied in the task at the time of the stimulation. Importantly, the temporal window that separates the firing of the pre- and post- synaptic cell or, here, neural populations, is the key element for plastic changes to occur and for determine the relation of causality (Keysers and Gazzola, 2014). Meeting the directional, and thus temporal, constraints of the connection, we induced a potentiation after the experimental session (eV5-V1_80), while no behavioural effect was prompted by the control session having opposite direction of stimulation (cV1-V5_80), as determined by the timing between the pulses (+20 vs. -20 ms).

State dependency: The pivotal element of this study is the specificity of the results on a functional level. The sensitivity threshold for motion was specifically improved for the direction congruent with that of the stimulus presented at the time of ccPAS, although the stimulation targeted the MT/V5 area, crucially involved in the detection of both the right and left directions of motion (Beckers and Hömberg, 1992; Bullier, 2001; Pascual-Leone and Walsh, 2001; Cattaneo and Silvanto, 2008). Despite this spatial overlap, TMS allows targeting of functionally distinct neuronal populations based on their state of activation using an appropriate intensity of stimulation (Silvanto and Cattaneo, 2017). In the experimental session (eV5-V1_80) we delivered the first ccPAS pulse, time-locked to the task, over MT/V5 containing neurons tuned to the viewed direction that, since primed by the stimulus, were activate by subthreshold TMS having lower activation threshold. It is indeed known that the threshold for active neurons is lower than for those inactive, thus, TMS exerts a differential impact on these pre-activated functionally distinct neural populations. We then delivered the second ccPAS pulse time locked to the first pulse over V1, complying with PAS principles (Stefan et al., 2000; Rizzo et al., 2009), at threshold intensity to specifically empower the functional connectivity between MT/V5 primed neurons and V1 area. In the intensity control session (cV5-V1_100), the MT/V5 pulse was delivered at threshold, that is an intensity sufficient to activate all neurons, thus losing functional specificity. One could expect to have a generalised improvement as it occurred in our previous study (Romei et al., 2016a), instead, we found no change in motion sensitivity. It is plausible that absolute differences of TMS intensity may account for these different results, Romei and colleagues stimulated at a fix intensity of 70% of the maximum output stimulator, this factor, albeit unlikely, cannot be disentangled. Another possibility resides again in the state of MT/V5 neurons at the time of ccPAS phase; it is worth to remind that in the previous study, as opposed to the present one, ccPAS was applied at complete rest. Here, we hypothesise that the same lateral inhibition processes, physiologically engaged during stimulus view (Alais and Blake, 1998), would be activated by high-intensity TMS also for those neuronal pools not tuned to the congruent direction. In this scenario, both the congruent and non-congruent pathways would be activated and suppressed by lateral inhibition phenomena; a competitive processing resulting

in a net zero-effect, resembling the “reset” TMS effect observed in some TMS-adaptation paradigms induced and tested online (see Silvanto and Cattaneo, 2017). However, in absence of more explicit measures of neural activity changes, our assumptions of MT/V5-V1 connectivity manipulation are only based on indirect evidence; further investigations (e.g. electrophysiological) may elucidate to what extent functional changes occurred in the targeted pathway as a consequence of ccPAS.

Summarising, our results provide the first behavioural evidence that neural plasticity induced by TMS in the ccPAS paradigm can be targeted on specific neural pathways, based on the functional selectivity. Only neurons tuned to the presented stimulus benefit from the strengthening of neural connections – giving rise to direction-selective induction of plasticity reflected in a functional specific performance improvement. When TMS is applied at a higher intensity, the stimulation intensity is likely to be sufficient to activate neurons regardless of whether they have been activated by the visual stimulus, and allegedly because of lateral inhibition considerations, no behavioural plasticity is induced.

CHAPTER IV

Grounding motor resonance in the PMv-M1 connectivity

4.1 Introduction

Evolution equipped the human beings with a malleable neural system that allows the processing of others' actions, indispensable to benefit from shared social contexts created through everyday non-verbal social interactions.

The view of an action executed by a conspecific, evokes a covert activity of the primary motor cortex (M1) that is specifically tuned to the movement observed (Fadiga et al., 1995; Strafella and Paus, 2000; Aziz-Zadeh et al., 2002; Maeda et al., 2002; Urgesi et al., 2006; Alaerts et al., 2009). This phenomenon called motor resonance (MR) has been demonstrated by several transcranial magnetic stimulation (TMS) studies that tested the corticospinal excitability of the primary motor cortex (M1) during action observation and is considered the expression of the activity of the action observation network (AON) involved in the processing of others' actions (Avenanti et al., 2013a; Naish et al., 2014). Converging evidence suggest that the AON transforms the visual information sourced from the middle temporal gyrus (MTG) onto motor representations in the ventral portion of the premotor cortex (PMv) of the onlooker through the inferior parietal lobule (IPL) processing (Jeannerod, 2001; Rizzolatti and Craighero, 2004; Grafton, 2009; Caspers et al., 2010; Sinigaglia, 2013), and accordingly modulates the activity of M1 (Avenanti et al., 2007) allegedly through direct PMv-M1 cortico-cortical connections (Koch et al., 2010; Catmur et al., 2011).

The AON is subject to plastic modifications as showed by functional imaging studies that highlighted how motor experience biases the engagement of the network's nodes (Buccino et al., 2004; Calvo-Merino et al., 2005). During the developmental age (Biagi et al., 2016) but also through specific physical (Catmur et al., 2008), observational (Cross et al., 2009; Jastorff et al., 2009) or combined training (Cross et al., 2006, 2009) new motor representations can be acquired and old ones can be modelled (Catmur

et al., 2007; Catmur, 2013). Consistent results were obtained with TMS approaches showing that motor experience influences MR (Aglioti et al., 2008; Makris and Urgesi, 2013) and that rehearsal enhances or invert MR accordingly (Catmur et al., 2007; Jola et al., 2012). Gardner and colleagues (Gardner et al., 2015) emphasise the role of the pathways that consent the information to flow within the cortical hubs of the AON, and showed that the familiarity for the movements modulates the effective connectivity of the network. Taken together these findings demonstrate that MR probed by TMS represents a reliable index to assess the expression of the AON processing and that the AON malleability is associated with the change of both the activity of its hubs and the information flow within them. However, there is no causative evidence about the impact that connectivity exerts on the processing of the AON.

A novel dual-coil TMS protocol, denominated cortico-cortical paired associative stimulation (ccPAS; Rizzo et al., 2009), offers the unique possibility to exogenously induce plastic alterations in the connectivity between two cortical sites of the AON. It is assumed that the ccPAS, by repeatedly delivering pairs of TMS pulses with a connection-specific interpulse interval (IPI), activates the pathways connecting the two targeted sites, and prompts physiological changes at the synaptic level (Arai et al., 2011; Buch et al., 2011). The underlying mechanisms reminds on a larger scale the cellular phenomenon known as spike-timing-dependent plasticity (STDP) where the repetitive activation of neuronal circuits can induce long-term modulation in the cellular response in compliance with the temporal order of pre- and post-synaptic firing (Bi and Poo, 2001; Caporale and Dan, 2008; Keyzers and Gazzola, 2014).

Here we aim to demonstrate for the first time that the AON processing is amenable to modulations by altering the AON connectivity via non-invasive brain stimulation technique. To this purpose, we take advantage of the ccPAS protocol to modulate the synaptic efficiency of the AON using the PMv-M1 connectivity as a test-bed circuit. Specifically, we hypothesise that if the ccPAS boosts the PMv-M1 flow of information then AON functionality will be fostered leading to enhanced MR.

4.2 Methods

Sample

Forty-five right handed healthy volunteers with normal or corrected-to-normal visual acuity (23 females and 22 males) ranging from 19 and 34 years (mean \pm s.d.; 24 ± 3) were recruited for the study. None of them suffered of medical conditions or contraindication to TMS (Rossi et al., 2009; Rossini et al., 2015). The local ethic committee in accordance with the Declaration of Helsinki approved experiment procedures and participants gave written informed consent before taking part to it.

General experimental design

TMS applied over the cortical representation of the M1 hand, specifically the first dorsal interosseous (FDI) and abductor digiti minimi (ADM) muscles, probed the cortico-spinal excitability during the observation (OBS) of right finger movements (either index or little finger) and in a resting condition (REST). Cortico-spinal excitability in OBS and REST conditions was tested before (PRE), immediately (POST0) and 30 minutes (POST30) after the administration of a ccPAS protocol aimed at modulating the physiological connectivity between PMv and M1. Each testing session of (PRE, POST0, POST20) consisted of two blocks of \sim 4 minutes, with 16 OBS and 10 REST trials. The order of the experimental conditions was randomly determined for each participant but counterbalanced and was consistent throughout the experiment (i.e. 23 participants: OBS-REST; 22 participants: REST-OBS). Participants were randomly assigned to 3 groups that differed by the ccPAS configuration that was delivered. Specifically, the IPI parameter was manipulated in order to induce strengthening (PMv-to-M1) or weakening (M1-to-PMv) of the PMv-M1 connectivity. In the third ccPAS setup (SHAM) no effective TMS was applied. ccPAS phase lasted approximately 13 min.

Apparatus and stimuli

During the testing phase, participants were asked to keep their right hand out of sight laying palm-down on the arm tablet attached to the chair on which they sat. Centrally and at approximately 80 cm of

distance from participants' head, visual stimuli were displayed on a 24" LED screen Acer GN246HL-Bbid with a full HD resolution (1920 x 1080 pixels) and a refresh rate of 60 Hz. MATLAB software (version R2013b; The MathWorks Inc., Natick, MA) and the Psychophysics Toolbox extensions (Brainard, 1997; Pelli, 1997; Kleiner et al., 2007) served stimuli presentation and triggered TMS pulses.

The experiment was divided in blocks, each of which had 2 experimental conditions i.e. OBS and REST. Regardless of the experimental condition, trials had a common triple-screen structure and a common duration of 7000 ms; each trial began with a first screen of the duration of 1000 ms depicting a fixation cross, followed by a TMS-screen of 3000 ms displaying either the fixation cross or a clip (according to the ongoing experimental condition), and ended up with a blank screen of 3000 ms.

In the OBS condition, the TMS-screen consisted of videos depicting abductive/adductive movements of the right index (IND) or little (LIT) finger of two male and two female Caucasian hands. Each clip began with the hand still for 1200 ms and then initiated the movement that was interrupted after 1800 ms. One complete abductive/adductive movement lasted about 1 second, the finger moved on the horizontal plan of the hand and lift-and-displace movement were avoided, in order to generate movements requiring the maximum activity of the abductive muscles of the fingers. The hands, bare-jewellery and with no distinctive peculiarities (e.g. tattoos), were presented in palm-down position from an overhead view and rotated of 90 degrees clockwise or anti-clockwise from an egocentric perspective to exclude visuo-spatial compatibility effects. Each video consisted of 45 frames and each frame remained onscreen for 4 complete screen refreshes, corresponding approximately to 67 ms, still providing a fluid perception of the movement. Stimuli were presented twice in a pseudorandomized order for the factorial combination of the three conditions (4 hand model × 2 finger moved × 2 hand orientation × 2 repetitions) resulting in a total of 32 trials per block.

The TMS-screen of the REST condition consisted of a fixation cross.

The background for all the frames of the displayed stimuli was white coloured. The perpendicular intersection of two black lines of 2 degrees of visual angle composed the fixation cross. Videos were

inscribed in a virtual square that subtended a visual arc of 13.8 degrees per side. In every trial a single TMS pulse was delivered to probe corticospinal excitability at five randomized intervals ranging from 2400 and 3200 ms after the beginning of the trial. This timing assured that TMS was always administered within the TMS-screen and during the movement in the OBS condition (from 200 to 1000 ms after the movement onset), therefore the TMS intertrial interval (ITI) was 7000 ± 800 ms.

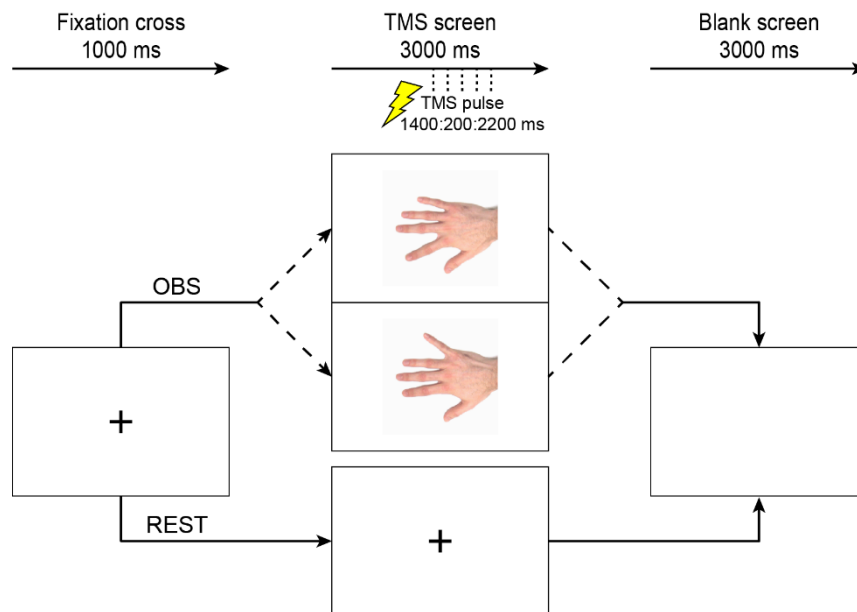


Fig.4.1 Schematic representation of trials. In OBS trials (above), after the fixation cross (1000 ms), a rotated hand (90° either clockwise or anti-clockwise) appeared, between 1400 and 2200 ms after the presentation of the hand and during the movement of the finger (IND or LIT) a TMS was delivered, followed a blank screen for 3000 ms. In REST trials (below), the trial was identical, but instead of the hand, the fixation cross remained.

TMS and electromyographic recording

TMS was delivered through figure-of-eight coils (50 mm wing external diameter). The optimal scalp position (OSP) and the resting motor threshold (rMT) of each participant was determined using a Magstim BiStim2 device that generates a monophasic waveform. The coil was held tangentially to the scalp with an orientation of ~45 degrees with respect to the midsagittal line inducing a posterior-to-anterior current in the brain, optimal to activate the cortico-spinal tract with a monophasic TMS (Brasil-Neto et al., 1992; Kammer et al., 2001). Motor evoked potentials (MEPs) were recorded simultaneously from the FDI and the ADM muscles of the right hand, agonists muscles for index and little fingers

abduction respectively, using bipolar surface Ag-AgCl electrodes using a belly-tendon montage by means of a Biopac MP-35 (BIOPAC Systems, Inc., Goleta, CA) electromyograph. EMG signal was band-pass filtered (30-500 kHz) and digitized (sampling rate 20 kHz). OSP was defined as the coil position where a TMS pulse delivered at fixed intensity over the left M1 evoked an MEP of the maximal amplitude in the FDI muscle of the contralateral hand. The rMT was defined as the minimal intensity able to evoke at least five out of 10 MEPs with an amplitude $> 50 \mu\text{V}$ in the relaxed FDI, holding the coil over the OSP and is expressed as the percentage of the maximum stimulator output (MOS) of the TMS machine (Rossini et al., 1994). On average the rMT of this study was (Mean \pm SD) $40 \pm 7 \%$ of the MOS.

During the testing phase, single pulses TMS (spTMS) were administered to participants over the OSP through a Magstim Rapid2 device that generates a biphasic waveform. Stimulation intensity was set in order to produce MEPs of approximately 1 mV, and coil were oriented in order to induce an anterior-to-posterior current in the brain with respect to the first phase of the waveform generated, optimal to activate transynaptically the cortico-spinal tract using a biphasic TMS (Kammer et al., 2001; Di Lazzaro et al., 2004). By means of the SoftTaxic Navigator system (Electro Medical Systems, Bologna, Italy) individual Talairach coordinates corresponding to the projection of M1 OSP on the brain surface were calculated and corresponded to (Mean \pm SD) $x = -36 \pm 5.9$; $y = -13 \pm 9.2$; $z = 56 \pm 4.6$. The neuro-navigator system automatically estimates Talairach coordinates from an MRI-constructed stereotaxic template based on the digitized scalp of each participant acquired using a Polaris Vicra digitizer (Northern Digital INC. Ontario, Canada).

In the plasticity induction phase, 90 pairs of pulses were administered at rest to PMv and M1 site locations through two coils at a frequency of ~ 0.13 Hz (a pair of stimuli every 7 s, total duration ~ 11 minutes). PMv stimuli were delivered at 110% of the rMT, using the Magstim BiStim2. The coil was held tangentially to the scalp to induce a lateral-anterior to medial-posterior current in the brain. Anatomically, the site was located in the antero-ventral aspect of the precentral gyrus at the border with the pars opercularis of the inferior frontal gyrus (Brodmann's area 6/44), identified at Talairach

coordinates $x = -52$; $y = 10$; $z = 24$ (Avenanti et al., 2013a). Their projection on the brain surface estimated by means of the neuro-navigation system corresponded to (Mean \pm SD) $x = -53 \pm 2$; $y = 10 \pm 0.9$; $z = 24 \pm 1.6$. M1 stimulation settings were identical to those of the testing phase.

ccPAS is expected to be effective when the relevant connection is repeatedly activated in compliance with its physiological constraints. Therefore, to optimally activate the PMv-M1 connection, each pulse of a ccPAS cycle was delivered with parameters in accordance to previous dual-site TMS studies (Davare et al., 2009; Mars et al., 2009; Buch et al., 2010) which demonstrated interactions between these areas at rest when delivering a pulse over PMv, at 110% of the rMT, 8 ms before (interpulse interval; IPI) M1 suprathreshold pulse. In keeping, the PMv-to-M1 ccPAS group that repeatedly received a PMv pulse followed by a M1 pulse with 8 ms IPI, meeting the physiological constraints of the connection, was conceived to strengthen the PMv-M1 connectivity (Buch et al., 2011; Johnen et al., 2015) and thus enhance MR. In opposition, the M1-to-PMv group received an inverse stimulation being M1 activated 8 ms before PMv, that is a configuration shown to lead to a dumping of physiological PMv-M1 effects (Buch et al., 2011). Therefore, one could expect a correspondent decrease in MR following such ccPAS, however, this correspondence is not obvious on a functional level (Fiori et al., submitted), still it may represent an ideal control condition for IPI. In the third group (SHAM) the PMv-to-M1 ccPAS was administrated with the coils tilted for inducing an ineffective stimulation, thus controlling for captious variables such as unspecific TMS effect.

Overall the active ccPAS configurations reproduced that of previous studies (Buch et al., 2011; Johnen et al., 2015) that successfully manipulated PMv-M1 connectivity. However, two points are worth of clarification. In the present experiment, a TMS device that generates a biphasic waveform pulse was used to stimulate M1; to overcome this potential ambiguity, we rotated the coil in order that the second and most effective phase of the pulse induced a posterior-to-anterior current in the brain, thus matching that used in the cited previous studies, and nevertheless, this adjustment has been shown to be effective by another study of our lab (Fiori et al. submitted). Concerning the second point, ccPAS

cycles were delivered at a higher rate (0.13 Hz vs 0.1 Hz), a variation introduced to maintain consistency between the ccPAS and the testing phase were pulses were randomly delivered at an average ITI of 7 s (see Apparatus and Stimuli section). Although targeting parietal areas and M1, ccPAS protocols administrated with cycles faster than 0.1 Hz have been reported by previous literature (Koch et al., 2013; Veniero et al., 2013; Chao et al., 2015). The rationale of a relatively long ITI (i.e. at least 5 s) is that no temporal summation of the ccPAS cycles (leading to a sort of repetitive-TMS protocol) must be ensured.

Data analysis

EMG signal analysis was conducted through a MATLAB script. For MEP analysis, the peak-to-peak amplitude was extracted computing the maximum and the minimum values in the time window between 15 and 60 ms after the spTMS. Since background EMG activity is known to modulate MEP amplitudes (Devanne et al., 1997) muscular activity before the TMS pulse was estimated by calculating the mean rectified signal 100 ms prior to TMS. MEPs with amplitude < 0.1 mV and MEPs with preceding background EMG deviating from the mean of the relative session for either the mean rectified or the peak-to-peak indices by more than 2 S.D., were removed from further analysis (21%).

Raw peak-to-peak MEP data acquired during the REST condition were submitted to a 2 x 3 x 3 mixed ANOVA with Muscle (FDI, ADM) and Session (PRE, POST0, POST20) as within group conditions and Stimulation (PMv-to-M1, M1-to-PMv, Sham) as between group condition. ANOVA showed no significant effects (see Results).

In order to assess the occurrence of motor resonance phenomenon in the OBS condition before any ccPAS intervention (Session PRE), a preliminary 2 x 2 x 3 mixed ANOVA with Muscle (FDI, ADM) and Movement (IND, LIT) as within group conditions and Stimulation (PMv-to-M1, M1-to-PMv, Sham) as between group condition was performed on normalised data; specifically, the mean MEP amplitude of each muscle was expressed as the ratio of the mean MEPs amplitude determined for the REST of the same session, as follows:

$$\frac{\text{Mean(OBS)}}{\text{Mean(REST)}}$$

To test whether ccPAS altered the muscle-specific sensitivity in the OBS condition, a sensitivity index of motor resonance was calculated across time for each muscle by subtracting the average MEP recorded during the non-agonist movement to that of the agonist movement (i.e. $\text{FDI}_{\text{ind}} - \text{FDI}_{\text{lit}}$; $\text{ADM}_{\text{lit}} - \text{ADM}_{\text{ind}}$) and dividing this difference to the square root of the mean of the variance of these two conditions, as follows:

$$\frac{\text{Mean}(\text{MEP}_{\text{agonist}}) - \text{Mean}(\text{MEP}_{\text{nonagonist}})}{\sqrt{\frac{\sigma^2(\text{MEP}_{\text{agonist}}) + \sigma^2(\text{MEP}_{\text{nonagonist}})}{2}}}$$

D' transformed data were analysed through a 2 x 3 x 3 mixed ANOVA with Muscle (FDI, ADM) and Session (PRE, POST0, POST20) as within group conditions and Stimulation (PMv-to-M1, M1-to-PMv, Sham) as between group condition. Finally, for each subject an index of muscle-specific sensitivity modulation was computed by averaging the muscles and then subtracting the transformed D' values of POST0 to those of PRE session, as follows:

$$\text{Mean}(D'_{\text{POST0}}) - \text{Mean}(D'_{\text{PRE}})$$

Planned two-tailed Student's t-tests for independent samples were conducted comparing the modulation index of the 3 groups of stimulation (i.e. PMv-to-M1 vs. M1-to-PMv; M1-to-PMv vs. Sham; PMv-to-M1 vs. Sham).

Statistical analyses were performed using the STATISTICA software (version 12; StatSoft Inc., 2014). ANOVA post hoc analyses were performed with the Duncan test; results were considered significant with $p < 0.05$.

4.3 Results

Rest condition

A mixed ANOVA was performed on raw data of MEP amplitude to verify that M1 excitability per se was not altered across time. The analysis with factors Muscle x Session x Stimulation showed neither main effects nor interactions ($p > 0.13$), indicating that ccPAS did not alter M1 excitability per se.

Observation condition

The mixed ANOVA conducted on normalised data of MEP amplitude collected during the observation condition before ccPAS with factors Muscle, Movement and Stimulation showed a significant interaction between Muscle and Movement ($F_{1,42} = 17.1$, $p < 0.001$), indexing the motor resonance phenomenon. Post hoc analysis revealed that when the observed movement was congruent to the muscle, MEPs were higher ($FDI_{IND} 109 \pm 31\%$; $ADM_{LIT} 106 \pm 24\%$) compared to the incongruent movement ($FDI_{LIT} 101 \pm 22\%$; $ADM_{IND} 99 \pm 24\%$) for both FDI ($p = 0.003$) and ADM muscle ($p = 0.017$). No other main effects nor interactions resulted significant ($p > 0.42$), hence assuring comparability of motor resonance phenomenon across the groups of stimulation before the ccPAS intervention.

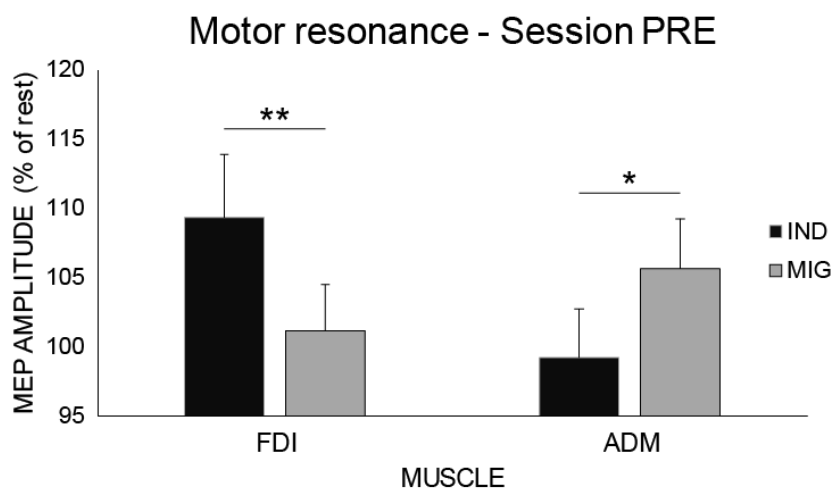


Fig.4.2 Motor resonance at before ccPAS intervention (PRE). Chart representing the Muscle x Movement interaction, no significant differences between groups of stimulation are observable. Error bars denote s.e.m., asterisks indicate significant post-hoc comparisons ($*p < 0.05$, $**P < 0.01$).

| | PMv-to-M1 | | M1-to-PMv | | Sham | |
|------------|------------------------------|------------------------------|------------------------------|------------------------------|------------------------------|------------------------------|
| | IND | MIG | IND | MIG | IND | MIG |
| FDI | 114 ± 35% (1.01 ± .34 mV) | 103 ± 21% (1.01 ± .34 mV) | 114 ± 34% (1.18 ± .39 mV) | 102 ± 25% (1.05 ± .29 mV) | 101 ± 22% (1.11 ± .23 mV) | 98 ± 21% (1.08 ± .22 mV) |
| ADM | 101 ± 32% (.75 ± .50 mV) | 105 ± 33% (.76 ± .49 mV) | 103 ± 21% (.88 ± .58 mV) | 110 ± 21% (.90 ± .57 mV) | 94 ± 17% (1.09 ± .77 mV) | 102 ± 15% (1.16 ± .78 mV) |

Table 4.1 Values of MEP amplitudes expressed as percentage of rest across groups, before ccPAS.

In the present experiment we operationalised motor resonance in a signal detection theory framework. Motor facilitation should be sensitive enough to distinguish on the basis of its activity between two different observed actions. An optimal muscular specific tuning of the onlooker's system would maximise the sensitivity of motor representations to discriminate between the observation of a compatible action (signal) and an incompatible action (noise). For this reason we transformed data in d' values and considered them as an index of sensitivity of FDI and ADM representations during action observation, in other words, motor resonance.

To test changes in motor resonance, a Muscle x Session x Stimulation mixed ANOVA was performed on the D' index. The analysis revealed only a significant interaction Session x Stimulation ($F_{4,84} = 3.59$, $p = 0.009$), that indicate a change of muscle-specific sensitivity over time depending on the stimulation applied, while others effect did not reach the significance threshold ($p > 0.16$). Post hoc analyses of the significant interaction revealed that if compared to Session PRE, the PMv-to-M1 stimulation led to enhanced motor resonance (POST0; $p = 0.005$) such effect was no longer present after 20 minutes (POST20; $p = 0.67$). Motor resonance values remained unaltered after the M1-to-PMv ($p > 0.25$) and the fictitious Sham ($p > 0.91$) stimulations. Moreover, whilst the sensitivity of the three groups of ccPAS was comparable in the session PRE ($p > 0.41$) PMv-to-M1 group of ccPAS, differed significantly from both the M1-to-PMv ($p = 0.009$) and the Sham ($p = 0.044$) groups in the POST0 session. These results demonstrate that PMv-to-M1 ccPAS, empowering PMv-M1 connectivity, strengthened motor resonance phenomenon.

Muscle-specific sensitivity

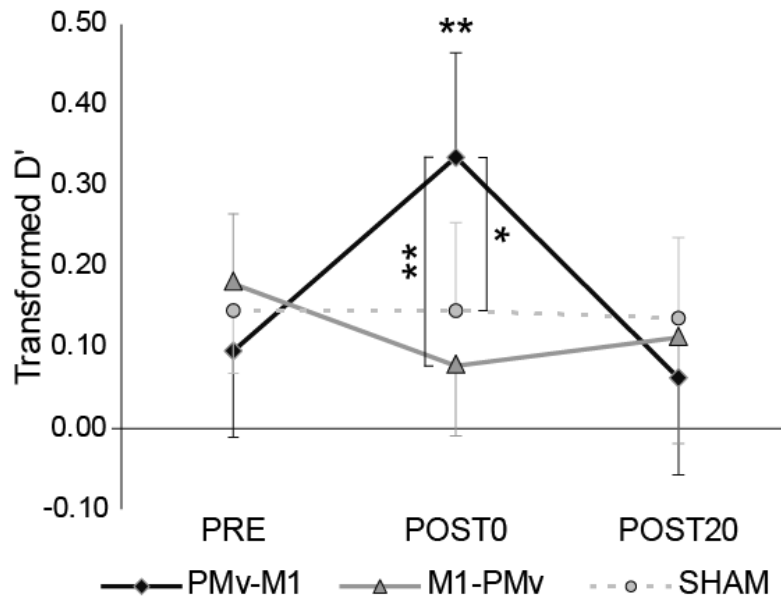


Fig.4.2 Chart represents the Session x Stimulation interaction. Error bars denote s.e.m., asterisks indicate significant post-hoc comparisons (* $p < 0.05$, ** $P < 0.01$).

In line with our hypothesis, the main ANOVA highlighted a dramatic change in muscle-specific sensitivity occurring at POST0 as a function of the ccPAS setup applied. Planned t-tests were conducted to compare the magnitude and the direction of the modulation between the three groups of stimulation. Analyses revealed that PMv-to-M1 and M1-to-PMv ccPAS showed a different modulatory effect ($t = 4.09$, $df = 28$, $p < 0.001$), the first setup increased the muscle-specific sensitivity ($+0.24 \pm 0.23$) while the latter slightly decreased it (-0.1 ± 0.22). PMv-to-M1 modulatory effect also differed from the Sham ccPAS setup ($t = 2.54$, $df = 28$, $p = 0.017$) that had no effect on the sensitivity (0 ± 0.28). Modulations of M1-to-PMv and Sham groups did not differ each other ($t = 1.09$, $df = 28$, $p = 0.28$).

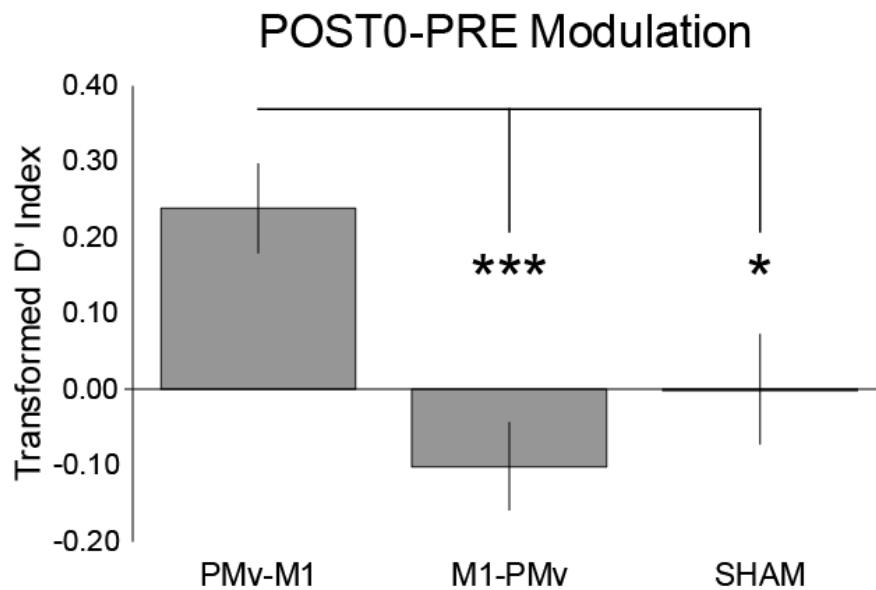


Fig.4.3 Index of ccPAS modulation at POST0. Error bars denote s.e.m., asterisks indicate significant t-test comparisons (* $p < 0.05$, *** $P < 0.001$).

4.4 Discussion

We studied the impact of ccPAS induced changes in the synaptic association between the PMv and M1, frontal motor nodes of the AON, on the M1 neurophysiological response to the observation of other's movement as probed by spTMS, i.e. the motor resonance phenomenon. Participants presented with brief clips displaying simple hand movements of the right index or little finger showed a modulation of left M1 activity specifically tuned to the movement observed. Changes in motor resonance were observed immediately after the ccPAS administration for the PMv-to-M1 group of stimulation. This ccPAS setup, aimed at strengthening the PMv-M1 connectivity, led to enhanced motor resonance. Importantly, this effect was due neither to a mere consequence of TMS nor to unspecific TMS reactions, as a matter of fact, motor resonance was unaltered after either the stimulation of the same areas in reversed order (M1-to-PMv group) or ineffective ccPAS application (SHAM group).

The motor resonance, evidenced by the analysis of the corticospinal excitability evoked by spTMS of M1 during passive action observation, has been regarded as a physiological index of the embodiment of the seen action (Fadiga et al., 1995, 2005; Naish et al., 2014) and is allegedly prompted by the

processing of the AON, and directly from its frontal core area, PMv (Hari et al., 1998; Nishitani and Hari, 2000; Avenanti et al., 2007). Motor resonance is recognised as a rather convincing evidence of action observation processing considering also its dependence on the individual way of performing the motor act (Montagna et al., 2005), reflecting an individual experienced-based coupling between execution and observation as blatantly highlighted by counter-mirror training paradigms (Catmur et al., 2007, 2011). In keeping, the stimuli presented in the current experiment were conceived to elicit interindividual unambiguous motor response, to make sure that every participant would have executed the observed action in a similar manner, that is requiring the highest involvement of the agonist muscles of the movement observed. Another key feature of motor resonance is its occurrence regardless of the spatial compatibility between the observed and the observer's effector position during a movement, to demonstrate that the observed action is topographically mapped onto the observer's motor system (Urgesi et al., 2006). In accordance, the stimuli were presented rotated in either directions by 90 degrees with respect to the first-person perspective and the posture of participants' hand, therefore excluding an interpretation of our effects as due to a PMv-M1 connectivity role in spatial compatibility functions.

The importance of the present study resides in the test-bed demonstration that the novel ccPAS protocol may represent a pivotal technique instrumental not only to change mere patterns of physiological interactions between cortical areas, but also to modulate essential high cognitive functions, here, the processing of other's actions. To address this point, we focused on the well-known connectivity of the PMv-M1 circuitry. Anatomical and physiological studies on the connectivity between the homologue PMv area of monkeys and M1 showed that it consists of dense glutamatergic cortico-cortical projections (Muakkassa and Strick, 1979; Tokuno and Nambu, 2000; Cerri et al., 2003; Shimazu et al., 2004; Dum and Strick, 2005) through which the first exerts a powerful influence on the latter's activity (Shimazu et al., 2004). In humans dual-site TMS (dsTMS) studies tested the characteristics of the PMv-M1 interactions at rest (Davare et al., 2008; Bäumer et al., 2009). Moreover, this connectivity at an IPI of 8 ms has been related to several cognitive tasks, proving its crucial role in implementing

hand shaping for overt movements during action execution (Davare et al., 2008), action planning (Davare et al., 2009; Buch et al., 2010), and action reprogramming (Neubert et al., 2010), as well as for covert movements during action observation as connecting the late nodes of the AON (Koch et al., 2010; Catmur et al., 2011).

Effects of motor resonance modulation were obtained through the repetitive activation of the neural pathway linking PMv to M1 able to induce phenomena of plasticity that resembles those of Hebbian learning for cause modalities and outcomes. According to Hebbian principles, synapses increase their efficacy when the presynaptic neuron repeatedly assists the postsynaptic target neuron in the generation of action potentials (Hebb, 1949; Caporale and Dan, 2008). This LTP mechanisms of STDP represents the neural basis of plastic adaptation and implies the concepts of persistence, intended as consistency of firing, and causality, defined as temporal consequentiality (Keysers and Gazzola, 2014). By inverting the temporal order of the inputs (i.e. post-pre), STDP may also result in a net weakening of synaptic efficacy denoting phenomena of LTD (Levy and Steward, 1983; Keysers and Gazzola, 2014). In compliance with the rules of the STDP mechanism, the ccPAS protocol may selectively enhance or weaken the synaptic efficacy of cortico-cortical connections if the physiological constraints are met (Romei et al., 2016b). ccPAS induced plastic changes have been shown in the motor (Koganemaru et al., 2009; Rizzo et al., 2009; Buch et al., 2011; Veniero et al., 2013; Johnen et al., 2015) and in the visual system (Romei et al., 2016a) following the repetitive activation through TMS of the anatomical neural pathway connecting the targeted regions with an optimal IPI. IPI determines the temporal order which cues the directionality of the stimulation.

We administered ccPAS with the optimal settings to activate PMv-M1 connectivity as informed by dsTMS reporting both inhibition at rest (Davare et al., 2008; Buch et al., 2010) and facilitation during action observation (Catmur et al., 2011). Assuming a hierarchy in the PMv-M1 flow of information (Nishitani and Hari, 2000; Avenanti et al., 2007), in the present experiment we conceptualised PMv as the pre- and M1 as the post-synaptic node of the cortical route tested. For this reason, we expected to

induce an LTP-like effect with the PMv-to-M1 ccPAS setup. It was unclear whether an LTD-like plasticity could be obtained using the M1-to-PMv ccPAS setup. Proof of principle of this protocol efficacy in inducing plastic changes in the PMv-M1 pathway is represented by a neurophysiological study (Buch et al., 2011) that probed with a dsTMS paradigm PMv-M1 interactions before and after the application of the ccPAS protocol and were further corroborated by neuroimaging evidence reporting improved functional connectivity between the targeted areas (Johnen et al., 2015). Buch and colleagues (Buch et al., 2011) showed the emergency of LTP-like mechanisms after PMv-to-M1 ccPAS during both rest and action planning conditions. They also reported a veiled reduction of M1 output measured after the application of M1-to-PMv ccPAS setup that is ascribable to diminished PMv-M1 connectivity following LTD-like mechanisms. Nonetheless this setup had no significant effects on spTMS trials, and no behavioural effect in another study conducted in our laboratories (Fiori, in press). It is arguable that the subtle changes reported by Buch's group can be uncovered only by very sensitive measures. Here we report no substantial modulatory effect of this setup even though motor resonance values are slightly reduced. However, this null result represents a valid control condition ruling out explanations of the experimental effects that account for mere effects of areas stimulation or timing.

Information about the optimal ccPAS setup are mainly based on evidence of cortico-cortical interactions uncovered at rest by means of the dsTMS paradigm. The cognitive state of the participant is a remarkable factor; although administered at rest, ccPAS had no effect on M1 excitability probed at rest, while it was only affected during the observation condition. In line with our results, Buch and co-workers (Buch et al., 2011) reported no modulation of spTMS over M1 at rest but increased MEP amplitudes in the task condition (i.e. movement preparation). Noteworthy, if the ccPAS had a simple effect on the function, one would expect to induce an aftereffect in accordance with the sign of the connectivity boosted as revealed by dsTMS. Hence, in the case of LTP-like induction at rest, the inhibitory PMv-M1 connectivity boost would predict enhanced inhibitory interactions at rest and, eventually, reduced facilitation during action observation. In contrast, the effects have no regard of the cognitive state at the time of plasticity induction; The expression of the modulation was indeed

dependent on the cognitive state of the subject at the time of testing, therefore accounting for a mere empowering of the transmission of the information encoded by PMv and conveyed to M1.

Neurons with mirror-like characteristics recently observed in macaque M1 (Dushanova and Donoghue, 2010; Kraskov et al., 2014) suggest that the motor resonance phenomenon probed by spTMS may be explained by this class of M1 neurons, thus excluding a cortico-cortical modulation of PMv mirror activity. On account, dsTMS experiment reporting a modulation of corticospinal excitability during action observation (Koch et al., 2010; Catmur et al., 2011) are subject to explanations that involve the influence exerted by part of PMv projections, directly onto descending M1 pyramidal tract neurons (Kraskov et al., 2009), thus implying a subcortical instead of a cortical modulation. As a matter of fact, evidence supports the view that ccPAS (Koganemaru et al., 2009; Rizzo et al., 2009; Chao et al., 2015) and the analogous perifero-cortical PAS (Stefan et al., 2000; Di Lazzaro et al., 2009a, 2009b; Müller-Dahlhaus et al., 2010) operate at a cortical level. We therefore affirm that M1 output change induced by PMv-to-M1 ccPAS is the result of the modulation of the cortical PMv-M1 connectivity that acquires a causal role in the transmission of information encoded by the AON.

It is to determine whether the modulation of motor resonance was uniquely due to an improved synaptic efficacy in the circuit PMv-M1 or if they were consequence of a broader modification of connectivity weights in the wider action observation stream. Very similar parameters to the present PMv-to-M1 ccPAS were used in the fMRI study by Johnen and colleagues (Johnen et al., 2015) that reported increased functional connectivity in the connection targeted, as well as among the broader “dorsolateral network” for motor programming in which the targeted areas are encompassed (Turella and Lingnau, 2014). Accordingly, we demonstrate that the modulation of the motor resonance phenomenon we have induced was consequence of the repetitive PMv-M1 connectivity activation and one may argue that it was not only due to a change in the PMv-M1 information flow, but also to an altered connectivity affecting the other nodes of the wider AON. In keeping, it has been shown that, after interferent TMS, compensatory plasticity may occur in the network nodes other than the

stimulated ones, suggesting a redistribution of functional weights aimed at compensating the artificially-induced imbalance (O'Shea et al., 2007; Hartwigsen et al., 2012; Avenanti et al., 2013a).

Here we demonstrate the potentiality of selectively foster the information processed by PMv and affecting M1 and thus the possibility to exogenously regulate the internal motor simulation of the observed action prompted by the activity of the AON. The physiological approach used here show an appreciable effect of ccPAS, being effective in modifying the AON response to the observation of simple human movements, nonetheless, data in support of a behavioural change in the processing of observed actions are lacking. It is unlikely that the simple stimuli used here may provoke a notable behavioural effect in the normal population, perhaps more complex stimuli would be more appropriate to highlight behavioural changes. Nevertheless, this study may pave the way to future research aimed at testing the physiological and behavioural effects of prolonged PMv-to-M1 ccPAS sessions either in neurological patients suffering from neural lesions and disconnection syndromes or in population with pathological conditions exhibiting impairments in the sphere of the social cognition.

CHAPTER V

Strengthening PMv-STS feedback projections enhances action prediction accuracy

5.1 Introduction

When we observe other people, we represent and understand their actions once deployed, but also, we tend to predict the outcomes of these actions whilst being executed. The ability of foreseeing other's initiated actions could represent an enormous advantage for the human being, in terms of preservation of the individual (e.g. fights) and in the social context of everyday life (e.g. cooperative actions, sports), since enables to anticipate rather than react to others' movements. The neural substrate of this process has been suggested by neuroimaging studies (Grafton et al., 1996; Buccino et al., 2001; Chong et al., 2008; Gazzola and Keysers, 2009; Kilner et al., 2009; Caspers et al., 2010), that highlighted the compelling engagement of a system named Action Observation Network (AON) during the observation of other people actions, and includes the superior temporal sulcus (STS), the inferior parietal lobule (IPL) and the ventral premotor cortex (PMv). Compelling evidence demonstrate that this system internally simulates the observed actions anticipating the forthcoming sensory outcome (Kilner et al., 2004; Aglioti et al., 2008; Urgesi et al., 2010; Abreu et al., 2012; Avenanti et al., 2013b, 2017; Makris and Urgesi, 2013). Since the early stages, the transformation of the sensory inputs of an observed action leads the onlooker to activate those internal motor representations engaged for executing the same action (Fadiga et al., 2005; Gazzola and Keysers, 2009; Avenanti et al., 2013b; Paracampo et al., 2016). In keeping with the concept that action perception compels a close relationship between action and sensation, it has been suggested that the this system has emerged from the Hebbian associations implemented during motor execution since the early stages of individuals' life (Heyes, 2001; Keysers and Perrett, 2004; Catmur et al., 2007; Keysers and Gazzola, 2014). This prefigures the development of internal models that bridge motor commands to sensory outcomes and vice versa in execution and observation, respectively. Therefore well experienced actions

rather than untrained (Calvo-Merino et al., 2005; Cross et al., 2013; Makris and Urgesi, 2013), or impossible (Costantini et al., 2005; Avenanti et al., 2007), will preferentially activate AON simulative processes when observed leading to more accurate predictions (Hecht et al., 2001; Graf et al., 2007; Aglioti et al., 2008; Urgesi et al., 2012).

These concepts have been framed within the predictive coding account (Kilner et al., 2007a, 2007b; Friston et al., 2011). During action execution the internal models are thought to involve two competitive processes; the forward model allows the agent to predict sensory and proprioceptive consequences of the movement being implemented, while the inverse model selects the motor command to be carried out to achieve a desired end-state (Wolpert et al., 2003). During observation, the simulation of these processes occurs in reversed order, it is triggered by the subthreshold activation of the motor command that best matches the observed sensory input and is actively inferred through the inverse model. The subsequent engagement of the forward model allows the observer to predict the sensory consequences of that command and thus of the ongoing observed action (Wilson and Knoblich, 2005; Gazzola and Keysers, 2009). In this framework, the AON is conceptualized as an anticipation device that provides sensory outcomes inferring the most likely cause of an action by reducing the prediction error, thanks to recurrent interactions among the areas of the system (Kilner et al., 2007b; Friston et al., 2011). This functioning of the AON cannot rely just on the elaboration of isolated areas, rather the feed-forward and -backward flow of information (Schippers and Keysers, 2011; Gardner et al., 2015) that reciprocally interlaces the hubs of the AON circuit and is granted by dense anatomical connections (Hecht et al., 2013; Borra and Luppino, 2016) plays a leading role. In this dynamic theorization of the AON the feed-forward STS→IPL→PMv connectivity conveys the visual information from the perceptual reality that, through sensorimotor transformations, is mapped onto motor commands, while the feed-back PMv→IPL→STS connectivity generates the upcoming sensory consequences of the action and compare them to the incoming inputs from the perceptual reality in STS (Gazzola and Keysers, 2009). If a mismatch is detected, the feed-forward stream will send a prediction error that allow the refinement of the motor command selection and will therefore lead to update the prediction (Kilner et al., 2007b;

Friston et al., 2011). This theorisation is compatible with the findings of Schippers and Keysers (2011) that, during the observation of a predictable action, showed how the initial feedforward flow of information is stopped while the feedback flow takes over. Gardner et al. (Gardner et al., 2015) reported a dampening of effective connectivity in the feedforward flow for STS→IPL and a non-significant dampening for IPL→PMv viewing familiar, compared to unfamiliar, observed actions. These findings are compatible with the notion of decreased prediction error and decreased sensory input for well experienced and thus more predictable actions (Schippers and Keysers, 2011). However, data also showed dampened effective connectivity for IPL→STS feedback flow in the same condition. These controversial findings partially support the predictive coding assumptions, still, they provide only correlational and inconclusive evidence, therefore a more direct approach.

To address this issue, we aimed to manipulate the AON feedback connectivity to test the impact on the predictive abilities of healthy individuals. If the predictive coding model accurately reflects the processing that brings the individual to predict the consequences of other's actions, then boosting the feedback connectivity should empower the comparison processing between the internal model and the sensory input of the perceptual reality and thus lead to a more accurate prediction of the ongoing observed action. The final goal of the present study is to demonstrate that increasing the feedback flow of information can improve the accuracy in the prediction of other people's action.

To achieve our purpose, we took advantage of a transcranial magnetic stimulation (TMS) protocol called cortico-cortical paired associative stimulation (ccPAS; Koganemaru et al., 2009; Rizzo et al., 2009) that is thought to mimic on physiologically interconnected neural populations those mechanisms of spike timing dependent plasticity (STDP) demonstrated in neural cells (see Bi and Poo, 2001; Caporale and Dan, 2008). In keeping, ccPAS delivered using configurations that comply with the Hebbian rules (Hebb, 1949; Keysers and Gazzola, 2014; Romei et al., 2016b) lead to neurophysiological and behavioural changes that are consistent with an alteration of the information flows between the targeted cortical sites. This protocol has been shown to cause both in motor areas part of the AON (Chiappini and

Avenanti, 2018) and in visual areas (Romei et al., 2016a) phenomena resembling long-term potentiation (LTP-like). Hence, the goal of the present study is to enhance the behavioural expression of a functional connectivity by empowering the information flow in the underlying anatomical connection. Specifically, we aim to apply ccPAS to a hybrid motor-visual connection, namely PMv→STS, and test the consequences of such modulation on the behavioural performance at a human action prediction task.

5.2 Methods

Sample

Seventy right handed participants with normal or corrected-to-normal vision (38 females) aged 18-33 years took part in the study. None of them suffered from medical conditions or contraindication to TMS. The local ethic committee in accordance with the Declaration of Helsinki approved experiment procedures and participants gave written informed consent before taking part to it.

Design

Participants were tested for their accuracy in an action prediction task (AP) and in a non-human prediction task (nHP), before and in 3 timepoints after (0, 20 and 40 min) the end of a session of ccPAS (see Fig.5.1, panel A). Before the beginning of the experimental procedure each participant was randomly assigned to one of the six ccPAS conditions (see Fig.5.1, panel B) and underwent a session of familiarisation for both tasks. The order of the tasks (i.e. AP-nHP or nHP-AP) was counterbalanced across participants.

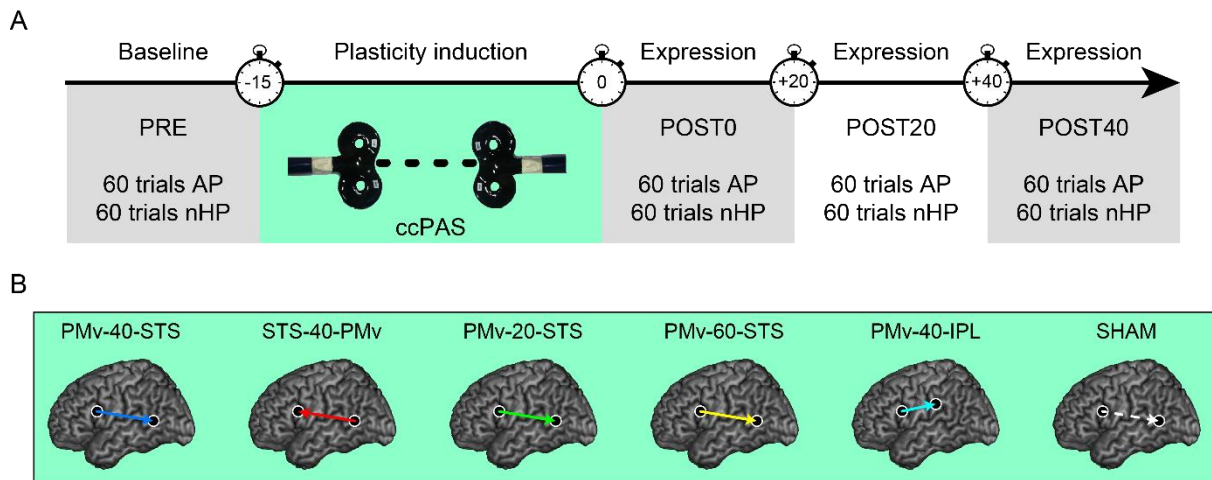


Fig.5.1 Experiment timeline (A) and schematic representation of ccPAS configurations applied during the plasticity induction phase (B).

Task & stimuli

In the action prediction task (AP), participants were asked to observe 60 clips (640 x 480 pixels, 30 fps) representing a human right hand reaching for one of two possible objects of common use. Each clip begins with the hand resting on a plane surface (right side of the screen), that after a variable delay (1000-2000 ms), started a reach-and-grasp movement towards one of the two objects (left side of the screen) placed at ~45 cm from the hand starting position on the same surface, one to the right and the other to the left of the hand midline, still, very close one another. However, only a portion of the complete movement was shown (from 30 to 70% of the movement duration), the last sequences of the action were indeed occluded and a random dot screen appeared (150 ms). A response screen (until response) asked the observer to guess which one of the two objects was going to be grasped by the actor's hand. The objects placed to the left and to the right of the hand were depicted below the question always on the left and on the right of the screen, respectively. Participants had to express their decision by pressing one of two computer keys always in spatial accordance with the objects position (i.e. left key - left object and right key - right object). Video clips included 8 nonprofessional actors (4 females; 23.6 ± 1.1 years of age) getting 8 different pairs of objects (i.e., lighter vs. plastic cup; highlighter vs. corkscrew; deodorant spray vs. coffeepot; mug vs. book; clothespin vs. nutcracker;

spatula vs. tea cup; little ball vs. big ball; fork vs. stapler) that required different affordances, implying different grips (power vs. precision). Since the hand-object interaction was occluded this task tapped onto the processing of the kinematic cues (i.e. hand trajectory, hand shaping) to discriminate the forthcoming grasped object (see Fig.5.2, panel A-C).

The non-human prediction task (NP) was conceived to reproduce as faithfully as possible the AP task, thus maintaining the concept, the temporal structure and the technical features but the stimuli were represented by irregular polygons instead of hands/objects, to animate a movement undoubtedly non-biological. In 60 videoclips, generated using the Adobe Flash Professional software, a black form on the right of the screen moved towards one of two forms placed on the left of the screen and the displacement was interrupted at 30-70% of the movement duration. Participants were asked to predict which of the two left-side forms was going to be joined and fitted by pressing one of two possible keys, as in the AP task, the targets placed to the right and to the left of the black shape were always placed on the right and the left of the response screen respectively, and there was spatial accordance between them and the response keys (i.e. left key - left target and right key - right target). Stimuli for the targets included 8 different pairs of forms associated to 8 different black moving forms. The trajectories of the black forms during the animation were developed to grossly reproduce those of the hands in the AP task. Analogously, the shape of the black form could change a little during the displacement to assume a configuration that could optimally match one of the two possible targets, mimicking the shaping of the fingers occurring in the AP task (see Fig.5.2, panel D-F).

Both the tasks were already used in previous study conducted in our lab and the stimuli were selected throughout a validation process. The final set of stimuli included 60 AP and 60 nHP clips (30 requiring left response + 30 right response) having an average of correct recognition of ~75%, based on the score of 51 subjects tested.

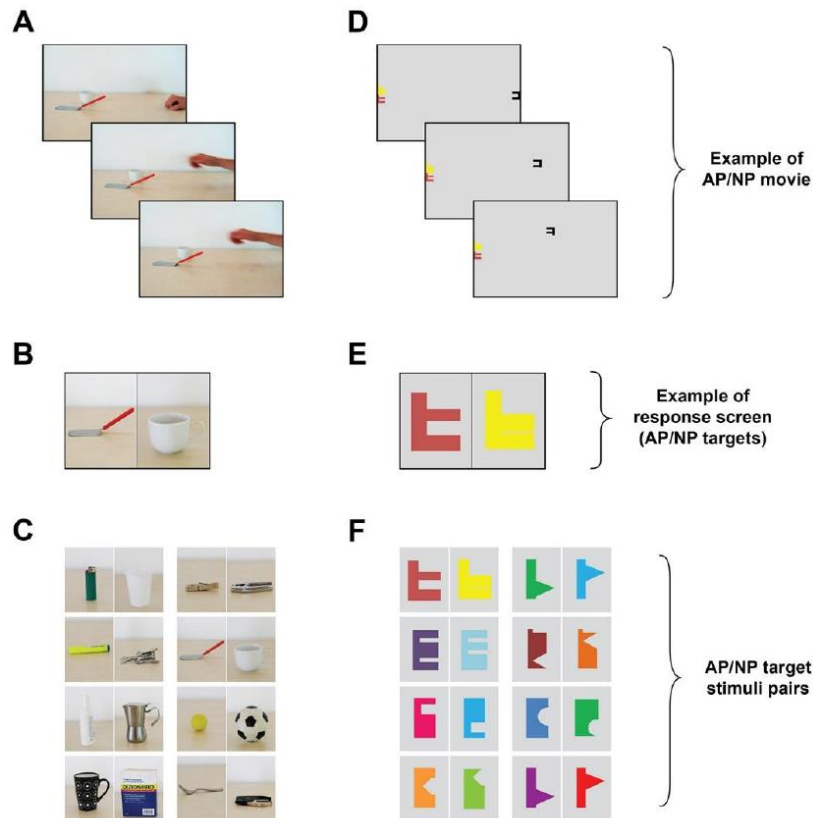


Fig.5.2 Trials and stimuli. Hands (A) or black forms (D) moved towards one of the two possible targets (B, E), whilst assuming an optimal configuration to join the target. A) example of an AP task trial; D) Example of nHP trial. B) Pair of possible AP targets; E) Pair of possible nHP targets. C) AP stimuli used, in pairs; F) nHP stimuli used, in pairs

ccPAS and sites localisation

We administered ccPAS over two cortical areas of the left hemisphere via two figure-of-eight coils (5 cm external wing diameter) connected to two Magstim BiStim2 (Magstim, UK) generating monophasic waveforms, aiming to repeatedly activate the cortico-cortical pathway linking the targeted areas. 90 pairs of pulses were delivered at a rate of 0.1 Hz for 15 min with an intensity of 105% of the resting motor threshold (rMT; see below).

Participants could be randomly assigned to one of the following possible configurations of ccPAS (Fig.5.1, panel B):

1. Experimental group (PMv-40-STS), first pulse to PMv second to STS, ISI of 40 ms
2. Control group order (STS-40-STS), first pulse to STS second to PMv, ISI of 40 ms. This configuration allowed to exclude effects due to the order of the pulses.

3. Control group ISI-long (PMv-60-STS), first pulse to PMv second to STS, ISI of 60 ms. This configuration controlled for the optimal ISI to activate the PMv-STS pathway.
4. Control group ISI-short (PMv-20-STS), first pulse to PMv second to STS, ISI of 20 ms. This configuration further controlled for the optimal ISI to activate the PMv-STS pathway.
5. Control group area (PMv-40-IPL), first pulse to PMv second to IPL, ISI of 40 ms. This configuration controlled for the specificity of the pathway at a determined ISI.

In a further group (SHAM) of 14 additional participants (8 females, age 19-27 years) we controlled for any unspecific TMS or tasks practice effect; the experiment procedure was identical to other groups, and a PMv-40-STS ccPAS was administered, however, the coils were held perpendicular to prevent TMS interaction with participant's brain.

In the experimental group, the ISI of 40 ms was selected as the optimal timing to activate the PMv-STS connection based on preliminary data collected in our lab using transcranial evoked potentials (TEPs). Single TMS pulses were delivered at rest over PMv at 105% of the rMT, while an electroencephalographic (EEG) system recorded the electrophysiological response of the brain. The analyses revealed a response change compared to sham TMS at ~40 ms over the T7, TP7, P7 electrodes of the 10-20 EEG system, corresponding to the posterior portion of STS, as confirmed by a sLORETA source analysis, suggesting a PMv-STS interaction at this timing.

In order to stimulate efficiently the targeted areas, we opted to adopt a standard parameter for the stimulation of the motor areas that is in relation with the individual rMT. We decided to stimulate all the areas above the rMT (at 105%), this allowed to keep the intensity consistent across the areas and to be consistent with our previous TMS-EEG experiment. There is no unidirectional and conclusive agreement on the optimal intensity for the stimulation of silent non-motor areas such as STS and IPL, but our strategy and intensity values are slightly below (105 vs 110% of rMT) those for other successful TMS manipulations on the action observation topic (Grossman et al., 2005; Cattaneo et al., 2010), furthermore, adopting a different arbitrary and yet unjustified intensity than that of PMv could have

caused confounding interpretations. For this reasons, before the beginning of the experiment, we assessed for each participant the rMT, defined as the minimum intensity to produce 5 out of 10 consecutive motor evoked potentials (MEPs) of at least 50 μ V with single pulses of TMS delivered over the left primary motor cortex (M1) (Rossini et al., 2015). MEPs were recorded from the relaxed right hand through surface Ag/AgCl electrodes with a belly-tendon montage, the active electrode was placed on the first dorsal interosseous muscle, the reference on the metacarpophalangeal joint of the index finger, the ground on the wrist. Electromyographic signal was band-pass filtered (30-500 Hz) and digitised at a sample rate of 20 kHz using a Biopac MP-35 (Biopac, USA), TMS pulses were delivered using a single Magstim BiStim2 device holding the coil at $\sim 45^\circ$ to the sagittal midline inducing a posterior-anterior current direction to optimally activate M1 (Kammer et al., 2001). The mean rMT \pm s.d. was $42\% \pm 7$ of the maximum output stimulator and it was consistent across groups of ccPAS.

To determine the scalp sites to stimulate during ccPAS, a SofTaxis Neuronavigation System (ElectroMedical System, IT) was used. 4 craniometric points (left & right preauricular, nasion, inion landmarks) and ~ 90 scalp points were digitally recorded thanks to a Polaris Vicra spatial digitizer (Northern Digital, CAN). This method provides an individual estimated magnetic resonance image (MRI) that is warped on the 3D digitized representation of the participant's scalp and allows to navigate the MRI in the Talairach stereotactic frame ensuring accurate localisations of the brain sites with < 5 mm of dispersion (Carducci and Brusco, 2012). We searched for the target sites at the Talairach coordinates $[x = -52, y = 10, z = 24]$ for PMv (Avenanti et al., 2012a, 2013a; Tidoni et al., 2013), $[x = -52, y = -53, z = 9]$ for STS and $[x = -52, y = -28, z = 23]$ for IPL and we marked on a tight cup the exact spot for the following stimulation depending on the ccPAS configuration applied. The coil was held at $\sim 90^\circ$ from the sagittal midline with the handle pointing forward to induce a posterior-to-anterior current in PMv, at $\sim 90^\circ$ from the sagittal midline with the handle pointing backward to induce an anterior-to-posterior current in STS and at $\sim 45^\circ$ from the sagittal midline (due to space concerns) with the handle pointing backward to induce an anterior-to-posterior current in IPL. We used the neuronavigation system to estimate the coordinates of the cortical surface of the sites that were targeted with TMS, which resulted

in (mean \pm s.d.) [$x = -53.0 \pm 2.0$, $y = 10.3 \pm 2.7$, $z = 23.0 \pm 6.9$] for PMv, [$x = -54.6 \pm 3.1$, $y = -54.4 \pm 3.6$, $z = 9.4 \pm 1.5$] for STS and [$x = -57.5 \pm 3.1$, $y = -25.6 \pm 1.5$, $z = 24.8 \pm 2.0$] for IPL.

Data analysis

To check for eventual baseline differences across groups and to verify that participants scored overall a performance in line with the data obtained in the validation phase (~75%) for both the AP and the nHP tasks, a preliminary analysis was conducted on the accuracy rates of all the participants assigned to the 5 groups and the sixth SHAM group (84 subjects), before ccPAS (PRE). A 2 x 6 mixed ANOVA with the factors Task (AP, nHP) as within subjects condition and ccPAS (PMv-40-STS, PMv-60-STS, PMv-20-STS, STS-40-PMv, PMv-40-IPL, SHAM) as a between subjects condition was conducted.

To exclude from the analysis any unspecific TMS difference and practice effects, accuracy rates of each participant were transformed to z-scores using the mean and the standard deviation values of the SHAM group (Candidi et al., 2011). These data were then entered into a 2 x 4 x 5 mixed ANOVA with the factors Task (AP, nHP) and Time (PRE, POST0, POST20, POST40) as within subjects condition and ccPAS (PMv-40-STS, PMv-60-STS, PMv-20-STS, STS-40-PMv, PMv-40-IPL) as a between subjects condition. Since this analysis showed a significant triple interaction, the main ANOVA was split by the factor Task, resulting in two 2 x 5 ANOVAs with factors Time and ccPAS. Where appropriate, t-tests corrected for multiple comparisons with the Bonferroni method were performed. Values are expressed in the form: mean \pm standard error.

5.3 Results

The preliminary Task x ccPAS ANOVA on the accuracy rates recorded before ccPAS of the 84 participants including the SHAM group, revealed no significant effects or interaction (all p s > 0.28), indicating that at baseline, all the groups of ccPAS were comparable. Furthermore, the analysis showed that participants had average accuracy rates (Table 5.1) similar to that expected based on the validation process.

| | PMv-40-STS | STS-40-PMv | PMv-20-STS | PMv-60-STS | PMv-20-IPL | SHAM |
|-----|------------|------------|------------|------------|------------|--------|
| AP | 70% ±2 | 70% ±2 | 72% ±2 | 70% ±2 | 76% ±1 | 74% ±2 |
| nHP | 71% ±5 | 70% ±4 | 72% ±2 | 72% ±4 | 78% ±2 | 74% ±3 |

Table5.1 Accuracy rates (mean ± s.e.) of the six groups of ccPAS before the stimulation.

The Task x Time x ccPAS ANOVA conducted on the corrected z-score of the accuracy, showed a main effect of Time ($F_{3,195} = 3.42$, $p = 0.012$), an interaction Task x Time ($F_{3,195} = 8.84$, $p < 0.001$), a marginally significant interaction of Time x ccPAS ($F_{12,195} = 1.78$, $p = 0.053$) and, most remarkably, the interaction Task x Time x ccPAS was significant ($F_{12,195} = 2.66$, $p = 0.003$). Neither other main effects nor interactions resulted significant (other $ps > 0.13$). The three-way interaction, indicating that different ccPAS configurations had differential effects on task performances over time, was split by the factor “Task” in two ANOVAs.

The ccPAS x Time ANOVA conducted on the corrected z-score of the accuracy of the AP task, showed a main effect of Time ($F_{3,195} = 8.81$, $p < 0.001$), and most importantly, the ccPAS x Time interaction resulted significant ($F_{12,195} = 3.05$, $p < 0.001$) indicating a change over Time of the performance depending on the ccPAS applied. The main effect of ccPAS was just marginally significant ($p = 0.062$). Post-hoc analysis showed an improvement in the accuracy index in the PMv-40-STS compared to the PRE Time (mean ± s.e.: $-48\% \pm 24\%$) at POST0 (mean ± s.e.: $93\% \pm 21\%$, $p < 0.001$), POST20 (mean ± s.e.: $80\% \pm 28\%$, $p = 0.005$) and POST40 (mean ± s.e.: $32\% \pm 22\%$, $p = 0.008$). Comparisons between the PRE and the POST times in the other groups was not significant (other $ps > 0.22$). Hence, the PMv-40-STS ccPAS was the only configuration that enhanced the performance to the AP task of the tested participants. The effect of ccPAS begin immediately after the stimulation and lasted for at least 40 min (Fig.5.3, panel A-E).

The ccPAS x Time ANOVA conducted on the corrected z-score of the accuracy of the nHP task, showed neither main effects nor interactions $p > 0.43$. This analysis shows that ccPAS did not affect subjects' performance to the nHP task, regardless of the ccPAS configuration applied (Fig.5.3, panel F).

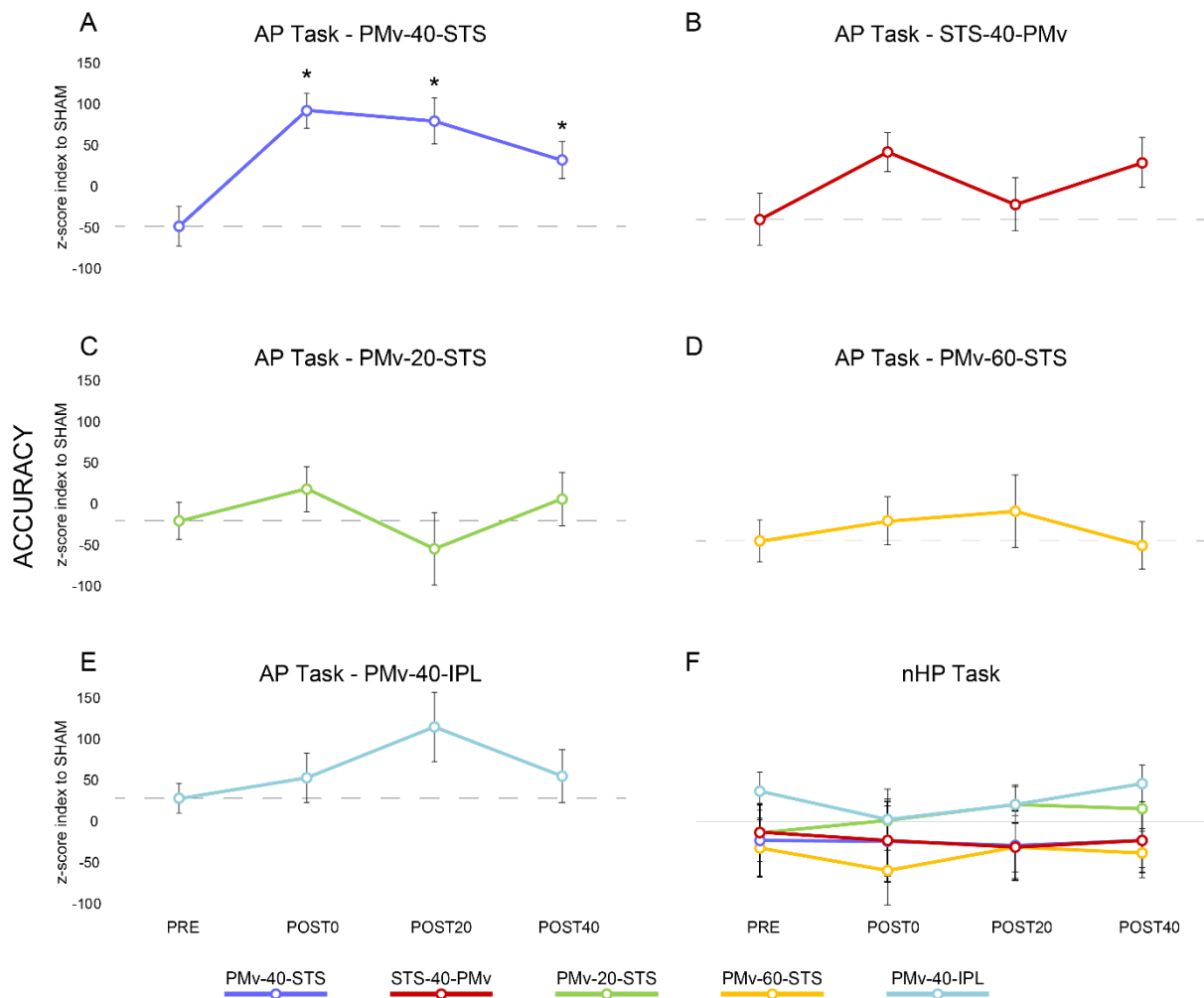


Fig.5.3 Accuracy at the tasks. A-E panels show the significant ccPAS x Time interaction in the AP task; F panel illustrates performance at the nHP task, no main effects or interactions were revealed. Error bars denote s.e.m., asterisks (*) indicate significant post-hoc comparisons versus the respective PRE session.

5.4 Discussion

This study provides evidence that the feedback connections of the AON subserve predictive functions and are amenable of ccPAS modulation. We found that the long-term exogenous potentiation between two main nodes of the AON, namely the PMv-STS connectivity, via ccPAS enhances the accuracy in predicting viewed human actions, that is the functional expression of these feedback connections, as

assumed by the predictive coding theory of action perception (Kilner et al., 2007a). Specifically, participants' behavioural performance, indexed by accuracy rates in the AP task, is boosted up to at least 40 min after a session of ccPAS with the optimal configuration to repeatedly activate the PMv-STS pathway. The AP task tapped into participants' ability to predict the possible outcome of human hands reaching and grasping an object. The selection between the two possible objects target of the movement could rely on kinematic cues of reaching direction and hand preshaping, since the last phases of the movement were occluded. No substantial behavioural modulations were reported in those subjects that underwent ccPAS with configurations that differed for the order of the stimulation (STS-40-IPL), the IPI (PMv-60-STS and PMv-20-STS), or the site of stimulation (PMv-40-IPL). In the control nHP task, tapping into the ability to predict the target of the displacement of geometrical forms, no performance changes were noticeable before and after stimulation, regardless of the ccPAS configuration applied.

The peculiar characteristic of ccPAS is that it is supposed to induce brain plasticity by mimicking those STDP mechanisms that prompt to alterations of the synaptic efficiency (Koganemaru et al., 2009; Veniero et al., 2013; Johnen et al., 2015). A crucial rule of the Hebbian learning concerns the causality of the stimulation to modulate the efficiency of the synapse (Hebb, 1949). The trademark of causality is the temporal precedence (Keysers and Gazzola, 2014), that in the present case is expressed as the IPI, that has to be optimal to allow the action potential (AP) of the pre-synaptic node to assist the AP of the postsynaptic node. Specifically, to produce LTP-like mechanisms in the PMv-to-STS connectivity we adopted 40 ms IPI that, based on data obtained in our lab (see *Methods* section), is the transfer time of the information that flows from the presynaptic (PMv) to the postsynaptic (STS) site. Therefore, knowing that the PMv neurons take part in causing action potentials in STS neurons after 40 ms, via the PMv-40-STS ccPAS we provoked repeated activations of this pathway echoing the laws of the Hebbian learning (Hebb, 1949).

From an anatomical point of view, the stimulated PMv-STS pathway is likely to be indirect. Studies from macaques (Petrides and Pandya, 2009), chimpanzees and humans (Hecht et al., 2013) show a stream of fibres that connects the caudal part of the STS with the frontal premotor cortices through the arcuate fasciculus that mingles with the fibres originating from the IPL and courses through the second and the third branches of the superior longitudinal fasciculus. This is likely a multi-synaptic pathway, mediated by anterior portion of the frontal operculum (Brodmann area 45) or the IPL in the caudal sector of the supramarginal gyrus and the angular gyrus (Petrides and Pandya, 2009; Hecht et al., 2013; Borra and Luppino, 2016). Although STDP mechanisms have been shown in monosynaptic connections (e.g. Markram et al., 1997), STDP-like modifications can be induced also in polysynaptic connections, as shown and often replicated using the first perifero-cortical PAS protocol; by repeatedly pairing the electrical stimulation of a peripheral afferent nerve with TMS over M1, a modulation of the coupling between somatosensory afferents and intrinsic motor circuits were observed with STDP-like properties (Stefan et al., 2000; Wolters et al., 2003).

Concerning the ccPAS configurations controlling for the timing, there is evidence that the presynaptic neuron must fire ~20 ms or less before the postsynaptic neuron for LTP to occur, while if the first fires 20 ms or less after the second, LTD phenomena may arise (Bi and Poo, 1998; Zhang et al., 1998). Consistently with the cited studies, we found neither changes in performance coherent with LTP-like effects when the ccPAS IPI was set at ± 20 ms around the experimental timing of 40 ms (PMv-20-STS and PMv-60-STS configurations), nor performance worsening, expression of LTD-like phenomena, after the application of ccPAS with reversed stimulation order, so that the presynaptic fired before the postsynaptic site (STS-40-PMv); it is presumable that the 40 ms latency was too long for LTD to establish. However, it should be remarked that at cellular level, the timing for LTP and LTD induction changes considerably depending on the type of synapses tested. For example, hippocampal pyramidal neurons of rats produced LTP when presynaptic occurred 15 ms before postsynaptic action potentials (APs), while LTD was induced with synchronous stimulation or with the post APs preceding pre APs by 25 to 200 ms (Debanne et al., 1998); in inhibitory synapses of rat neocortical cells, LTP was induced by

presynaptic APs arriving 410-510 ms and LTD up to 250 ms after the postsynaptic APs; in retinotectal cells of xenopus frogs, LTP occurs when the presynaptic neuron fire ~20 ms or less before the postsynaptic neuron, while if the first fires 20 ms or less after the second, LTD phenomena arise (Zhang et al., 1998). In human cells, it was shown in hippocampal cell cultures that ± 20 ms asynchronies in pre- and post- synaptic APs determined LTP or LTD (Bi and Poo, 1998), while the time window for the same effects was ± 10 ms in neocortical preparations (Markram et al., 1997). Albeit indirect evidence suggests the involvement of similar cellular mechanisms, this parallelism on the temporal rules governing STDP and STDP-like phenomena are purely speculative, since invasive neuronal recording are lacking.

The STS-40-PMv configuration, rather than LTD-like mechanisms in the PMv-to-STS connection, could be expected to induce LTP-like plasticity in the feedforward STS \rightarrow IPL \rightarrow PMv connection, leading to a potentiation of the system expressed by an enhancement of the behavioural performance. Data do not support this hypothesis, and a plausible explanation is that the 40 ms IPI does not meet the temporal constraints of the feedforward connectivity, or it is at least a suboptimal timing (preliminary TMS-EEG data indicate an optimal timing of ~50 ms), indeed, as the graph suggests, the slight increase visually detectable at Post0 did not survive correction for multiple comparisons (corrected $p = 0.28$; uncorrected $p = 0.018$). In the PMv-40-IPL configuration, anatomical-specific effects were tested, and data confirm that no change occurred. Altogether these findings suggest that behavioural enhancement is consistent with a LTP-like phenomenon exogenously induced using PMv-40-STS ccPAS configuration. The absence of effects in the control groups indicates that performance changes were not merely due to TMS, and that ccPAS is effective only if the temporal, directional and topographical constraints of the connection are met.

The tasks were repeated three times after the end of ccPAS at regular intervals of 20 min up to 40 min with the aim of monitoring participant's performance along time. Previous experiments found effects following ccPAS protocol that seem to depend on the connectivity manipulated, on the underlying function and on the nature of the adopted measures. For example, neurophysiological effects after

ccPAS of motor regions were shown to last over 1 h at rest (Rizzo et al., 2009; Lu et al., 2012b; Chao et al., 2015) or during action preparation (Buch et al., 2011), but less than 20 min when probed during an action observation task (Chiappini and Avenanti, 2018); behavioural changes have been shown to last at least 30-40 min in motor performance (Koganemaru et al., 2009; Rizzo et al., 2009; Fiori et al., 2018), and up to 1h in visual perception (Romei et al., 2016a). In the present study, the behavioural effects were observable immediately after ccPAS and lasted for at least 40 min. These findings demonstrate a long-lasting behavioural change in the processing of observed actions that is consistent the induction of a LTP-like mechanism in the PMv-STs connectivity. The fast evolution of the effects is more likely to reflect a strengthening of the synaptic efficacy proper of associative plasticity phenomena, rather than structural changes such as synaptogenesis or fibres sprouting (Stefan et al., 2000).

Participants' accuracy increased specifically for the action AP task involving human agents, while the performance in the control nHP task, requiring to predict which is going to be the target between two possible of a geometrical form displacement, was unaltered across time and groups of stimulation. The nHP task was conceived to match the AP task for both difficulty and the nature of information to be used for the prediction, i.e. motion trajectory and agent configuration to join the target. The absence of effects in the nHP task is in line with our expectations that were guided by the notion that the AON is strongly engaged viewing executable actions, that are in one's own motor repertoire (Press, 2011), indeed, its responses are more robust for humans than for animals (Buccino et al., 2004) or non-biological (Tai et al., 2004; Costantini et al., 2005; Engel et al., 2008) movements, and responses are weaker viewing humans moving with atypical non-human kinematics (Dayan et al., 2007; Casile et al., 2010). Although, PMv engagement has been also associated to the prediction of abstract non-biological sequences of stimuli (Schubotz and von Cramon, 2004), Avenanti (Avenanti et al., 2017) provided causative evidence supporting the key role of the left PMv in the prediction of human actions outcomes, and excluding a prominent role of the area in non-human predictions. For these reasons, the enhancement of the AON functioning through the potentiation of the PMv-STs connectivity was

expected to induce a specific behavioural enhancement in the AP task requiring predictive simulation of everyday human movements.

This experiment provides evidence that the PMv-STS connectivity is amenable of exogenous modulation via ccPAS if the physiological constraints of the connections are met. Furthermore, our findings fit the predictive coding theory of the AON, demonstrating that the PMv-STS connection, as part of the feedback PMv→IPL→STS connectivity of this system for the processing of observed human actions, if enhanced, increases the accuracy rates of healthy individuals at a human action prediction task, whilst preserves unaltered the performance at a non-biological prediction task. We believe that the selective enhancement of the information flowing from the frontal to the temporal frontal regions of the AON fostered the comparison between the predicted sensory outcome prompted by PMv motor simulative processes and incoming sensory inputs coded in STS.

GENERAL DISCUSSION

The proper functioning of a neural network hinges on the efficient connectivity between its nodes, indispensable for carrying essential information to be processed as well as modulatory inputs for the fine-tuning of the site activity. The aim of the research presented here was to provide further comprehension of the neural mechanisms that underpins everyday cognitive process essential for the social life of the human beings, and doing so by taking advantage of the ccPAS paradigm that is based on the plastic properties of the brain. Importantly, ccPAS is a novel conception TMS protocol able to induce associative plasticity mechanisms in the targeted cortical sites, that has been developed throughout the studies exposed in the present thesis.

In everyday life we face other people acting with non-verbal communication, and automatically or intentionally, we assign to their movements a meaning, allowing us to adjust our behaviour accordingly. Others' actions are complex stimuli involving a low-level visual analysis of the elements moving, a unification of them as a whole biological entity, a transformation of the visual inputs into motor representations, and finally an interpretation of them, in consideration of a priori knowledge and current contextual information. Furthermore, to readily react, interpretation is needed to be as fast as possible, therefore, we constantly try to accurately foresee what would be the outcome of such viewed movement.

The processing of stimuli of such complexity, engage a broad cortical network that encompass low and high level visual cortices, motor areas and hybrid visuo-motor regions known as the AON (Nishitani and Hari, 2000; Caspers et al., 2010). Its core regions involve STS, IPL and PMv (Keysers and Perrett, 2004; Cattaneo and Rizzolatti, 2009; Grafton, 2009; Caspers et al., 2010; Cattaneo et al., 2010), but they receive major visual inputs from visual areas for motion coding, such as the MT/V5+ complex (Vaina et al., 2001), and exert a prominent role in the modulation of M1 during action observation, giving rise to motor resonance phenomena (Fadiga et al., 2005; Avenanti et al., 2007; Catmur et al., 2011). Following both the most influential theories on action understanding, i.e. direct matching hypothesis (Rizzolatti

and Craighero, 2004) and prediction coding account (Kilner et al., 2007b), functionality of the AON highly relies on the flow of the information between the nodes of the system. The predictive coding perspective particularly emphasise the recursive feedforward-feedback interactions that, according to the theory, support the dynamic exchange of information between the various cortical representations, organised hierarchically (Kilner et al., 2007a, 2007b; Kilner, 2011). However, for a mechanistic understanding of the AON works and specifically, how the information is passed along the nodes of the system to make sense of other's people actions, a manipulation of the information flow was needed. Specifically, the aim was to test the models of connectivity within the AON by providing neurophysiological and behavioural evidence of the impact caused by the connectivity manipulation induced via ccPAS.

In the first experiments (Chapter 1) the efficacy of ccPAS in inducing behavioural changes in the PMv-M1 circuit was demonstrated. Before this, four ccPAS studies investigated motor behavioural changes following ccPAS, with non-conclusive results. In the most recent study, parietal-to-motor ccPAS led to no behavioural changes, as tested by the Purdue pegboard test for eye-hand fine movements coordination (Chao et al., 2015). Rizzo and colleagues (2009) tested left-to-right and right-to-left ccPAS over the M1s, and found a performance improvements at CRT tasks similar to that reported by Koganemaru and co-workers (2009). Nonetheless, these results seem not completely conclusive given the absence of a real control of stimulation or of tasks. Results of more complex manual tasks are instead less consistent, Rizzo's group (2011) found no changes, while Koganemaru's group did (2009). It is possible that such differences are accounted by task (complex finger opposition sequences vs. 9-hole pegboard test) or ccPAS configuration differences. Still, behavioural results following motor ccPAS were not conclusive, and most importantly, had never been tested on the PMv-M1 circuit. This cortico-cortical connection is of outstanding interest being involved in carrying to M1 basic information for preparing and reprogramming manual movements encoded in PMv (Davare et al., 2009; Buch et al., 2010), as well as for conveying specific modulatory information to M1 during action observation, considered crucial for the embodiment of other's motor acts, as shown by TMS research (Fadiga et al.,

2005; Avenanti et al., 2007; Koch et al., 2010; Catmur et al., 2011). Furthermore, the susceptibility to plasticity induction via ccPAS in the PMv-M1 connectivity had been recently demonstrated with neurophysiological and neuroimaging tools (Buch et al., 2011; Johnen et al., 2015). We therefore probed the sensitivity of PMv-M1 circuit to ccPAS manipulation on a behavioural level, and we found that the PMv-to-M1 ccPAS, meant to strengthen the connection, improved motor performance after 30 minutes from the end of the stimulation, while opposite direction (M1-to-PMv) or sham ccPAS did not. Behavioural changes were assessed by means of the 9-hole pegboard test that requires overt motor movements, but that likely taps on the visual transformations that PMv performs to adequately grasp the objects (Kantak et al., 2012). Importantly, this is also the function attributed to PMv during action perception that consent the simulation of the ongoing action (Gallese et al., 1996; Rizzolatti and Craighero, 2004; Pobric and Hamilton, 2006).

The second study presented in this thesis (Chapter II) coupled for the first time ccPAS and the visual system. The AON processing maps onto motor representations the visual inputs sourcing from the occipital regions, to modulate this hybrid network, we firstly needed to verify the efficacy of ccPAS on low-level visual percepts on a behavioural level. We accomplished this by applying ccPAS on a system for motion perception that comprises feedforward and feedback interactions (Lamme and Roelfsema, 2000), functionally analogous to the AON conceptualised by the predictive coding account (Kilner et al., 2007b). Re-entrant projections from MT/V5 to V1 had been shown to have a critical role for awareness of the visual motion to arise (Pascual-Leone and Walsh, 2001; Silvanto et al., 2005a). Our work demonstrates that fostering the information flowing via the MT/V5-V1 re-entrant projections (Pascual-Leone and Walsh, 2001; Silvanto et al., 2005a), positively influences the sensitivity to global motion kinematograms. Although more direct evidence such as electrophysiological measures are still lacking, the results matched the hypotheses formulated on the basis of previous functional evidence and on those mechanisms resembling of Hebbian associative plasticity that can be induced through ccPAS as demonstrated on motor areas. In keeping behavioural changes appeared only 30 minutes after the end of stimulation and were critically dependent on the compliance of physiological and directional

constraints of the connection targeted. It is therefore reasonable to expect that the visual system responsible for low-level motion coding follows the rules evidenced to be critical for the instauration of Hebbian-like phenomena in more frontal systems. Moreover, induced effects on the pathway targeted seemed to follow the predominant anisotropy, thus suggesting that ccPAS is suitable for selectively targeting either forward or backward connections, likely depending on the parameters used (e.g. optimal timing for feedback rather than feedforward connections).

The study reported in Chapter III further explored both the MT/V5-V1 connection and the ccPAS protocol applications. Here, the purpose of selectively improving perception of a specific feature, the neural substrate of which relies on overlapping neuronal pools of the same cortical site, was accomplished by taking advantage of the state dependency properties of TMS (Silvanto and Muggleton, 2008a, 2008b) used for the first time to implement the ccPAS protocol. The previous study (Chapter II) marked the starting point of this experimental work that has methodological connotations. Applying an experimental paradigm in which ccPAS administration was coupled with visual presentation of a stimulus moving in a specific direction, perception of that primed direction benefited from the ccPAS manipulation, whilst the opposite was not affected. These findings corroborate the knowledge on the tuning to a particular motion direction of MT/V5 neurons (Maunsell and Van Essen, 1983b; Albright, 1984; Bartels et al., 2008). Most importantly, they are in agreement with the results obtained in the study of Chapter II, thus supporting its conclusions, and they widen the applications of ccPAS for future research by narrowing and optimising to functional level the spatial resolution of this stimulation protocol.

Experiments presented in Chapter IV, the focused on the internal simulation of actions observed and on the PMv-M1 circuit. We demonstrated that the ccPAS configuration identical to previous literature (Buch et al., 2011; Johnen et al., 2015), shown to be suitable for inducing plastic changes in action execution tasks, as evidenced by physiological measures, was useful for modulating motor resonance phenomena occurring during action observation (Fadiga et al., 1995). Research on mirror neurons

(Gallese et al., 1996; Rizzolatti et al., 1996) and embodied cognition theories for action understanding (Jeannerod, 2001; Rizzolatti et al., 2001; Gallese, 2007) found strong empirical support when motor resonance phenomena revealed by TMS over M1 were evidenced (Fadiga et al., 1995), being the neurophysiological demonstration in humans that the motor system covertly activates to simulate the observed actions in a muscle-specific fashion as during their execution (see Naish et al., 2014). This study, thus demonstrates for the first time that empowering PMv-M1 circuit, impacts on the neurophysiological index of the AON functioning. We therefore provided evidence supporting the view that this connectivity is centrally involved in conveying AON information to M1 for embodiment of others' movements (Koch et al., 2010; Catmur et al., 2011) that may contribute to action understanding (Pobric and Hamilton, 2006), and we demonstrated for the first time the possibility of manipulating AON emergent phenomena by manipulating the underlying connectivity. However, no behavioural evidence supports the view that these induced alterations corresponded to a behavioural change in making sense of others' individuals acting.

Finally, the study of Chapter V aimed at verifying the functions of feedback PMv-STs connectivity in the prediction of others' actions. Research suggests that the humans' motor system represents ongoing actions in a predictive fashion (Kilner et al., 2004; Friston, 2010; Urgesi et al., 2010; Avenanti et al., 2013a, 2017; Ondobaka et al., 2015) and scholars theorised models of the AON that work as an anticipatory device for engaging forward internal models (Kilner et al., 2007a, 2007b; Friston et al., 2011). This predictive coding account regards the AON as a recursive system that dynamically exchanges the information from visual-to-motor areas to simulate the early kinematics of an observed action in a complete motor act and from motor-to-visual areas to compare the motor prediction to the incoming visual inputs. However, this model received only partial empirical support by correlational studies that analysed the flow of feedforward and feedback information during the active prediction of known actions using granger causal modelling (Kokal and Keysers, 2010; Schippers and Keysers, 2011). To understand the role of connectivity within the AON we modulated the flow of information between its motor-visual nodes, namely PMv and STS, and measured the behavioural response in an action

prediction task. In this study we demonstrated that the strengthening of feedback connectivity led to improved performance at the prediction task. The specificity of effects when temporal, directional and anatomical constraints were satisfied, strongly suggests that the optimal ccPAS configuration improved the targeted pathway at a timing that, according to a preliminary TMS-EEG study, functionally links the PMv and STS sites during action observation, allegedly with the involvement of the third core node of the AON, i.e. IPL. Given the predictive nature of the task and the specific improvements with biomechanical human (but not with non-human) stimuli, we believe that the behavioural effects evidenced are attributable to an empowering of the information flowing backwards, from frontal motor regions to temporal visual areas, crucially involved in the prediction of human movements. Importantly, the experiments show that ccPAS administered over AON sites can critically change the perception of actions. For the sake of clarity, it should be noted that in absence of functional connectivity evidence, the only behavioural results cannot account for possible alterations of other functionally connected or functionally related regions indirectly driven by the unbalance of the network caused by ccPAS, as Johnen and co-workers showed (2015). Specifically, we cannot exclude the possibility that our feedback connectivity manipulation had empowering or compensative secondary effects on other circuits, for instance on the feedforward flow, that may have contributed to the behavioural change observed. In conclusion, this study represents a first precedent for exogenously manipulating action perception in the healthy population.

Appendices A and B, report methodological experiments that explored systematically the connectivity of motor-related cortical areas of the left (Appendix A) or right (Appendix B) hemisphere with left M1 at long-time latencies through a dual-coil TMS paradigm. This paradigm has been widely used to test interactions between areas occurring at defined latencies especially between motor areas (Reis et al., 2008). Classically the latencies considered are relatively short (2-30 ms; Ferbert et al., 1992; Civardi et al., 2001; Davare et al., 2008; Bäumer et al., 2009; Cattaneo and Barchiesi, 2011; Arai et al., 2012; see also Reis et al., 2008 for a review). However, functionally relevant interplays at longer latencies might occur (Gerloff et al., 1998; Mochizuki et al., 2004b; Ni et al., 2009) and may underlie indirect pathways

(Gerloff et al., 1998; Neubert et al., 2010) or slower physiological mechanisms (Kukawadia et al., 2005; Irlbacher et al., 2007), conducive to the fine-tuning of the motor system. In these experiments we show the time-course of interactions between 6 motor-related areas and left M1, emphasising peculiar interplays that are dependent on the conditioning site and on the intensity of conditioning stimulation. These data can be of notable interest also for informing with precision the optimal timing of intercortical motor interactions for setting ccPAS interventions.

The studies presented in this thesis significantly expand on previous knowledge about the cortical connectivity responsible for the functional exchange of information within the systems involved in the coding of movement and observed actions. Findings are consistent with the existent literature in the field and provide behavioural or neurophysiological evidence in support of theoretical models. In parallel, a work of research and development of the ccPAS protocol has been undertaken to provide unambiguous evidence on the methodological aspects of its administration. Before the experiments performed during this doctoral project, the impact of this powerful tool was only tested on motor related areas and with unclear results on behavioural motor performance. We showed instead the possibility to affect motor behaviour, low-level visual perception and the processing of stimuli characterised by visuo-motor coupling. Moreover, ccPAS was successfully administered not only on feedforward connections, but also on feedback circuits with spatial accuracy at a functional scale. Although these results are very promising, more evidence in support of the underlying neural physiological mechanisms of the ccPAS are needed to comprehensively understand the phenomena triggered. Nevertheless, evidence of functional improvements on cognitive abilities crucial for the human beings are encouraging for the development of future strategies for diseases prompting to motor performance decay, stroke rehabilitation, and disorders characterised by reduced or altered brain connectivity.

APPENDIX A

Long-latency modulation of motor cortex excitability by ipsilateral posterior inferior frontal gyrus and pre-supplementary motor area²

A1.1 Introduction

Interactions between premotor and motor brain regions are critical for understanding motor network functioning. The posterior inferior frontal cortex (including the posterior sector of the inferior frontal gyrus, pIFG, and the ventral premotor cortex, PMv) and the supplementary motor complex (including the pre-supplementary motor area, pre-SMA, and the supplementary motor area, SMA) are key regions within the motor system linking cognition to action (Picard and Strick, 2001; Rushworth et al., 2004; Hoshi and Tanji, 2007; Nachev et al., 2008; Avenanti and Urgesi, 2011; Davare et al., 2011; Swann et al., 2012; Rizzolatti et al., 2014; Urgesi et al., 2014). Both inferior frontal and supplementary areas have sparse projections to the spinal cord, whereas their most posterior premotor sectors (i.e., PMv and SMA) possess extensive projections to the primary motor cortex (M1) to influence motor output (Muakkassa and Strick, 1979; Dum and Strick, 1996; Tokuno and Nambu, 2000; Fujii et al., 2002; Prabhu et al., 2009). Such projections appear less abundant in the most rostral sectors of inferior frontal and supplementary regions, particularly in the pre-SMA, which appears to exert its influence over motor output via indirect interconnected pathways (Dum and Strick, 1996; Fujii et al., 2002; Mars et al., 2009). Yet, rostral premotor regions appear critical for motor functions, and neuroimaging and neurophysiological studies indicate strong connectivity between rostral premotor cortices and M1 (Hoshi and Tanji, 2007; Nachev et al., 2008; Swann et al., 2012; Rizzolatti et al., 2014).

Functional imaging studies have highlighted premotor-motor functional coupling at rest (De Luca et al., 2006; Power et al., 2011) and disruption of this coupling in a number of neurological conditions affecting

² Published paper: Fiori F, Chiappini E, Soriano M, Paracampo R, Romei V, Borgomaneri S, Avenanti A (2016) Long-latency modulation of motor cortex excitability by ipsilateral posterior inferior frontal gyrus and pre-supplementary motor area. *Sci Rep* 6:1–11

the motor system (Grefkes et al., 2008; Tessitore et al., 2012). However, these functional connectivity studies rely on an approach that is correlational in nature and characterised by low temporal resolution. Therefore, brain stimulation techniques might be better suited for highlighting the time-course of rostral premotor-M1 causal interactions.

Dual-site transcranial magnetic stimulation (dsTMS) is a valuable neurophysiological method for non-invasively mapping causal connectivity with high temporal resolution (Ferber et al., 1992; Di Lazzaro et al., 1999; Civardi et al., 2001; Cattaneo and Barchiesi, 2011; Rothwell, 2011). In the dsTMS protocol, a conditioning stimulus (CS) is administered over a target (e.g., premotor) region to activate hypothetical pathways (through direct or indirect connections) from the site of stimulation to M1. The CS is followed by a test stimulus (TS) that is administered over M1 to induce motor-evoked potentials (MEPs) in contralateral muscles. Both facilitation and inhibition may occur at the TS site (i.e., M1), evidencing different neurophysiological interactions between the stimulated areas depending on CS intensity and the inter-stimulus intervals (ISIs) between CS and TS. The dsTMS paradigm has been extensively used to investigate interhemispheric connections between homologous M1 sites (Ferber et al., 1992; Di Lazzaro et al., 1999; De Gennaro et al., 2003; Li et al., 2007; Sattler et al., 2014). More recently, interactions between non-primary motor areas and M1 have started to be investigated (Mochizuki et al., 2004a; Koch et al., 2006, 2007; Cattaneo and Barchiesi, 2011). Using dsTMS, studies have focused on how M1 excitability is influenced by a CS administered over posterior inferior frontal cortices (Davare et al., 2008, 2009, 2010; Bäumer et al., 2009; Cattaneo and Barchiesi, 2011) and the supplementary motor complex (Civardi et al., 2001; Mars et al., 2009; Cattaneo and Barchiesi, 2011; Arai et al., 2012). These studies have focused on short-latency connectivity using various ISIs of < 15 ms, and have shown that a CS over premotor areas can modulate MEPs induced by the TS over M1 only at specific ISIs of ~ 4–8 ms, evidencing time-dependent effects. Moreover, these studies suggest that the excitatory or inhibitory nature of premotor-to-motor short-latency interactions depends on TMS intensity, as partially distinct neural populations are recruited depending on TMS intensities. For example, Bäumer and colleagues (2009) showed that a relatively low subthreshold CS over posterior

inferior frontal regions (80% of active motor threshold; aMT) and a higher intensity CS (90% of resting motor threshold; rMT) produced facilitation and inhibition of MEPs, respectively. These findings highlighted the intensity- and time-dependent nature of short-latency premotor-motor interactions. Previous dsTMS studies have mainly used short ISIs to explore ipsilateral premotor-motor interactions. However, neural interactions within the motor system likely occur on different time-scales. Indeed, longer-latency interactions with ISIs up to 150 ms have been documented between M1 and contralateral motor-related areas (Mochizuki et al., 2004b; Ni et al., 2009) and studies have shown altered long-latency M1-M1 interhemispheric interactions (at an ISI of 40 ms) in neurological conditions affecting motor control (Li et al., 2007; Sattler et al., 2014). Thus, motor network functioning may be based on optimal tuning between short-latency, as well as long-latency, interactions. The goal of this study was to explore, for the first time, the dynamics of long-latency rostral premotor-motor interactions. To this aim, we used dsTMS over PMv-M1 and pre-SMA-M1 circuits, and tested the effect of ISI (between 40 and 150 ms) and CS intensity on MEP amplitude modulation (Fig.A1.1). Our findings show that long-latency functional connections do exist between rostral premotor and motor areas, and that specific time intervals and intensities are crucial for observing causal influences of PMv and pre-SMA over M1 excitability during a resting state. Although these interactions likely involve indirect pathways, tracking the time-course of long-latency PMv-M1 and pre-SMA-M1 interactions is important not only for understanding cortico-cortical connectivity (and its disruption in clinical conditions), but also for developing novel information-based (Romei et al., 2016b) non-invasive transcranial brain stimulation methods aimed at manipulating connectivity, such as the cortico-cortical paired associative stimulation (ccPAS) protocol (Arai et al., 2011; Buch et al., 2011; Veniero et al., 2013; Romei et al., 2016a, 2016b) which relies on the critical ISIs identified by dsTMS.

A1.2 Methods

Participants

Twelve healthy volunteers (7 females; mean age \pm S.D.; 24.8 ± 2 years), free of any contraindications to TMS (Rossi et al., 2009) gave written informed consent prior to the study. All participants were right-handed according to the Edinburgh Handedness Inventory (Oldfield, 1971). The experimental protocol was approved by the Bioethics committee of the University of Bologna and was carried out in agreement with legal requirements and international norms (Declaration of Helsinki, 1964). The methods carried out in this work are in accordance with approved guidelines. None of the participants reported adverse reactions to TMS.

General design

Participants took part in an experimental session and a control session separated by 7 ± 3 days. MEPs induced by a TS delivered over the left M1 were collected from the right first dorsal interosseous (FDI). In the experimental session, we performed 4 experimental blocks, differing as a function of the CS site (PMv or pre-SMA) and CS intensity (subthreshold: 90% rMT; or suprathreshold: 110% rMT) (Fig.A1.1, panel A). In each experimental block, we randomly intermixed spTMS trials (TS alone) and dsTMS trials (TS preceded by a CS with an ISI randomly set at 40, 60, 80, 100, 120 or 150 ms). In this way, we investigated PMv-M1 and pre-SMA-M1 intensity-dependent causal interactions and identified temporal windows sensitive to the influence of premotor conditioning over M1 excitability. A control experiment was performed by administering the TS over the left M1 and the CS over the contralateral (right) dorsal premotor cortex (PMd). Both in the experimental and control sessions, MEPs induced by spTMS were collected in two separate blocks serving as a baseline (see Fig.A1.1).

Experimental procedure

Participants sat with both hands relaxed and were instructed to keep their eyes closed with the purpose of obtaining a signal as stable as possible and minimising the influence of potentially distracting visual

stimuli. Electromyographic (EMG) recording was performed through Ag/AgCl surface electrodes placed over the right FDI in a belly-tendon montage. EMG signals were acquired by means of a Biopac MP-35, band-pass filtered (30–500 Hz) and sampled at 5 kHz. TMS pulses were delivered via 2 figure-of-eight coils (50 mm wing coil outer diameter), each of which was connected to a Magstim 200 monophasic stimulator. The left M1 was identified as the hotspot where the TS induced the largest MEP amplitudes with the coil held tangentially to the scalp, at a $\sim 45^\circ$ angle to the midline, inducing a posterior-to-anterior current (Di Lazzaro et al., 2004; Rossini et al., 2015). The TS intensity was set to produce a MEP amplitude of about 1.0–1.5 mV (mean \pm S.D.: $51\% \pm 11$ of the maximum stimulator output, MSO).

The experimental session consisted of 4 experimental blocks testing PMv-M1 interactions (in two blocks) or pre-SMA interactions (in the other two blocks). The control session consisted of 2 control blocks testing PMd-M1 interactions. For each stimulated area, 2 CS intensities were used (i.e., 90% or 110% of rMT) and were tested in separate blocks. The rMT was defined as the MSO intensity that induced a MEP with $>50 \mu\text{V}$ amplitude in 5 out of 10 consecutive trials (Rossini et al., 2015). The mean rMT was $40\% \pm 7$ of the MSO. Each of the experimental blocks included 152 trials (32 spTMS trials and 120 dsTMS trials: 20 trials for each of the 6 ISIs, i.e., 40, 60, 80, 100, 120 and 150 ms). Each of the 2 control blocks included 52 trials (32 trials of spTMS and 20 trials of dsTMS using a 40-ms ISI). Block and trial orders were randomised. Additionally, at the beginning of the first session (either the experimental or the control session) we collected a block of 10 spTMS trials constituting the baseline/pre block; at the end of the second session, we collected another block of 10 spTMS trials, constituting the baseline/post block.

The control session was motivated by a preliminary off-line analysis performed on data from 7 participants who were initially tested in the experimental session only. This analysis revealed that the CS over both the PMv and the pre-SMA tended to consistently reduce MEPs at a 40-ms ISI. Thus, to rule out that this inhibitory modulation was due to nonspecific effects (e.g., the coil click), we tested these participants in the control session, in which a CS was applied over the PMd. These seven participants

were tested first in the main experiment and then in the control experiment. The remaining participants were tested in the opposite order.

Brain localisation

Brain conditioning sites were identified using established methods. The left PMv location was identified with the EMS SofTaxic Navigator system, which automatically estimates coordinates in Talairach space from a magnetic resonance imaging-constructed stereotaxic template. Skull landmarks and ~80 points providing a uniform representation of the scalp were digitised by means of a Northern Digital Polaris Vicra digitiser (Carducci and Brusco, 2012; Tidoni et al., 2013; Jacquet and Avenanti, 2015). An individual estimated magnetic resonance image (MRI) was obtained for each subject through a 3D warping procedure fitting a high-resolution MRI template with the participant's scalp model and craniometric points. This procedure ensures a global localisation accuracy of ~5 mm (Carducci and Brusco, 2012). We targeted the PMv using the following Talairach coordinates: $x = -54$, $y = 10$, $z = 24$ (Avenanti et al., 2012a, 2013a). The coil was placed at ~45° to the midline to induce a ventro-lateral to medio-posterior current (Bäumer et al., 2009). Based on previous research, we used craniometric methods to identify the pre-SMA and PMd scalp positions. The pre-SMA was stimulated 4 cm anterior to the vertex on the sagittal midline as in previous research (Mars et al., 2009; Buch et al., 2011; Arai et al., 2012), with the coil handle pointing forward to induce an anterior-posterior current (Arai et al., 2012). The right PMd was stimulated 2 cm anterior and 1 cm medial with respect to the right M1 hotspot for inducing MEPs in the left FDI, and the coil was held at ~90° from the midline, inducing a latero-medial current (Mochizuki et al., 2004a, 2004b; Bestmann et al., 2005).

The SofTaxic Navigator system was used to estimate the projection of the targeted scalp positions on the brain surface, confirming correct coil placement for all the sites (Avenanti et al., 2012a, 2013a; Carducci and Brusco, 2012; Tidoni et al., 2013; Jacquet and Avenanti, 2015). The estimated Talairach coordinates for the left M1 (i.e., the FDI optimal scalp position) were (mean ± S.D.): $x = -38.3 \pm 5.0$, $y = -19.4 \pm 6.1$, $z = 58.7 \pm 3.0$. Brain surface Talairach coordinates for the PMv were: $x = -54.8 \pm 1.3$, $y = 9.1$

± 1.0 , $z = 24 \pm 1.0$; coordinates for the pre-SMA were: $x = 0.1 \pm 0.3$, $y = 9.8 \pm 6.5$, $z = 67.9 \pm 1.4$; right PMd: $x = 22.2 \pm 6.8$, $y = -3.5 \pm 7.2$, $z = 63.5 \pm 7.4$ (Fig.A1.1, panel B).

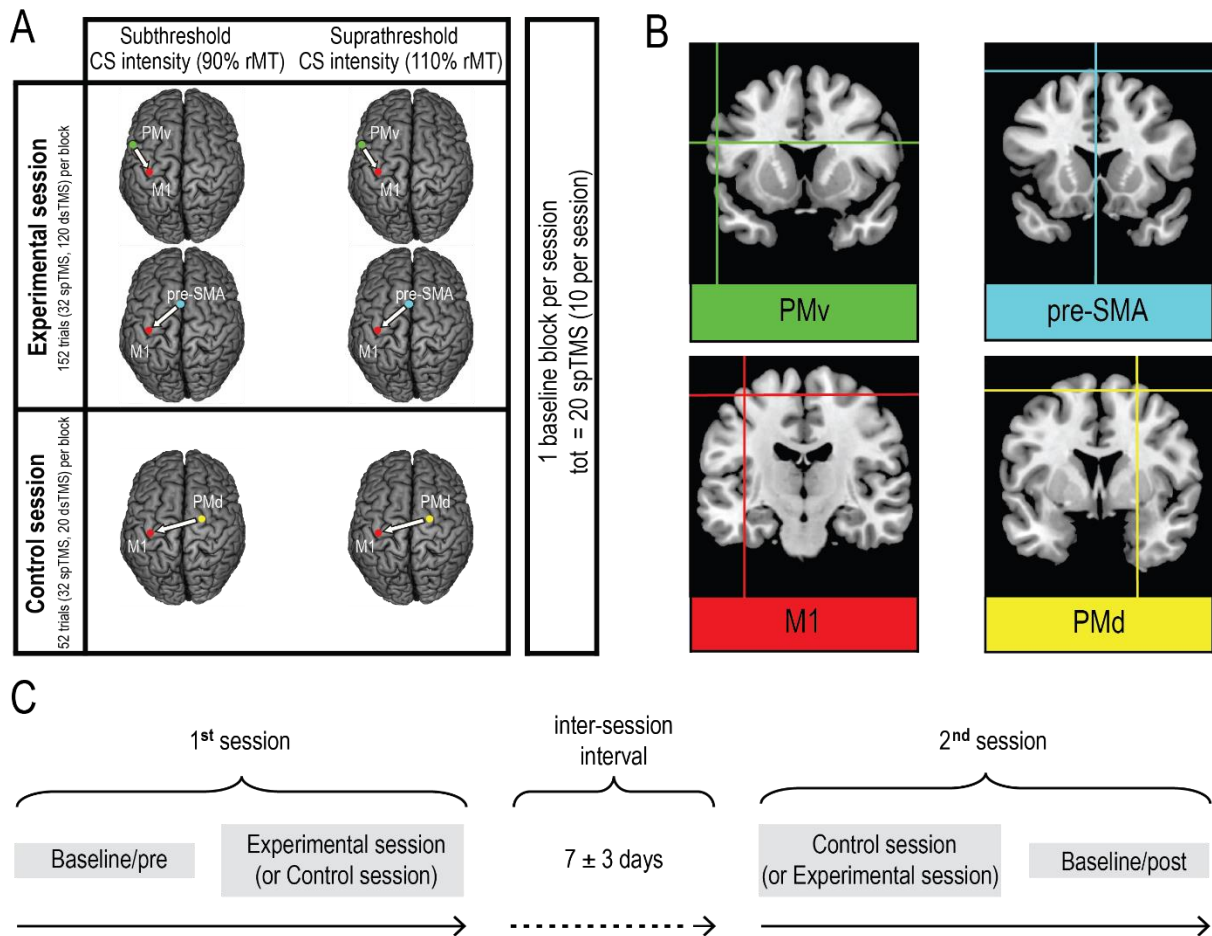


Fig.A1.1 A) Schematic representation of the experimental and control sessions. For each experimental and control block, brain stimulation sites, CS intensity and number of trials are reported. The baseline consisted of a total of 20 spTMS trials, recorded during the experimental session (10 MEPs) and the control session (10 MEPs). The baseline trials were collected at the beginning or at the end of each session. B) Brain stimulation sites. Coordinates in Talairach space corresponding to the projection of the stimulated scalp sites on the brain surface were estimated through neuronavigation software (left mean PMv coordinates \pm S.D.: $x = -54.8 \pm 1.3$, $y = 9.1 \pm 1.0$, $z = 24 \pm 1.0$; pre-SMA: $x = 0.1 \pm 0.3$, $y = 9.8 \pm 6.5$, $z = 67.9 \pm 1.4$; left M1: $x = -38.3 \pm 5.0$, $y = -19.4 \pm 6.1$, $z = 58.7 \pm 3.0$; and right PMd: $x = 22.2 \pm 6.8$, $y = -3.5 \pm 7.2$, $z = 63.5 \pm 7.4$) and then reconstructed on a standard template using MRICron software (v 1.40 <http://www.mricron.com>). C) Experiment timeline.

Data analysis

In each block, the mean peak-to-peak MEP amplitude was computed for the spTMS condition and each dsTMS condition. Any trace showing EMG activity 100 ms prior to the TMS pulses was excluded (~4%).

In each condition, MEPs with amplitudes deviating from the mean by more than 2.5 S.D. were removed

from the analysis (~3%). A preliminary one-way ANOVA was conducted on mean MEPs elicited by spTMS in all the experimental, control and baseline blocks (8 levels: PMv/subthreshold, PMv/suprathreshold, pre-SMA/ subthreshold, pre-SMA/suprathreshold, PMd/subthreshold, PMd/suprathreshold, baseline/pre, baseline/post). The ANOVA was not significant ($F_{7,88} = 1.01$, $P = 0.43$), indicating that motor excitability measured by spTMS stimulation was comparable across experimental, control and baseline blocks. For each participant, we averaged MEPs across the pre- and post-baseline blocks and used this value to normalise MEP amplitudes in the different conditions of each experimental block (i.e., spTMS-MEPs, and dsTMS-MEPs at ISIs from 40 to 150 ms were divided by the baseline spTMS-MEPs) and control block (i.e., spTMS-MEPs and dsTMS-MEPs at a 40-ms ISI were divided by the baseline spTMS-MEPs).

Two separate CS intensity (subthreshold and suprathreshold) × Condition (spTMS, and dsTMS at ISIs from 40 to 150 ms) ANOVAs were performed on normalised MEP amplitudes (% of baseline), one for each conditioned area (PMv and pre-SMA). A post-hoc analysis was performed with the Newman-Keuls test in order to compare dsTMS-MEPs relative to spTMS-MEPs within each area, and to correct for multiple comparisons. This analysis revealed the critical ISIs at which a CS over a target region influenced M1 excitability. To compare the modulatory effects revealed by dsTMS in the different areas, we also subtracted normalised MEP amplitudes in the spTMS condition from those in the dsTMS condition, in order to directly compare inhibitory/facilitatory effects in the PMv-M1 and pre-SMA-M1 circuits. Subsequently we submitted these modulation indices to a series of Area x CS intensity ANOVAs, one for each critical ISI.

Data from the control experiment were analysed following the same procedure used for data from the experimental session. Thus, MEPs elicited by spTMS and dsTMS were normalised using the previously computed grand average baseline, and submitted to a CS intensity (subthreshold and suprathreshold) × Condition (spTMS, and dsTMS at a 40-ms ISI) ANOVA. Moreover, to compare the modulatory effect (dsTMS minus spTMS normalised MEP amplitudes) induced by dsTMS stimulation at a 40-ms ISI with

the brain stimulation sites examined in the experimental session, a further Area (PMv, pre-SMA, PMd) × CS intensity (subthreshold and suprathreshold) ANOVA was computed.

A1.3 Results

Identification of critical ISIs: PMv-M1 experimental blocks

To explore intensity-dependent causal interactions from PMv to M1, dsTMS was performed in two experimental blocks where participants received a TS over the left M1 preceded by a CS over the ipsilateral PMv either at a subthreshold or a suprathreshold CS intensity. A CS intensity (2 levels: subthreshold and suprathreshold) × Condition (7 levels: spTMS, and dsTMS with 40–150-ms ISIs) ANOVA conducted on normalised MEP amplitudes (% of baseline) showed a main effect of Condition ($F_{6,66} = 4.19$, $P = 0.001$; $\eta_p^2 = 0.28$) while the main effect of CS intensity did not reach significance ($F_{1,11} = 0.18$, $P = 0.68$). However, we found a CS intensity × Condition interaction ($F_{6,66} = 2.90$, $P = 0.014$; $\eta_p^2 = 0.21$; Fig.A1.2, panel A), showing that the modulatory effect of dsTMS depended on CS intensity. A post-hoc analysis (performed with Newman-Keuls test) was used to identify critical ISIs at which MEPs evoked by dsTMS differed from MEPs evoked by spTMS, and to check the influence of CS intensity.

In the subthreshold CS intensity block, MEPs in the dsTMS conditions at 40- and 150-ms ISIs (mean amplitude relative to the baseline: 87.5% and 83.4%, respectively) were lower than MEPs in the spTMS condition (104.6%; all $P < 0.008$). Similarly, in the suprathreshold CS intensity block, MEPs in the dsTMS conditions at 40- and 150-ms ISIs (84.1% and 81.7%, respectively) were lower than MEPs in the spTMS condition (101.5%; all $P < 0.005$). Moreover, MEP amplitudes induced by dsTMS at these two ISIs were comparable for subthreshold and suprathreshold CS intensity (all $P > 0.44$). Interestingly, in the suprathreshold CS block, dsTMS MEP amplitudes at an ISI of 60 ms were marginally larger than spTMS MEP amplitudes (113.6% vs. 101.5%; $P = 0.057$) and significantly larger than dsTMS MEP amplitudes collected in the subthreshold CS block at the same ISI (113.6% vs. 95.9%; $P = 0.005$), indicating timing-specific dsTMS intensity-dependent effects. No other significant comparisons were found ($P > 0.19$).

We further explored the dsTMS effects at an ISI of 60 ms by using a more lenient post-hoc test (Duncan test). This showed that, relative to the MEP amplitudes in the spTMS conditions, MEP amplitudes in the dsTMS condition at a 60-ms ISI were significantly larger following a suprathreshold CS ($P = 0.015$) but tended to be suppressed by a subthreshold CS ($P = 0.095$). These findings should be interpreted with caution as they show a non-significant trend detected with a less conservative post-hoc test, and future investigations should ascertain the validity of this trend. If confirmed, it would provide further support to the notion that dsTMS exerts timing-specific and intensity-dependent facilitatory and inhibitory effects over the pIFC-M1 circuit driven by supra- and subthreshold CS, respectively.

Identification of critical ISIs: pre-SMA-M1 experimental blocks.

To investigate causal interactions from pre-SMA to M1, participants were also tested in two additional experimental blocks in which subthreshold (90% of rMT) or suprathreshold (110% of rMT) CS intensities were administered over the pre-SMA. The CS intensity (2 levels: subthreshold and suprathreshold) × Condition (7 levels: spTMS, and dsTMS with 40–150-ms ISIs) ANOVA conducted on normalised MEP amplitudes (% of baseline) showed a main effect of Condition ($F_{6,66} = 3.02$, $P = 0.011$, $\eta_p^2 = 0.22$; Fig.A1.2, panel B) accounted for by the significant decrease in MEP amplitudes between the spTMS condition and the dsTMS condition at an ISI of 40 ms (110.9% vs. 100.2%; $P = 0.016$). No other dsTMS conditions (i.e., ISIs 60–150 ms) were different from the spTMS condition (all $P > 0.68$). Neither the main effect of CS intensity nor the CS site × CS intensity interaction was significant in the ANOVA ($F < 0.73$, $P > 0.41$).

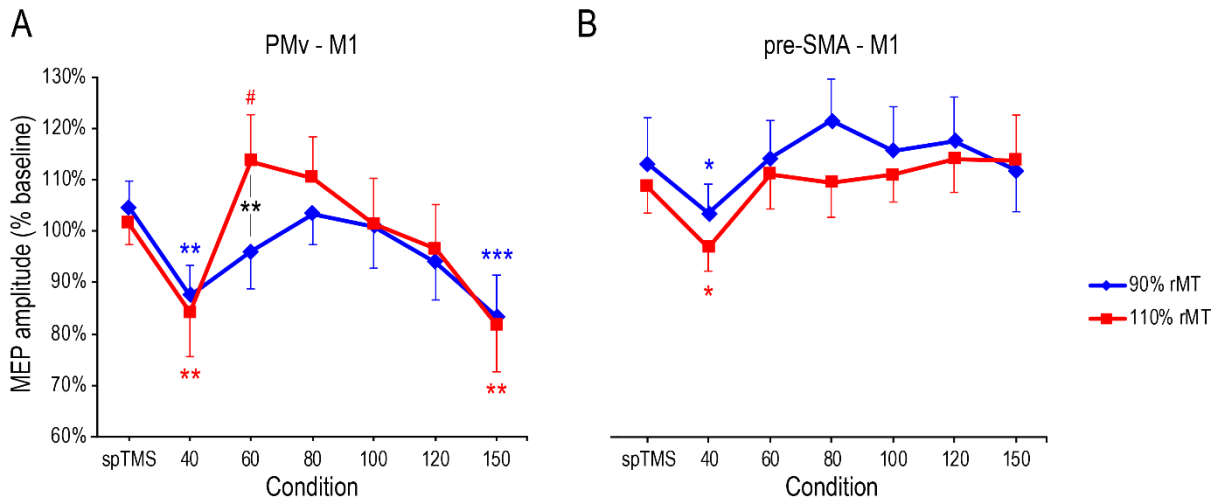


Fig.A1.2. Normalised MEP amplitudes (% baseline). The graph illustrates the CS intensity (90% and 110% of rMT) \times Condition (spTMS, and dsTMS with 40-150-ms ISIs) interaction in A) PMv-M1 blocks and B) pre-SMA-M1 blocks. Error bars denote s.e.m. Hash marks and asterisks indicate marginally significant and significant post-hoc comparisons, respectively (Newman-Keuls test, # $P < 0.06$, * $P < 0.05$, *** $P < 0.001$).

Control session: PMd-M1 control blocks.

The analysis of MEPs in the experimental blocks revealed that the CS over both the PMv and the pre-SMA reduced MEP amplitudes at a 40-ms ISI. To rule out that this inhibitory modulation was due to nonspecific effects (e.g., the coil click; Furubayashi et al., 2000; Serino et al., 2009), participants were further tested in a control session on a separate day. This included two short counterbalanced control blocks in which subthreshold (90% of rMT) or suprathreshold (110% of rMT) CS intensities were applied over a brain region that is not believed to influence motor excitability at about a 40 ms ISI (at least when using CS intensities similar to those used here), namely, the contralateral (right) PMd (Koch et al., 2006; Ni et al., 2009). Both PMd-M1 control blocks included dsTMS trials (a TS preceded by a CS with an ISI of 40 ms) randomly intermixed with spTMS trials (TS alone).

The CS intensity (2 levels: subthreshold and suprathreshold) \times Condition (2 levels: spTMS, and dsTMS with a 40 ms ISI) ANOVA conducted on normalised MEP amplitudes (% of baseline) showed no significant effects ($F < 0.93$, $P > 0.36$) confirming the lack of PMd influence over M1 at an ISI of 40 ms.

Comparing ISI-specific modulatory effects in premotor-motor circuits.

The two main analyses detected three critical ISIs at which dsTMS revealed clear modulatory effects of at least one CS site over M1 excitability, i.e., 40, 60 and 150 ms. To directly compare such effects in the two PMv-M1 and pre-SMA-M1 circuits, for each experimental block and critical ISI, we computed a modulation index on normalised MEPs (% of baseline) as the difference between dsTMS MEPs and spTMS MEPs of the same block. Then we submitted this index to a series of CS site x CS intensity ANOVAs, one for each critical ISI.

In the earliest, 40-ms ISI, the main analyses reported above revealed inhibitory effects in both PMv-M1 and pre-SMA-M1 circuits. To test site-specificity, we analysed the modulation index computed at the 40-ms ISI using a CS site (2 levels: PMv and pre-SMA) x CS intensity (2 levels: subthreshold and suprathreshold) ANOVA. This analysis did not show any main effects or interactions ($F < 0.84$, $P > 0.38$), suggesting the inhibitory influence of premotor stimulation at an ISI of 40 ms was comparable across PMv/pre-SMA sites and sub/suprathreshold CS intensities. Then, we included data from the control experiment in a CS site (3 levels: PMv, pre-SMA, PMd) x CS intensity (2 levels: subthreshold and suprathreshold) ANOVA. This second analysis showed the main effect of the CS site ($F_{2,22} = 5.15$, $P = 0.015$, $\eta_p^2 = 0.32$; Fig.A1.3, panel A), but not the main effect of CS intensity, nor a CS site x CS intensity interaction ($F < 0.18$, $P > 0.67$). Post-hoc tests (Newman-Keuls) revealed a significant difference between PMv and PMd (mean modulatory indices: -17.2% vs. 0.6% ; $P = 0.012$) and a nearly significant difference between pre-SMA and PMd (-10.7% vs. 0.6% ; $P = 0.057$), both indicating stronger M1 suppression for PMv and pre-SMA conditioning than for PMd conditioning when the critical 40-ms ISI was tested.

At an ISI of 60 ms, the main analysis reported in the previous paragraph revealed an intensity-dependent modulation in the PMv-M1 circuit but not in the pre-SMA-M1 circuit. To test site-specificity, we performed a CS site (2 levels: PMv and pre-SMA) x CS intensity (2 levels: subthreshold and suprathreshold) ANOVA on the modulation index. The analysis showed a significant interaction ($F_{1,11} = 8.00$, $P = 0.016$, $\eta_p^2 = 0.42$; Fig.A1.3, panel B), suggesting a differential impact of CS intensity depending on the CS site. The post-hoc analysis showed that when the CS was administered over the PMv site, the

modulatory index was greater for suprathreshold than for subthreshold CS intensity (12.2% vs. -8.7%; $P = 0.006$), whereas the modulatory index was comparable with suprathreshold and subthreshold pre-SMA conditioning (2.5% and 1.1%; $P = 0.78$). Additionally, the modulatory index tended to be larger for PMv than for pre-SMA conditioning when a suprathreshold intensity was used ($P = 0.07$), whereas it tended to be lower for PMv than for pre-SMA when a subthreshold intensity was used ($P = 0.07$). The two main effects were non-significant ($F < 2.10$, $P > 0.18$).

Finally, at a 150-ms ISI, the main analysis showed a reduction in MEPs when subthreshold or suprathreshold CS intensities were administered over PMv, but not over pre-SMA. The CS site (2 levels: PMv and pre-SMA) \times CS intensity (2 levels: subthreshold and suprathreshold) ANOVA on the modulation index demonstrated site-specific modulation by showing a significant main effect of the CS site ($F_{1,11} = 8.80$, $P = 0.013$, $\eta_p^2 = 0.44$; Fig.A1.3, panel C). This indicates stronger suppression for PMv (-20.5%) than for pre-SMA conditioning (1.9%) at a 150-ms ISI. Neither the main effect of CS intensity nor the CS site \times CS intensity interaction was significant ($F < 1$, $P > 0.58$).

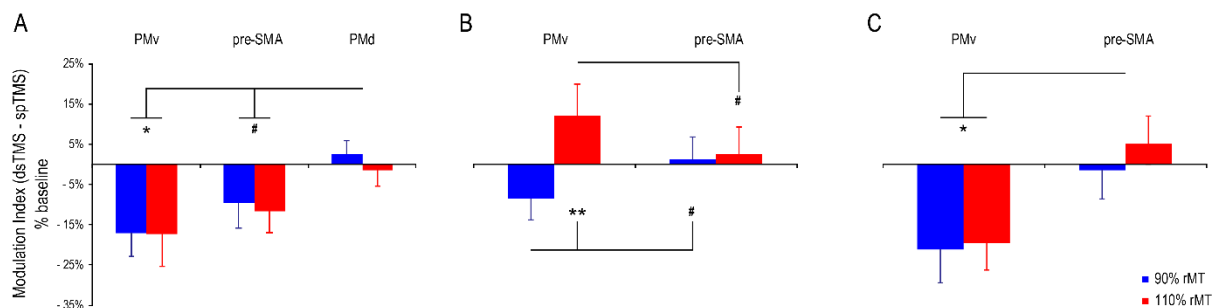


Fig.A1.3. Modulatory effects revealed by dsTMS (dsTMS minus spTMS normalised MEP amplitudes) in the targeted areas at each critical ISI. A) 40-ms ISI, including data from the control experiment; B) 60-ms ISI; C) 150-ms ISI. Error bars denote s.e.m. Hash marks and asterisks indicate marginally significant and significant post-hoc comparisons, respectively (Newman-Keuls test, # $P < 0.07$, * $P < 0.05$, ** $P < 0.01$).

A1.4 Discussion

The causal interactions between PMv and M1 or pre-SMA and M1 are still scarcely known, since the available dsTMS data mostly pertain to short temporal windows (CS-TS ISI < 15 ms) that are supposed to tap into direct anatomical connections. Here we have shown that long-latency PMv-M1 and pre-

SMA-M1 connections also robustly influence M1 output, likely through indirect pathways. We performed a systematic dsTMS investigation of the PMv-M1 and pre-SMA-M1 circuits, and tested their interactions using a wider temporal window (with ISIs ranging from 40 to 150 ms) and varying CS intensities (90 or 110% of the rMT). Our findings revealed several distinct time intervals at which PMv and pre-SMA influence M1 output during a resting state. Specifically, three critical time intervals of rostral premotor-motor interactions were revealed, corresponding to ISIs of 40, 60 and 150 ms. These timings showed different site-specific and intensity-dependent effects of the CS on the amplitude of MEPs evoked by left M1 stimulation.

A strong modulatory influence of premotor stimulation over M1 activity was found in the earliest tested time interval (i.e., when the CS was administered over PMv or pre-SMA 40 ms prior to the TS). To rule out the possibility that these inhibitory modulations were due to nonspecific effects such as the coil click or TMS-related somatosensory stimulation of the scalp, a control experiment targeting the right PMd was performed. The results showed that dsTMS over PMd-M1 at a 40-ms ISI did not modulate MEPs, relative to those evoked by spTMS (TS alone). Similar null findings with dsTMS at a 40-ms ISI have been reported in previous studies when the CS was administered to parietal or (pre)motor control areas at CS intensities similar to those used here (Valls-Solé et al., 1992; Strigaro et al., 2015). Taken together, the previous and present findings suggest that the MEP reduction found at a 40-ms ISI reflects anatomic- and time-specific rostral premotor-motor connectivity and cannot be attributed to nonspecific effects. The 40-ms ISI appeared to be a key time-interval for highlighting both PMv-M1 and pre-SMA-M1 interactions, despite the functional differences shown by these areas within the motor network at different ISIs. It is worth noting that M1 modulation by pre-SMA conditioning occurred only with a 40-ms ISI, while longer ISIs did not significantly affect M1 excitability. A different pattern of modulatory causal influence could be observed following PMv conditioning at longer ISIs. Indeed, PMv stimulation brought about a second peak of intensity-independent inhibition when the CS was delivered 150 ms before M1 stimulation. Interestingly, at a 60-ms ISI, we also observed a CS intensity-dependent M1 modulation due to PMv conditioning. The direction of the modulation that PMv exerts over M1 was

contingent upon the CS intensity applied: M1 excitability tended to be enhanced only if the CS had a suprathreshold intensity. Moreover, using a more lenient post-hoc correction, we found a tendency for suppression with a subthreshold CS at this ISI. Although these trends should be interpreted with caution, intensity-dependent effects at the 60-ms ISI were specific to the pIFC-M1 circuit, as no similar modulations were detected with pre-SMA conditioning.

This pattern of PMv-M1 interactions fits with the well-known role of the PMv in regulating motor output. Neurophysiological studies in human and non-human primates suggest that posterior inferior frontal regions are involved in action planning and exert fine-tuned control over M1 by transforming sensory information into specific motor programs (Fogassi et al., 2001; Shimazu et al., 2004; Hoshi and Tanji, 2007; Prabhu et al., 2009). Importantly, these studies indicate that connections between inferior frontal regions and M1 are critically involved in conveying information used to optimally adapt hand configuration to the object to be grasped, providing evidence that these connections play an important role in the fine control of low-level motor parameters (Shimazu et al., 2004; Hoshi and Tanji, 2007; Prabhu et al., 2009; Rizzolatti et al., 2014). This appears in line with our data showing that the PMv exerted a time- and intensity-dependent excitatory and inhibitory influence over M1 excitability, and with the fact that this such PMv influence could be found well before M1 stimulation (i.e., with the 150-ms ISI).

Intensity-dependent bidirectional facilitatory and inhibitory influences have been reported in studies exploring short-latency PMv-M1 interactions (e.g., at an ISI of 4–6 ms; Bäumer et al., 2009). The intensity-dependent switch in the net modulatory effect of posterior inferior frontal cortex stimulation has been interpreted as recruitment of different classes of intra-cortical interneurons in M1 (Bäumer et al., 2009), possibly due to the activation of different neural populations with different activation thresholds in the PMv. This explanation is supported by monkey studies showing that, while connections between the premotor cortex and M1 are excitatory, specifically glutamatergic, there are, nonetheless, synapses on both pyramidal neurons and inhibitory interneurons within M1 (Tokuno and

Nambu, 2000). Thus, the highlighted pattern of CS intensity dependence may reflect distinct involvements of underlying inhibitory and facilitatory PMv-M1 circuits. They may implicate distinct intra-cortical M1 interneurons, but also third cortical or subcortical structures, considering the long-latency timings explored in the present study. Gerloff et al. (Gerloff et al., 1998) suggested that long-latency interhemispheric interactions (with ISIs > 50 ms) might be mediated, to a certain extent, by subcortical regions. In keeping with this idea, Neubert and colleagues (Neubert et al., 2010), combining dsTMS and diffusion-weighted magnetic resonance imaging, suggested that subcortical pathways involving the basal ganglia mediate interactions between the PMv and contralateral M1 conducive to action reprogramming at relatively early latencies (ISI of 12 ms). Admittedly, the CS-induced modulations of MEPs at these long latencies might not be solely ascribed to direct connections between the conditioning brain site and M1, but might be based on the recruitment of larger scale CS-related brain networks involving indirect pathways (Massimini et al., 2005; Bortoletto et al., 2015a). Our data do not provide any information about the specific pathway involved in the long-latency influence of PMv or pre-SMA over M1 and this represents a potential limitation of our study. However, it appears that these routes are at least partially separate, considering the site-specific effects in our results.

Intensity-dependent bidirectional PMv-M1 influences may reflect mechanisms for action control, as suggested by previous dsTMS studies addressing short-latency (6–8 ms ISIs) PMv-M1 interactions during active tasks: inhibitory modulations typical of the resting state turn into facilitations during action planning and execution (Davare et al., 2008; Buch et al., 2010). Similarly, in action selection, PMv facilitatory effects turn into inhibitory effects during action reprogramming, when contextual information prompts a switch to a different motor response (Neubert et al., 2010). Thus, the fine-grained regulation of M1 output, as a consequence of the CS intensity used over PMv, supports the notion that the PMv acts as a modulator, able to activate different cells and generate relevant information for M1 to emit a specific motor command.

The pre-SMA stimulation revealed an inhibitory (but not excitatory) influence over M1 only at a 40-ms ISI, regardless of CS intensity, whereas PMv stimulation showed more complex facilitatory and inhibitory modulations at different time points. This is in keeping with the stronger modulatory effects reported with PMv stimulation relative to pre-SMA stimulation by Picazio and colleagues at short-time latencies (Picazio et al., 2014) and further supports the key role of the PMv in the fine tuning of corticomotor output.

The distinct long-latency influences of the PMv and the pre-SMA on M1 excitability may reflect their distinct roles in the hierarchy of action control. The frontal lobe is structured as a hierarchy of processes mediating the temporal arrangement and cognitive control of behaviour (Koechlin et al., 2003; Badre et al., 2009). A cascade of control processes mediating sensory, contextual and episodic control are implemented in prefrontal and premotor areas. Considering the roles of the PMv and the pre-SMA in planning and controlling actions (Picard and Strick, 2001; Rushworth et al., 2004; Hoshi and Tanji, 2007; Nachev et al., 2007; Swann et al., 2012; Rizzolatti et al., 2014), it might be suggested that these regions play partially distinct roles in the frontal hierarchy and in the regulation of M1 neurons. While the PMv is also engaged in relatively simple motor tasks and exerts a fine-tuned modulatory influence over M1 neurons, the pre-SMA is involved in higher-level action planning and plays a particularly prominent role in cognitively demanding motor tasks (Gerloff et al., 1997; Rushworth et al., 2004; Nachev et al., 2008; Pool et al., 2013; Rizzolatti et al., 2014). The pre-SMA (and the supplementary motor complex in general) releases high-level commands for subsequent downstream motor processes, and it is supposed to exert an influence over M1 for action initiation. This may explain why the dsTMS protocol in our resting conditions with no active motor task revealed only an influence of the pre-SMA over M1 at the shortest 40-ms ISI which did not depend on CS intensity. However, it could be speculated that earlier (i.e., longer-latency ISIs) and more fine-tuned modulatory influences of the pre-SMA over M1 could be revealed during complex motor tasks, in keeping with a higher-level role for this region in action control. Further studies are needed to test this hypothesis.

In sum, using dsTMS, we revealed the existence of long-latency premotor-motor interactions consisting of modulation of M1 motor output by PMv or pre-SMA conditioning at critical time intervals. The reported modulations highlight the distinct roles of the PMv and pre-SMA in causally influencing motor output in resting-state conditions. Moreover, they are consistent with the general concept that investigations of motor connectivity during a resting state can provide insights into the functions of motor networks (Grefkes et al., 2008). Our results show fine-grained premotor modulation of M1 excitability that is site-specific and both time- and intensity-dependent. Investigations of long-latency premotor-M1 interactions are important for understanding cortico-cortical connectivity at rest, and can pave the way for future investigations during active motor tasks and/or cognitive tasks where premotor-motor connectivity might be involved (Koch et al., 2007, 2010, Borgomaneri et al., 2015a, 2015b). Moreover, tracking the specific time courses of PMv-M1 and pre-SMA-M1 interactions in the healthy brain can pave the way for investigations of pathological conditions. While our study does not provide evidence for the specific pathways that might mediate these neurophysiological interactions, our data allow us to identify specific time intervals in which premotor regions can influence M1 output. These time intervals are of potential interest, as they may be amenable to connectivity manipulations, for example, via the cc-PAS protocol, which relies on the critical ISIs identified by dsTMS data (Arai et al., 2011; Buch et al., 2011; Veniero et al., 2013; Romei et al., 2016a). Future applications of these protocols may be promising for clinical conditions where connectivity across functional networks is altered (Grefkes et al., 2008; Carter et al., 2010; Avenanti et al., 2012b; Katak et al., 2012).

APPENDIX B

Long-latency interhemispheric interactions between motor-related areas and the primary motor cortex: a dual site TMS study³

A2.1 Introduction

Motor network functioning is based on neural interactions between different premotor and motor areas. The frontal lobe contains multiple premotor areas that are involved in action planning and execution and in a number of motor and cognitive processes including motor imagery (Jeannerod, 2001; Fourkas et al., 2008; Cattaneo et al., 2009), action perception (Avenanti et al., 2013b; Rizzolatti et al., 2014) and language production and comprehension (Bracco et al., 2009; de Vega et al., 2014). Premotor areas are known to act in concert with the primary motor cortex (M1) during motor behaviour and, interestingly, part of this interplay occurs via interhemispheric interactions (Koch et al., 2006; Fujiyama et al., 2016). Neuroimaging studies have revealed high functional coupling between activity in premotor regions and the contralateral M1 even when people are at rest (Biswal et al., 1995; De Luca et al., 2006; Fox and Raichle, 2007). However, these studies rely on a correlational approach characterised by low temporal resolution (Bortoletto et al., 2015b; Valchev et al., 2015). Neurophysiological techniques appear better suited for disclosing the time-course of premotor-M1 causal interactions. Yet, how premotor and motor areas in one hemisphere causally interact with the contralateral M1 is still poorly understood.

Evidence of premotor-motor interhemispheric interactions can be gathered using the dual-site transcranial magnetic stimulation (dsTMS) protocol (Ferber et al., 1992; Gerloff et al., 1998; Di Lazzaro et al., 1999; Hanajima et al., 2001; Mochizuki et al., 2004b; Ni et al., 2009; Fiori et al., 2016). In the dsTMS paradigm, a suprathreshold test stimulus (TS) administered to M1 is preceded by a conditioning stimulus (CS) administered to an interconnected brain region (e.g., in the contralateral hemisphere) at

³ Published paper: Fiori F, Chiappini E, Candidi M, Romei V, Borgomaneri S, Avenanti A (2017) Long-latency interhemispheric interactions between motor-related areas and the primary motor cortex: a dual site TMS study. *Sci Rep* 7:14936

a selected inter-stimulus interval (ISI). The CS activates hypothetical pathways (employing direct/indirect connections) from the conditioning site to M1 and modulates the amplitude of motor evoked potentials (MEPs) elicited by the TS. Depending on CS intensity, location, and the ISI between the CS and the TS, both facilitatory and inhibitory influences on M1 activity can be detected (Rothwell, 2011), thus providing causal physiological evidence for the directionality and timing of cortico-cortical interactions.

Seminal dsTMS studies have reported that M1 stimulation in one hemisphere inhibits the excitability of the contralateral M1 (Ferber et al., 1992; Gerloff et al., 1998; Di Lazzaro et al., 1999; Hanajima et al., 2001). This effect takes place via transcallosal pathways and is referred to as interhemispheric inhibition. A large body of studies reported short-latency interhemispheric interactions (ISIs < 15 ms) between the left and right M1 (Ferber et al., 1992; Gerloff et al., 1998; Di Lazzaro et al., 1999; Hanajima et al., 2001; De Gennaro et al., 2003; Reis et al., 2008; Romei et al., 2008). However, longer-latency interactions between the two M1 areas have also been documented (Gerloff et al., 1998; Mochizuki et al., 2004b; Ni et al., 2009). Those interactions are altered in neurological conditions affecting motor control (Li et al., 2007; Sattler et al., 2014), suggesting that motor network functioning might hinge on the optimal tuning between short- and long-latency interhemispheric interactions.

More recently, dsTMS has been employed to investigate connectivity between non-homologous areas, i.e., between premotor areas in one hemisphere and the contralateral M1. Studies have documented that M1 excitability can be affected not only by conditioning the contralateral M1 but also by a CS administered over the contralateral dorsal premotor cortex (PMd; Mochizuki et al., 2004a; Bäumer et al., 2006; Koch et al., 2006; Boorman et al., 2007) or the ventral premotor cortex (PMv; Buch et al., 2010; Neubert et al., 2010; Picazio et al., 2014). Moreover, studies have tested the influence of a CS over the supplementary motor area (SMA) on M1 excitability (Civardi et al., 2001; Mars et al., 2009; Neubert et al., 2010; Arai et al., 2012) – it should be noted that in this case the CS likely affects SMA bilaterally, and thus the modulatory effects on M1 may also reflect the influence of the ipsilateral SMA.

Importantly, all these studies have focused on short ISIs only (typically < 20 ms), while investigations of long-lasting interactions have been mainly limited to homologous M1 areas only. Studies of long-latency interactions between premotor areas and the contralateral M1 are scarce. To the best of our knowledge, only two studies have investigated such interactions. Ni and co-workers (2009) tested the influence of right M1 (rM1) and right PMd (rPMd) conditioning on the excitability of the left M1 (lM1). Mochizuki and colleagues (2004b) investigated the influence of a CS administered over right motor-related areas (rM1 and a dorso-lateral premotor site at the border between rPMd and the right PMv, rPMv) on the excitability of lM1. These studies have documented longer-latency premotor-motor interhemispheric interactions, supporting the notion that motor network functioning might rely on interactions at different time-scales. However, they did not clarify the issue of anatomical specificity, i.e., whether different sectors of premotor cortex (i.e., from ventral to medial areas) exert different effects on contralateral M1 excitability. Notably, these studies reported very similar modulatory effects when testing interhemispheric interactions between non-homologous areas (i.e., when a CS was administered over rPMd and a TS over lM1) and when testing motor-motor interhemispheric interactions (i.e., a CS over rM1 and a TS over lM1). This raises the possible concern that, at long ISIs, causal interactions from premotor/motor sites to contralateral M1 may reflect a nonspecific spreading of activation across motor structures. Indeed, long-latency interactions likely reflect complex and indirect pathways (Gerloff et al., 1998; Neubert et al., 2010). However, the apparently nonspecific interhemispheric effects reported in the two previous studies of Mochizuki *et al.* (2004b) and Ni *et al.* (2009) could be partly due to the high suprathreshold CS intensities used. Indeed, in those studies, lower (i.e., subthreshold) CS intensities were only used at a single long-latency ISI of 50 ms (Ni et al., 2009), but not at later ISIs.

In a third, recent study by Fiori *et al.* (2016), our group also tested long-latency interactions between a rostral medial premotor site and lM1. Although we found site-specific effects of medial premotor subthreshold and suprathreshold conditioning over M1, our study did not focus on interhemispheric interactions, and thus did not include rM1 as a control CS site.

Therefore, an important and yet unanswered question is to what extent distinct ventral, dorsal and medial sectors of the premotor cortex in one hemisphere exert site-specific modulatory effects over the contralateral M1 resulting in a long-latency influence that is distinct from the influence exerted by M1 over its contralateral homologue. Disclosing site-specific premotor-motor interactions requires a systematic investigation of the effect of the CS location, but also CS intensity, as different TMS intensities can recruit partially distinct neural populations (Serino et al., 2009; Fiori et al., 2016). All these issues are addressed in the present study, which investigated how CS intensity and CS location within different premotor and motor areas in one hemisphere impacted the excitability of the contralateral M1 at long ISIs. To this aim, we used a dsTMS protocol while recording MEPs at rest. To compare our data with those of Ni *et al.* (2009), Mochizuki *et al.* (2004b) and Fiori *et al.* (2016), we focused on the influence that a CS over right hemispheric motor areas exerts over the contralateral M1. Therefore, the TS was administered over IM1, and MEPs were recorded from the right hand. The TS was either administered alone (single pulse TMS) or preceded by a CS over one of four sites: rM1, rPMv, rPMd and the SMA (for technical reasons, the SMA was stimulated bilaterally, as in previous research; Civardi et al., 2001; Mars et al., 2009; Neubert et al., 2010; Arai et al., 2012). To explore long-latency interactions, the ISI between the CS and the TS was varied between six time-intervals (40, 60, 80, 100, 120 and 150 ms). Furthermore, to test the effect of CS intensity, we administered either a subthreshold CS (i.e., 90% of the resting motor threshold, rMT) or a suprathreshold CS (i.e., 110% of rMT). This experimental design allowed us to track the time course and the CS-intensity dependence of inter-hemispheric premotor-motor interactions. Our study shows that different sectors of the premotor cortex exert site-specific modulatory influences over the contralateral M1. Moreover, our study highlights, for the first time, the strong modulatory influence exerted by rPMv over IM1. Our findings suggest that long-latency PMv-M1 interhemispheric interactions may be a novel, powerful target for modulating motor network functioning in both healthy and damaged brains (Weiller et al., 1992; Johansen-Berg et al., 2002).

A2.2 Methods

Participants

Fifteen right-handed healthy participants (6 males; mean age \pm S.D.: 25.2 \pm 2.3 years) took part in this study. All participants gave their informed written consent before being tested. The experimental procedures were approved by the University of Bologna Bioethics committee and were in accordance with the 1964 Declaration of Helsinki. The methods carried out in this study are in accordance with approved guidelines. No adverse reactions to TMS were noticed during stimulation or reported by participants (Rossini et al., 2015).

Procedure

Participants underwent 8 blocks of stimulation, following a 4 (CS site: rPMv, rPMd, SMA or rM1) \times 2 (CS intensity: 90% and 110% of the rMT) blocked factorial design. Additionally, in each block, the TS was either administered alone (single pulse TMS: spTMS) or coupled with a preceding CS (dsTMS) delivered at one of 6 ISIs (40, 60, 80, 100, 120 or 150 ms). The order of the blocks and the TMS conditions (spTMS/dsTMS at various ISIs) within each block were randomised. Each block consisted of 152 trials (120 dsTMS trials, 20 at each ISI, and 32 spTMS trials) with a fixed inter-trial interval of 6 s. The block was split into 2 parts (with a short break in between) and lasted about 18 minutes. A 5 minutes break was allowed between blocks. Due to the overall duration of the experiment, testing was divided into two sessions conducted on two different days (4 blocks per day), separated by 7 \pm 3 days. Participants sat on a comfortable chair. They were asked to shut their eyes and keep both hands relaxed while testing, with the aim of obtaining a stable electromyographic (EMG) signal and minimising any visual distractions.

Electromyography and TMS

Silver/silver chloride electrodes were placed in a belly-tendon montage on the right first dorsal interosseous (FDI) muscle. EMG signals from the FDI were recorded by means of a Biopac MP-35

(Biopac, USA) electromyograph, using a band-pass filter of 30–500 Hz and a sampling rate of 5000 Hz. TMS pulses were administered via two 50-mm butterfly-shaped coils, each of which was connected to a Magstim 200 monophasic transcranial stimulator (Magstim, UK).

The TS was administered over IM1 with the intersection of the coil placed tangentially to the scalp, at a $\sim 45^\circ$ angle away from the midline, inducing a posterior-to-anterior current direction (Kammer et al., 2001; Di Lazzaro et al., 2004). The IM1 was identified as the optimal scalp position for inducing the largest MEPs in the right FDI. The TS intensity was set in order to induce MEPs of ~ 1 mV amplitude. The corresponding mean stimulator output \pm S.D. was $53.4\% \pm 11.5$ on day 1 and $52.6\% \pm 13.0$ on day 2 ($P=0.49$). The CS was administered over rM1 (corresponding to the hotspot for evoking the largest MEPs in the left FDI), and over rPMv, rPMd and SMA, all of which were localised using established methods (see next paragraph). The CS intensity was either subthreshold or suprathreshold, corresponding to 90% and 110% of the rMT, respectively. The rMT was defined as the lowest stimulator intensity able to evoke a MEP larger than $50 \mu\text{V}$ with 50% probability. The mean rMT \pm S.D. across participants was $40.3\% \pm 6.5$ on day 1 and $41.4\% \pm 8.0$ on day 2.

Stimulation sites

To localise the stimulation sites, we used established functional, craniometric and stereotaxic procedures. Each target site was identified on the scalp based on the most established procedure (e.g., functional methods for M1), and then the position of the coil was verified using a neuronavigation system (Fiori et al., 2016). Both the IM1 and the rM1 scalp sites were localised using functional procedures, i.e., by identifying the FDI motor hotspot. The rPMd scalp site was determined by placing the coil 2.5 cm anterior and 1 cm medial relative to rM1 as in previous research^{22,31,44}. For this stimulation site, the TMS coil was rotated away from the sagittal midline by $\sim 90^\circ$, inducing a lateral-to-medial current (Mochizuki et al., 2004b; Ni et al., 2009). When stimulating the SMA, the coil was positioned 4 cm anterior to the Cz position in the 10–20 system (Verwey et al., 2002; Matsunaga et al.,

2005; Arai et al., 2012; Lu et al., 2012a), and the handle of the coil was pointed forward to induce an anterior-to-posterior current (Verwey et al., 2002; Arai et al., 2012).

The rPMv scalp site was identified using a neuronavigation system (Davare, 2006; Davare et al., 2009; Cattaneo, 2010; Fiori et al., 2016). We used the SofTaxis Navigator system (EMS; Electro Medical Systems, Bologna, Italy), as in previous studies (Bertini et al., 2010; Tidoni et al., 2013; Fiori et al., 2016; Paracampo et al., 2016; Avenanti et al., 2017; Valchev et al., 2017). This system automatically estimates Talairach coordinates from a magnetic resonance imaging (MRI)-constructed stereotaxic template. Based on the MRI template, we estimated the scalp position corresponding to rPMv (on the anterior ventral aspect of the precentral gyrus, at the border with the posterior part of the inferior frontal gyrus) using the Talairach coordinates $x = 52$, $y = 7$, $z = 24$. The centre of the coil was positioned over this location with the handle pointing anteriorly, inducing a posterior-to-anterior current (Avenanti et al., 2007, 2012a; Davare et al., 2009; Jacquet and Avenanti, 2015).

The neuronavigation system was also used to estimate the coordinates of the target locations (lM1, rM1, rPMv, rPMd and SMA) projected onto the cortical surface of the MRI template (see Fig.A2.1). For each participant, skull landmarks (nasion, inion and 2 preauricular points) and about 80–100 points providing a model of the scalp were digitised through a Polaris Vicra digitiser (Northern Digital). An estimated MRI was created for each participant using a 3D warping algorithm that fits a high-resolution MRI template to the acquired landmarks and scalp model. This estimation has been proven to ensure a spatial accuracy of ~ 5 mm, a level of precision closer to that obtained using individual MRIs than can be achieved using other localisation methods (Carducci and Brusco, 2012). The mean \pm S.E.M. estimated Talairach coordinates were: lM1: $x = -39.3 \pm 1.0$, $y = -19.0 \pm 1.6$, $z = 58.6 \pm 0.9$; rM1: $x = 37.6 \pm 1.2$, $y = -18.5 \pm 1.8$, $z = 58.6 \pm 1.1$; rPMv: $x = 54.3 \pm 0.9$, $y = 7.3 \pm 0.5$, $z = 23.4 \pm 0.4$; rPMd: $x = 25.8 \pm 2.0$, $y = 1.0 \pm 2.2$, $z = 62.9 \pm 1.6$; and SMA: $x = 0.6 \pm 0.2$, $y = 4.9 \pm 1.8$, $z = 63.8 \pm 1.6$. These estimated coordinates are consistent with the boundaries of human M1, PMv, PMd and SMA regions as defined by a meta-analysis of neuroimaging studies (Mayka et al., 2006). They are also consistent with previous TMS

studies that used individual's MRI data to localise these areas for stimulation (Verwey et al., 2002; Di Lazzaro et al., 2004; Mochizuki et al., 2004a; Matsunaga et al., 2005; O'Shea et al., 2007; Arai et al., 2011; Buch et al., 2011; Catmur et al., 2011; Lu et al., 2012a; Randhawa et al., 2013).

Data analysis

Neurophysiological data were analysed offline. Due to a technical issue, data from one female participant were lost, so the final sample consisted of fourteen individuals. EMG activity was visually inspected, and trials showing muscle activity 100 ms before the TMS artefact were removed from the analysis (~4%). In each block, the mean peak-to-peak MEP amplitude was calculated for dsTMS and spTMS conditions. In each condition, MEPs with an amplitude ≥ 2 S.D. from the mean were excluded from the analysis (~3% of trials).

A repeated measures ANOVA with the factors CS site (4 levels: rPMv, rPMd, rM1 and SMA) and CS intensity (2 levels: 90% and 110% rMT) was first conducted on raw MEP amplitudes induced by spTMS (TS alone). Neither of the main effects was significant, nor was the interaction (all $P > 0.26$), demonstrating that MEPs induced by spTMS were comparable across the eight blocks. Then, MEPs elicited by spTMS were used to normalise the MEP amplitudes induced by dsTMS: in each block (i.e., for each combination of CS site and CS intensity), an index of dsTMS modulation was computed for each ISI by subtracting MEPs elicited by spTMS within the same block from MEPs elicited by dsTMS (dsTMS MEP – spTMS MEP). Normalised dsTMS modulation indices were submitted to a repeated measures ANOVA with the factors CS site (4 levels: rPMv, rPMd, rM1 and SMA), CS intensity (2 levels: 90% and 110% of rMT) and ISI (6 levels: 40, 60, 80, 100, 120 and 150 ms). Partial η^2 (η_p^2) was computed as a measure of effect size for significant main effects and interactions. By convention, η_p^2 effect sizes of ~0.01, ~0.06, and ~0.14 are considered small, medium, and large, respectively (Cohen, 1992).

The ANOVA showed a significant three-way interaction (see Results section) which was further explored with six separate CS site x CS intensity ANOVAs, one for each ISI. In these further ANOVAs, we directly tested the critical question of whether rPMv, rPMd or SMA exert site-specific modulatory influences

over IM1 that differ from the modulatory influence exerted by rM1. We used post-hoc pairwise comparisons (Duncan's tests) to analyse significant effects involving the factor CS site. Additionally, to better interpret the pattern of results shown in the ANOVAs, we used one-sample t-tests to test whether dsTMS modulation indices (dsTMS MEP – spTMS MEP) differed significantly from zero (i.e., whether MEPs in the dsTMS conditions were different from the corresponding spTMS condition).

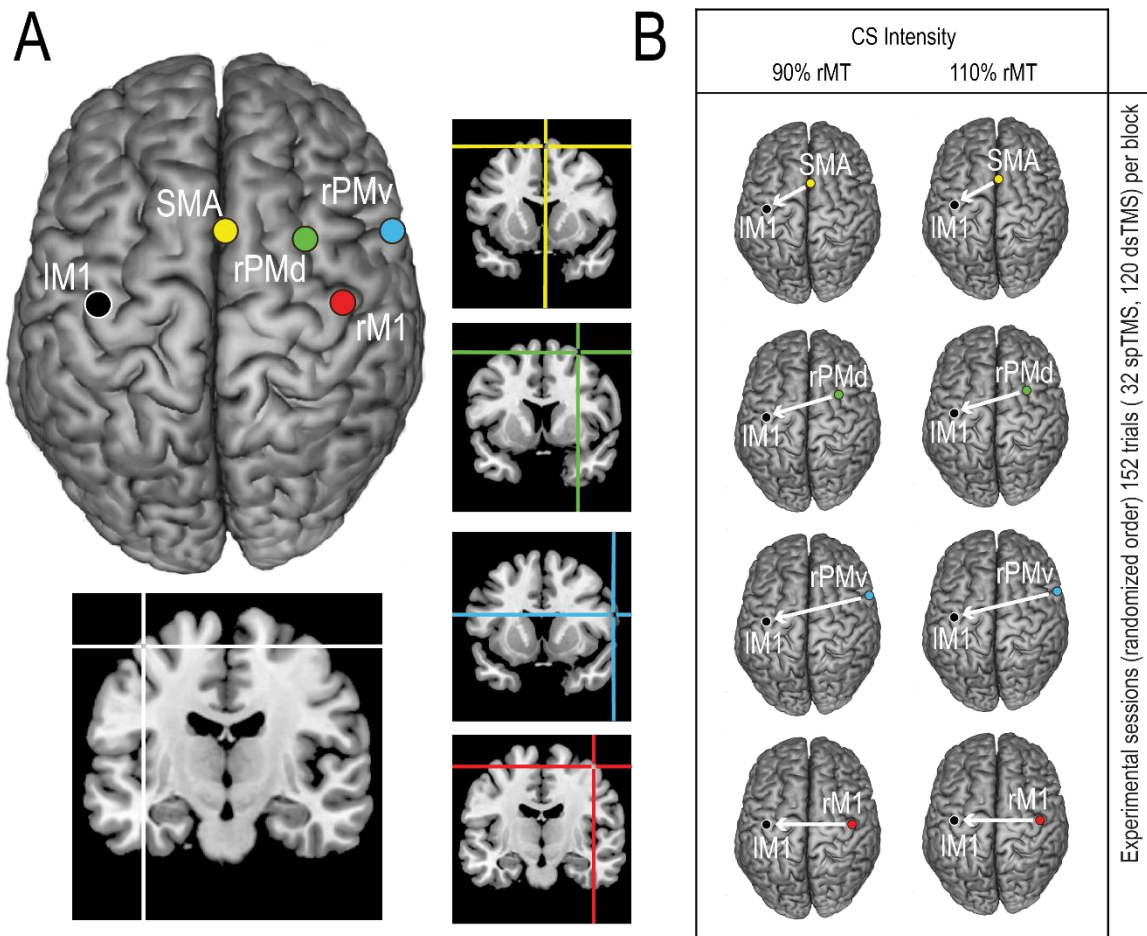


Fig.A2.1 A) Brain stimulation sites. Coordinates in Talairach space corresponding to the projection of the stimulated scalp sites onto the brain surface were estimated through a neuronavigation system and reconstructed on a standard template using MRIcron software (v 1.40, www.mricron.com). B) Schematic representation of the experimental blocks. For each experimental block, brain stimulation sites, CS intensity and number of trials are reported.

A2.3 Results

The CS site x CS intensity x ISI ANOVA on dsTMS MEP indices (i.e., dsTMS MEP – spTMS MEP) showed

a main effect of CS site ($F_{3,39} = 4.58$, $p = 0.008$; $\eta_p^2 = 0.26$), a main effect of ISI ($F_{5,65} = 7.92$, $p = 0.00001$; $\eta_p^2 = 0.38$), a CS site x ISI interaction ($F_{15,195} = 1.90$, $p = 0.025$; $\eta_p^2 = 0.13$) and a three-way CS site x CS intensity x ISI interaction ($F_{15,195} = 1.89$, $p = 0.026$; $\eta_p^2 = 0.13$). The three-way interaction indicates that the combined influence of CS intensity and ISI on MEP amplitudes varied as a function of the CS site, thus providing initial support to the hypothesis of site-specific effects. To further explore the three-way interaction and test site-specific modulatory influences of premotor/motor conditioning on IM1 excitability, separate CS site x CS intensity ANOVAs were performed, one for each ISI (Fig.A2.2, see also Fig.A2.3).

40-ms ISI

The CS site x CS intensity ANOVA performed on the dsTMS modulation index collected at a 40-ms ISI showed a main effect of CS site ($F_{3,39} = 7.26$, $p = 0.001$; $\eta_p^2 = 0.36$; Fig.A2.2, panel A). Post-hoc comparisons suggested that this main effect was accounted for by the more negative dsTMS modulation index values obtained with rPMv conditioning (mean MEP contrast \pm S.E.M. = -0.29 mV \pm 0.08) relative to rPMd (-0.01 mV \pm 0.02; $p = 0.001$), rM1 (-0.13 mV \pm 0.05; $p = 0.012$) and SMA conditioning (-0.11 mV \pm 0.04; $p = 0.009$). This result reflects greater inhibition of MEPs due to rPMv conditioning, compared to the other conditioning sites. Moreover, the dsTMS modulation indices were comparable in the rM1 and SMA conditions ($p = 0.81$), and more negative in those conditions than in the rPMd condition (rM1: $p = 0.065$; SMA: $p = 0.086$). The ANOVA did not show a main effect of CS intensity or an interaction between the two factors ($p > 0.21$), suggesting that the site-specific modulations at a 40-ms ISI were not affected by CS intensity.

One-sample t-tests were performed to further explore the main effect of CS site. These analyses showed that the dsTMS modulation index (across the two CS intensities) was significantly less than zero (i.e., dsTMS MEPs were inhibited relative to spTMS MEPs) in the rPMv, rM1 and SMA conditions (all $p < 0.027$), but not in the rPMd condition ($p = 0.78$). Thus, conditioning the rPMv, rM1 and SMA with dsTMS elicited motor inhibition relative to (unconditioned) spTMS MEPs.

60-ms ISI

At this ISI, no significant effects were detected (Fig.A2.2, panel B). The CS site x CS intensity ANOVA showed no significant main effect of CS site ($F_{3,39} = 2.47$, $p = 0.076$; $\eta_p^2 = 0.16$) and no main effect of, or interaction with, CS intensity ($p > 0.65$).

80-ms ISI

This ANOVA showed a significant CS site x CS intensity interaction ($F_{3,39} = 3.20$, $p = 0.034$; $\eta_p^2 = 0.20$; Fig.A2.2, panel C), but no significant main effects (all $p > 0.54$). The interaction was due to the different influences exerted by subthreshold and suprathreshold CS intensities across CS sites. Post-hoc analyses showed that when the CS was administered over rM1, more positive dsTMS modulation index values were obtained with a suprathreshold CS compared to a subthreshold CS ($0.18 \text{ mV} \pm 0.07$ vs. $-0.06 \text{ mV} \pm 0.05$; $p = 0.031$). An opposite pattern of rPMv, rPMd and SMA conditioning was appreciable by visual inspection (i.e., more positive dsTMS modulation indices for a subthreshold CS than for a suprathreshold CS), but the relevant post-hoc tests did not reach statistical significance (all $p > 0.15$). The CS site x CS intensity interaction was also due to larger (more positive) dsTMS modulation indices with suprathreshold rM1 conditioning than with suprathreshold rPMv conditioning ($p = 0.042$). Also, a larger dsTMS modulation index was found with subthreshold conditioning when the CS was delivered to the SMA than when it was administered over rM1 ($p = 0.051$). No other comparisons were significant ($p > 0.49$).

One-sample t-tests were used to further explore the significant interaction. These tests showed that dsTMS modulation indices were significantly greater than zero (i.e., dsTMS MEPs were facilitated relative to spTMS MEPs) when using a suprathreshold CS over rM1 ($p = 0.025$), and a subthreshold CS over rPMd ($p = 0.019$) and the SMA ($p = 0.056$). Facilitation with a subthreshold CS over the SMA was marginally significant ($p = 0.056$), and facilitation with a subthreshold CS over rPMv did not reach significance ($p = 0.21$). No other conditions showed dsTMS modulation indices different from zero (all $p > 0.22$).

100- and 120-ms ISIs

At these ISIs, no significant effects were detected (Fig.A2.2, panels D, E). The CS site x CS intensity ANOVAs showed no significant main effects of CS site at 100 ms ($F_{3,39} = 2.31$, $p = 0.092$; $\eta_p^2 = 0.15$) or 120 ms ($F_{3,39} = 2.45$, $p = 0.08$; $\eta_p^2 = 0.16$) and no main effects of, or interactions with, CS intensity (all $p > 0.36$).

150-ms ISI

The ANOVA showed a main effect of CS site ($F_{3,39} = 3.46$, $p = 0.026$; $\eta_p^2 = 0.21$), but no main effect of CS intensity ($p = 0.96$). It also showed a significant CS site x CS intensity interaction ($F_{3,39} = 3.63$, $p = 0.021$; $\eta_p^2 = 0.22$; Fig.A2.2, panel F). Post-hoc analyses showed more negative dsTMS modulation indices when suprathreshold conditioning was administered over rPMv ($-0.21 \text{ mV} \pm 0.09$) and rM1 ($-0.20 \text{ mV} \pm 0.07$) relative to rPMd ($0.08 \text{ mV} \pm 0.05$; all $p < 0.01$) and SMA ($0.10 \text{ mV} \pm 0.07$; all $p < 0.006$), which in turn did not differ from one another ($p = 0.8$). Suprathreshold conditioning of rPMv and rM1 induced comparable dsTMS modulation indices ($p = 0.84$). One-sample t-tests indicated that rPMv and rM1 dsTMS modulation indices were significantly different from zero (i.e., dsTMS MEPs were inhibited relative to spTMS MEPs; all $p < 0.037$). No other conditions showed dsTMS modulation indices different from zero (all $p > 0.16$).

Post-hoc analyses also showed that the comparison between suprathreshold and subthreshold CS intensities was significant when the CS was administered over the SMA ($p = 0.028$), but not when the CS was administered over rPMv, rM1 or rPMd (all $p > 0.19$). When the CS was administered over the SMA, dsTMS modulation indices were negative for a subthreshold CS and positive for a suprathreshold CS. However, those dsTMS modulation indices did not significantly differ from zero, as shown by one-sample t-tests (all $p > 0.16$).

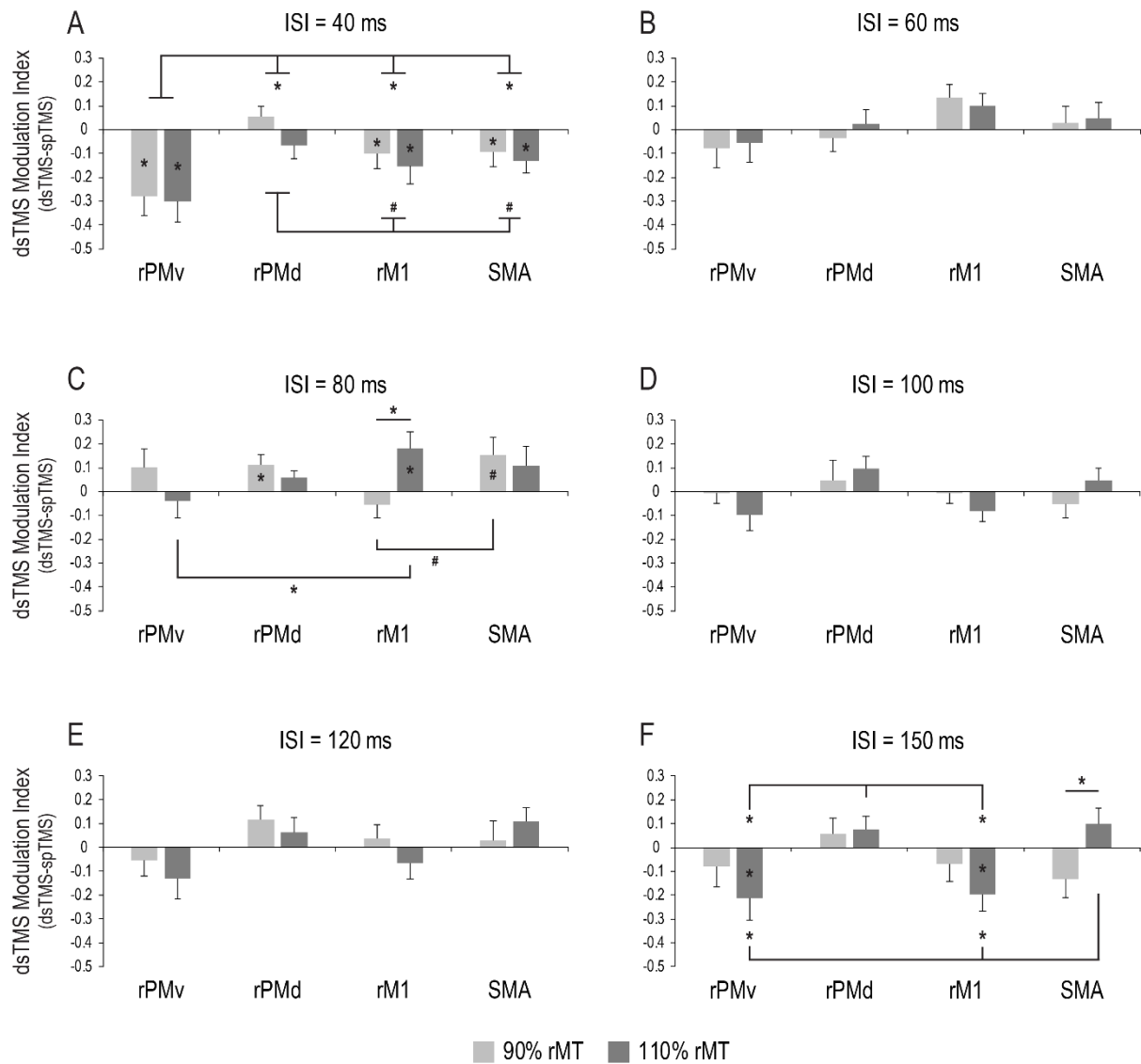


Fig.A2.2. Changes in IM1 excitability induced by conditioning of right motor areas. The CS site (rPMv, rPMd, rM1 and SMA) x CS intensity (90% and 110% of rMT) interaction is shown separately for each ISI (40, 60, 80, 100, 120, 150 ms) in panels (A-F). On the y-axis of each panel, the amplitude of MEPs induced by dsTMS is represented relative to MEPs induced by spTMS (dsTMS – spTMS) to normalise the data. Error bars denote S.E.M. Hash marks and asterisks indicate marginally significant and significant comparisons, respectively (see text).

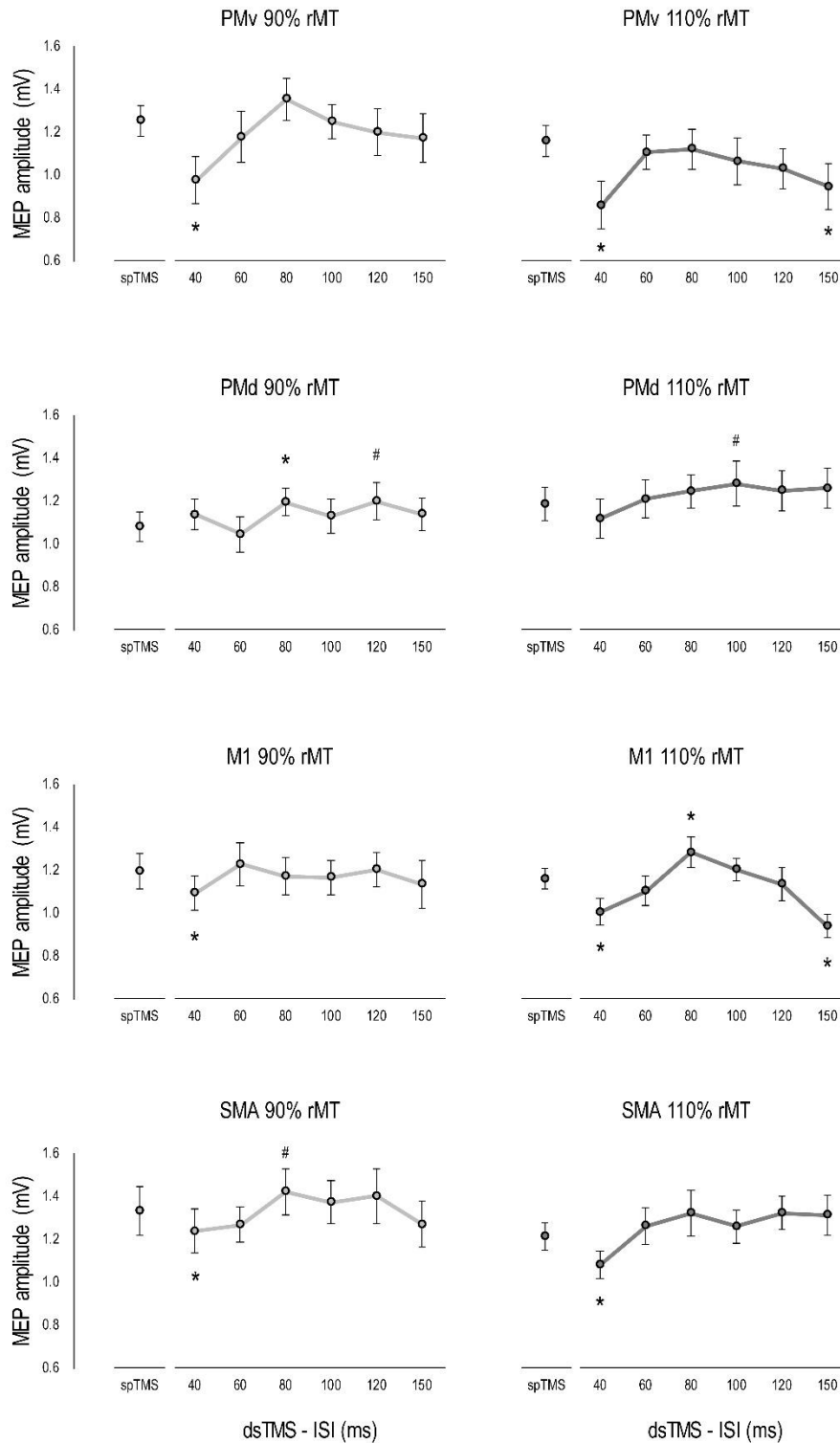


Fig.A2.3. Changes in IM1 excitability. Raw MEP amplitudes (in mV) induced by spTMS and dsTMS in each block (i.e., in each combination of CS site and CS intensity). Asterisks (*) indicate significant comparisons between dsTMS and spTMS MEPs ($p < 0.05$) and harsh marks (#) indicate non-significant trends ($0.09 < p < 0.06$). In addition to the comparisons reported in the text (ISI = 40,80,150, see Fig.A2.2), here, further exploratory t-tests were conducted for those ISIs not associated with significant effects in the CS site x CS intensity ANOVAs (ISI = 60,100, 120). These comparisons show sparse non-significant modulatory effects of premotor conditioning that did not emerge using our stringent criterion of site-specificity.

A2.4 Discussion

Motor network functioning might depend on the optimal tuning of neural interactions between different nodes of the network. These interplays include interhemispheric interactions between homologous (Ferber et al., 1992; Gerloff et al., 1998; Avenanti et al., 2012b) and non-homologous areas (Boorman et al., 2007; Picazio et al., 2014). The functional interactions between these interconnected regions of the motor network likely occur at different time scales, and can be optimally explored using causal methods with high temporal resolution like the dsTMS protocol.

As reported in the introduction, the only two previous dsTMS studies demonstrating the existence of long-latency premotor-motor interhemispheric interactions in healthy humans (Mochizuki et al., 2004b; Ni et al., 2009) showed that the effects of stimulating non-homologous areas (i.e., PMd-M1) were very similar to the effects of stimulating homologous areas (i.e., M1-M1), thus leaving unresolved the issue of the anatomical specificity of long-latency interhemispheric interactions in the human motor system. We hypothesised that the apparent lack of specificity reported in previous studies might stem from the limited number of conditions being tested. Thus, in the present study, we provided a systematic investigation of long-latency interactions (ISIs from 40 to 150 ms) between primary and non-primary motor areas of the right hemisphere (rM1, rPMv, rPMd and bilateral SMA) and lM1. We investigated the effects of ISI, CS site and CS intensity (subthreshold vs. suprathreshold intensity) on lM1 excitability, while participants were at rest.

Our study highlights three key time points (i.e., 40-, 80- and 150-ms ISIs) at which site-specific MEP modulations occurred. The first inhibitory modulation of lM1 was detected when the CS was administered over rPMv, rM1 and the SMA at a 40-ms ISI. The 80-ms ISI revealed an intensity-dependent excitatory influence of rM1 conditioning, while the 150-ms ISI highlighted intensity-dependent inhibitory influences of rPMv and rM1.

In keeping with previous studies testing long-latency cortico-cortical interactions (Mochizuki et al., 2004b; Ni et al., 2009; Fiori et al., 2016), most of the interactions detected across the CS sites and ISIs

were inhibitory. Monkey studies indicate that interhemispheric interactions occur mainly through transcallosal pathways connecting homologous areas in the two hemispheres (Marconi et al., 2003; Boussaoud et al., 2005). Transcallosal connections are constituted by excitatory fibres originating from a target (motor) area in one hemisphere (i.e., where the CS is administered) and synapsing over interneurons in the contralateral homologue. Excitatory signals conveyed by transcallosal connections activate local circuits in the homologous area that are mainly characterised by GABAergic neurons (Somogyi et al., 1998), consequently resulting in a net reduction of motor output. However, in view of the long ISIs we explored in this study, it is also very likely that complex and indirect cortico-subcortical pathways might have been involved in the observed interhemispheric inhibitions (at ISIs of 40 and 150 ms), as well as interhemispheric facilitations (at an ISI of 80 ms). Yet, our study clearly demonstrates that MEP modulations are site- and intensity-specific, even at long ISIs.

A major point of novelty of our study is the investigation of long-latency interhemispheric PMv-M1 interactions. Indeed, previous studies testing long-latency interhemispheric interactions mainly focused on M1-M1 or PMd-M1. In a previous study, Mochizuki *et al.* (2004b) conditioned a dorsolateral premotor site (2 cm anterior to M1), and thus might have influenced the most dorsal aspects of PMv, whereas here we centered the CS over an anterior sector of the PMv proper. Conditioning rPMv resulted in a strong modulatory influence over IM1 in the explored time window. This modulatory influence was particularly conspicuous in the first critical ISI (40 ms). This ISI was characterised by a strong inhibitory influence of rPMv conditioning on IM1 excitability. Inhibition was greater when the CS was administered over rPMv relative to the other CS sites. A reduction in IM1 excitability was also detected with rM1 and SMA conditioning, replicating previous findings of a peak in interhemispheric inhibition when a CS was administered at a 40-ms ISI over similar sites (Gerloff et al., 1998; Ni et al., 2009; Fiori et al., 2016). Varying CS intensity produced no substantial differences in IM1 excitability when the CS was administered to rPMv, rM1 or the SMA. Additionally, no IM1 modulation was elicited by either subthreshold or suprathreshold conditioning of rPMd. The lack of IM1 modulation when the CS was administered over rPMd is in keeping with previous data (Fiori et al., 2016), and rules out the

possibility that IM1 suppression with rPMv, rM1 or SMA conditioning might be due to nonspecific factors such as the coil click (Furubayashi et al., 2000). In summary, data collected across the four CS sites with a 40-ms ISI provide strong support for our hypothesis of site-specific interhemispheric interactions between motor-related areas, and suggest these interactions are relatively insensitive to the intensity of the CS. Yet, it should be acknowledged that we only tested two CS intensities, both near to rMT. Thus, future studies might use lower (< 90% rMT) or higher (> 110% rMT) CS intensities in order to further test intensity-dependent modulations at this ISI.

The marked modulatory influence elicited by PMv conditioning appears in line with studies using different TMS protocols and reporting strong effects of premotor conditioning on M1. Studies have shown that administering low-frequency repetitive TMS (rTMS) over ventral and lateral premotor sites can lead to stronger modulation of M1 than administering rTMS over M1 itself (Gerschlagler et al., 2001; Münchau et al., 2002; Avenanti et al., 2007, 2013b), and can affect a more widespread fronto-parietal network (Chouinard et al., 2003). In the dsTMS study of Fiori *et al.* (2016), conditioning the posterior inferior frontal cortex – at the border with the PMv – led to stronger (ipsilateral) M1 modulations than conditioning a medial premotor site (pre-SMA) did, and this stronger modulation was observed at several long-latency ISIs. Picazio *et al.* (2014) used dsTMS to test short-latency premotor-motor interactions. The authors reported that conditioning a right inferior frontal site – partially overlapping with our PMv site – exerted a stronger modulatory influence over IM1 than conditioning a control site (i.e., the pre-SMA). Taken together, these findings suggest that PMv sites can exert strong modulatory influences over M1. Our findings build upon previous evidence by showing that rPMv conditioning inhibits the contralateral M1 at 40 ms after the CS, and this inhibition is even larger than that induced by conditioning the homologous M1.

In monkeys, direct (heterotopic) connections between premotor cortices and the contralateral M1 have been demonstrated (Marconi et al., 2003; Boussaoud et al., 2005), although they are believed to play a minor role in motor functioning, with most neural interactions occurring between homologous areas.

Thus, the effects exerted by rPMv stimulation over IM1 could be mainly ascribed to the recruitment of indirect pathways linking the two areas. Because of the stronger effects of rPMv relative to rM1 conditioning at the 40-ms ISI, the rPMv-IPMv-IM1 pathway appears more plausible than the rPMv-rM1-IM1 pathway, although, in view of the long ISI, even more indirect cortico-subcortical pathways could be hypothesised (Neubert et al., 2010).

An effect of rPMv conditioning was also observed at the longest ISI of 150 ms, although in this case the modulation was not specific to rPMv. In keeping with the study of Mochizuki *et al.* (2004b; that conditioned M1 and a premotor site more dorsal and posterior than our PMv site), we found that suprathreshold CS intensities administered over rPMv or rM1 led to reductions in contralateral IM1 excitability. Our data expand on previous evidence by showing that the inhibitory effects were specific to suprathreshold conditioning of rPMv and rM1, as they were not found with rPMd or SMA conditioning, or with subthreshold CS intensities. Thus, our study suggests that the second long-latency peak of inhibition found at a 150-ms ISI might reflect site-specific interactions involving homologous (rM1-IM1) as well as non-homologous areas (rPMv-IM1). Our data allow us to firmly rule out the possibility that interhemispheric inhibition at an ISI of 150 ms reflects nonspecific spreading of activation to any premotor site. Yet, future studies will need to test the possibility that spreading activation across rM1 and rPMv specifically accounts for the suppression of IM1 excitability at this ISI.

In addition to inhibitory interhemispheric interactions, we also found some evidence of facilitatory interhemispheric interactions. Motor facilitations were selectively detected at an ISI of 80 ms. Greater dsTMS MEP modulation indices were obtained with rM1 conditioning when using a suprathreshold CS relative to a subthreshold CS. Suprathreshold rM1 conditioning also increased IM1 excitability relative to spTMS. An opposite pattern of modulation across the other premotor CS sites was detectable by visual inspection (i.e., larger dsTMS MEPs induced by subthreshold relative to suprathreshold CS). Yet, subthreshold conditioning of rPMd and SMA significantly increased IM1 excitability relative to spTMS.

Previous studies have already documented short-latency M1 facilitation when the CS was administered over the contralateral M1, rPMd or the SMA. These effects were detected with both subthreshold and suprathreshold CS intensities, although not always in a consistent way (Ferber et al., 1992; Hanajima et al., 2001; Bäumer et al., 2006; Arai et al., 2012). The mechanism underlying such short-latency interhemispheric interactions is likely different from that underlying our long-latency modulations. However, it is interesting to note that these previous investigations concluded that premotor-M1 interactions and M1-M1 interactions were mediated by different populations of neurons in M1, suggesting site-specific mechanisms.

Our data appear to be in keeping with previous evidence that rPMd conditioning requires subthreshold intensities to produce interhemispheric facilitation in the contralateral M1 (Civardi et al., 2001; Bäumer et al., 2006), and suggest that this rule may apply to long-latency interactions at an ISI of about 80 ms. On the other hand, different rules might apply to short- and long-latency interactions involving rM1 and SMA. At an 80-ms ISI, our data are not consistent with evidence that subthreshold rM1 conditioning²⁹ and suprathreshold, but not subthreshold, SMA conditioning (Arai et al., 2012) induce short-latency M1 facilitation. Yet, in those studies, the intensity of subthreshold conditioning (60–90% of active motor threshold) was much lower than that used in the present study, and the intensity of suprathreshold conditioning (140% of active motor threshold) was higher.

The selectivity of MEP facilitation for suprathreshold rM1 conditioning likely reflects site-specific and intensity-dependent interactions between the two homologous M1 areas. A possible alternative interpretation is that suprathreshold conditioning of rM1 may have caused a spreading of the magnetic stimulation to nearby premotor CS sites (e.g., rPMd or SMA), resulting in attenuated activation of those sites, similar to that caused by subthreshold CS intensities over the same sites. However, the M1-M1 facilitatory effect with suprathreshold conditioning was more consistent than the premotor-M1 facilitatory effects with subthreshold conditioning, thus speaking in favor of site-specific interactions

between the two M1 areas. Nevertheless, future studies will have to clarify whether the same circuit mediates the effects observed with rM1 and premotor conditioning at an ISI of 80 ms.

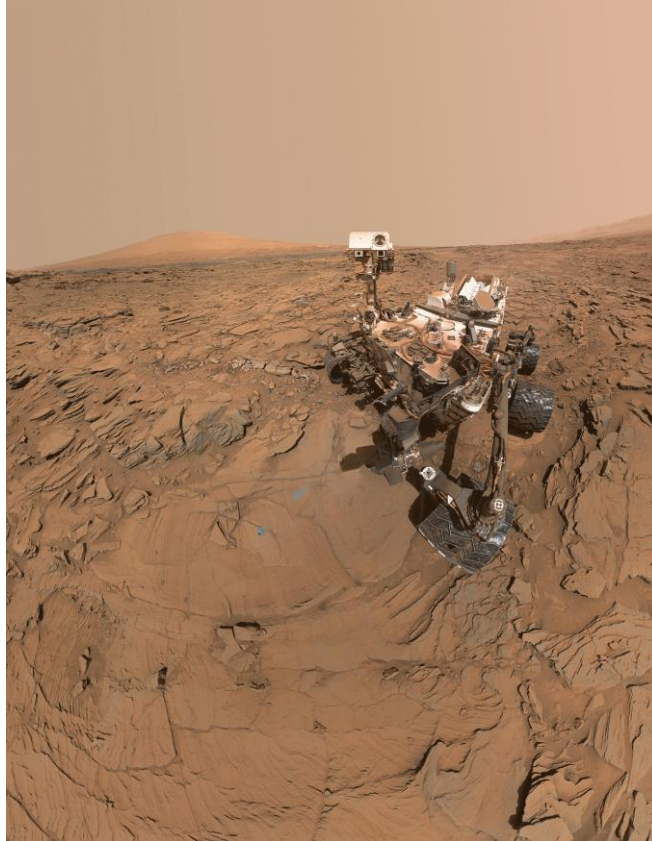
A potential limitation of our study is the use of only two levels of CS intensity. The investigation of an input-output curve with additional CS intensities (i.e., lower subthreshold and higher suprathreshold intensities) may further highlight intensity-dependent interhemispheric interactions at specific ISIs. Moreover, based on the previous studies of Ni *et al.* (2009) and Mochizuki *et al.* (2004b), we focused on right-to-left interhemispheric interactions in right-handed participants only. In this regard, future studies might test whether asymmetrical interactions occur at late ISIs, similar to those reported with short ISIs (Koch *et al.*, 2006; Boorman *et al.*, 2007; Rizzo *et al.*, 2009). Yet, the selected CS intensities and the focus on right-to-left cortico-cortical interactions were sufficient to support our hypothesis that long-latency interhemispheric interactions cannot be reduced to a nonspecific spreading of activation across motor structures.

In conclusion, our study documents site- and intensity-dependent inhibitory and facilitatory modulations of IM1 excitability by stimulation of contralateral premotor and motor regions in the right hemisphere. Our data highlight prominent and distinct modulatory roles of rPMv, rM1 and SMA over IM1 across the explored ISIs of 40–150 ms. Although the reported modulations at 40-, 80- and 150-ms ISIs likely reflect not only the recruitment of direct pathways but also large indirect cortico-cortical and cortico-subcortical pathways (Gerloff *et al.*, 1998; Massimini *et al.*, 2005; Neubert *et al.*, 2010; Bortoletto *et al.*, 2015b), our study clarifies that long-latency interhemispheric interactions do not reflect a nonspecific spreading of activation across motor structures (Mochizuki *et al.*, 2004b; Ni *et al.*, 2009). Rather, they reflect intensity-dependent, site- and time-specific mechanisms.

The investigation of long-latency interhemispheric interactions is important for understanding the rules governing motor network functioning at rest, and can lay the groundwork for further exploration during motor and/ or cognitive tasks that involve premotor-to-motor connectivity (Fourkas *et al.*, 2006; Catmur *et al.*, 2011; Borgomaneri *et al.*, 2015a, 2015b) or connections between other sectors of the

motor system (Koch et al., 2007, 2009; Plow et al., 2014). Tracking the specific time course of interhemispheric interactions between homologous and non-homologous brain areas in the healthy population can provide novel insights into clinical conditions associated with altered connectivity patterns. Our study does not clarify which pathways mediate these neurophysiological interactions. Nevertheless, our findings point to specific time intervals at which motor and premotor areas can affect contralateral M1 output. Studies of the exact time scales of these interactions are of potential interest, as they might be crucial for manipulating the functionality of these motor connections. For example, one might apply novel TMS protocols such as the cortico-cortical paired associative stimulation (cc-PAS), which can modify the functional connectivity between interconnected nodes (Buch et al., 2011; Veniero et al., 2013; Johnen et al., 2015; Romei et al., 2016a). Future applications of these kinds of non-invasive neurostimulation protocols are promising for clinical profiles characterised by altered connectivity across functional networks (Johansen-Berg et al., 2002; Avenanti et al., 2012b).

- May the curiosity be with you -



REFERENCES

- Abrahamyan A, Clifford CWG, Arabzadeh E, Harris JA (2011) Improving Visual Sensitivity with Subthreshold Transcranial Magnetic Stimulation. *J Neurosci* 31:3290–3294.
- Abreu AM, Macaluso E, Azevedo RT, Cesari P, Urgesi C, Aglioti SM (2012) Action anticipation beyond the action observation network: A functional magnetic resonance imaging study in expert basketball players. *Eur J Neurosci* 35:1646–1654.
- Aglioti SM, Cesari P, Romani M, Urgesi C (2008) Action anticipation and motor resonance in elite basketball players. *Nat Neurosci* 11:1109–1116.
- Agyei SB, van der Weel FRR, van der Meer ALH (2016) Development of Visual Motion Perception for Prospective Control: Brain and Behavioral Studies in Infants. *Front Psychol* 7:1–14.
- Alaerts K, Swinnen SP, Wenderoth N (2009) Is the human primary motor cortex activated by muscular or direction-dependent features of observed movements? *Cortex* 45:1148–1155.
- Alais D, Blake R (1998) Interactions between global motion and local binocular rivalry. *Vision Res* 38:637–644.
- Albert NB, Robertson EM, Miall RC (2009) The Resting Human Brain and Motor Learning. *Curr Biol* 19:1023–1027.
- Albright TD (1984) Direction and orientation selectivity of neurons in visual area MT of the macaque. Direction and Orientation Selectivity of Neurons in Visual Area MT of the Macaque. *J Neurophysiol* 52:1106–1130.
- Antonov I, Antonova I, Kandel ER, Hawkins RD (2003) Activity-dependent presynaptic facilitation and hebbian LTP are both required and interact during classical conditioning in *Aplysia*. *Neuron* 37:135–147.
- Arai N, Lu M-K, Ugawa Y, Ziemann U (2012) Effective connectivity between human supplementary motor area and primary motor cortex: a paired-coil TMS study. *Exp Brain Res* 220:79–87.
- Arai N, Müller-Dahlhaus FJM, Murakami T, Bliem B, Lu M-K, Ugawa Y, Ziemann U (2011) State-Dependent and Timing-Dependent Bidirectional Associative Plasticity in the Human SMA-M1 Network. *J Neurosci* 31:15376–15383.
- Avenanti A, Annala L, Serino A (2012a) Suppression of premotor cortex disrupts motor coding of peripersonal space. *Neuroimage* 63:281–288.
- Avenanti A, Annala L, Candidi M, Urgesi C, Aglioti SM (2013a) Compensatory plasticity in the action observation network: Virtual lesions of STS enhance anticipatory simulation of seen actions. *Cereb Cortex* 23:570–580.
- Avenanti A, Bolognini N, Maravita A, Aglioti SM (2007) Somatic and Motor Components of Action Simulation. *Curr Biol* 17:2129–2135.
- Avenanti A, Candidi M, Urgesi C (2013b) Vicarious motor activation during action perception: beyond correlational evidence. *Front Hum Neurosci* 7:185.

- Avenanti A, Coccia M, Làdavas E, Provinciali L, Ceravolo MG (2012b) Low-frequency rTMS promotes use-dependent motor plasticity in chronic stroke. A randomized trial. *Neurology* 78:256–264.
- Avenanti A, Paracampo R, Annella L, Tidoni E, Aglioti SM (2017) Boosting and Decreasing Action Prediction Abilities Through Excitatory and Inhibitory tDCS of Inferior Frontal Cortex. *Cereb Cortex*:1–15.
- Avenanti A, Urgesi C (2011) Understanding “what” others do: Mirror mechanisms play a crucial role in action perception. *Soc Cogn Affect Neurosci* 6:257–259.
- Aziz-Zadeh L, Maeda F, Zaidel E, Mazziotta JC, Iacoboni M (2002) Lateralization in motor facilitation during action observation: A TMS study. *Exp Brain Res* 144:127–131.
- Badre D, Hoffman J, Cooney JW, D’Esposito M (2009) Hierarchical cognitive control deficits following damage to the human frontal lobe. *Nat Neurosci* 12:515–522.
- Barracough NE, Xiao D, Baker CI, Oram MW, Perrett DI (2005) Integration of Visual and Auditory Information by Superior Temporal Sulcus Neurons Responsive to the Sight of Actions. *J Cogn Neurosci* 17:377–391.
- Bartels A, Logothetis NK, Moutoussis K (2008) fMRI and its interpretations: an illustration on directional selectivity in area V5/MT. *Trends Neurosci* 31:444–453.
- Bastos AM, Vezoli J, Bosman CA, Schoffelen J-M, Oostenveld R, Dowdall JR, De Weerd P, Kennedy H, Fries P (2015) Visual areas exert feedforward and feedback influences through distinct frequency channels. *Neuron* 85:390–401.
- Bäumer T, Bock F, Koch G, Lange R, Rothwell JC, Siebner HR, Münchau A (2006) Magnetic stimulation of human premotor or motor cortex produces interhemispheric facilitation through distinct pathways. *J Physiol* 572:857–868.
- Bäumer T, Schippling S, Kroeger J, Zittel S, Koch G, Thomalla G, Rothwell JC, Siebner HR, Orth M, Münchau A (2009) Inhibitory and facilitatory connectivity from ventral premotor to primary motor cortex in healthy humans at rest - A bifocal TMS study. *Clin Neurophysiol* 120:1724–1731.
- Beckers G, Hömberg V (1992) Cerebral visual motion blindness: transitory akinetopsia induced by transcranial magnetic stimulation of human area V5. *Proc R Soc B* 249:173–178.
- Bedny M, Konkle T, Pelphrey K, Saxe R, Pascual-Leone A (2010) Sensitive period for a multimodal response in human visual motion area MT/MST. *Curr Biol* 20:1900–1906.
- Bertini C, Leo F, Avenanti A, Làdavas E (2010) Independent mechanisms for ventriloquism and multisensory integration as revealed by theta-burst stimulation. *Eur J Neurosci* 31:1791–1799.
- Beste C, Wascher E, Güntürkün O, Dinse HR (2011) Improvement and impairment of visually guided behavior through LTP- and LTD-like exposure-based visual learning. *Curr Biol* 21:876–882.
- Bestmann S, Baudewig J, Siebner HR, Rothwell JC, Frahm J (2005) BOLD MRI responses to repetitive TMS over human dorsal premotor cortex. *Neuroimage* 28:22–29.
- Bestmann S, Duque J (2016) Transcranial Magnetic Stimulation: Decomposing the Processes Underlying Action Preparation. *Neuroscientist* 22:392–405.

- Bi G, Poo M (1998) Synaptic modifications in cultured hippocampal neurons: dependence on spike timing, synaptic strength, and postsynaptic cell type. *J Neurosci* 18:10464–10472.
- Bi G, Poo M (2001) Synaptic Modification by Correlated Activity: Hebb's Postulate Revisited. *Annu Rev Neurosci* 24:139–166.
- Biagi L, Cioni G, Fogassi L, Guzzetta A, Sgandurra G, Tosetti M (2016) Action observation network in childhood: a comparative fMRI study with adults. *Dev Sci* 19:1075–1086.
- Binkofski F, Buccino G, Posse S, Seitz RJ, Rizzolatti G, Freund HJ (1999) A fronto-parietal circuit for object manipulation in man: evidence from an fMRI-study. *Eur J Neurosci* 11:3276–3286.
- Binkofski F, Buxbaum LJ (2013) Two action systems in the human brain. *Brain Lang* 127:222–229.
- Biswal B, Zerrin Yetkin F, Haughton VM, Hyde JS (1995) Functional connectivity in the motor cortex of resting human brain using echo-planar mri. *Magn Reson Med* 34:537–541.
- Bliss T V., Collingridge GL (1993) A synaptic model of memory: long-term potentiation in the hippocampus. *Nature* 361:31–39.
- Bliss T V., Lømo T (1973) Long-lasting potentiation of synaptic transmission in the dentate area of the anaesthetized rabbit following stimulation of the perforant path. *J Physiol* 232:331–356.
- Boorman ED, O'Shea J, Sebastian C, Rushworth MFS, Johansen-Berg H (2007) Individual differences in white matter microstructure reflect variation in functional connectivity during action choice_Supplemental data. *Curr Biol* 17:1426–1431.
- Borgomaneri S, Gazzola V, Avenanti A (2015a) Transcranial magnetic stimulation reveals two functionally distinct stages of motor cortex involvement during perception of emotional body language. *Brain Struct Funct* 220:2765–2781.
- Borgomaneri S, Vitale F, Gazzola V, Avenanti A (2015b) Seeing fearful body language rapidly freezes the observer's motor cortex. *Cortex* 65:232–245.
- Borra E, Gerbella M, Rozzi S, Luppino G (2017) The macaque lateral grasping network: A neural substrate for generating purposeful hand actions. *Neurosci Biobehav Rev* 75:65–90.
- Borra E, Luppino G (2016) Functional anatomy of the macaque temporo-parieto-frontal connectivity. *Cortex*:1–21.
- Borst A (2014) Neural Circuits for Elementary Motion Detection. *J Neurogenet* 28:361–373.
- Bortoletto M, Pellicciari MC, Rodella C, Miniussi C (2015a) The interaction with task-induced activity is more important than polarization: A tDCS study. *Brain Stimul* 8:269–276.
- Bortoletto M, Veniero D, Thut G, Miniussi C (2015b) The contribution of TMS-EEG coregistration in the exploration of the human cortical connectome. *Neurosci Biobehav Rev* 49:114–124.
- Boussaoud D, Tanné-Gariépy J, Wannier T, Rouiller EM (2005) Callosal connections of dorsal versus ventral premotor areas in the macaque monkey: a multiple retrograde tracing study. *BMC Neurosci* 6:67.

- Bracco L, Giovannelli F, Bessi V, Borgheresi A, Di Tullio A, Sorbi S, Zaccara G, Cincotta M (2009) Mild cognitive impairment: Loss of linguistic task-induced changes in motor cortex excitability. *Neurology* 72:928–934.
- Brainard DH (1997) The Psychophysics Toolbox. *Spat Vis* 10:433–436.
- Brasil-Neto JP, Cohen LG, Panizza M, Nilsson J, Roth BJ, Hallett M (1992) Optimal Focal Transcranial Magnetic Activation of the Human Motor Cortex. *J Clin Neurophysiol* 9:132–136.
- Buccino G, Binkofski F, Fink GR, Fadiga L, Fogassi L, Gallese V, Seitz RJ, Zilles K, Rizzolatti G (2001) Action observation activates premotor and parietal areas in a somatotopic manner: an fMRI study. *Eur J Neurosci* 13:400–404.
- Buccino G, Vogt S, Ritzl A, Fink GR, Zilles K, Freund HJ, Rizzolatti G (2004) Neural circuits underlying imitation learning of hand actions: An event-related fMRI study. *Neuron* 42:323–334.
- Buch ER, Johnen VM, Nelissen N, O’Shea J, Rushworth MFS (2011) Noninvasive Associative Plasticity Induction in a Corticocortical Pathway of the Human Brain. *J Neurosci* 31:17669–17679.
- Buch ER, Mars RB, Boorman ED, Rushworth MFS (2010) A Network Centered on Ventral Premotor Cortex Exerts Both Facilitatory and Inhibitory Control over Primary Motor Cortex during Action Reprogramming. *J Neurosci* 30:1395–1401.
- Bullier J (2001) Integrated model of visual processing. *Brain Res Rev* 36:96–107.
- Burnat K, Hu T-T, Kossut M, Eysel UT, Arckens L (2017) Plasticity beyond V1 - Reinforcement of motion perception upon binocular central retinal lesions in adulthood. *J Neurosci* 37:1231–17.
- Calvo-Merino B, Glaser DE, Grèzes J, Passingham RE, Haggard P (2005) Action observation and acquired motor skills: An fMRI study with expert dancers. *Cereb Cortex* 15:1243–1249.
- Candidi M, Stienen BMC, Aglioti SM, de Gelder B (2011) Event-Related Repetitive Transcranial Magnetic Stimulation of Posterior Superior Temporal Sulcus Improves the Detection of Threatening Postural Changes in Human Bodies. *J Neurosci* 31:17547–17554.
- Caporale N, Dan Y (2008) Spike timing-dependent plasticity: a Hebbian learning rule. *Annu Rev Neurosci* 31:25–46.
- Carducci F, Brusco R (2012) Accuracy of an individualized MR-based head model for navigated brain stimulation. *Psychiatry Res - Neuroimaging* 203:105–108.
- Carter AR, Astafiev S V., Lang CE, Connor LT, Rengachary J, Strube MJ, Pope DLW, Shulman GL, Corbetta M (2010) Resting interhemispheric functional magnetic resonance imaging connectivity predicts performance after stroke. *Ann Neurol* 67:365–375.
- Casile A, Dayan E, Caggiano V, Hendler T, Flash T, Giese MA (2010) Neuronal encoding of human kinematic invariants during action observation. *Cereb Cortex* 20:1647–1655.
- Caspers S, Zilles K, Laird AR, Eickhoff SB (2010) ALE meta-analysis of action observation and imitation in the human brain. *Neuroimage* 50:1148–1167.
- Castiello U (2005) The neuroscience of grasping. *Nat Rev Neurosci* 6:726–736.

- Casula EP, Pellicciari MC, Picazio S, Caltagirone C, Koch G (2016) Spike-timing-dependent plasticity in the human dorso-lateral prefrontal cortex. *Neuroimage* 143:204–213.
- Catmur C (2013) Sensorimotor learning and the ontogeny of the mirror neuron system. *Neurosci Lett* 540:21–27.
- Catmur C, Gillmeister H, Bird G, Liepelt R, Brass M, Heyes C (2008) Through the looking glass: Counter-mirror activation following incompatible sensorimotor learning. *Eur J Neurosci* 28:1208–1215.
- Catmur C, Mars RB, Rushworth MFS, Heyes C (2011) Making mirrors: premotor cortex stimulation enhances mirror and counter-mirror motor facilitation. *J Cogn Neurosci* 23:2352–2362.
- Catmur C, Walsh V, Heyes C (2007) Sensorimotor Learning Configures the Human Mirror System. *Curr Biol* 17:1527–1531.
- Cattaneo L (2010) Tuning of ventral premotor cortex neurons to distinct observed grasp types: A TMS-priming study. *Exp Brain Res* 207:165–172.
- Cattaneo L, Barchiesi G (2011) Transcranial Magnetic Mapping of the Short-Latency Modulations of Corticospinal Activity from the Ipsilateral Hemisphere during Rest. *Front Neural Circuits* 5:1–13.
- Cattaneo L, Caruana F, Jezzini A, Rizzolatti G (2009) Representation of goal and movements without overt motor behavior in the human motor cortex: a transcranial magnetic stimulation study. *J Neurosci* 29:11134–11138.
- Cattaneo L, Rizzolatti G (2009) The mirror neuron system. *Arch Neurol* 66:557–560.
- Cattaneo L, Sandrini M, Schwarzbach J (2010) State-dependent TMS reveals a hierarchical representation of observed acts in the temporal, parietal, and premotor cortices. *Cereb Cortex* 20:2252–2258.
- Cattaneo Z, Silvanto J (2008) Investigating visual motion perception using the transcranial magnetic stimulation-adaptation paradigm. *Neuroreport* 19:1423–1427.
- Cavina-Pratesi C, Monaco S, Fattori P, Galletti C, McAdam TD, Quinlan DJ, Goodale MA, Culham JC (2010) Functional Magnetic Resonance Imaging Reveals the Neural Substrates of Arm Transport and Grip Formation in Reach-to-Grasp Actions in Humans. *J Neurosci* 30:10306–10323.
- Cerri G, Shimazu H, Maier MA, Lemon RN (2003) Facilitation From Ventral Premotor Cortex of Primary Motor Cortex Outputs to Macaque Hand Muscles. *J Neurophysiol* 90:832–842.
- Chao CC, Karabanov AN, Paine R, Carolina De Campos A, Kukke SN, Wu T, Wang H, Hallett M (2015) Induction of motor associative plasticity in the posterior parietal cortex-primary motor network. *Cereb Cortex* 25:365–373.
- Cheeran B, Ritter C, Rothwell JC, Siebner HR (2009) Mapping genetic influences on the corticospinal motor system in humans. *Neuroscience* 164:156–163.
- Cheeran B, Talelli P, Mori F, Koch G, Suppa A, Edwards M, Houlden H, Bhatia K, Greenwood R, Rothwell JC (2008) A common polymorphism in the brain-derived neurotrophic factor gene (BDNF) modulates human cortical plasticity and the response to rTMS. *J Physiol* 586:5717–5725.

- Chen N, Bi T, Zhou T, Li S, Liu Z, Fang F (2015) Sharpened cortical tuning and enhanced cortico-cortical communication contribute to the long-term neural mechanisms of visual motion perceptual learning. *Neuroimage* 115:17–29.
- Chiappini E, Avenanti A (2018) Motor resonance enhancement following induction of Hebbian-like plasticity in premotor-motor areas. *Press*.
- Chong TTJ, Cunnington R, Williams MA, Kanwisher N, Mattingley JB (2008) fMRI Adaptation Reveals Mirror Neurons in Human Inferior Parietal Cortex. *Curr Biol* 18:1576–1580.
- Chouinard PA, Van Der Werf YD, Leonard G, Paus T (2003) Modulating neural networks with transcranial magnetic stimulation applied over the dorsal premotor and primary motor cortices. *J Neurophysiol* 90:1071–1083.
- Civardi C, Cantello R, Asselman P, Rothwell JC (2001) Transcranial Magnetic Stimulation Can Be Used to Test Connections to Primary Motor Areas from Frontal and Medial Cortex in Humans. *Neuroimage* 14:1444–1453.
- Cohen J (1992) A power primer. *Psychol Bull* 112:155–159.
- Costantini M, Galati G, Ferretti A, Caulo M, Tartaro A, Romani GL, Aglioti SM (2005) Neural Systems Underlying Observation of Humanly Impossible Movements: An fMRI Study. *Cereb Cortex* 15:1761–1767.
- Cross ES, Hamilton AF de C, Grafton ST (2006) Building a motor simulation de novo: Observation of dance by dancers. *Neuroimage* 31:1257–1267.
- Cross ES, Kraemer DJM, Hamilton AF de C, Kelley WM, Grafton ST (2009) Sensitivity of the action observation network to physical and observational learning. *Cereb Cortex* 19:315–326.
- Cross ES, Stadler W, Parkinson J, Schütz-Bosbach S, Prinz W (2013) The influence of visual training on predicting complex action sequences. *Hum Brain Mapp* 34:467–486.
- Davare M (2006) Dissociating the Role of Ventral and Dorsal Premotor Cortex in Precision Grasping. *J Neurosci* 26:2260–2268.
- Davare M, Kraskov A, Rothwell JC, Lemon RN (2011) Interactions between areas of the cortical grasping network. *Curr Opin Neurobiol* 21:565–570.
- Davare M, Lemon RN, Olivier E (2008) Selective modulation of interactions between ventral premotor cortex and primary motor cortex during precision grasping in humans. *J Physiol* 586:2735–2742.
- Davare M, Montague K, Olivier E, Rothwell JC, Lemon RN (2009) Ventral premotor to primary motor cortical interactions during object-driven grasp in humans. *Cortex* 45:1050–1057.
- Davare M, Rothwell JC, Lemon RN (2010) Causal Connectivity between the Human Anterior Intraparietal Area and Premotor Cortex during Grasp. *Curr Biol* 20:176–181.
- Dayan E, Casile A, Levit-Binnun N, Giese MA, Hendler T, Flash T (2007) Neural representations of kinematic laws of motion: evidence for action-perception coupling. *Proc Natl Acad Sci U S A* 104:20582–20587.

- Dayan E, Censor N, Buch ER, Sandrini M, Cohen LG (2013a) Noninvasive brain stimulation: From physiology to network dynamics and back. *Nat Neurosci* 16:838–844.
- Dayan E, Censor N, Buch ER, Sandrini M, Cohen LG (2013b) Noninvasive brain stimulation: from physiology to network dynamics and back. *Nat Neurosci* 16:838–844.
- Dayan E, Cohen LG (2011) Neuroplasticity subserving motor skill learning. *Neuron* 72:443–454.
- De Gennaro L, Ferrara M, Bertini M, Pauri F, Cristiani R, Curcio G, Romei V, Fratello F, Rossini PM (2003) Reproducibility of callosal effects of transcranial magnetic stimulation (TMS) with interhemispheric paired pulses. *Neurosci Res* 46:219–227.
- De Luca M, Beckmann CF, De Stefano N, Matthews PM, Smith SM (2006) fMRI resting state networks define distinct modes of long-distance interactions in the human brain. *Neuroimage* 29:1359–1367.
- de Vega M, León I, Hernández JA, Valdés M, Padrón I, Ferstl EC (2014) Action Sentences Activate Sensory Motor Regions in the Brain Independently of Their Status of Reality. *J Cogn Neurosci* 26:1363–1376.
- Debanne D, Gahwiler BH, Thompson SM (1998) Long-term synaptic plasticity between pairs of individual CA3 pyramidal cells in rat hippocampal slice cultures. *J Physiol* 507:237–247.
- Dehaene S, Changeux JP, Naccache L, Sackur J, Sergent C (2006) Conscious, preconscious, and subliminal processing: a testable taxonomy. *Trends Cogn Sci* 10:204–211.
- Desimone R, Duncan J (1995) Neural Mechanisms of Selective Visual Attention. *Annu Rev Neurosci* 18:193–222.
- Dettmers C, Nedelko V, Schoenfeld MA (2015) Impact of left versus right hemisphere subcortical stroke on the neural processing of action observation and imagery. *Restor Neurol Neurosci* 33:701–712.
- Devanne H, Lavoie BA, Capaday C (1997) Input-output properties and gain changes in the human corticospinal pathway. *Exp Brain Res* 114:329–338.
- Di Lazzaro V, Dileone M, Pilato F, Profice P, Oliviero A, Mazzone P, Insola A, Capone F, Ranieri F, Tonali PA (2009a) Associative motor cortex plasticity: Direct evidence in humans. *Cereb Cortex* 19:2326–2330.
- Di Lazzaro V, Dileone M, Profice P, Pilato F, Oliviero A, Mazzone P, Di Iorio R, Capone F, Ranieri F, Florio L, Tonali PA (2009b) LTD-like plasticity induced by paired associative stimulation: Direct evidence in humans. *Exp Brain Res* 194:661–664.
- Di Lazzaro V, Oliviero A, Pilato F, Saturno E, Dileone M, Mazzone P, Insola A, Tonali PA, Rothwell JC (2004) The physiological basis of transcranial motor cortex stimulation in conscious humans. *Clin Neurophysiol* 115:255–266.
- Di Lazzaro V, Oliviero A, Profice P, Insola A, Mazzone P, Tonali PA, Rothwell JC (1999) Direct demonstration of interhemispheric inhibition of the human motor cortex produced by transcranial magnetic stimulation. *Exp Brain Res* 124:520–524.

- di Pellegrino G, Fadiga L, Fogassi L, Gallese V, Rizzolatti G (1992) Understanding motor events: a neurophysiological study. *Exp Brain Res* 91:176–180.
- Dienes Z (2011) Bayesian versus orthodox statistics: Which side are you on? *Perspect Psychol Sci* 6:274–290.
- Dum RP, Strick PL (1991) The origin of corticospinal projections from the premotor areas in the frontal lobe. *J Neurosci* 11:667–689.
- Dum RP, Strick PL (1996) Spinal cord terminations of the medial wall motor areas in macaque monkeys. *J Neurosci* 16:6513–6525.
- Dum RP, Strick PL (2005) Frontal lobe inputs to the digit representations of the motor areas on the lateral surface of the hemisphere. *J Neurosci* 25:1375–1386.
- Dushanova J, Donoghue J (2010) Neurons in primary motor cortex engaged during action observation. *Eur J Neurosci* 31:386–398.
- Ehrsson HH, Fagergren A, Jonsson T, Westling G, Johansson RS, Forssberg H (2000) Cortical activity in precision- versus power-grip tasks: an fMRI study. *J Neurophysiol* 83:528–536.
- Engel A, Burke M, Fiehler K, Bien S, Rosler F (2008) How moving objects become animated: The human mirror neuron system assimilates non-biological movement patterns. *Soc Neurosci* 3:368–387.
- Fadiga L, Craighero L, Olivier E (2005) Human motor cortex excitability during the perception of others' action. *Curr Opin Neurobiol* 15:213–218.
- Fadiga L, Fogassi L, Pavesi G, Rizzolatti G (1995) Motor facilitation during action observation: a magnetic stimulation study. *J Neurophysiol* 73:2608–2611.
- Fagg AH, Arbib MA (1998) Modeling parietal-premotor interactions in primate control of grasping. *Neural Networks* 11:1277–1303.
- Felleman DJ, Van Essen DC (1991) Distributed hierarchical processing in the primate cerebral cortex. *Cereb Cortex* 1:1–47.
- Ferbert A, Priori A, Rothwell JC, Day BL, Colebatch JG, Marsden CD (1992) Interhemispheric inhibition of the human motor cortex. *J Physiol* 453:525–546.
- Fiori F, Chiappini E, Avenanti A (2018) Enhancing goal-directed action performance following TMS manipulation of associative plasticity in ventral premotor-motor pathway. *Neuroimage*.
- Fiori F, Chiappini E, Candidi M, Romei V, Borgomaneri S, Avenanti A (2017) Long-latency interhemispheric interactions between motor-related areas and the primary motor cortex: a dual site TMS study. *Sci Rep* 7:14936.
- Fiori F, Chiappini E, Soriano M, Paracampo R, Romei V, Borgomaneri S, Avenanti A (2016) Long-latency modulation of motor cortex excitability by ipsilateral posterior inferior frontal gyrus and pre-supplementary motor area. *Sci Rep* 6:1–11.
- Fogassi L, Gallese V, Buccino G, Craighero L, Fadiga L, Rizzolatti G (2001) Cortical mechanism for the visual guidance of hand grasping movements in the monkey: A reversible inactivation study. *Brain* 124:571–586.

- Fourkas AD, Avenanti A, Urgesi C, Aglioti SM (2006) Corticospinal facilitation during first and third person imagery. *Exp Brain Res* 168:143–151.
- Fourkas AD, Bonavolontà V, Avenanti A, Aglioti SM (2008) Kinesthetic imagery and tool-specific modulation of corticospinal representations in expert tennis players. *Cereb Cortex* 18:2382–2390.
- Fox MD, Raichle ME (2007) Spontaneous fluctuations in brain activity observed with functional magnetic resonance imaging. *Nat Rev Neurosci* 8:700–711.
- Frégnac Y, Pananceau M, René A, Huguet N, Marre O, Levy M, Shulz DE (2010) A re-examination of Hebbian-covariance rules and spike timing-dependent plasticity in cat visual cortex in vivo. *Front Synaptic Neurosci* 2:147.
- Fregni F, Boggio PS, Nitsche M, Bermanpohl F, Antal A, Feredoes E, Marcolin MA, Rigonatti SP, Silva MTA, Paulus W, Pascual-Leone A (2005) Anodal transcranial direct current stimulation of prefrontal cortex enhances working memory. *Exp Brain Res* 166:23–30.
- Friston KJ (2010) The free-energy principle: a unified brain theory? *Nat Rev Neurosci* 11:127–138.
- Friston KJ, Mattout J, Kilner JM (2011) Action understanding and active inference. *Biol Cybern* 104:137–160.
- Fujii N, Mushiaki H, Tanji J (2002) Distribution of Eye- and Arm-Movement-Related Neuronal Activity in the SEF and in the SMA and Pre-SMA of Monkeys. *J Neurophysiol* 87:2158–2166.
- Fujiyama H, Van Soom J, Rens G, Cuypers K, Heise KF, Levin O, Swinnen SP (2016) Performing two different actions simultaneously: The critical role of interhemispheric interactions during the preparation of bimanual movement. *Cortex* 77:141–154.
- Furubayashi T, Ugawa Y, Terao Y, Hanajima R, Sakai K, MacHii K, Mochizuki H, Shiio Y, Uesugi H, Enomoto H, Kanazawa I (2000) The human hand motor area is transiently suppressed by an unexpected auditory stimulus. *Clin Neurophysiol* 111:178–183.
- Gallese V (2007) Before and below “theory of mind”: embodied simulation and the neural correlates of social cognition. *Philos Trans R Soc B Biol Sci* 362:659–669.
- Gallese V, Fadiga L, Fogassi L, Rizzolatti G (1996) Action recognition in the premotor cortex. *Brain* 119 (Pt 2):593–609.
- Gangitano M, Mottaghy FM, Pascual-Leone A (2001) Phase-specific modulation of cortical motor output during movement observation. *Neuroreport* 12:1489–1492.
- Gardner T, Goulden N, Cross ES (2015) Dynamic modulation of the action observation network by movement familiarity. *J Neurosci* 35:1561–1572.
- Gattass R, Gross CG (1981) Visual topography of striate projection zone (MT) in posterior superior temporal sulcus of the macaque. *J Neurophysiol* 46:621–638.
- Gazzola V, Keysers C (2009) The observation and execution of actions share motor and somatosensory voxels in all tested subjects: Single-subject analyses of unsmoothed fMRI data. *Cereb Cortex* 19:1239–1255.

- Gerbella M, Rozzi S, Rizzolatti G (2017) The extended object-grasping network. *Exp Brain Res* 235:2903–2916.
- Gerloff C, Cohen LG, Floeter MK, Chen R, Corwell B, Hallett M (1998) Inhibitory influence of the ipsilateral motor cortex on responses to stimulation of the human cortex and pyramidal tract. *J Physiol* 510:249–259.
- Gerloff C, Corwell B, Chen R, Hallett M, Cohen LG (1997) Stimulation over the human supplementary motor area interferes with the organization of future elements in complex motor sequences. *Brain* 120:1587–1602.
- Gerschlagner W, Siebner HR, Rothwell JC (2001) Decreased corticospinal excitability after subthreshold 1 Hz rTMS over lateral premotor cortex. *Neurology* 57:449–455.
- Giese MA, Poggio T (2003) Cognitive neuroscience: Neural mechanisms for the recognition of biological movements. *Nat Rev Neurosci* 4:179–192.
- Gilaie-Dotan S (2016) Visual motion serves but is not under the purview of the dorsal pathway. *Neuropsychologia* 89:378–392.
- Gilbert CD, Li W (2013) Top-down influences on visual processing. *Nat Rev Neurosci* 14:350–363.
- Girelli M, Luck SJ (1997) Are the Same Attentional Mechanisms Used to Detect Visual Search Targets Defined by Color, Orientation, and Motion? *J Cogn Neurosci* 9:238–253.
- Goodale MA, Milner AD (1992) Separate visual pathways for perception and action. *Trends Neurosci* 15:20–25.
- Graf M, Reitzner B, Corves C, Casile A, Giese M, Prinz W (2007) Predicting point-light actions in real-time. *Neuroimage* 36:22–32.
- Grafton ST (2009) Embodied cognition and the simulation of action to understand others. *Ann N Y Acad Sci* 1156:97–117.
- Grafton ST, Arbib MA, Fadiga L, Rizzolatti G (1996) Localization of grasp representations in humans by positron emission tomography. *Exp Brain Res* 112:103–111.
- Grefkes C, Nowak DA, Eickhoff SB, Dafotakis M, Küst J, Karbe H, Fink GR (2008) Cortical connectivity after subcortical stroke assessed with functional magnetic resonance imaging. *Ann Neurol* 63:236–246.
- Grèzes J, Decety J (2001) Functional Anatomy of Execution, Mental Simulation, Observation, and Verb Generation of Actions: A Meta-Analysis. *Hum Brain Mapp* 19:1–19.
- Grol MJ, Majdandzic J, Stephan KE, Verhagen LM, Dijkerman HC, Bekkering H, Verstraten FAJ, Toni I (2007) Parieto-Frontal Connectivity during Visually Guided Grasping. *J Neurosci* 27:11877–11887.
- Groppa S, Werner-Petroll N, Münchau A, Deuschl G, Rushworth MFS, Siebner HR (2012) A novel dual-site transcranial magnetic stimulation paradigm to probe fast facilitatory inputs from ipsilateral dorsal premotor cortex to primary motor cortex. *Neuroimage* 62:500–509.

- Gross CG (1991) Contribution of striate cortex and the superior colliculus to visual function in area MT, the superior temporal polysensory area and inferior temporal cortex. *Neuropsychologia* 29:497–515.
- Grossman ED, Battelli L, Pascual-Leone A (2005) Repetitive TMS over posterior STS disrupts perception of biological motion. *Vision Res* 45:2847–2853.
- Hamilton AF de C, Grafton ST (2006) Goal Representation in Human Anterior Intraparietal Sulcus. *J Neurosci* 26:1133–1137.
- Hamilton AF de C, Grafton ST (2007) The motor hierarchy : from kinematics to goals and intentions. In: *Attention and Performance* (Haggard P, Rosetti Y, Kawato M, eds). Oxford: Oxford University Press.
- Hamzei F, Lämpchen CH, Glauche V, Mader I, Rijntjes M, Weiller C (2012) Functional Plasticity Induced by Mirror Training. *Neurorehabil Neural Repair* 26:484–496.
- Hanajima R, Ugawa Y, Machii K, Mochizuki H, Terao Y, Enomoto H, Furubayashi T, Shio Y, Uesugi H, Kanazawa I (2001) Interhemispheric facilitation of the hand motor area in humans. *J Physiol* 531:849–859.
- Hari R, Forss N, Avikainen S, Kirveskari E, Salenius S, Rizzolatti G (1998) Activation of human primary motor cortex during action observation: a neuromagnetic study. *Proc Natl Acad Sci U S A* 95:15061–15065.
- Hartwigsen G, Bestmann S, Ward NS, Woerbel S, Mastroeni C, Granert O, Siebner HR (2012) Left Dorsal Premotor Cortex and Supramarginal Gyrus Complement Each Other during Rapid Action Reprogramming. *J Neurosci* 32:16162–16171.
- He SQ, Dum RP, Strick PL (1993) Topographic organization of corticospinal projections from the frontal lobe: motor areas on the lateral surface of the hemisphere. *J Neurosci* 13:952–980.
- Hebb DO (1949) *The organization of behavior*.
- Hecht EE, Gutman DA, Preuss TM, Sanchez MM, Parr LA, Rilling JK (2013) Process versus product in social learning: Comparative diffusion tensor imaging of neural systems for action execution-observation matching in macaques, chimpanzees, and humans. *Cereb Cortex* 23:1014–1024.
- Hecht H, Vogt S, Prinz W (2001) Motor learning enhances perceptual judgment: A case for action-perception transfer. *Psychol Res* 65:3–14.
- Heyes C (2001) Causes and consequences of imitation. *Trends Cogn Sci* 5:253–261.
- Hochstein S, Ahissar M (2002) View from the Top: Review Hierarchies and Reverse Hierarchies in the Visual System. *Neuron* 36:791–804.
- Horn U, Roschka S, Eyme K, Walz AD, Platz T, Lotze M (2016) Increased ventral premotor cortex recruitment after arm training in an fMRI study with subacute stroke patients. *Behav Brain Res* 308:152–159.
- Hoshi E, Tanji J (2007) Distinctions between dorsal and ventral premotor areas: anatomical connectivity and functional properties. *Curr Opin Neurobiol* 17:234–242.

- Hotson JR, Braun D, Herzberg W, Boman D (1994) Transcranial magnetic stimulation of extrastriate cortex degrades human motion direction discrimination. *Vision Res* 34:2115–2123.
- Huang YZ, Edwards MJ, Rounis E, Bhatia KP, Rothwell JC (2005) Theta burst stimulation of the human motor cortex. *Neuron* 45:201–206.
- Hupé JM, James AC, Payne BR, Lomber SG, Girard P, Bullier J (1998) Cortical feedback improves discrimination between figure and background by V1, V2 and V3 neurons. *Nature* 394:784–787.
- Irlbacher K, Brocke J, Mechow J V., Brandt SA (2007) Effects of GABAA and GABAB agonists on interhemispheric inhibition in man. *Clin Neurophysiol* 118:308–316.
- Jackson A, Mavoori J, Fetz EE (2006) Long-term motor cortex plasticity induced by an electronic neural implant. *Nature* 444:56–60.
- Jacquet PO, Avenanti A (2015) Perturbing the action observation network during perception and categorization of actions' goals and grips: State-dependency and virtual lesion TMS effects. *Cereb Cortex* 25:598–608.
- Jastorff J, Kourtzi Z, Giese MA (2009) Visual learning shapes the processing of complex movement stimuli in the human brain. *J Neurosci* 29:14026–14038.
- Jeannerod M (2001) Neural Simulation of Action: A Unifying Mechanism for Motor Cognition. *Neuroimage* 14:S103–S109.
- Jeannerod M, Arbib MA, Rizzolatti G, Sakata H (1995) Grasping objects: the cortical mechanisms of visuomotor transformation. *Trends Neurosci* 18:314–320.
- Johansen-Berg H, Rushworth MFS, Bogdanovic MD, Kischka U, Wimalaratna S, Matthews PM (2002) The role of ipsilateral premotor cortex in hand movement after stroke. *Proc Natl Acad Sci* 99:14518–14523.
- Johnen VM, Neubert F-X, Buch ER, Verhagen LM, O'Reilly J, Mars RB, Rushworth MFS (2015) Causal manipulation of functional connectivity in a specific neural pathway during behaviour and at rest. *Elife* 2015:1–23.
- Jola C, Abedian-Amiri A, Kuppuswamy A, Pollick FE, Grosbras MH (2012) Motor simulation without motor expertise: Enhanced corticospinal excitability in visually experienced dance spectators. *PLoS One* 7.
- Jones CB, Lulic T, Bailey AZ, Mackenzie TN, Mi YQ, Tommerdahl M, Nelson AJ (2016) Metaplasticity in human primary somatosensory cortex: effects on physiology and tactile perception. *J Neurophysiol* 115:2681–2691.
- Kalia M (2008) Brain development: anatomy, connectivity, adaptive plasticity, and toxicity. *Metabolism* 57:2–5.
- Kammer T (1999) Phosphenes and transient scotomas induced by magnetic stimulation of the occipital lobe: Their topographic relationship. *Neuropsychologia* 37:191–198.

- Kammer T, Beck S, Thielscher A, Laubis-Hermann U, Topka H (2001) Motor threshold in humans: a transcranial magnetic stimulation study comparing different pulse waveforms, current directions and stimulator types. *Clin Neurophysiol* 112:250–258.
- Kantak SS, Stinear JW, Buch ER, Cohen LG (2012) Rewiring the brain: potential role of the premotor cortex in motor control, learning, and recovery of function following brain injury. *Neurorehabil Neural Repair* 26:282–292.
- Kennedy H, Bullier J (1985) A double-labeling investigation of the afferent connectivity to cortical areas V1 and V2 of the macaque monkey. *J Neurosci* 5:2815–2830.
- Keysers C, Gazzola V (2014) Hebbian learning and predictive mirror neurons for actions, sensations and emotions. *Philos Trans R Soc B Biol Sci* 369:20130175.
- Keysers C, Perrett DI (2004) Demystifying social cognition: A Hebbian perspective. *Trends Cogn Sci* 8:501–507.
- Kidgell DJ, Mason J, Frazer A, Pearce AJ (2016) I-wave periodicity transcranial magnetic stimulation (iTMS) on corticospinal excitability. A systematic review of the literature. *Neuroscience* 322:262–272.
- Kilner JM (2011) More than one pathway to action understanding. *Trends Cogn Sci* 15:352–357.
- Kilner JM, Friston KJ, Frith CD (2007a) The mirror-neuron system: a Bayesian perspective. *Neuroreport* 18:619–623.
- Kilner JM, Friston KJ, Frith CD (2007b) Predictive coding: An account of the mirror neuron system. *Cogn Process* 8:159–166.
- Kilner JM, Neal A, Weiskopf N, Friston KJ, Frith CD (2009) Evidence of mirror neurons in human inferior frontal gyrus. *J Neurosci* 29:10153–10159.
- Kilner JM, Vargas C, Duval S, Blakemore S-J, Sirigu A (2004) Motor activation prior to observation of a predicted movement. *Nat Neurosci* 7:1299–1301.
- Kleiner M, Brainard DH, Pelli DG, Ingling A, Murray R, Broussard C (2007) What's new in psychtoolbox-3. *Perception* 36:1–16.
- Kobayashi M, Hutchinson S, Theoret H, Schlaug G, Pascual-Leone A (2004) Repetitive TMS of the motor cortex improves ipsilateral sequential simple finger movements. *Neurology* 62:91–98.
- Koch G, Fernández del Olmo M, Cheeran B, Ruge D, Schippling S, Caltagirone C, Rothwell JC (2007) Focal stimulation of the posterior parietal cortex increases the excitability of the ipsilateral motor cortex. *J Neurosci* 27:6815–6822.
- Koch G, Franca M, Fernandez Del Olmo M, Cheeran B, Milton R, Alvarez Saucó M, Rothwell JC (2006) Time Course of Functional Connectivity between Dorsal Premotor and Contralateral Motor Cortex during Movement Selection. *J Neurosci* 26:7452–7459.
- Koch G, Ponzo V, Di Lorenzo F, Caltagirone C, Veniero D (2013) Hebbian and Anti-Hebbian Spike-Timing-Dependent Plasticity of Human Cortico-Cortical Connections. *J Neurosci* 33:9725–9733.

- Koch G, Ruge D, Cheeran B, Fernandez Del Olmo M, Pecchioli C, Marconi B, Versace V, Lo Gerfo E, Torriero S, Oliveri M, Caltagirone C, Rothwell JC (2009) TMS activation of interhemispheric pathways between the posterior parietal cortex and the contralateral motor cortex. *J Physiol* 587:4281–4292.
- Koch G, Versace V, Bonni S, Lupo F, Gerfo E Lo, Oliveri M, Caltagirone C (2010) Resonance of cortico-cortical connections of the motor system with the observation of goal directed grasping movements. *Neuropsychologia* 48:3513–3520.
- Koechlin E, Ody C, Kouneiher F (2003) The Architecture of Cognitive Control in the Human Prefrontal Cortex. *Science* (80-) 302:1181–1185.
- Koganemaru S, Mima T, Nakatsuka M, Ueki Y, Fukuyama H, Domen K (2009) Human motor associative plasticity induced by paired bihemispheric stimulation. *J Physiol* 587:4629–4644.
- Koivisto M, Mäntylä T, Silvanto J (2010) The role of early visual cortex (V1/V2) in conscious and unconscious visual perception. *Neuroimage* 51:828–834.
- Kokal I, Keysers C (2010) Granger causality mapping during joint actions reveals evidence for forward models that could overcome sensory-motor delays. *PLoS One* 5:1–10.
- Kolster H, Peeters R, Orban GA (2010) The Retinotopic Organization of the Human Middle Temporal Area MT/V5 and Its Cortical Neighbors. *J Neurosci* 30:9801–9820.
- Kraskov A, Dancause N, Quallo MM, Shepherd S, Lemon RN (2009) Corticospinal Neurons in Macaque Ventral Premotor Cortex with Mirror Properties: A Potential Mechanism for Action Suppression? *Neuron* 64:922–930.
- Kraskov A, Philipp R, Waldert S, Vigneswaran G, Quallo MM, Lemon RN (2014) Corticospinal mirror neurons. *Philos Trans R Soc Lond B Biol Sci* 369:20130174.
- Krause B, Cohen Kadosh R (2014) Not all brains are created equal: the relevance of individual differences in responsiveness to transcranial electrical stimulation. *Front Syst Neurosci* 8:25.
- Kroliczak G, Cavina-Pratesi C, Goodman DA, Culham JC (2007) What Does the Brain Do When You Fake It? An fMRI Study of Pantomimed and Real Grasping. *J Neurophysiol* 97:2410–2422.
- Kuhtz-Buschbeck JP, Ehrsson HH, Forssberg H (2001) Human brain activity in the control of fine static precision grip forces: An fMRI study. *Eur J Neurosci* 14:382–390.
- Kukawadia S, Wagle-Shukla A, Morgante F, Gunraj C, Chen R (2005) Interactions between long latency afferent inhibition and interhemispheric inhibitions in the human motor cortex. *J Physiol* 563:915–924.
- Lamme VAF (2006) Towards a true neural stance on consciousness. *Trends Cogn Sci* 10:494–501.
- Lamme VAF, Roelfsema PR (2000) The distinct modes of vision offered by feedforward and recurrent processing. *Trends Neurosci* 23:571–579.
- Lamme VAF, Supèr H, Landman R, Roelfsema PR, Spekreijse H (2000) The role of primary visual cortex (V1) in visual awareness. *Vision Res* 40:1507–1521.

- Lamme VAF, Supèr H, Spekreijse H (1998) Feedforward, horizontal, and feedback processing in the visual cortex. *Curr Opin Neurobiol* 8:529–535.
- Lang CE, Schieber MH (2004) Reduced Muscle Selectivity During Individuated Finger Movements in Humans After Damage to the Motor Cortex or Corticospinal Tract. *J Neurophysiol* 91:1722–1733.
- Laycock R, Crewther DP, Fitzgerald PB, Crewther SG (2007) Evidence for Fast Signals and Later Processing in Human V1/V2 and V5/MT+: A TMS Study of Motion Perception. *J Neurophysiol* 98:1253–1262.
- Levi A, Shaked D, Tadin D, Huxlin K (2014) Is improved contrast sensitivity a natural consequence of visual training? *J Vis* 14:1158–1158.
- Levy WB, Steward O (1983) Temporal contiguity requirements for long-term associative potentiation/depression in the hippocampus. *Neuroscience* 8:791–797.
- Li JY, Espay AJ, Gunraj CA, Pal PK, Cunic DI, Lang AE, Chen R (2007) Interhemispheric and ipsilateral connections in Parkinson’s disease: Relation to mirror movements. *Mov Disord* 22:813–821.
- List J, Kübke JC, Lindenberg R, Külzow N, Kerti L, Witte V, Flöel A (2013) Relationship between excitability, plasticity and thickness of the motor cortex in older adults. *Neuroimage* 83:809–816.
- Lu M-K, Arai N, Tsai C-H, Ziemann U (2012a) Movement related cortical potentials of cued versus self-initiated movements: Double dissociated modulation by dorsal premotor cortex versus supplementary motor area rTMS. *Hum Brain Mapp* 33:824–839.
- Lu M-K, Tsai C-H, Ziemann U (2012b) Cerebellum to motor cortex paired associative stimulation induces bidirectional STDP-like plasticity in human motor cortex. *Front Hum Neurosci* 6:1–9.
- Maeda F, Kleiner-Fisman G, Pascual-Leone A (2002) Motor facilitation while observing hand actions: specificity of the effect and role of observer’s orientation. *J Neurophysiol* 87:1329–1335.
- Makris S, Urgesi C (2013) Neural underpinnings of superior action prediction abilities in soccer players. *Soc Cogn Affect Neurosci* 10:342–351.
- Mansur CG, Fregni F, Boggio PS, Riberto M, Gallucci-Neto J, Santos CM, Wagner T, Rigonatti SP, Marcolin MA, Pascual-Leone A (2005) A sham stimulation-controlled trial of rTMS of the unaffected hemisphere in stroke patients. *Neurology* 64:1802–1804.
- Marconi B, Genovesio A, Giannetti S, Molinari M, Caminiti R (2003) Callosal connections of dorso-lateral premotor cortex. *Eur J Neurosci* 18:775–788.
- Markram H, Gerstner W, Sjöström PJ (2011) A history of spike-timing-dependent plasticity. *Front Synaptic Neurosci* 3:1–24.
- Markram H, Lubke J, Frotscher M, Sakmann B (1997) Regulation of synaptic efficacy by coincidence of postsynaptic APs and EPSPs. *Science* (80-) 275:213–215.
- Mars RB, Klein MC, Neubert F-X, Olivier E, Buch ER, Boorman ED, Rushworth MFS (2009) Short-Latency Influence of Medial Frontal Cortex on Primary Motor Cortex during Action Selection under Conflict. *J Neurosci* 29:6926–6931.

- Marzi CA (2010) Asymmetry of interhemispheric communication. *Wiley Interdiscip Rev Cogn Sci* 1:433–438.
- Massimini M, Ferrarelli F, Huber R, Esser SK, Singh H, Tononi G (2005) Breakdown of Cortical Effective Connectivity During Sleep. *Science* (80-) 309:2228–2232.
- Mathiowetz V, Volland G, Kashman N, Weber K (1985) Adult norms for the Box and Block Test of manual dexterity. *Am J Occup Ther* 39:386–391.
- Matsunaga K, Maruyama A, Fujiwara T, Nakanishi R, Tsuji S, Rothwell JC (2005) Increased corticospinal excitability after 5 Hz rTMS over the human supplementary motor area. *J Physiol* 562:295–306.
- Maunsell JHR, Newsome WT (1987) Visual Processing In Monkey Extrastriate Cortex. *Annu Rev Neurosci* 10:363–401.
- Maunsell JHR, Van Essen DC (1983a) The connections of the middle temporal visual area (MT) and their relationship to a cortical hierarchy in the macaque monkey. *J Neurosci* 3:2563–2586.
- Maunsell JHR, Van Essen DC (1983b) Functional Properties of Neurons in Middle Temporal Visual Area of the Macaque Monkey. I. Selectivity for Stimulus Direction, Speed, and Orientation. *J Neurophysiol* 49:1127–1147.
- Mayka MA, Corcos DM, Leurgans SE, Vaillancourt DE (2006) Three-dimensional locations and boundaries of motor and premotor cortices as defined by functional brain imaging: A meta-analysis. *Neuroimage* 31:1453–1474.
- Miall RC (2003) Connecting mirror neurons and forward models. *Neuroreport* 14:2135–2137.
- Mishkin M, Ungerleider LG (1982) Contribution of striate inputs to the visuospatial functions of parieto-preoccipital cortex in monkeys. *Behav Brain Res* 6:57–77.
- Mochizuki H, Huang YZ, Rothwell JC (2004a) Interhemispheric interaction between human dorsal premotor and contralateral primary motor cortex. *J Physiol* 561:331–338.
- Mochizuki H, Terao Y, Okabe S, Furubayashi T, Arai N, Iwata NK, Hanajima R, Kamakura K, Motoyoshi K, Ugawa Y (2004b) Effects of motor cortical stimulation on the excitability of contralateral motor and sensory cortices. *Exp Brain Res* 158:519–526.
- Montagna M, Cerri G, Borroni P, Baldissera F (2005) Excitability changes in human corticospinal projections to muscles moving hand and fingers while viewing a reaching and grasping action. *Eur J Neurosci* 22:1513–1520.
- Muakkassa KF, Strick PL (1979) Frontal lobe inputs to primate motor cortex: evidence for four somatotopically organized “premotor” areas. *Brain Res* 177:176–182.
- Muir RB, Lemon RN (1983) Corticospinal neurons with a special role in precision grip. *Brain Res* 261:312–316.
- Mukamel R, Ekstrom AD, Kaplan J, Iacoboni M, Fried I (2010) Single-Neuron Responses in Humans during Execution and Observation of Actions. *Curr Biol* 20:750–756.
- Müller-Dahlhaus FJM, Ziemann U, Classen J (2010) Plasticity resembling spike-timing dependent synaptic plasticity: The evidence in human cortex. *Front Synaptic Neurosci* 2:1–11.

- Münchau A, Bloem BR, Irlbacher K, Trimble MR, Rothwell JC (2002) Functional connectivity of human premotor and motor cortex explored with repetitive transcranial magnetic stimulation. *J Neurosci* 22:554–561.
- Murata A, Fadiga L, Fogassi L, Gallese V, Raos V, Rizzolatti G (1997) Object representation in the ventral premotor cortex (area F5) of the monkey. *J Neurophysiol* 78:2226–2230.
- Nachev P, Kennard C, Husain M (2008) Functional role of the supplementary and pre-supplementary motor areas. *Nat Rev Neurosci* 9:856–869.
- Nachev P, Wydell H, O'Neill K, Husain M, Kennard C (2007) The role of the pre-supplementary motor area in the control of action. *Neuroimage* 36.
- Naish KR, Houston-Price C, Bremner AJ, Holmes NP (2014) Effects of action observation on corticospinal excitability: Muscle specificity, direction, and timing of the mirror response. *Neuropsychologia* 64:331–348.
- Nelles G, Jentzen W, Jueptner M, Müller S, Diener HC (2001) Arm Training Induced Brain Plasticity in Stroke Studied with Serial Positron Emission Tomography. *Neuroimage* 13:1146–1154.
- Neubert F-X, Mars RB, Buch ER, Olivier E, Rushworth MFS (2010) Cortical and subcortical interactions during action reprogramming and their related white matter pathways_Supporting Information. *Proc Natl Acad Sci U S A* 107.
- Ni Z, Gunraj C, Nelson AJ, Yeh I-J, Castillo G, Hoque T, Chen R (2009) Two phases of interhemispheric inhibition between motor related cortical areas and the primary motor cortex in human. *Cereb Cortex* 19:1654–1665.
- Nishitani N, Hari R (2000) Temporal dynamics of cortical representation for action. *Proc Natl Acad Sci U S A* 97:913–918.
- Nishitani N, Hari R (2002) Viewing lip forms: Cortical dynamics. *Neuron* 36:1211–1220.
- Nitsche MA, Nitsche MS, Klein CC, Tergau F, Rothwell JC, Paulus W (2003) Level of action of cathodal DC polarisation induced inhibition of the human motor cortex. *Clin Neurophysiol* 114:600–604.
- Nowicka A, Tacikowski P (2011) Transcallosal transfer of information and functional asymmetry of the human brain. *Laterality* 16:35–74.
- O'Shea J, Johansen-Berg H, Trief D, Gobel S, Rushworth MFS (2007) Functionally Specific Reorganization in Human Premotor Cortex. *Neuron* 54:479–490.
- Oldfield RC (1971) The assessment and analysis of handedness: the Edinburgh inventory. *Neuropsychologia* 9:97–113.
- Ondobaka S, de Lange FP, Wittmann M, Frith CD, Bekkering H (2015) Interplay between conceptual expectations and movement predictions underlies action understanding. *Cereb Cortex* 25:2566–2573.
- Orban GA, Van Essen DC, Vanduffel W (2004) Comparative mapping of higher visual areas in monkeys and humans. *Trends Cogn Sci* 8:315–324.

- Oxford Grice K, Vogel KA, Le V, Mitchell A, Muniz S, Vollmer MA (2003) Adult norms for a commercially available Nine Hole Peg Test for finger dexterity. *Am J Occup Ther* 57:570–573.
- Palmer CE, Bunday KL, Davare M, Kilner JM (2016) A Causal Role for Primary Motor Cortex in Perception of Observed Actions. *J Cogn Neurosci* 28:2021–2029.
- Paracampo R, Pirruccio M, Costa M, Borgomaneri S, Avenanti A (2018) Visual, sensorimotor and cognitive routes to understanding others' enjoyment: an individual differences rTMS approach to empathic accuracy. *Neuropsychologia*:1–13.
- Paracampo R, Tidoni E, Borgomaneri S, di Pellegrino G, Avenanti A (2016) Sensorimotor Network Crucial for Inferring Amusement from Smiles. *Cereb Cortex*:1–14.
- Pascual-Leone A, Tarazona F, Keenan J, Tormos JM, Hamilton R, Catala MD (1998) Transcranial magnetic stimulation and neuroplasticity. *Neuropsychologia* 37:207–217.
- Pascual-Leone A, Walsh V (2001) Fast backprojections from the motion to the primary visual area necessary for visual awareness. *Science* (80-) 292:510–512.
- Pelli DG (1997) The VideoToolbox software for visual psychophysics: transforming numbers into movies. *Spat Vis* 10:437–442.
- Petrides M, Pandya DN (2009) Distinct parietal and temporal pathways to the homologues of Broca's area in the monkey. *PLoS Biol* 7.
- Philip BA, Frey SH (2016) Increased functional connectivity between cortical hand areas and praxis network associated with training-related improvements in non-dominant hand precision drawing. *Neuropsychologia* 87:157–168.
- Picard N, Strick PL (2001) Imaging the premotor areas. *Curr Opin Neurobiol* 11:663–672.
- Picazio S, Veniero D, Ponzio V, Caltagirone C, Gross J, Thut G, Koch G (2014) Prefrontal control over motor cortex cycles at beta frequency during movement inhibition. *Curr Biol* 24:2940–2945.
- Plow EB, Cattaneo Z, Carlson TA, Alvarez GA, Pascual-Leone A, Battelli L (2014) The Compensatory dynamic of inter-hemispheric interactions in visuospatial attention revealed using rTMS and fMRI. *Front Hum Neurosci* 8:226.
- Pobric G, Hamilton AF de C (2006) Action Understanding Requires the Left Inferior Frontal Cortex. *Curr Biol* 16:524–529.
- Pool E-M, Rehme AK, Fink GR, Eickhoff SB, Grefkes C (2013) Network dynamics engaged in the modulation of motor behavior in healthy subjects. *Neuroimage* 82:68–76.
- Power JD, Cohen AL, Nelson SM, Wig GS, Barnes KA, Church JA, Vogel AC, Laumann TO, Miezin FM, Schlaggar BL, Petersen SE (2011) Functional Network Organization of the Human Brain. *Neuron* 72:665–678.
- Prabhu G, Shimazu H, Cerri G, Brochier T, Spinks RL, Maier MA, Lemon RN (2009) Modulation of primary motor cortex outputs from ventral premotor cortex during visually guided grasp in the macaque monkey. *J Physiol* 587:1057–1069.

- Press C (2011) Action observation and robotic agents: Learning and anthropomorphism. *Neurosci Biobehav Rev* 35:1410–1418.
- Prieto EA, Barnikol UB, Soler EP, Dolan K, Hesselmann G, Mohlberg H, Amunts K, Zilles K, Niedeggen M, Tass PA (2007) Timing of V1/V2 and V5+ activations during coherent motion of dots: An MEG study. *Neuroimage* 37:1384–1395.
- Ptak R, Schnider A, Fellrath J (2017) The Dorsal Frontoparietal Network: A Core System for Emulated Action. *Trends Cogn Sci* 21:589–599.
- Puce A, Perrett DI (2003) Electrophysiology and brain imaging of biological motion. *Philos Trans R Soc Lond B Biol Sci* 358:435–445.
- Raiguel S, Van Hulle MM, Xiao DK, Marcar VL, Lagae L, Orban GA (1997) Size and shape of receptive fields in the medial superior temporal area (MST) of the macaque. *Neuroreport* 8:2803–2808.
- Randhawa BK, Farley BG, Boyd LA (2013) Repetitive transcranial magnetic stimulation improves handwriting in parkinson's disease. *Parkinsons Dis* 2013:1–9.
- Raos V, Umiltà M-A, Murata A, Fogassi L, Gallese V (2006) Functional properties of grasping-related neurons in the ventral premotor area F5 of the macaque monkey. *J Neurophysiol* 95:709–729.
- Redcay E (2008) The superior temporal sulcus performs a common function for social and speech perception: Implications for the emergence of autism. *Neurosci Biobehav Rev* 32:123–142.
- Reis J, Swayne O, Vandermeeren Y, Camus M, Dimyan MA, Harris-Love M, Perez MA, Ragert P, Rothwell JC, Cohen LG (2008) Contribution of transcranial magnetic stimulation to the understanding of cortical mechanisms involved in motor control. *J Physiol* 586:325–351.
- Ridding MC, Ziemann U (2010) Determinants of the induction of cortical plasticity by non-invasive brain stimulation in healthy subjects. *J Physiol* 588:2291–2304.
- Rizzo V, Bove M, Naro A, Tacchino A, Mastroeni C, Avanzino L, Crupi D, Morgante F, Siebner HR, Quartarone A (2011) Associative cortico-cortical plasticity may affect ipsilateral finger opposition movements. *Behav Brain Res* 216:433–439.
- Rizzo V, Siebner HR, Morgante F, Mastroeni C, Girlanda P, Quartarone A (2009) Paired associative stimulation of left and right human motor cortex shapes interhemispheric motor inhibition based on a hebbian mechanism. *Cereb Cortex* 19:907–915.
- Rizzolatti G, Cattaneo L, Fabbri-Destro M, Rozzi S (2014) Cortical mechanisms underlying the organization of goal-directed actions and mirror neuron-based action understanding. *Physiol Rev* 94:655–706.
- Rizzolatti G, Craighero L (2004) the Mirror-Neuron System. *Annu Rev Neurosci* 27:169–192.
- Rizzolatti G, Fadiga L, Gallese V, Fogassi L (1996) Premotor cortex and the recognition of motor actions. *Cogn Brain Res* 3:131–141.
- Rizzolatti G, Fogassi L, Gallese V (2001) Neurophysiological mechanisms underlying the understanding and imitation of action. *Nat Rev Neurosci* 2:661–670.

- Rodman HR, Albright TD (1989) Single-unit analysis of pattern-motion selective properties in the middle temporal visual area (MT). *Exp Brain Res* 75:53–64.
- Romei V, Chiappini E, Hibbard PB, Avenanti A (2016a) Empowering Reentrant Projections from V5 to V1 Boosts Sensitivity to Motion. *Curr Biol* 26:2155–2160.
- Romei V, De Gennaro L, Fratello F, Curcio G, Ferrara M, Pascual-Leone A, Bertini M (2008) Interhemispheric transfer deficit in alexithymia: A transcranial magnetic stimulation study. *Psychother Psychosom* 77:175–181.
- Romei V, Thut G, Silvanto J (2016b) Information-Based Approaches of Noninvasive Transcranial Brain Stimulation. *Trends Neurosci*:1–14.
- Rossi S, Hallett M, Rossini PM, Pascual-Leone A (2009) Safety, ethical considerations, and application guidelines for the use of transcranial magnetic stimulation in clinical practice and research. *Clin Neurophysiol* 120:2008–2039.
- Rossini PM et al. (2015) Non-invasive electrical and magnetic stimulation of the brain, spinal cord, roots and peripheral nerves: Basic principles and procedures for routine clinical and research application: An updated report from an I.F.C.N. Committee. *Clin Neurophysiol* 126:1071–1107.
- Rothwell JC (2011) Using transcranial magnetic stimulation methods to probe connectivity between motor areas of the brain. *Hum Mov Sci* 30:906–915.
- Rushworth MFS, Walton ME, Kennerley SW, Bannerman DM (2004) Action sets and decisions in the medial frontal cortex. *Trends Cogn Sci* 8:410–417.
- Rust NC, Mante V, Simoncelli EP, Movshon JA (2006) How MT cells analyze the motion of visual patterns. *Nat Neurosci* 9:1421–1431.
- Sattler V, Dickler M, Michaud M, Meunier S, Simonetta-Moreau M (2014) Does abnormal interhemispheric inhibition play a role in mirror dystonia? *Mov Disord* 29:787–796.
- Schippers MB, Keysers C (2011) Mapping the flow of information within the putative mirror neuron system during gesture observation. *Neuroimage* 57:37–44.
- Schubotz RI, von Cramon YD (2004) Sequences of Abstract Nonbiological Stimuli Share Ventral Premotor Cortex with Action Observation and Imagery. *J Neurosci* 24:5467–5474.
- Schwarzkopf DS, Silvanto J, Rees G (2011) Stochastic resonance effects reveal the neural mechanisms of transcranial magnetic stimulation. *J Neurosci* 31:3143–3147.
- Serino A, Annella L, Avenanti A (2009) Motor properties of peripersonal space in humans Ferrari PF, ed. *PLoS One* 4:e6582.
- Shimazu H, Maier MA, Cerri G, Kirkwood PA, Lemon RN (2004) Macaque ventral premotor cortex exerts powerful facilitation of motor cortex outputs to upper limb motoneurons. *J Neurosci* 24:1200–1211.
- Siebner HR et al. (2009a) Consensus paper: Combining transcranial stimulation with neuroimaging. *Brain Stimul* 2:58–80.

- Siebner HR, Hartwigsen G, Kassuba T, Rothwell JC (2009b) How does transcranial magnetic stimulation modify neuronal activity in the brain? Implications for studies of cognition. *Cortex* 45:1035–1042.
- Silvanto J (2015) Why is “blindsight” blind? A new perspective on primary visual cortex, recurrent activity and visual awareness. *Conscious Cogn* 32:15–32.
- Silvanto J, Cattaneo Z (2017) Common framework for “virtual lesion” and state-dependent TMS: The facilitatory/suppressive range model of online TMS effects on behavior. *Brain Cogn* 119:32–38.
- Silvanto J, Cowey A, Lavie N, Walsh V (2005a) Striate cortex (V1) activity gates awareness of motion. *Nat Neurosci* 8:143–144.
- Silvanto J, Lavie N, Walsh V (2005b) Double dissociation of V1 and V5/MT activity in visual awareness. *Cereb Cortex* 15:1736–1741.
- Silvanto J, Muggleton N, Walsh V (2008) State-dependency in brain stimulation studies of perception and cognition. *Trends Cogn Sci* 12:447–454.
- Silvanto J, Muggleton NG (2008a) Testing the validity of the TMS state-dependency approach: Targeting functionally distinct motion-selective neural populations in visual areas V1/V2 and V5/MT+. *Neuroimage* 40:1841–1848.
- Silvanto J, Muggleton NG (2008b) A novel approach for enhancing the functional specificity of TMS: Revealing the properties of distinct neural populations within the stimulated region. *Clin Neurophysiol* 119:724–726.
- Silvanto J, Muggleton NG, Cowey A, Walsh V (2007) Neural adaptation reveals state-dependent effects of transcranial magnetic stimulation. *Eur J Neurosci* 25:1874–1881.
- Sinigaglia C (2013) What type of action understanding is subserved by mirror neurons? *Neurosci Lett* 540:59–61.
- Sokolov AA, Erb M, Grodd W, Tatagiba MS, Frackowiak RSJ, Pavlova MA (2014) Recovery of biological motion perception and network plasticity after cerebellar tumor removal. *Cortex* 59:146–152.
- Somogyi P, Tamás G, Lujan R, Buhl EH (1998) Salient features of synaptic organisation in the cerebral cortex. In: *Brain Research Reviews*, pp 113–135.
- Stefan K, Kunesch E, Cohen LG, Benecke R, Classen J (2000) Induction of plasticity in the human motor cortex by paired associative stimulation. *Brain* 123 Pt 3:572–584.
- Strafella A, Paus T (2000) Modulation of cortical excitability during action observation: a transcranial magnetic stimulation study. *Neuroreport* 11:2289–2292.
- Strigaro G, Ruge D, Chen J-C, Marshall L, Desikan M, Cantello R, Rothwell JC (2015) Interaction between visual and motor cortex: a transcranial magnetic stimulation study. *J Physiol* 593:2365–2377.
- Sun FT, Miller LM, Rao AA, D’Esposito M (2007) Functional connectivity of cortical networks involved in bimanual motor sequence learning. *Cereb Cortex* 17:1227–1234.

- Swann NC, Cai W, Conner CR, Pieters TA, Claffey MP, George JS, Aron AR, Tandon N (2012) Roles for the pre-supplementary motor area and the right inferior frontal gyrus in stopping action: Electrophysiological responses and functional and structural connectivity. *Neuroimage* 59:2860–2870.
- Tai YF, Scherfler C, Brooks DJ, Sawamoto N, Castiello U (2004) The Human Premotor Cortex Is “Mirror” only for Biological Actions. *Curr Biol* 14:117–120.
- Taubert M, Lohmann G, Margulies DS, Villringer A, Ragert P (2011) Long-term effects of motor training on resting-state networks and underlying brain structure. *Neuroimage* 57:1492–1498.
- Tessitore A, Amboni M, Esposito F, Russo A, Picillo M, Marcuccio L, Pellecchia MT, Vitale C, Cirillo M, Tedeschi G, Barone P (2012) Resting-state brain connectivity in patients with Parkinson’s disease and freezing of gait. *Parkinsonism Relat Disord* 18:781–787.
- Thickbroom GW (2007) Transcranial magnetic stimulation and synaptic plasticity: Experimental framework and human models. *Exp Brain Res* 180:583–593.
- Thickbroom GW, Byrnes ML, Edwards DJ, Mastaglia FL (2006) Repetitive paired-pulse TMS at I-wave periodicity markedly increases corticospinal excitability: A new technique for modulating synaptic plasticity. *Clin Neurophysiol* 117:61–66.
- Tidoni E, Borgomaneri S, di Pellegrino G, Avenanti A (2013) Action simulation plays a critical role in deceptive action recognition. *J Neurosci* 33:611–623.
- Tokuno H, Nambu A (2000) Organization of nonprimary motor cortical inputs on pyramidal and nonpyramidal tract neurons of primary motor cortex: An electrophysiological study in the macaque monkey. *Cereb Cortex* 10:58–68.
- Tunik E, Rice NJ, Hamilton AF de C, Grafton ST (2007) Beyond grasping: Representation of action in human anterior intraparietal sulcus. *Neuroimage* 36:T77–T86.
- Turella L, Lingnau A (2014) Neural correlates of grasping. *Front Hum Neurosci* 8:686.
- Urgesi C, Candidi M, Avenanti A (2014) Neuroanatomical substrates of action perception and understanding: an anatomic likelihood estimation meta-analysis of lesion-symptom mapping studies in brain injured patients. *Front Hum Neurosci* 8:344.
- Urgesi C, Candidi M, Fabbro F, Romani M, Aglioti SM (2006) Motor facilitation during action observation: Topographic mapping of the target muscle and influence of the onlooker’s posture. *Eur J Neurosci* 23:2522–2530.
- Urgesi C, Maieron M, Avenanti A, Tidoni E, Fabbro F, Aglioti SM (2010) Simulating the future of actions in the human corticospinal system. *Cereb Cortex* 20:2511–2521.
- Urgesi C, Savonitto MM, Fabbro F, Aglioti SM (2012) Long- and short-term plastic modeling of action prediction abilities in volleyball. *Psychol Res* 76:542–560.
- Vaina LM, Solomon J, Chowdhury S, Sinha P, Belliveau JW (2001) Functional neuroanatomy of biological motion perception in humans. *Proc Natl Acad Sci U S A* 98:11656–11661.

- Valchev N, Curčić-Blake B, Renken RJ, Avenanti A, Keysers C, Gazzola V, Maurits NM (2015) cTBS delivered to the left somatosensory cortex changes its functional connectivity during rest. *Neuroimage* 114:386–397.
- Valchev N, Gazzola V, Avenanti A, Keysers C (2016) Primary somatosensory contribution to action observation brain activity-combining fMRI and cTBS. *Soc Cogn Affect Neurosci*:Epub.
- Valchev N, Tidoni E, Hamilton AF de C, Gazzola V, Avenanti A (2017) Primary somatosensory cortex necessary for the perception of weight from other people's action: A continuous theta-burst TMS experiment. *Neuroimage* 152:195–206.
- Vallar G, Bolognini N (2011) Behavioural facilitation following brain stimulation: Implications for neurorehabilitation. *Neuropsychol Rehabil* 21:618–649.
- Valls-Solé J, Pascual-Leone A, Wassermann EM, Hallett M (1992) Human motor evoked responses to paired transcranial magnetic stimuli. *Electroencephalogr Clin Neurophysiol* 85:355–364.
- Van Overwalle F, Baetens K (2009) Understanding others' actions and goals by mirror and mentalizing systems: A meta-analysis. *Neuroimage* 48:564–584.
- Veniero D, Ponzio V, Koch G (2013) Paired Associative Stimulation Enforces the Communication between Interconnected Areas. *J Neurosci* 33:13773–13783.
- Verwey WB, Lammens R, Honk J van (2002) On the role of the SMA in the discrete sequence production task: a TMS study. *Neuropsychologia* 40:1268–1276.
- Vesia M, Barnett-Cowan M, Elahi B, Jegatheeswaran G, Isayama R, Neva JL, Davare M, Staines WR, Culham JC, Chen R (2017) Human dorsomedial parieto-motor circuit specifies grasp during the planning of goal-directed hand actions. *Cortex* 92:175–186.
- Vetter P, Grosbras MH, Muckli L (2015) TMS over V5 disrupts motion prediction. *Cereb Cortex* 25:1052–1059.
- Vossel S, Geng JJ, Fink GR (2014) Dorsal and ventral attention systems: Distinct neural circuits but collaborative roles. *Neuroscientist* 20:150–159.
- Wagenmakers EJ, Marsman M, Jamil T, Ly A, Verhagen J, Love J, Selker R, Gronau QF, Šmíra M, Epskamp S, Matzke D, Rouder JN, Morey RD (2017) Bayesian inference for psychology. Part I: Theoretical advantages and practical ramifications. *Psychon Bull Rev*:1–23.
- Walsh V, Ellison A, Battelli L, Cowey A (1998) Task-specific impairments and enhancements induced by magnetic stimulation of human visual area V5. *Proc R Soc B Biol Sci* 265:537–543.
- Walsh V, Rushworth MFS (1999) A primer of magnetic stimulation as a tool for neuropsychology. *Neuropsychologia* 37:125–135.
- Weiller C, Chollet F, Friston KJ, Wise RJS, Frackowiak RSJ (1992) Functional reorganization of the brain in recovery from striatocapsular infarction in man. *Ann Neurol* 31:463–472.
- Wiestler T, Diedrichsen J (2013) Skill learning strengthens cortical representations of motor sequences. *Elife* 2013:e00801.

- Wilson M, Knoblich G (2005) The Case for Motor Involvement in Perceiving Conspicifics. *Psychol Bull* 131:460–473.
- Wolpert DM, Doya K, Kawato M (2003) A unifying computational framework for motor control and social interaction. *Philos Trans R Soc Lond B Biol Sci* 358:593–602.
- Wolters A, Sandbrink F, Schlottmann A, Kunesch E, Stefan K, Cohen LG, Benecke R, Classen J (2003) A Temporally Asymmetric Hebbian Rule Governing Plasticity in the Human Motor Cortex. *J Neurophysiol* 89:2339–2345.
- Wyatte D, Jilk DJ, O'Reilly RC (2014) Early recurrent feedback facilitates visual object recognition under challenging conditions. *Front Psychol* 5:1–10.
- Xerri C (2012) Plasticity of Cortical Maps. *Neurosci* 18:133–148.
- Zeki SM (2004) Thirty years of a very special visual area, Area V5. *J Physiol* 557:1–2.
- Zeki SM, Watson JD, Lueck CJ, Friston KJ, Kennard C, Frackowiak RS (1991) A direct demonstration of functional specialization in human visual cortex. *J Neurosci* 11:641–649.
- Zhang LI, Tao HW, Holt CE, Harris WA, Poo M (1998) A critical window for cooperation and competition among developing retinotectal synapses. *Nature* 395:37–44.
- Ziemann U, Paulus W, Nitsche MA, Pascual-Leone A, Byblow WD, Berardelli A, Siebner HR, Classen J, Cohen LG, Rothwell JC (2008) Consensus: Motor cortex plasticity protocols. *Brain Stimul* 1:164–182.
- Zihl J, von Cramon YD, Mai N (1983) Selective Disturbance of Movement. *Brain* 106:313–340.